

AD_____

AWARD NUMBER: W81XWH-05-2-0027

TITLE: IMPACT (Imaging and Molecular Markers for Patients with Lung Cancer: Approaches with Molecular Targets and Complementary, Innovative and Therapeutic Modalities)

PRINCIPAL INVESTIGATOR: Waun Ki Hong, M.D
Roy Herbst, M.D.,Ph.D.

CONTRACTING ORGANIZATION: University of Texas
M.D. Anderson Cancer Center
Houston, TX 77030

REPORT DATE: March 2007

TYPE OF REPORT: Annual

PREPARED FOR: U.S. Army Medical Research and Materiel Command
Fort Detrick, Maryland 21702-5012

DISTRIBUTION STATEMENT: Approved for Public Release;
Distribution Unlimited

The views, opinions and/or findings contained in this report are those of the author(s) and should not be construed as an official Department of the Army position, policy or decision unless so designated by other documentation.

REPORT DOCUMENTATION PAGE

Form Approved
OMB No. 0704-0188

Public reporting burden for this collection of information is estimated to average 1 hour per response, including the time for reviewing instructions, searching existing data sources, gathering and maintaining the data needed, and completing and reviewing this collection of information. Send comments regarding this burden estimate or any other aspect of this collection of information, including suggestions for reducing this burden to Department of Defense, Washington Headquarters Services, Directorate for Information Operations and Reports (0704-0188), 1215 Jefferson Davis Highway, Suite 1204, Arlington, VA 22202-4302. Respondents should be aware that notwithstanding any other provision of law, no person shall be subject to any penalty for failing to comply with a collection of information if it does not display a currently valid OMB control number. PLEASE DO NOT RETURN YOUR FORM TO THE ABOVE ADDRESS.

1. REPORT DATE 01-03-2007	2. REPORT TYPE Annual	3. DATES COVERED 1 Feb 2006 – 31 Jan 2007		
4. TITLE AND SUBTITLE IMPACT (Imaging and Molecular Markers for Patients with Lung Cancer: Approaches with Molecular Targets and Complementary, Innovative and Therapeutic Modalities)		5a. CONTRACT NUMBER		
		5b. GRANT NUMBER W81XWH-05-2-0027		
		5c. PROGRAM ELEMENT NUMBER		
6. AUTHOR(S) Waun Ki Hong, M.D., Roy Herbst, M.D., Ph.D. E-Mail: whong@mdanderson.org		5d. PROJECT NUMBER		
		5e. TASK NUMBER		
		5f. WORK UNIT NUMBER		
7. PERFORMING ORGANIZATION NAME(S) AND ADDRESS(ES) University of Texas M.D. Anderson Cancer Center Houston, TX 77030		8. PERFORMING ORGANIZATION REPORT NUMBER		
9. SPONSORING / MONITORING AGENCY NAME(S) AND ADDRESS(ES) U.S. Army Medical Research and Materiel Command Fort Detrick, Maryland 21702-5012		10. SPONSOR/MONITOR'S ACRONYM(S)		
		11. SPONSOR/MONITOR'S REPORT NUMBER(S)		
12. DISTRIBUTION / AVAILABILITY STATEMENT Approved for Public Release; Distribution Unlimited				
13. SUPPLEMENTARY NOTES Original contains colored plates: ALL DTIC reproductions will be in black and white.				
14. ABSTRACT The projects in this proposal specifically target several signal transduction pathways known to be critical for NSCLC pathogenesis including the EGFR pathway and the more downstream ras/raf/Mek/ERK pathway. These projects combine targeted approaches using molecular and imaging techniques to validate activity against a target and monitor response using imaging modalities specific to the receptor using either small molecules or targeted peptide approaches. The Developmental Research projects explore new areas including 1) the issue of high morbidity malignant pleural effusion thereby bringing the pulmonologists into the treatment of advanced disease with molecular therapies; and 2) prevention of lung cancer in youth through a highly interactive, entertaining CD-ROM program.				
15. SUBJECT TERMS lung cancer, molecular markers, molecular imaging				
16. SECURITY CLASSIFICATION OF: a. REPORT U		17. LIMITATION OF ABSTRACT UU	18. NUMBER OF PAGES 233	19a. NAME OF RESPONSIBLE PERSON USAMRMC
b. ABSTRACT U				19b. TELEPHONE NUMBER (include area code)
c. THIS PAGE U				

TABLE OF CONTENTS

INTRODUCTION	2
BODY	2
Project 1	2
Project 2	7
Project 3	11
Project 4	14
Project 5	18
Project 6	24
Core B Biostatistics and Data Management	33
Core C Molecular Pathology and Specimen Procurement	35
Core D Molecular Imaging	46
Developmental Research Project 1	47
Developmental Research Project 2.....	49
Career Development Project 1.....	52
KEY RESEARCH ACCOMPLISHMENTS	53
REPORTABLE OUTCOMES.....	56
CONCLUSIONS	57
REFERENCES	59
APPENDICES	62
Appendix A (Project 1 - Genentech approval memo)	
Appendix B (Project 1 - Approved animal protocol and letter)	
Appendix C (Revised Statement of Work for Project 5)	
Appendix D (Project 5 - Approved animal protocol and letter)	
Appendix E (Project 5 - The DoD approval letter of RAD001 trial)	
Appendix F (DRP-1- Memo of PI change and IRB approved letter)	
Appendix G (DRP2 - TALK- 1- Focus group)	
Appendix H (DRP2- TALK - 2 - Development)	
Appendix I (DRP2 - TALK - 3 - Script)	
Appendix J (Publications)	

IMPACT: Imaging and Molecular Markers for Patients with Lung Cancer: Approaches with Molecular Targets, Complementary, Innovative and Therapeutic Modalities

INTRODUCTION

Lung cancer is the most prevalent cancer worldwide and the leading cause of cancer-related mortality in both men and women in the United States. Conventional multimodality therapies (surgery, radiation and chemotherapy) have reached a therapeutic ceiling in improving the five-year overall survival rate of non-small cell lung cancer (NSCLC) patients, clinically in large part due to chemo- and radiation-resistant locoregional and metastatic spread but ultimately due to poor understanding of the disease and its resistance to the therapy.

Lung cancer is a heterogeneous disease, resulting from accumulated genetic abnormalities over years, which thus requires a coordinated attack in a truly integrated fashion on multiple altered signal pathways. An emerging targeted therapy aims to target key molecular abnormalities in cancer and has succeeded in some tumor types such as chronic myeloid leukemia (CML) (Druker et al., 2004; Druker and Sawyers et al., 2001; Druker and Talpaz et al., 2001), gastrointestinal stromal tumor (Demetri et al., 2002), colon cancer (Hurwitz et al., 2003), and breast cancer (Howell et al., 2005). Thus, the incorporation of targeted therapy into conventional treatments appears to be a new promising approach to treatment of lung cancer.

The program project IMPACT has proposed to integrate targeted therapy in the lung cancer research program when initial clinical results showed disappointing response rates and survival benefit of EGFR inhibitor Gefitinib (Iressa) for non-selected lung cancer patients (Herbst et al., 2002, 2003, 2004; Herbst, 2004; Kris et al., 2003; Giaccone et al., 2004). It aims to validate molecular mechanisms of targeted agents alone and in combination with chemo and/or radiation therapies in preclinical and clinical settings. It also aims to develop effective molecular imaging and cancer cell-targeted peptide-based delivery tools to help improve efficacy of the targeted agents. Specifically, our objectives are:

- To validate preclinically and clinically several key signaling pathways and their agents for therapeutic potentials alone or in combination with each other or with chemo and /or radiotherapy
- To explore applications of molecular imaging for targeted therapy and identify cancer cell-targeted peptides for systemic delivery of therapeutic and imaging agents
- To discover and evaluate new molecular abnormalities and therapeutic predictors in lung cancer
- To develop an educational program for teens and young adults for smoking risk and resultant lung cancer occurrence.

IMPACT is composed of 6 research projects, 1 Biostatistics Core, 1 Molecular Pathology Core, 1 Molecular Imaging Core, 2 career development projects, and 2 developmental research projects. Here we present their scientific progresses in the second grant year as follows.

BODY (PROGRESS REPORT)

Project 1: Targeting epidermal growth factor receptor signaling to enhance response of lung cancer to therapeutic radiation.

(PI and co-PI: Raymond E. Meyn, Ph.D., Ritsuko Komaki, M.D.)

In spite of significant technical advances including IMRT and chemoradiation, locally advanced lung cancer continues to have a dismal prognosis as many patients' tumors appear to be resistant to radiation therapy. The molecular basis for radiation resistance is not fully understood, but tumor cells have an enhanced survival response that involves increased capacity for DNA repair and suppressed apoptosis. Both apoptosis propensity and DNA repair capacity are thought to be partly controlled by the upstream signal transduction pathways triggered by EGFR activation, which is constitutively activated in many NSCLCs, and its activation leads to a radiation-resistant phenotype. We hypothesize that the response of NSCLC to radiation can be improved through the use of inhibitors of EGFR signaling.

Aim 1 To test the combination of external beam radiation and the selective EGFR-tyrosine kinase inhibitor erlotinib (Tarceva) in locally advanced NSCLC.

Update

As reported last year, erlotinib was substituted for gefitinib because gefitinib has caused interstitial pneumonia and withdrawn from the market, and erlotinib has also appeared effective in terms of prolonging overall survival times in lung cancer patients (Tsao et al., 2005). The revised protocol entitled *A Phase I/II Study of TARCEVA (erlotinib) in Combination with Chemoradiation in Patients with Stage IIIA/B Non-Small Cell Lung Cancer (NSCLC)* has been progressing through comprehensive review by our Institutional Review Board (IRB), the US Department of Defense (DoD), Genentech, and Food and Drug Administration (FDA), and was approved by Genentech on December 22, 2006 (see in the Appendix A – Project 1- Genentech approval letter). We expect final approvals by the IRB and DoD and to receive Investigational New Drug (IND) application approval from the FDA soon. The contract for the supply of erlotinib to M. D. Anderson Cancer Center by Genentech is currently under negotiation. Once the final approvals and the contract are completed, the trial will subsequently be opened.

Aim 2 To test the hypothesis that activation of the EGFR pathway leads to radiation resistance in NSCLC cells due to an enhanced capacity for repairing DNA lesions.

Studies conducted in this aim involved characterizing the signaling pathways downstream of EGFR activation in NSCLC cell lines and correlating radiation response and DNA repair capacity in the cell lines with their respective activation of EGFR.

Update

Last year, we examined the response of 4 NSCLC cell lines (A549, H1299, H322, and H358), which carry the wildtype EGFR, and normal human lung fibroblasts (e.g., the CCD-16 cell line) to gefitinib. Considerable progress was demonstrated in the last report using the A549 and H1299 cell lines.

We have now expanded these studies to erlotinib. First, we have measured the survival of human NSCLC cells exposed to combinations of erlotinib and ionizing radiation using clonogenic assays. The results for A549, H1299, H322, H358 and CCD-16 cells were reported in the previous progress report as mentioned above, and we have extended the study to now include the H460 cell line. H460 is a standard NSCLC line that has wild-type EGFR status and will allow us to compare our results with many published reports that used this line.

The H460 cells were pretreated with 5 μ M erlotinib for 24 hours and then the cells were irradiated. Pretreatment with erlotinib suppressed the clonogenic survival of these cells (Figure 1). Survival at 2 Gy (SF2) was reduced from $73.75\% \pm 4.15$ in the control to $54.3\% \pm 1.8$ ($P = 0.05$) in 5 μ M erlotinib-treated cells. Survival enhancement ratios (SER) were calculated by dividing the radiation dose that produced 10% cell survival on the radiation-only survival curve by that for the corresponding erlotinib plus ionizing radiation curve. SER for the H460 cells was 1.19 for 5 μ M erlotinib-treated cells. Erlotinib, when used alone, did not significantly reduce the plating efficiency of H460 cells compared to untreated controls. We are currently using these cell lines as a model to explore the underlying molecular mechanism that may be responsible for governing radioresponse of NSCLC cells downstream of EGFR.

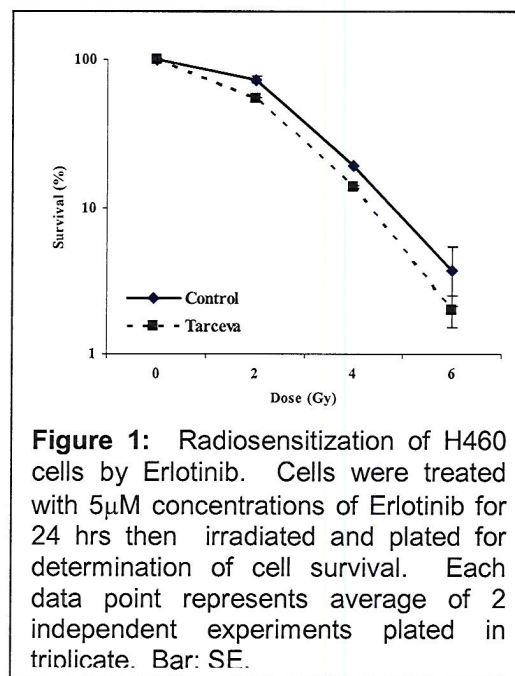


Figure 1: Radiosensitization of H460 cells by Erlotinib. Cells were treated with 5 μ M concentrations of Erlotinib for 24 hrs then irradiated and plated for determination of cell survival. Each data point represents average of 2 independent experiments plated in triplicate. Bar: SE.

As an initial investigation into the mechanism responsible for erlotinib-mediated radiosensitization, we examined the effect of erlotinib treatment on the expression of downstream targets in the EGFR signaling pathway. Dose-dependent decreases in the levels of pEGFR were observed in unirradiated A549 and H1299 cells following 24-hour treatment with erlotinib, in a preliminary experiment to be confirmed (Figure 2). Radiation activated pEGFR in these cell lines but this activation was suppressed by erlotinib correlating with its radiosensitizing effects (Figure 1). Thus, as we originally predicted, the key to understanding tumor cell radioresistance due to an abnormal activation of EGFR may lie in the signaling pathways downstream of this receptor.

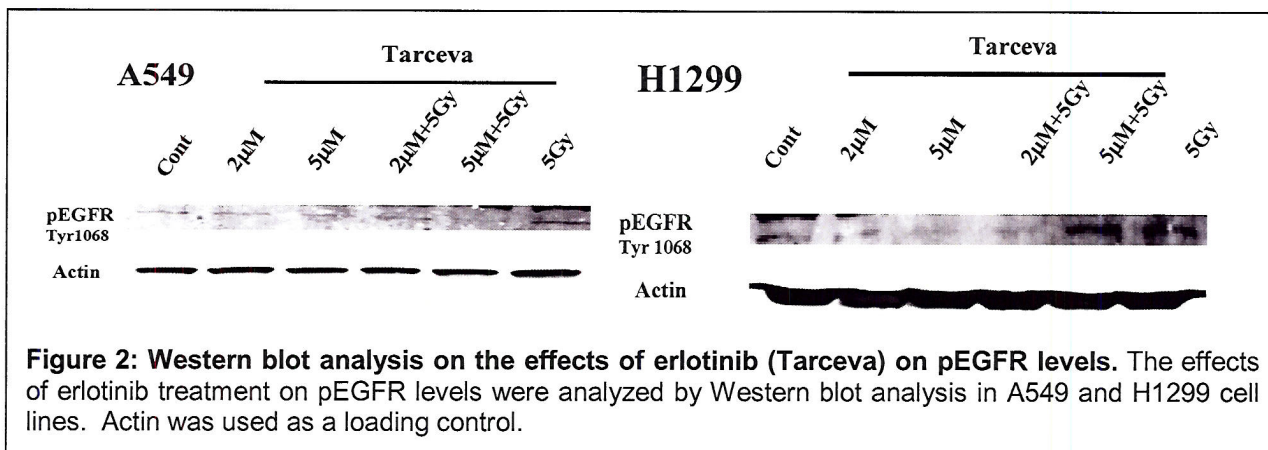


Figure 2: Western blot analysis on the effects of erlotinib (Tarceva) on pEGFR levels. The effects of erlotinib treatment on pEGFR levels were analyzed by Western blot analysis in A549 and H1299 cell lines. Actin was used as a loading control.

Aim 3 **To test the hypothesis that clinically useful inhibitors of EGFR signaling abrogate DNA repair capacity, restore apoptotic response and radiosensitize NSCLC cells.**

Update

As mentioned above, several clinically useful inhibitors of the EGFR pathway have already been developed and some are in clinical trials as single agents. Using the cell models developed in aim 2 above, we tested the ability of gefitinib and erlotinib to suppress DNA repair in NSCLC cells and normal human lung fibroblasts.

We have adopted two additional assays for the induction and repair of radiation-induced DNA double strand breaks (DSBs): the neutral comet assay and pulsed field gel electrophoresis (PFGE), to replace the host cell reactivation assay (HCR) used previously since these new assays are definitive for radiation-induced DSBs and superior to HCR. Briefly, in the neutral comet assay, the treated cells are imbedded in low melting point agarose and spread onto glass slides. Following cell lysis, the slides are subjected to electrophoresis for 20 min. The slides are then stained with SYBR green and the comet images are captured using a fluorescence microscope coupled to a CCD camera. Images are analyzed using CometScore software (TriTek, Sumerduck, VA), which yields the “Olive” tail moment as a relative measure of the DSBs. Cells were treated with either 2 μ M gefitinib or 5 μ M erlotinib for 24 hrs, irradiated with 20 Gy and analyzed using the neutral comet assay. The results are presented in Figures 3 and 4. As can be seen in Figure 3, the pretreatment with gefitinib inhibited the repair of DSBs (indicated as a return of the Olive moment to baseline levels) in both A549 and H1299 cells, especially over the first 2 hrs after irradiation while the initial level of radiation-induced DSBs in gefitinib (Iressa)-pretreated and sham (DMSO)-treated cells were identical at time 0.

As reported last year, both gefitinib and erlotinib produce a radioprotective effect on the normal human lung fibroblast line, CCD-16. The ability of these drugs to affect DSB repair in CCD-16 cells was assessed using the neutral comet assay. The results shown in Figure 4, indicate that both gefitinib and erlotinib enhance DSB repair in these normal cells which is consistent with the radioprotective effect previously described.

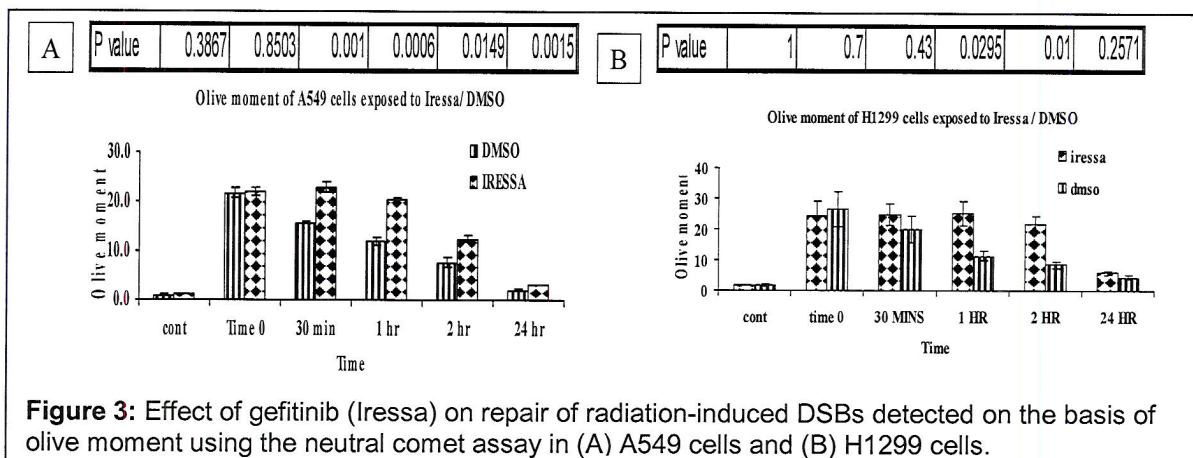


Figure 3: Effect of gefitinib (Iressa) on repair of radiation-induced DSBs detected on the basis of olive moment using the neutral comet assay in (A) A549 cells and (B) H1299 cells.

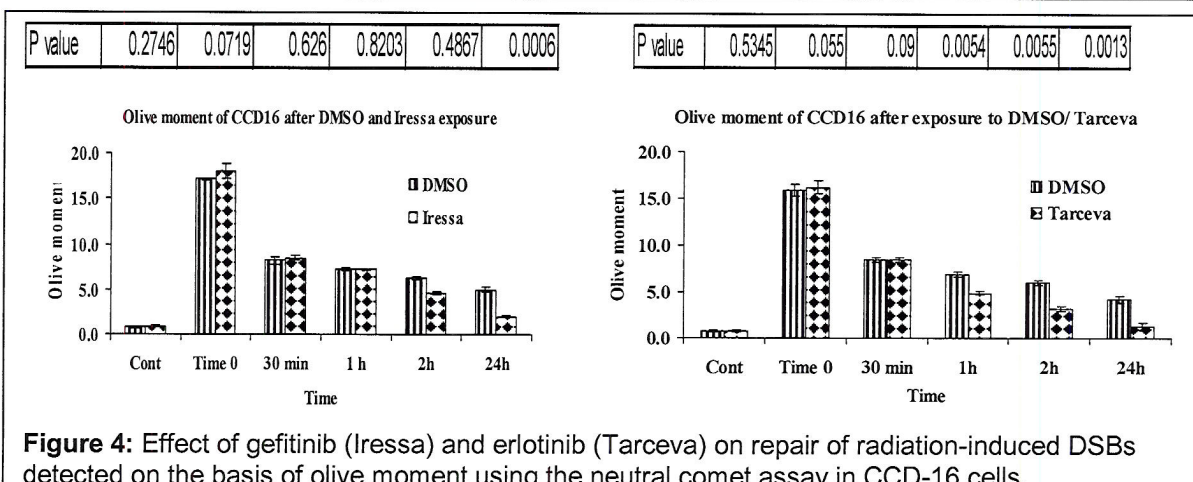


Figure 4: Effect of gefitinib (Iressa) and erlotinib (Tarceva) on repair of radiation-induced DSBs detected on the basis of olive moment using the neutral comet assay in CCD-16 cells.

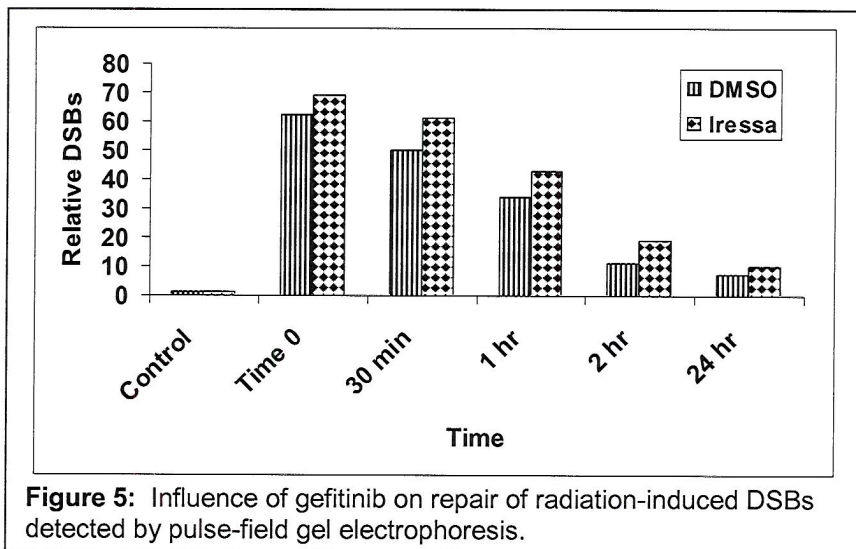


Figure 5: Influence of gefitinib on repair of radiation-induced DSBs detected by pulse-field gel electrophoresis.

To further confirm the findings, we have used PFGE technology to assess DSB repair following these same treatments. Our experimental protocol for this methodology has been published previously (Nishikawa et al., 2004). Briefly, after irradiation, cells are embedded in agarose plugs that are then subjected to digestion. The remaining DNA in the plugs is separated in an agarose

gel using a contour-clamped homogeneous electric field system at 1.5 V for 20 hr. The gel is then transferred to a nylon membrane for 3 days at room temperature. The membrane was then hybridized with a 32-P labeled human Alu probe for 18 hrs. The fraction of radioactivity released from the plug into the lane was determined using a phosphorimaging system. This fraction represents the relative number of DNA DSBs remaining after repair. Thus far, we have tested the ability of gefitinib to inhibit DSB repair in A549 cells. The results shown in Figure 5 indicate confirm that repair of radiation-induced DSBs is inhibited by gefitinib as seen previously in the Comet assay (Figure 3).

Aim 4 To test the hypothesis that targeting both EGFR and its downstream signaling pathways will have at least an additive radiosensitizing effect on NSCLC.

Update

We had previously begun to evaluate molecularly targeted agents that are designed to specifically target the Ras-Raf-Mek-ERK pathway downstream of EGFR. Testing of one such agent, sorafenib (BAY-43-9006), that targets Raf-kinase, has already been initiated and its radiosensitization of H1299 cells was reported last year. We have extended this analysis to other cell lines and began to examine the effect of sorafenib on the downstream signaling pathways of EGFR. Preliminary immunoblot analysis indicated that sorafenib suppresses the expression of activated vascular endothelial growth factor and platelet derived growth factor in H1299 cells (data not shown). We also confirmed a report in the literature that sorafenib suppressed the expression of the anti-apoptotic protein Mcl-1 (Rahmani et al., 2005).

Aim 5 To test whether the strategies developed in Specific Aims 2-4 have efficacy in a xenograft tumor model.

Update

This animal study was proposed for years 3 and 4. We prepared and submitted the animal protocol for review by our Animal Care and Use Committee (IACUC) which was approved on February 20, 2006. The approval letter and the animal protocol are attached in the Appendix B - Project 1. The experiments will commence this year.

Key Research Accomplishments

- Revised clinical protocol of erlotinib plus chemoradiation, informed consent, and submitted to the DoD and IRB. The IND application has also been revised and submitted. We are awaiting final approvals by the DoD, IRB, and FDA.
- Extended our model systems to include an additional NSCLC cell line, H460, and showed that it is radiosensitized by erlotinib.
- Demonstrated that erlotinib suppresses the radiation-induced activation of the EGFR.
- Demonstrated using two new assays, the neutral comet assay and pulsed field gel electrophoresis, that gefitinib suppresses the repair of radiation-induced DNA double strand breaks.
- Demonstrated that sorafenib suppresses activation of vascular endothelial growth factor receptor and platelet derived growth factor receptor in NSCLC cells.
- The animal protocol for xenograft model was prepared and approved.

Reportable Outcomes

Abstracts

1. Colin Brooks, Toshimistu Tanaka, Anupama Munshi, Jenny Liu, Nathan Wang, Marvette Hobbs, Raymond Meyn. Targeting EGFR signaling to enhance response of non-small lung cancer cells to radiation. The 98th AACR Annual Meeting, abstract: #4154, 2007.

Conclusions

Using additional cell lines, we have confirmed that clinically achievable concentrations of gefitinib and erlotinib sensitize NSCLC cell lines to radiation. This apparently small sensitization in cell lines with a single dose and exposure is expected to translate into significant clinical benefit. Using 4 independent assays, we have shown that gefitinib radiosensitizes NSCLC cells by suppressing the cellular capacity for repairing radiation-induced DSBs.

Project 2: Molecular Imaging of EGFR Expression and Activity in Targeting Therapy of Lung Cancer

(PI and co-PI: Juri Gelovani, M.D.; Roy Herbst, M.D., Ph.D.)

In the first funding year of IMPACT, our research focused on Specific Aims 1 and 2 as planned. During the second year, our work has focused on Aims 2 and 3 of this Project.

Aim 1 **To synthesize novel pharmacokinetically optimized ^{124}I and ^{18}F -labeled IPQA derivatives for PET imaging of EGFR kinase activity and conduct *in vitro* radiotracer accumulation studies in tumor cells expressing different levels of EGFR activity.**

No additional progress was made in the second year on this Aim.

Aim 2 **To assess the biodistribution (PK/PD) and tumor targeting by novel ^{124}I and ^{18}F -labeled EGFR kinase-specific IPQA derivatives using PET imaging in orthotopic mouse models of lung cancer and compare *in vivo* radiotracer uptake/retention with phospho-EGFR levels *in situ*.**

As reported last year, we identified 3-iodo-4-(phenylamino)quinazoline-6-acrylamide (IPQA) derivatives (JGAP-5 and JGAP-11) with improved water solubility. In the second year, our study focused on ^{131}I - and ^{124}I -JGAP5, which was synthesized by the IMPACT Imaging Core (Figure 1). It is noteworthy that the compound JGAP-5 was selected because it is highly soluble in

water and was expected to have less hepatobiliary clearance and, as a result, have a longer half-time of plasma circulation.

Initially, the ^{131}I -JGAP5 was assessed *in vitro* for accumulation and washout kinetics in human NSCLC cells with different EGFR signaling profiles (H441, H3255, PC14, H1975) (Figure 2A). The accumulation of JGAP5 in the NSCLC cells was almost similar to that previously observed with radio-iodinated mIPQA. Namely, the most progressive accumulation and the slowest washout were observed in H441 cells that overexpress TGF α and EGFR (positive autocrine loop) and in H3255 cells expressing dominant active mutant EGFR tyrosine kinase. In contrast, no progressive accumulation and almost complete washout (down to an equilibrium level of 1) was observed in PC14 cells with EGFR-independent growth (low EGFR) and in H1975 cells with dual mutations in EGFR tyrosine kinase domain that precludes JGAP5 from binding and covalent adduct formation. Further studies demonstrated that the accumulation of ^{131}I -JGAP5 at 60 min in these cell lines was inhibited by pre-treatment with EGFR TKI, gefitinib, in a dose-dependent manner (Figure 2B). The latter was especially dramatic in H3255 cells expressing dominant active mutant EGFR tyrosine kinase. Therefore, these *in vitro* radiotracer uptake and washout studies have demonstrated the highest uptake and retention of JGAP5 in cells with increased EGFR tyrosine kinase activity and high sensitivity to therapy with gefitinib.



Figure 1. Structure of the novel lead candidate JGAP5 with improved water solubility.

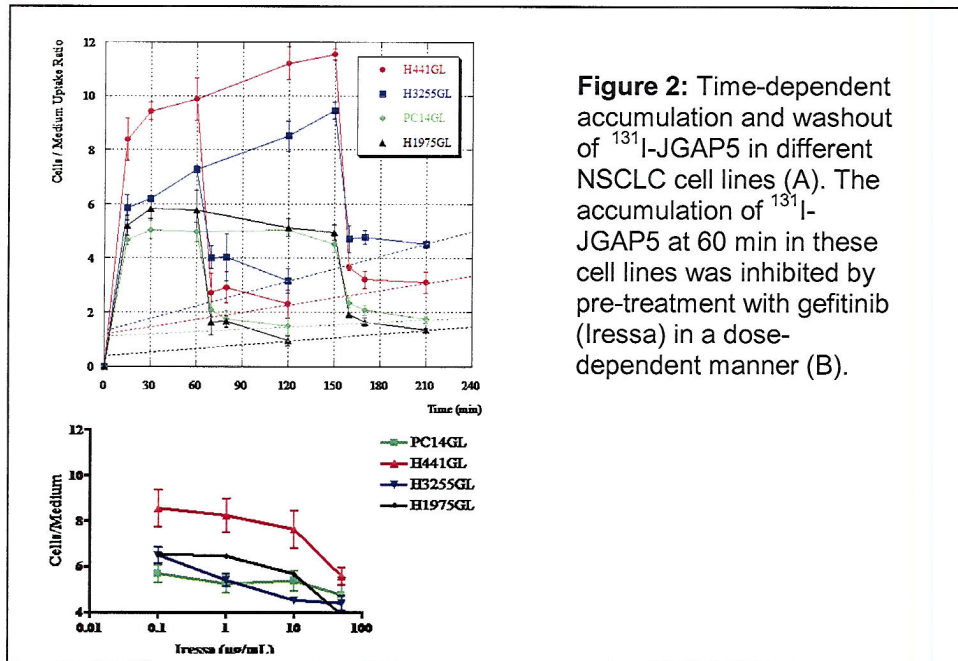


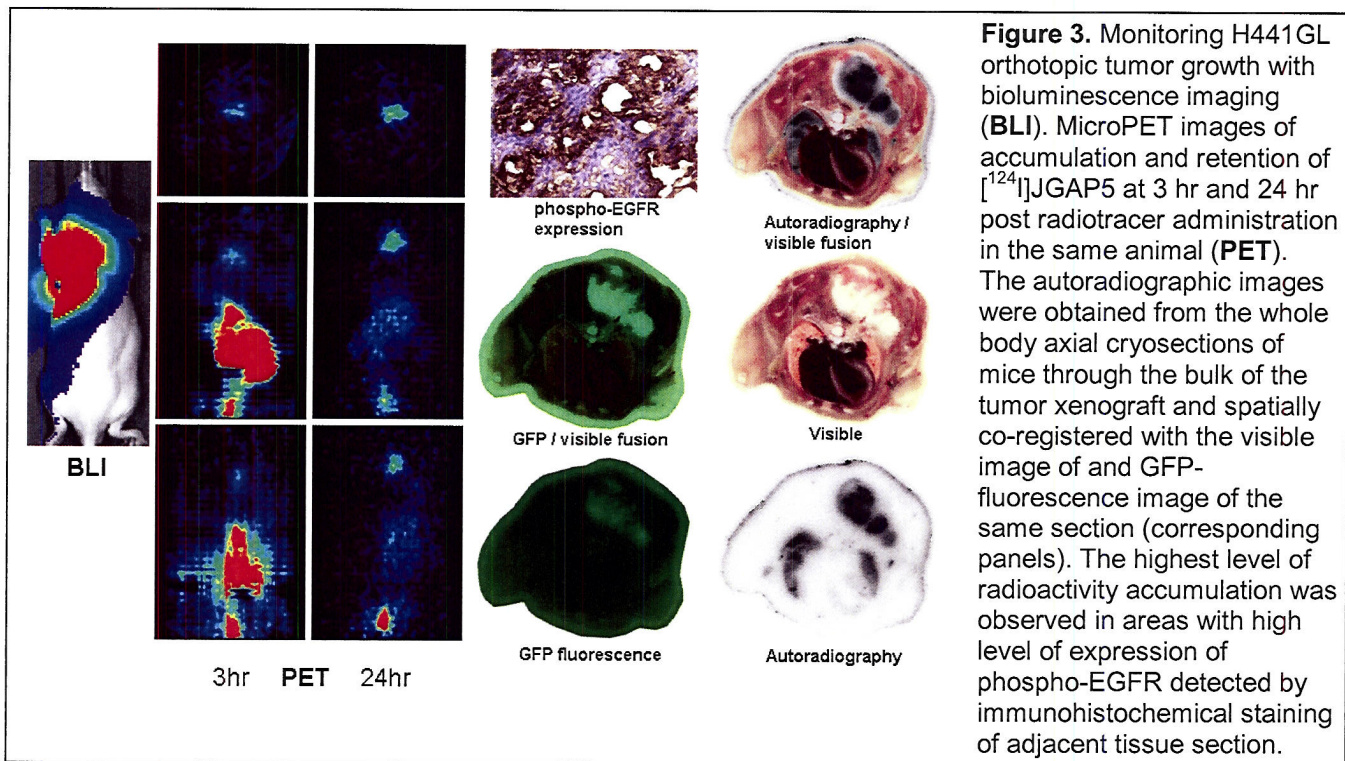
Figure 2: Time-dependent accumulation and washout of ^{131}I -JGAP5 in different NSCLC cell lines (A). The accumulation of ^{131}I -JGAP5 at 60 min in these cell lines was inhibited by pre-treatment with gefitinib (Iressa) in a dose-dependent manner (B).

Aim 3 Using selected ^{124}I or ^{18}F -labeled IPQA derivative, to conduct pre-clinical studies in animals with orthotopic models of lung cancer xenografts with different levels of EGFR expression/activity, and to assess the value of PET imaging as the inclusion criterion for therapy by EGFR inhibitors, as well as for monitoring the efficacy of treatment with EGFR-targeted drugs.

As part of Aim 3, we have initiated *in vivo* PET imaging studies with $[^{124}\text{I}]$ JGAP5 in mice bearing orthotopic xenografts of four human NSCLC cells that express TGF α at different levels and

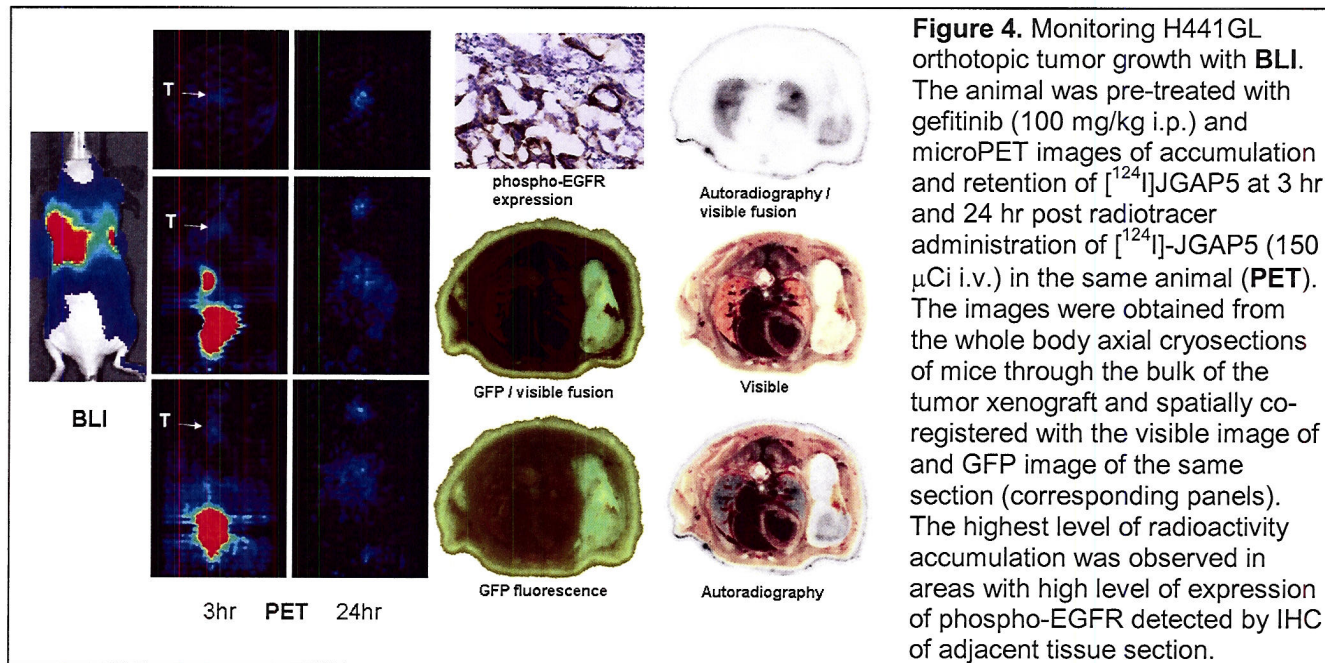
express either the wild-type or mutant EGFR tyrosine kinases (H441, H3255, PC14, H1975). As reported previously, these cell lines have been retrovirally transduced with enhanced green fluorescent protein (eGFP) – *Firefly luciferase* fusion reporter gene (GL) to facilitate non-invasive imaging in orthotopic NSCLC xenografts in mice. The GL reporter gene allows for fluorescence microscopic and FACS analysis of GL-expressing cells *in vitro* and bioluminescence imaging (BLI) of GL-expressing tumor xenografts in mice *in vivo*; tumor growth is monitored by measuring the total light output from the thorax of mice implanted into their lungs with different NSCLC cells (N = 6 mice per tumor type).

We found that the tumor growth rate was fastest in H441 xenografts, which generated a very strong BLI signal in two weeks post implantation (Figure 3; BLI panel). The H441 tumors accumulated significantly higher levels of [¹²⁴I]JGAP5, 7.42 ± 0.53 %ID/g (Figure 3; PET and autoradiography/visible panels) as compared to [¹²⁴I]mIPQA 4.30 ± 2.19 (p < 0.05) in our studies performed during previous reporting period. The highest levels of [¹²⁴I]JGAP5 accumulation were observed in tumor areas expressing high levels of phospho-EGFR (Figure 3; phospho-EGFR expression panel). The accumulation of [¹²⁴I]JGAP5 was also observed in hair follicles in the skin in lungs and bronchial epithelium, which serve as an “internal control tissues” (Figure 3; autoradiography/visible panel). In general, PET imaging of [¹²⁴I]-JGAP5 performed at 3 hours after intravenous (i.v.) administration of this radiotracer demonstrated substantial accumulation of this radiotracer in H441 and H3255 tumors. In contrast, significantly lower levels of [¹²⁴I]-JGAP5 accumulation were observed in PC14 and H1975 tumors (data not shown).



We also found that co-registration of autoradiographic images with corresponding anatomical images of the same sections, which were used to produce autoradiograms, provided high resolution images that explain the pattern of [¹²⁴I]-JGAP5 distribution at 3 hours post i.v. administration. Such pattern could not be visualized and analyzed by microPET, because it has a much lower resolution and sensitivity than autoradiography. Highly specific accumulation of [¹²⁴I]-JGAP5 was observed in hair follicles, subcutaneous fat layer, and in bronchi, which is consistent with high activity of EGFR in these tissues from the orthotopic H441 tumor mice

(Figure 4). The magnitude of accumulation of [¹²⁴I]-JGAP5 in these structures was also inhibited but in a lesser degree than in the H441 tumor tissue.



Key Research Accomplishments

- Demonstrated that the xenograft human NSCLC tumors accumulated significantly higher levels of [¹²⁴I]JGAP5 compared to [¹²⁴I]mIPQA measured by PET imaging studies, although the uptake and retention of JGAP5 *in vitro* in the human NSCLC cell lines with increased EGFR tyrosine kinase activity and high sensitivity to therapy with gefitinib was almost similar to those of [¹²⁴I]mIPQA. This result was found to be due to the the differential hepatobiliary clearance and water solubility properties of the compounds.
- Demonstrated that the accumulation of [¹²⁴I]JGAP5 was significantly decreased by pre-treatment of the mice with gefitinib as compared to non-treated animals, and the response was more sensitive than with [¹²⁴I]-mIPQA.
- Demonstrated the feasibility of PET imaging with [¹²⁴I]-JGAP5 for prediction of tumor responsiveness to therapy with EGFR TKIs.
- Observed the accumulation of [¹²⁴I]-JGAP5 in normal tissue structures expressing highly active EGFRs (i.e., hair follicle cells) that are currently used as surrogate biomarkers of EGFR activity/inhibition, providing additional proof of the approach to imaging EGFR tyrosine kinase activity with [¹²⁴I]-JGAP5.

Reportable Outcomes

Abstracts

- Nishii R, Pal A, Soghomonyan S, Balatoni J, Mushkudiani I, Yeh HH, Mukhopadhyay U, Volgin A, Shavrin A, Maxwell D, Tong W, Alauddin M, Bornmann W, Gelovani J. Molecular Imaging of Different EGFR Kinase Mutant NSCLC Carcinomas with [¹²⁴I]-mIPQA and [¹²⁴I]-JGAP5 PET for Prediction of Responsiveness to EGFR Kinase Inhibitors. *Proceedings of the 4th Annual Meeting of the Society of Molecular Imaging*, Hawaii. September 1-4, 2006.
- Nishii R, Mukhopadhyay U, Soghomonyan S, Volgin A, Alauddin MM, Gelovani J. PET with ¹⁸F-FDG and ¹⁸F-FMAU in the assessment of early response to EGFR-targeted therapy in mice bearing human NSCLC xenografts with different EGFR mutations. *Proceedings of the 53rd Annual Meeting of the Society for Nuclear Medicine*, CA. June 3-7, 2007.

Conclusions

Based on the progress at this point, we conclude that imaging with pharmacokinetically-optimized more water-soluble [¹²⁴I]-JGAP5 (as compared to [¹²⁴I]-mIPQA derivatives) should allow for identification of tumors with increased EGFR signaling. However, this series of compounds still remains suboptimal for the clinical use and we believe that a further decrease in lipophilicity of the series of IPQA-based compounds will result in additional improvement of AUC and the magnitude of the radiotracer accumulation in tumors vs lung.

Project 3: Targeted Peptide-based Systemic Delivery of Therapeutic and Imaging Agents to Lung Cancer

(PI and co-PI: Renata Pasqualini, Ph.D., Wadih Arap, M.D., Ph.D.)

The studies outlined in this proposal focus on the use of peptide sequences with selective lung tumor targeting properties. We will seek to validate these probes as delivery vehicles in drug and gene targeting approaches. This approach directly selects *in vivo* for circulating probes capable of preferential homing into tumors. The strategy will be to combine homing peptides in the context of phage as gene therapy vectors. Given that many of our peptides also target angiogenic vasculature in addition to tumor cells, these studies are likely to enhance the effectiveness of therapeutic apoptosis induction and imaging technology.

Aim 1 To select peptides targeting primary and metastatic tumors in lung cancer patients.

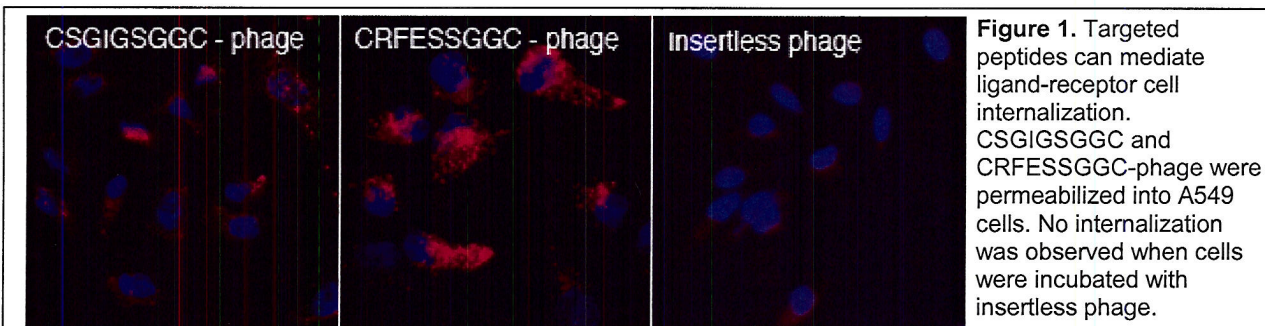
Last year, we showed that tumor cells could be grouped by profiles of their phage display-derived peptide ligands directed to differentially expressed cell surface receptors, and reported the identification and validation of peptide ligands recognizing lung cancer-associated molecular targets such as EGFR and possibly other tyrosine kinases receptors of Ephrin or FGF receptor families. In this grant year, thus, our focus was shifted to the Aim 2 as described below.

Aim 2 To validate receptors for targeting human lung cancer.

Update

As reported last year, we identified the lung cancer-targeting receptor EphA5 and validated ephrin-mimic peptides (CSGIGSGGC and CRFESSGGC) in lung cancer.

This year, we further evaluated whether targeting the EphA5 receptor by the ephrin-mimic peptides would mediate cell internalization. We used A549 line as a representative human lung cancer-derived cells expressing the EphA5 receptor on the cell surface. Each phage clone carrying either the peptides or control insertless phage was incubated with cells for 4h at 37°C. Both CSGIGSGGC and CRFESSGGC – phage were internalized into A549 cells while only background fluorescence was obtained when non-targeted control phage were used (Figure 1).



We have also demonstrated that the activation of the EphA5 receptor by the peptides CSGIGSGGC and CRFESSGGC lead to proliferation and/or survival of lung cancer cells. In the absence of sera, the peptides increased the proliferation of lung cancer cells by 4-fold (Figure 2). This effect was confirmed in two different human cell lines, which express the EphA5 receptor.

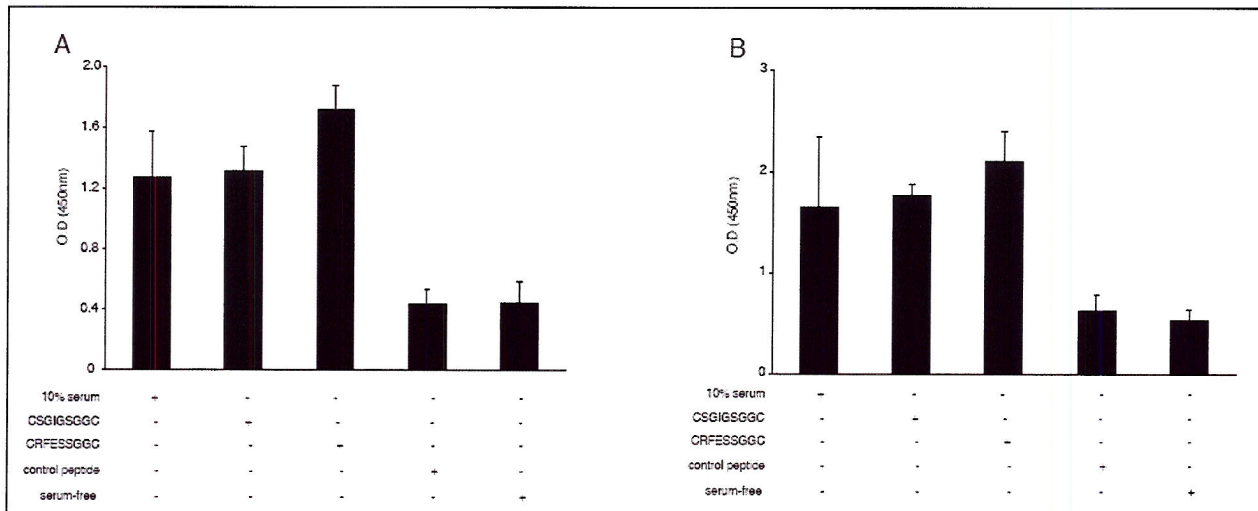


Figure 2. Biological effects of the peptides CSGIGSGGC and CRFESSGGC on lung cancer cells. Promotion of cell survival and proliferative response of starved lung cancer cells to the ephrin mimic peptides, control peptide and complete culture medium. (A) A549, (B) H460 cells. Concentrations of peptide were optimized previously. Values in the Y-axis correspond to the number of viable cells under each experimental condition evaluated after a 72h incubation period. Data bars represent the mean and corresponding standard error of the mean.

As described in the original grant proposal, we have identified circulating probes targeting the IL11R and GRP78 receptors and evaluated them as a “beacon” for the delivery of anti-cancer drugs (Arap et al; Zurita et al, 2004). Our preliminary data showed that these proapoptotic peptides (Arap et al, 2004; Zurita et al, 2004) targeted to the receptors specifically induce apoptosis in lung cancer cell lines. We are confirming these results and will present the data in next year’s report.

In collaboration with Dr. Wistuba, we examined the expression of GRP78, IL11R and EphA5 in lung cancer TMA containing 301 NSCLCs (192 adenocarcinomas and 109 squamous cell carcinomas) and 26 SCLCs with annotated clinical data. We performed analysis of immunostaining using microscopic evaluation by 2 independent observers, and consensus data were used for further analysis. Overall, high levels of GRP78, IL11R and EphA5 expression were detected in lung cancer tumor specimens. Significant differences in the expression of these markers were detected comparing both tumor types: a) GRP78 expression in NSCLCs histologies, adenocarcinoma and squamous cell carcinoma, was significantly higher in the cytoplasm and membrane of tumor cells compared with SCLC; b) IL11R showed higher levels of cytoplasmic expression but lower levels of membrane expression in NSCLCs; c) EphA5 expression was higher in NSCLC tumor cells compared with SCLC.

For NSCLCs adenocarcinoma and squamous cell carcinoma histologies, a detailed analysis comparing GRP78, IL11R and EphA5 expression in tumor cells with patients’ clinicopathologic features, including tumor histology, age, gender, smoking history, pathological TNM stage, disease free and overall survival, was performed. Significant differences in the expression of markers were detected comparing both NSCLC histologies with adenocarcinomas

demonstrating higher levels of cytoplasmic GRP78 ($P = 0.0003$) and cytoplasmic IL11R ($P < 0.0001$). In contrast, squamous cell carcinomas showed significantly higher expression for membrane GRP78 ($P = 0.003$) and EphA5 ($P = 0.002$). Only IL11R demonstrated correlation with smoking status, with tumors from ever smokers having higher levels ($P = 0.005$) of cytoplasmic IL11R than never smokers. No correlation between marker expression and disease free and overall survivals was detected. For more detailed data of the IHC analysis, please refer to Aim 4 of Project 3 in the Molecular Pathology Core of this report.

These findings suggest that these molecular receptor signatures within human tumors are suitable for targeted delivery of drugs.

Aim 3 To design tools for molecular imaging of lung tumors.

This year, we have assessed the expression of alpha v integrins in lung tumor cells and have established that the imaging vector targeting the integrin receptors we developed (Hajitou et al, Cell 2006) would be a suitable entity for imaging lung tumors *in vivo*. We are in the process of evaluating the efficiency of targeted delivery of luciferase and thymidine kinase in lung cancer animal models, in collaboration of Dr. Juri Gelovani, the Director of the IMPACT Molecular Imaging Core. Any definitive results will be presented in the next report.

Other promising receptor-ligand systems will be also leveraged for targeted imaging, such as vectors targeting EphA5, GRP78, and the IL11R, already validated in patient derived samples as described above and in the Molecular Pathology Core report.

Key Research Accomplishments

- Found that EphA5 mediated internalization of the ephrin-mimic peptides (CSGIGSGGC and CRFESSGGC).
- Found that CSGIGSGGC and CRFESSGGC increased the proliferation and/or survival of lung cancer cells expressing the EphA5 receptor.
- Demonstrated that overall, high levels of GRP78, IL11R and EphA5 expression were detected in lung cancer tumor specimens.
- Found that NSCLC adenocarcinomas had higher levels of cytoplasmic GRP78 ($P = 0.0003$) and cytoplasmic IL11R ($P < 0.0001$) than NSCLC squamous cell carcinoma. In contrast, squamous cell carcinomas showed significantly higher expression for membrane GRP78 ($P = 0.003$) and EphA5 ($P = 0.002$).
- Demonstrated that only IL11R expression had correlation with smoking status; Tumors from patients that ever smoked had higher levels of cytoplasmic IL11R than those from never smokers ($P = 0.005$). No correlation between the expression of markers and disease free and overall survivals was detected.

Reportable Outcomes

Manuscripts published in peer-reviewed Journals

- Souza GR, Levin CS, Hajitou, A, Pasqualini R, Arap W, and Miller JH. "In Vivo Detection of Gold-imidazole Self-assembly Complexes: NIR-SERS Signal Reporters", *Anal Chem* 78: 6232-7, 2006.
- Trepel M, Arap W, Pasqualini R. Selection, isolation, and identification of targeting peptides for ligand-directed gene delivery. *In: Gene Transfer: A Laboratory Manual*, New York: Cold Spring Harbor Laboratory Press. Ch. 30:359-69, 2007.

Project-Generated Resources

We are also generating an extensive database for targeting ligands and vascular receptors identified in our laboratory. This database is likely to be very useful as it can be integrated with

the system that is in place under the IMPACT Program to correlate clinical information and responses to therapy with the expression of selective molecular targets.

Conclusions and Future Plans

EphA5 protein overexpression in lung cancer cells in light of candidate ephrin mimics (GGS peptides) targeting these cells provides original evidence for EphA5 being a lung cancer marker and has potential functional implications.

Next, we will test the circulating peptides for IL11R and GRP78 *in vivo*, in lung cancer animal models, and evaluate their therapeutic properties. The most promising receptor-ligand systems will be developed into INDs after *in vivo* evaluation of anti-cancer activity.

We also plan to image the effects of other targeted peptides delivered to angiogenic vasculature using sophisticated vascular imaging technology. These studies should be highly informative and will shed light into the mechanistic aspects of the anti-tumor and anti-angiogenic activity in lung cancer.

Project 4: Inhibition of bFGF Signaling for Lung Cancer Therapy

(PI: Reuben Lotan, Ph.D.)

The survival of lung cancer patients is poor because this cancer is diagnosed at advanced stages. Therefore, improvements in early detection through the identification of molecular markers for diagnosis and for intervention combined with targeted chemoprevention are urgently needed. The molecular events involved in lung cancer pathogenesis are still being unraveled. Growth and angiogenesis promoting signaling pathways are amplified in lung cancer. Among them, the basic fibroblast growth factor (bFGF) and its trans-membrane tyrosine kinase receptors (FGFRs) have been demonstrated in NSCLC and associated with lung cancer development.

We hypothesize that bFGF triggers signaling pathways that contribute to malignant progression of lung cancers by stimulating tumor cell and endothelial cell proliferation and survival and augmenting angiogenesis. Therefore, agents that intervene in this pathway may be useful for lung cancer therapy either alone or in combination with cytotoxic agents. We will address the following specific aims in order to understand the mechanism(s) underlying the *in vitro* and *in vivo* effects of bFGF on lung cancer and endothelial cells and the ability of bFGF inhibitors to suppress the growth of NSCLC *in vitro* and *in vivo*.

Aim 1 Determine the effects of bFGF on *in vitro* growth, survival, motility, invasion and angiogenesis of NSCLC cells and endothelial cells.

Last year, we reported that bFGF stimulated the growth of immortalized mouse endothelial cells, which was suppressed by the bFGF inhibitor 5,10,15,20-tetrakis(methyl-4-pyridyl)-21H,23H-porphine-tetra-p-tosylate salt (TMPP).

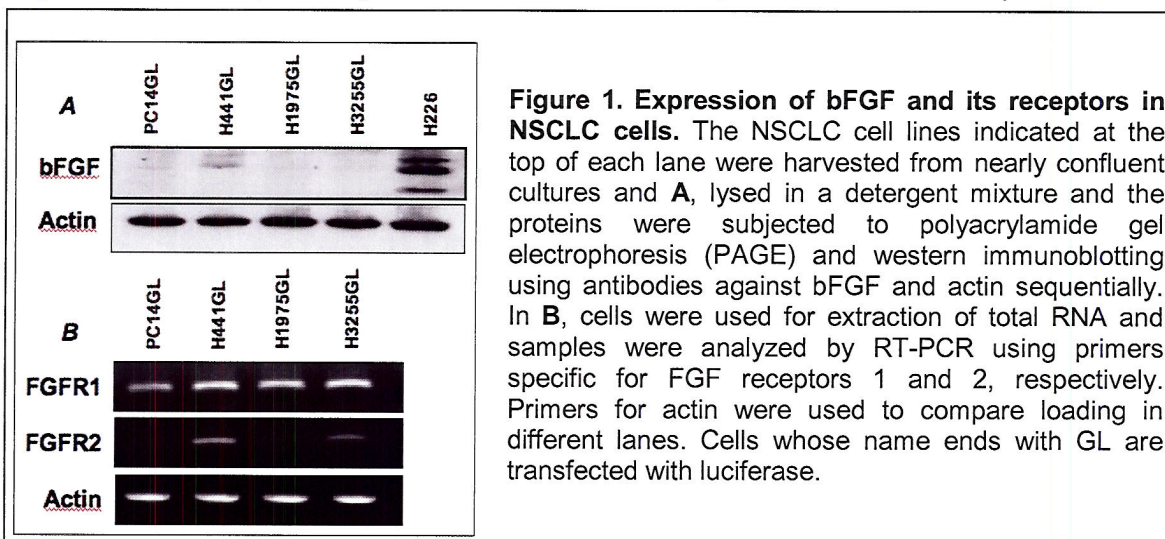
Update

We received NSCLC cell lines expressing the luciferase gene from Drs. Juri Gelovani and Andrei Volgin of the Imaging Core and began testing the effect of bFGF in these lines. The cell lines were transduced by viral supernatant collected from 293GPG retroviral packaging cell line, capable of producing high titers of recombinant Moloney murine leukemia virus particles that have incorporated the vesicular stomatitis virus G (VSV-G) protein transfected with SFGnesGL.

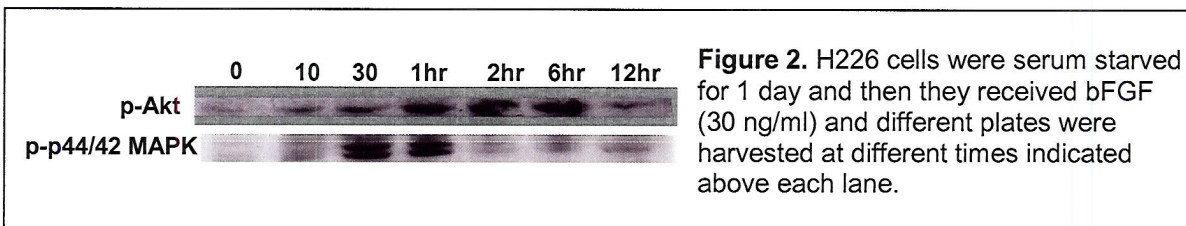
SFGnesGL is MoMLV-based retroviral double reporter construct, which represents an in-tandem fusion of the eGFP and firefly luciferase cDNAs. All cell lines underwent two rounds of sorting using BD FACS ARIA instrument. Percentages of positive cells were more than 96% as determined by FACS analysis.

However, we found that these cell lines had mycoplasma contamination and have applied various approaches to clean them from this infection including using specific antibiotics. The cleaned cells were again tested in Dr. Gelovani's laboratory for tumorigenicity in nude mice and after confirming that they have retained their tumorigenic potential, we then started our experiments using these cells.

First, we analyzed the expression of bFGF by western blotting and of FGF receptors 1 and 2 by RT-PCR in these lines. The results shown in Figure 1 indicated that the cell line H226 expressed high levels of bFGF, whereas the cell line H441GL expressed a low level and the other cell lines expressed very low or no bFGF. The analysis of FGF receptors demonstrated that all cell lines expressed FGFR-1, but only H441GL and H3255GL expressed FGFR-2 receptor.



Treatment of NSCLC cells with bFGF after serum starvation resulted in rapid and transient increase in phosphorylated ERK (p-p42/44) MAPK and Akt indicating that bFGF was mitogenic and enhanced survival pathway mediated by Akt (Figure 2).



We then examined the effects of bFGF on the growth of some of these cell lines. Figures 3 and 4 show representative data obtained in these experiments. The results in Figure 3 demonstrated that after 24 hr treatment with bFGF, the H226 and H358 cell lines were more sensitive than H441 to FGF and that PC14PE6 cells were almost non-responsive to bFGF.

We also found that extension of the treatment from the 1-day shown in Figure 3 to up to 5 days does not improve the overall growth stimulation (Figure 4A), and similar results for day 4 were obtained using a new method (Cytoquant, Diagnostica Stago, Asniers, France) relative to the

sulforhodamine B (SRB) method (Figure 4B).

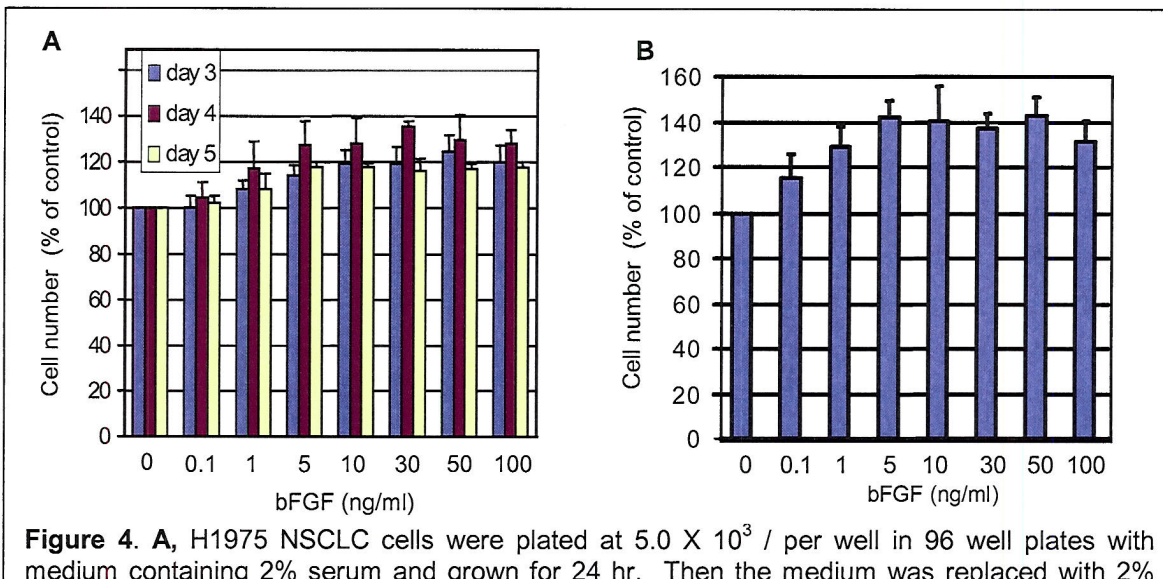
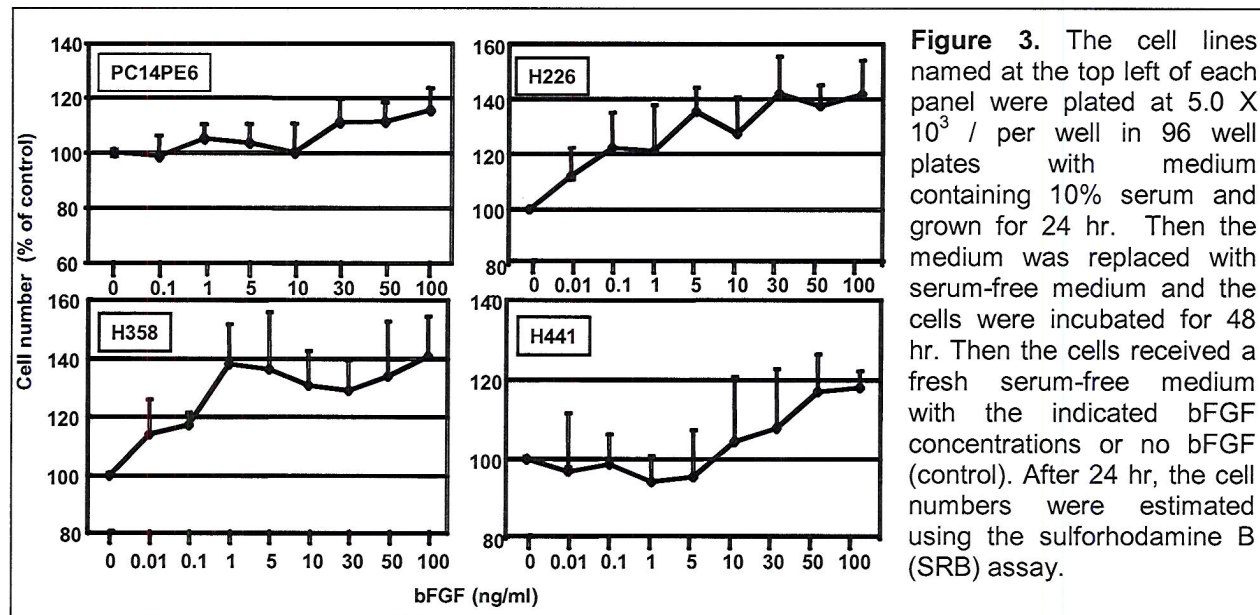


Figure 4. **A**, H1975 NSCLC cells were plated at 5.0×10^3 / per well in 96 well plates with medium containing 2% serum and grown for 24 hr. Then the medium was replaced with 2% serum containing medium and the cells were incubated with the indicated doses of bFGF or no bFGF for 3, 4, or 5 days. Medium with fresh bFGF was added on day 3. Cell number was estimated using the SRB assay. **B**, H1975 NSCLC cells were plated at 5.0×10^3 / per well in 96 well plates with medium containing 2% serum and grown for 24 hr. Then the medium was replaced with 2% serum containing medium and the cells were incubated with the indicated doses of bFGF or no bFGF for 4 days at which time their number was estimated using the Cyquant cell proliferation assay.

Aim 2 Evaluate the relative potency of several inhibitors of bFGF binding to receptor (i.e., TMPP and analogs) in inhibiting effects of bFGF detected in Specific Aim 1 and evaluate the effects of these inhibitors in combination with paclitaxel on *in vitro* growth and survival of tumor cells.

We did not work on this aim during the report period.

Aim 3 Evaluate anti-tumor activity (growth inhibition, apoptosis, suppression of angiogenesis) of the most effective inhibitor identified in Specific Aim 2 when used alone and in combination with paclitaxel in an orthotopic lung cancer model using luciferase-expressing NSCLC cells for *in vivo* bioluminescence imaging of tumor growth and response to treatment.

We did not work on this aim during the report period.

Aim 4 To investigate the expression of bFGF signaling components (bFGF, FGFR-1, FGFR-2, heparan sulfate, syndecan-1, and FGFR-3) by IHC staining of tissue microarrays (TMAs), and correlate the expression of bFGF/bFGFRs between tumor and non-malignant epithelial cells with angiogenesis.

As indicated in our recommendations in the previous annual report, we added Aim 4 to study additional components of bFGF signaling *in vivo*. In the period of 2005, we examined bFGF and receptors FGFR-1 and -2 expression in 71 normal bronchial epithelia, 128 bronchial hyperplasias, 23 squamous metaplasias, 78 squamous dysplasias, and 72 atypical adenomatous hyperplasias (AAH) using IHC. A semi-quantitative IHC analysis of cytoplasmic and nuclear expression was performed. We have concluded that bFGF signaling pathway may play an important role in NSCLC pathogenesis. Our analysis identified different expression patterns of bFGF and receptors in cytoplasm and nuclear cell compartments in normal and premalignant lung tissues (Behrens et al., 2006 AACR).

Update

During the last year (2006), in collaboration with the Pathology Core, the expression analysis of bFGF and receptors FGFR-1 and -2, and syndecan-1 has been performed in 321 NSCLC specimens placed in TMAs (Figure 5). This analysis has been added to the 372 epithelial specimens (including normal bronchial epithelium and lung cancer preneoplastic lesions)

examined during 2005. We increased the number of normal bronchial epithelium (N = 146) and bronchial hyperplasias (N = 174) specimens examined, and added Syndecan-1 IHC expression analysis to all epithelial samples. This new set of data is currently being analyzed.

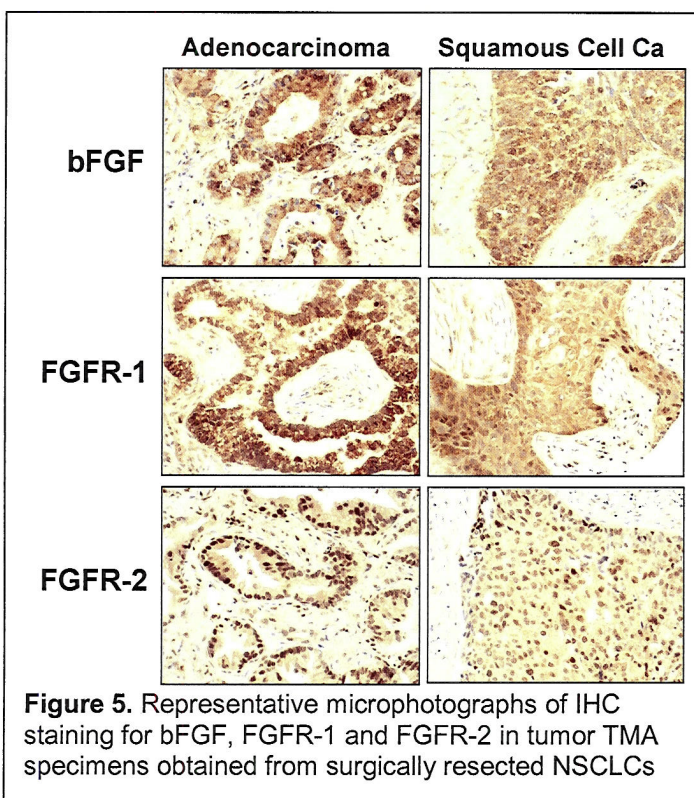


Figure 5. Representative microphotographs of IHC staining for bFGF, FGFR-1 and FGFR-2 in tumor TMA specimens obtained from surgically resected NSCLCs

In total, we performed semi-quantitative expression analysis of 196 lung adenocarcinomas (ADCA) and 125 SCC using formalin-fixed specimens in tissue microarrays using IHC. bFGF, FGFR-1, FGFR-2 were examined in tumor cells and SDC-1 in tumor (SDC-1T) and stromal (SDC-1S) cells.

Overall, we found high levels of expression of all markers in NSCLC. SCC expressed significantly higher levels of nuclear bFGF ($P = 0.01$), cytoplasmic FGFR-2 ($P = 0.006$), SDC-1T ($P < 0.0001$) and SDC-1S ($P < 0.0001$). ADCA expressed higher levels

($P < 0.0001$). ADCA expressed higher levels of nuclear FGFR-1 ($P < 0.0001$) and FGFR-2 ($P = 0.003$). Patient's clinical-pathologic data when correlated with expression of the markers showed different patterns of correlations in ADCA and SCC, especially for gender and smoking. In univariate analysis, in ADCA, females demonstrated higher levels of nuclear bFGF ($P = 0.03$), nuclear FGFR-1 ($P = 0.019$) and SDC-1T ($P = 0.03$) than males, while in SCC males had higher SDC-1T ($P = 0.02$). Among ADCAs, smokers demonstrated higher levels of cytoplasmic FGFR-1 ($P = 0.04$) and SDC-1S ($P = 0.02$) and lower levels of nuclear FGFR-1 ($P = 0.002$) and FGFR-2 ($P = 0.04$). Among SCCs, smokers demonstrated higher nuclear FGFR-2 ($P = 0.02$). A complex pattern of marker correlations was detected: ADCA and SCC showed correlation between nucleus and cytoplasm for FGFR-2 ($P = 0.0005$) and between cytoplasms of bFGF and FGFR-1 ($P < 0.03$) and FGFR-1 and FGFR-2 ($P < 0.0001$); only in ADCAs nuclear FGFR-1 correlated with nuclear bFGF and FGFR-2 ($P < 0.0001$ and 0.0003, respectively), and SDC-1T correlated with nuclear bFGF, FGFR-1 and FGFR-2 ($P = 0.04, 0.006$ and 0.02, respectively); in SCC, SDC-1T correlated with cytoplasmic bFGF and FGFR-2 ($P = 0.002$ and 0.02, respectively) and nuclear FGFR-1 ($P = 0.05$). SDC-1S only showed correlation with SDC-1T in SCC ($P = 0.0002$).

Key research accomplishments

- Established that some luciferase transfected NSCLC cell lines are sensitive and others are resistant to bFGF.
- Performed the first exhaustive analysis of the different bFGF signaling components (the growth factor, its receptors and the associated accessory molecule syndecan) in premalignant and malignant lung tissues using TMAs.

Reportable outcomes

Abstracts

- Behrens C, Lin H, Lee J, Hong WK, Wistuba II, Lotan R. Differential immunohistochemical expression patterns of fibroblast growth factor-2, receptors 1 and 2, and syndecan-1 in squamous cell carcinoma and adenocarcinoma of the lung. The 98th AACR Annual Meeting, abstract #: 6412, 2007.

Conclusions

Our findings of frequent activation and differential expression patterns of the bFGF signaling components in the two major forms of NSCLCs, adenocarcinomas and SCC, suggest that individual tumor characteristics must be considered to develop individualized therapeutic strategies. Also, the differential sensitivity of NSCLC cell lines *in vitro* to mitogenic effects of bFGF will allow us to interpret the effects of bFGF signaling inhibitors *in vivo*. For example, if we should find that an inhibitor exhibiting anti-tumor effects against a cell line that is not affected directly *in vivo*, we will explore the possibility that the *in vivo* effect might be due to targeting host endothelial cells instead of the tumor cells.

Project 5: Targeting mTOR and Ras signaling pathways for lung cancer therapy

(PI and co-PI: Fadlo R. Khuri, M.D., Shi-Yong Sun, Ph.D.)

Aim 1 To determine whether an mTOR inhibitor inhibits the growth of human NSCLC cells via G1 growth arrest or induction of apoptosis, and to identify the molecular determinants of mTOR inhibitor sensitivity.

Update

The work of the Aim was completed and reported in the 2006 annual report. We have concluded that both mTOR inhibitor rapamycin and RAD001 inhibit the growth of human NSCLC cells, but have minimal effects on cell cycle and apoptosis.

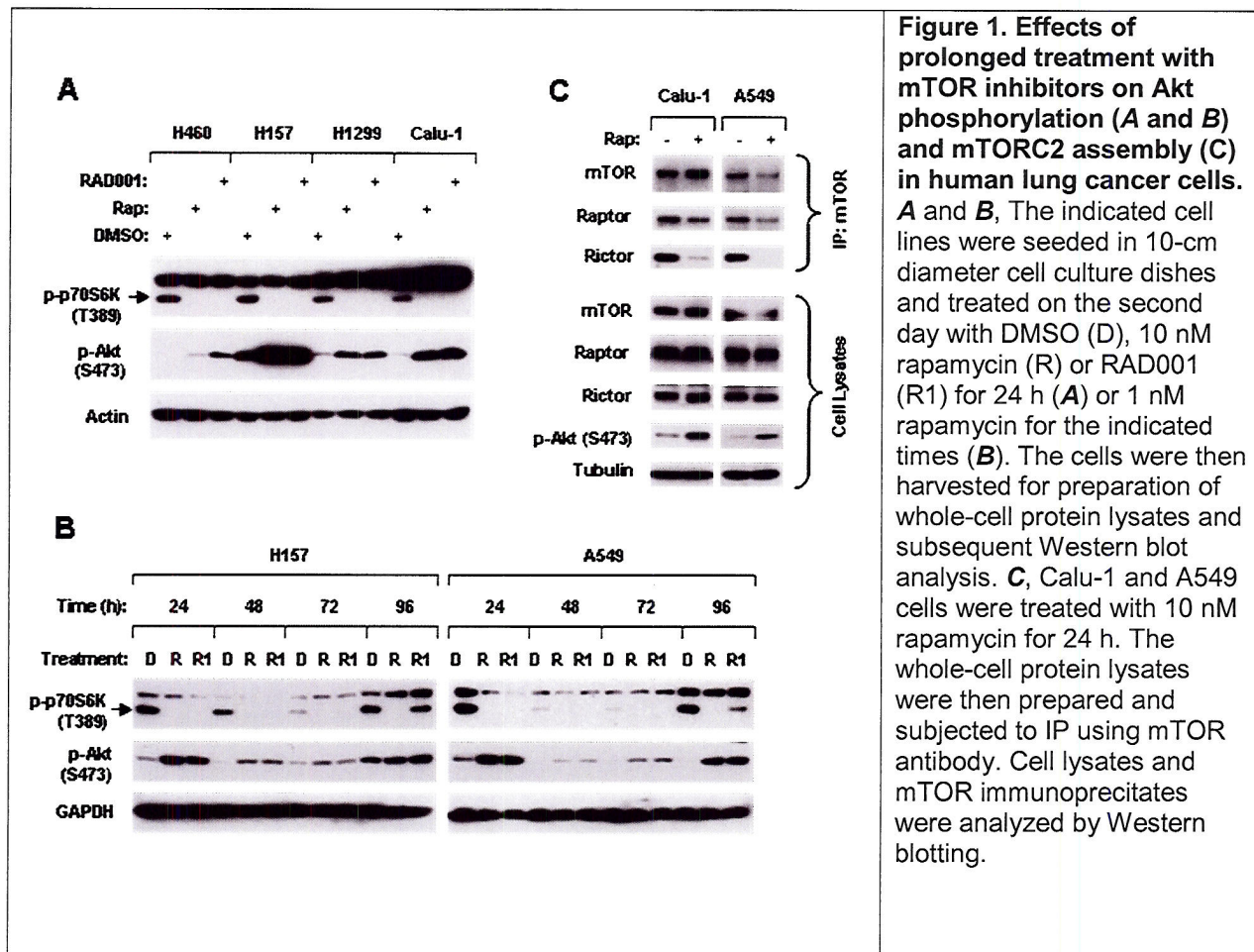
Using findings generated from this aim, an NIH R01 research grant proposal entitled “Enhancing mTOR-targeted Cancer Therapy” was prepared and successfully granted the 5-year award starting on August 15, 2006. One major objective of this proposal is to understand the mechanism by which mTOR inhibitors induce Akt activation in human NSCLC cells as well as other types of cancer cells.

Aim 2 To determine whether the effect of mTOR inhibitors on the growth of human NSCLC cells is enhanced in the presence of a PI3K inhibitor or a MAPK inhibitor.

In the 2006 progress report, we summarized the findings of the enhanced growth-inhibitory effects of the combination of the mTOR inhibitor rapamycin and the PI3K inhibitor LY294002, and of rapid Akt activation after mTOR inhibition. The work has been published in *Cancer Research* (Sun et al. *Cancer Res*, 2005). These results were also confirmed by other laboratories in different cancer cell lines and in RAD001-treated cancer specimens.

Update

Recent studies also show that prolonged treatment (24 h) with mTOR inhibitors disrupts mTOR-rictor complex (mTORC2), leading to inhibition of Akt in a few cancer cell lines (Sarbassov et al., 2006). Therefore, we studied the effects of long-term treatment with the mTOR inhibitor rapamycin on Akt activation in human NSCLC cells. In our cell systems, we found that prolonged treatment with mTOR inhibitors still increased Akt phosphorylation, albeit with inhibition of mTORC2 (Figure 1).



Furthermore, we established a rapamycin-resistant A549 NSCLC cell line, named A549-RR, by chronically exposing the cells to gradually increased concentrations of rapamycin over 6 months. This cell line is resistant to RAD001 as well. We found that the rapamycin-resistant cell line A549-RR, which was maintained in culture medium containing 1 μ M rapamycin, exhibited decreased levels of rictor in the mTORC2 and high levels of activated Akt compared with parental A549 cells (Figure 2).

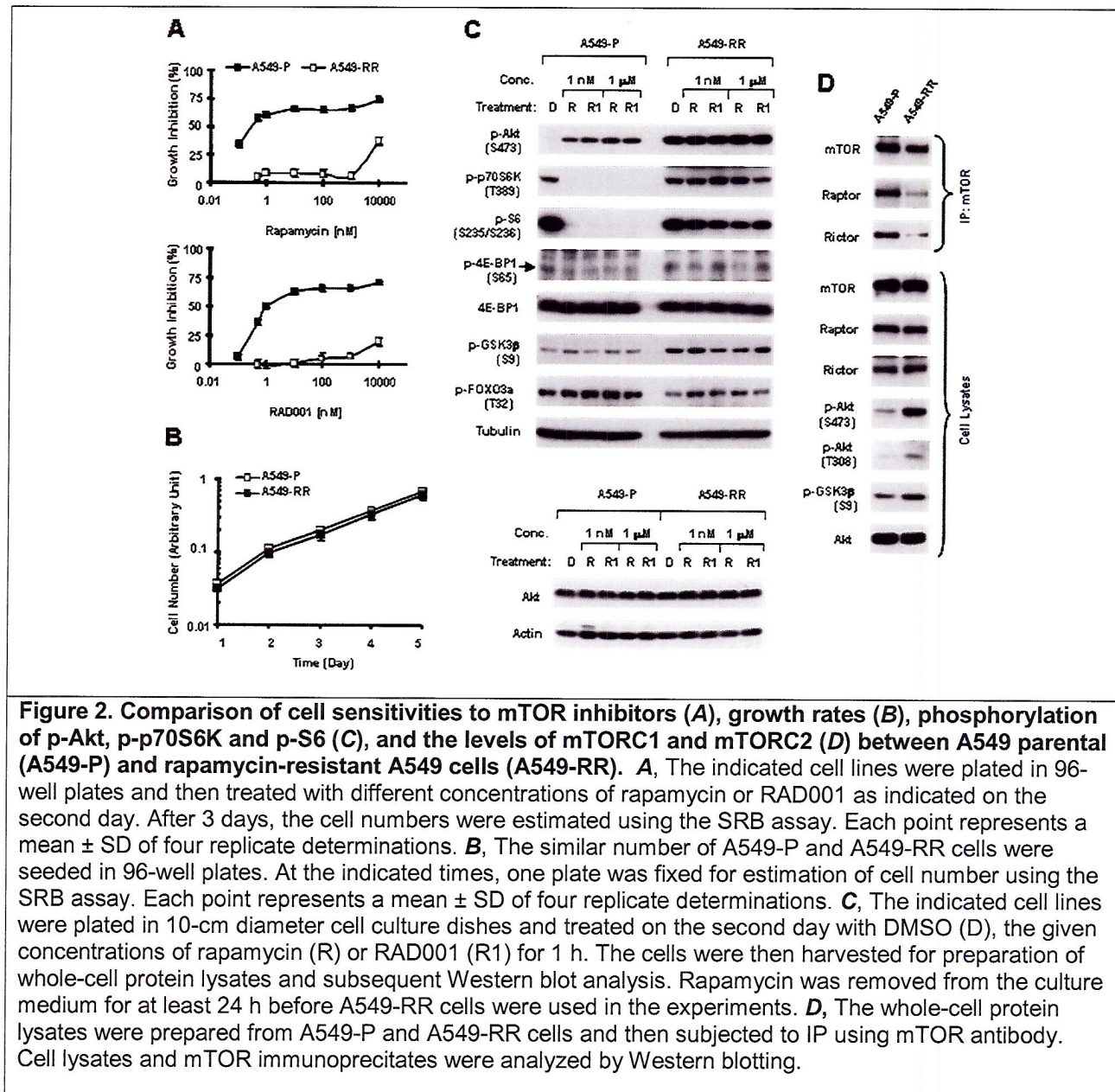


Figure 2. Comparison of cell sensitivities to mTOR inhibitors (A), growth rates (B), phosphorylation of p-Akt, p-p70S6K and p-S6 (C), and the levels of mTORC1 and mTORC2 (D) between A549 parental (A549-P) and rapamycin-resistant A549 cells (A549-RR). **A**, The indicated cell lines were plated in 96-well plates and then treated with different concentrations of rapamycin or RAD001 as indicated on the second day. After 3 days, the cell numbers were estimated using the SRB assay. Each point represents a mean \pm SD of four replicate determinations. **B**, The similar number of A549-P and A549-RR cells were seeded in 96-well plates. At the indicated times, one plate was fixed for estimation of cell number using the SRB assay. Each point represents a mean \pm SD of four replicate determinations. **C**, The indicated cell lines were plated in 10-cm diameter cell culture dishes and treated on the second day with DMSO (D), the given concentrations of rapamycin (R) or RAD001 (R1) for 1 h. The cells were then harvested for preparation of whole-cell protein lysates and subsequent Western blot analysis. Rapamycin was removed from the culture medium for at least 24 h before A549-RR cells were used in the experiments. **D**, The whole-cell protein lysates were prepared from A549-P and A549-RR cells and then subjected to IP using mTOR antibody. Cell lysates and mTOR immunoprecipitates were analyzed by Western blotting.

These compelling results indicate that long-term treatment with the mTOR inhibitor rapamycin in human NSCLC cells still induces Akt activation, which should be independent of mTORC2. Importantly, we found that when the rapamycin sensitivity of A549-RR cells was gradually restored upon withdrawal of rapamycin, a corresponding decline of phosphorylated Akt was observed, suggesting that Akt activation by the mTOR inhibitor rapamycin is associated with acquired rapamycin resistance (Figure 3).

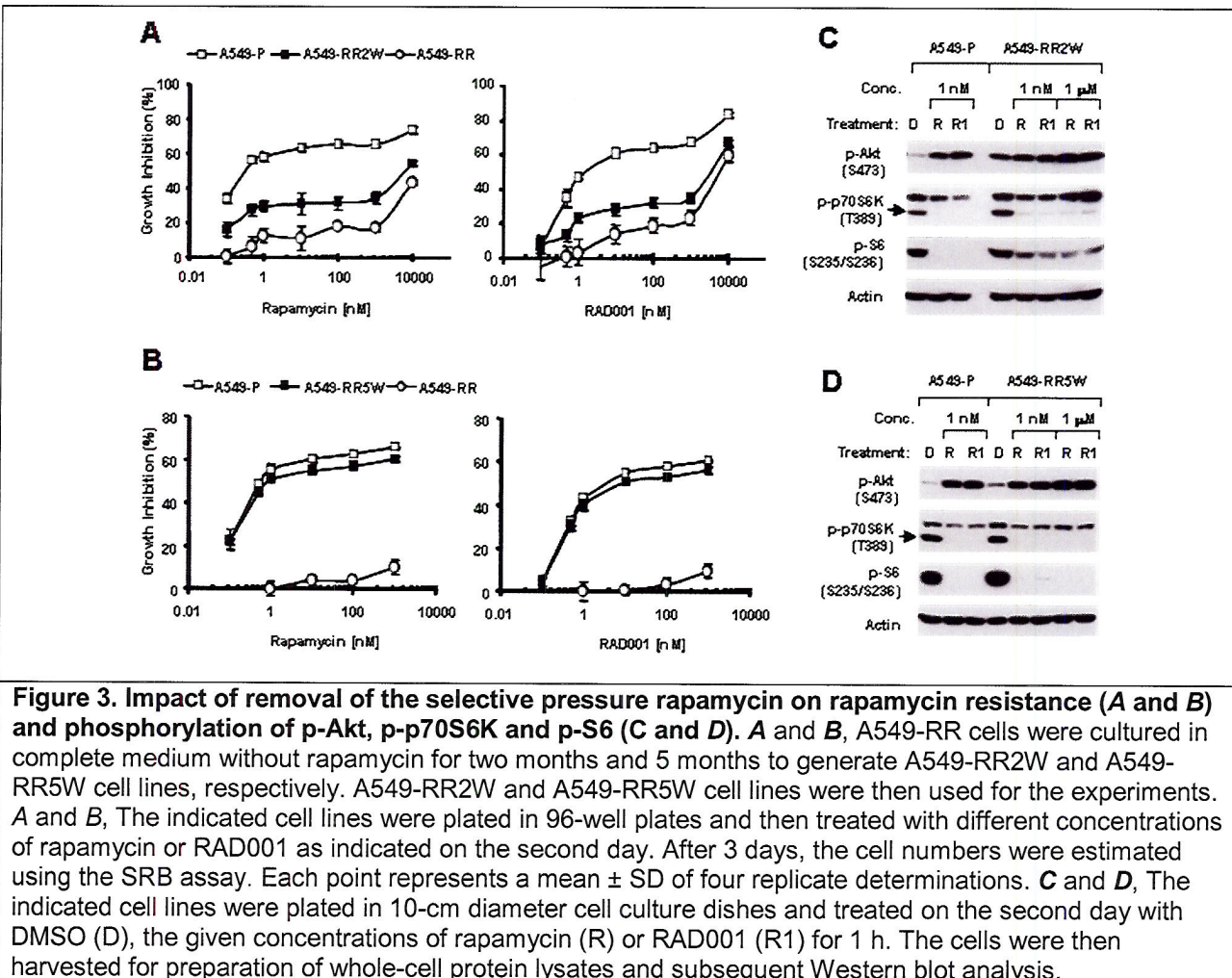
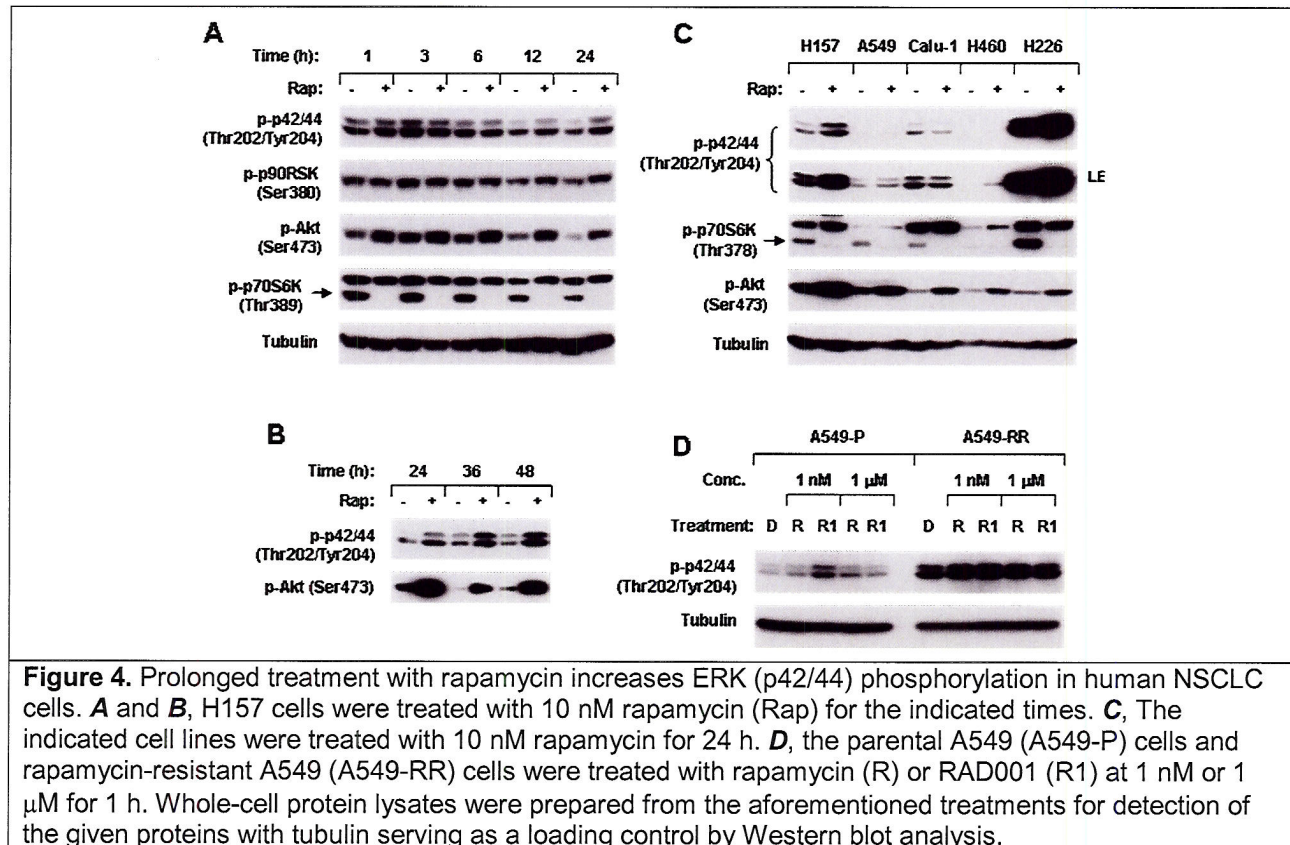


Figure 3. Impact of removal of the selective pressure rapamycin on rapamycin resistance (A and B) and phosphorylation of p-Akt, p-p70S6K and p-S6 (C and D). A and B, A549-RR cells were cultured in complete medium without rapamycin for two months and 5 months to generate A549-RR2W and A549-RR5W cell lines, respectively. A549-RR2W and A549-RR5W cell lines were then used for the experiments. A and B, The indicated cell lines were plated in 96-well plates and then treated with different concentrations of rapamycin or RAD001 as indicated on the second day. After 3 days, the cell numbers were estimated using the SRB assay. Each point represents a mean \pm SD of four replicate determinations. C and D, The indicated cell lines were plated in 10-cm diameter cell culture dishes and treated on the second day with DMSO (D), the given concentrations of rapamycin (R) or RAD001 (R1) for 1 h. The cells were then harvested for preparation of whole-cell protein lysates and subsequent Western blot analysis.

This finding thus provides a strong rationale for combining an mTOR inhibitor with a PI3K inhibitor or an Akt inhibitor in the clinical treatment of lung cancer. Moreover, we found that A549-RR cells were fully sensitive to PI3K inhibitors (i.e., LY294002 and wortmannin), further refining our recommended clinical treatment strategy targeting the mTOR signaling pathway through intermittent utilization of an mTOR inhibitor and a PI3K inhibitor to avoid the development of rapamycin resistance. A manuscript detailing the results is in review by *Clinical Cancer Research* (Wang et al., 2007).

We have also studied mTOR-inhibitor-induced ERK activation and enhancement of mTOR inhibitor-induced growth inhibition by the MEK inhibitor U0126. We found that prolonged treatment (> 12 h) with the mTOR inhibitor rapamycin increased ERK phosphorylation, in addition to rapidly increasing Akt phosphorylation, in some NSCLC cell lines (Figure 4A-4C). Interestingly, we detected increased levels of p-ERK (p-p42/44) in the rapamycin-resistant cell line A549-RR compared to those in the parental A549-P cells (Figure 4D), suggesting that ERK activation is involved in rapamycin resistance. These findings provide a scientific rationale for combination of an mTOR inhibitor, such as rapamycin, with a MEK/ERK inhibitor, such as U0126.



We also studied the effects of rapamycin combined with U0126 on the growth of human NSCLC cells in both short- (3 d) and long-term (10 d) treatments. With both 3-day (Figure 5A) and 10-day (Figure 5B) treatments, the combination of rapamycin and U0126 had better growth-inhibitory effects than each single agent alone in both H460 and H157 cells. Collectively, these results indicate that co-targeting mTOR and MEK/ERK signaling pathways augments the inhibition of the growth of human NSCLC cells.

Aim 3 To determine whether restoration of the Ras-dependent death signaling pathway enhances the growth inhibitory effect of an mTOR inhibitor in human NSCLC cells

Update

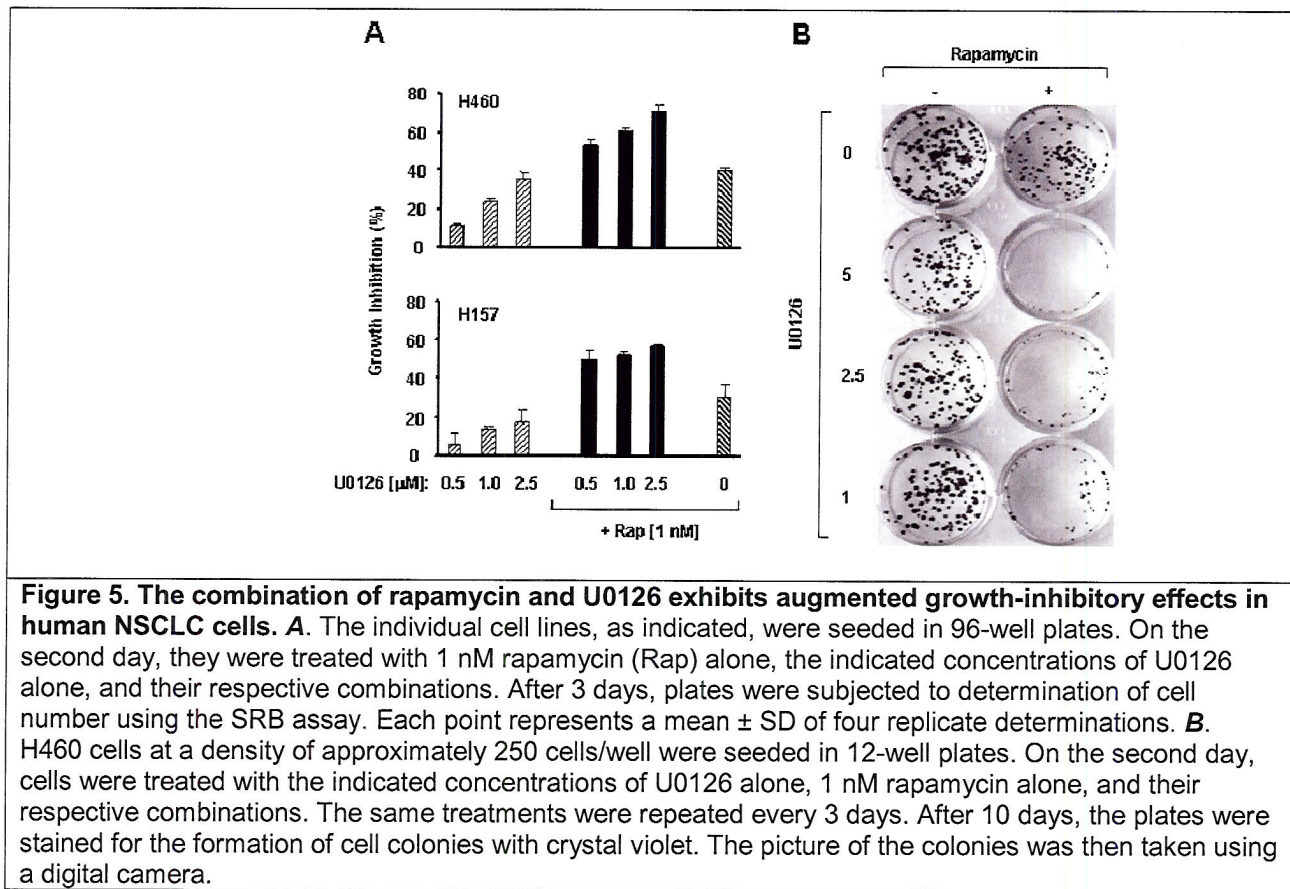
Our results from pursuing the study of this Aim have been disappointing up to this point. We were unable to reproduce published results indicating that RASSF2 induced apoptosis when overexpressed in human lung cancer cells such as A549 (Vos et al. 2003). Considering the promising findings of the combinations of mTOR inhibitors with LY294002 or U0126 on the growth inhibitory effects on NSCLC cells *in vitro*, we propose to revise this aim as follows (please refer to the Revised Statements of Work, Appendix C: Project 5 – Revised Statement of Work):

Revised Aim 3: To evaluate the efficacies of the combinations of rapamycin with LY294002 or U0126 in nude mice models of lung cancer xenografts *in vivo*.

To this end, we will conduct the following experiments:

- 1) Evaluate the efficacy of RAD001 combined with LY294002 on the growth of human lung cancer xenografts in comparison with each single agent.
- 2) Evaluate the efficacy of RAD001 combined with U0126 on the growth of human lung cancer xenografts in comparison with each single agent.
- 3) Analyze the modulation of p-Akt, p-ERK and key proteins such as p-p70S6 and p-S6 by mTOR signaling in xenograft tissues exposed to the aforementioned treatments by Western blot analysis and IHC.

The approval letter of Emory Institutional Animal Care and Use Committee as of October 06, 2006, and animal protocols are attached in Appendix D – Project 5 – Approved Animal protocol and IACUC letter.



Aim 4 To conduct a pilot clinical biochemical induction trial to investigate the effect of RAD001 in operable NSCLC patients and identify molecular determinants of RAD001 sensitivity and prognosis

The aim of this study is to test whether a preoperative dose of RAD001, a synthetic mTOR inhibitor, can be administered safely to patients for 21 days prior to resection of operable lung cancer. The plan is to accrue a total of 60 patients over 2 to 3 years, with correlation between biochemical modulation of the mTOR signaling pathway (as assayed by p-mTOR, p-AKT, p-S6, and p-4E-BP1) with metabolic modulation as assayed by PET scans obtained prior to initiation of the mTOR inhibitor and on the last preoperative dose.

Update

After a comprehensive protocol review and revision by all parties (the Emory IRB, Novartis Pharmaceuticals, Department of Defense USAMRMC, and the FDA), the protocol "Phase IB

trial of RAD001 in patients with operable non-small cell lung cancer (NSCLC)" was approved on January 15, 2007, and the IND was granted. The USAMRMC approval letter is attached in the Appendix E - Project 5 - RAD001 trial. The drug RAD001 has been received from Novartis. We initiated the trial on February 6, 2007.

Key Research Accomplishments

- Demonstrated that long-term treatment with an mTOR inhibitor in human NSCLC cells still increases Akt activity while inhibiting mTOR-riktor activity.
- Demonstrated that Akt activation during mTOR-targeted therapy is associated with acquired rapamycin resistance, thus providing a strong scientific rationale for combining mTOR inhibitors with agents that inhibit Akt activation, directly or indirectly (e.g., a PI3K inhibitor), in the clinical treatment of lung cancer.
- Demonstrated that a rapamycin-resistant cell line is fully sensitive to PI3K inhibitors, suggesting a more rational treatment strategy targeting mTOR-signaling pathway through intermittent utilization of an mTOR inhibitor and a PI3K inhibitor to avoid the development of rapamycin resistance.
- Demonstrated that co-targeting of mTOR and MEK/ERK signaling pathways exhibits enhanced growth-inhibitory effect of NSCLC cells.
- The phase 1B clinical protocol was approved and will open on February 06, 2007.

Reportable Outcomes

Manuscript in Revision

- Wang X, Yue P, Fu H, Khuri, Sun S-Y. Prolonged treatment with mTOR inhibitors increases Akt phosphorylation, which is associated with development of rapamycin resistance, despite inhibition of mTOR complex 2 in human lung cancer cells. *Clin Cancer Res* (in revision), 2007.

Project-Generated Grants

- Awarded NIH R01 research grant entitled "Enhancing mTOR-targeted Cancer Therapy" in 2006. Principal Investigator: Shi-Yong Sun, Ph.D.

Conclusions

Targeting the mTOR axis appears to be a promising strategy against lung cancer. Given the nature of the complexity of lung cancer signaling pathways, including mTOR signaling, it is essential to understand the biology of lung cancer and the mechanism of action for the therapeutics of interest in order to efficiently treat lung cancer through application of mechanism-driven therapeutic regimens. Thus, we have demonstrated the scientific rationale for our effort in pursuing mTOR-targeted lung cancer therapy.

Project 6: Identification and Evaluation of Molecular Markers in Non-Small Cell Lung Cancer (NSCLC)

(PI and co-PI: Ralf Krahe, Ph.D., Li Mao, M.D.)

A better understanding of the lung cancer biology and an identification of genes involved in tumor initiation, progression and metastasis are an important first step leading to the development of new prognostic markers and targets for therapy. In the same context, identification of reliable predictive markers for response or resistance to therapy in NSCLC patients is also desperately desired for optimal delivery of targeted therapy and/or standard chemotherapy. The proposed studies aim to identify the two types of markers that would

eventually help develop smarter clinical trials, which will selectively recruit patients who are more likely to respond to one regimen over another and lead to improvement of overall therapeutic outcomes.

Aim 1 To expression profile by DNA microarray technology aerodigestive cancers - with primary focus on adenocarcinoma and squamous cell carcinoma (SCC) of the lung, and head and neck squamous cell carcinoma (HNSCC), including primary tumors and normal adjacent tissue, and (where available) metastatic lesions.

Update

Expression profiling of HNSCC and NSCLC

Our ongoing experiments and analyses have focused on the HNSCC sample set for which tissue samples were available.

We have completed expression profiling of 29 matched tumor/normal pairs of HNSCCs, 12 matching lymph node metastases and 4 HNSCC cell lines. A manuscript reporting the findings of profiling was submitted to *Cancer* (Colella et al., 2007). Using HNSCC as a prototypic solid tumor of epithelial origin, we identified genes involved in head and neck cancer tumor initiation, progression and metastasis. In particular, taking advantage of genetically matched samples, including normal adjacent tissues, primary tumors and lymph node metastases, we identified tumor-associated gene expression signatures that were common to both primary tumors and metastases (Figure 1). These results are consistent with the notion that the metastatic potential is already encoded in the bulk of the primary tumor.

By using genetically matched samples we were also able to identify a limited set of 46 dysregulated genes uniquely associated with HNSCC metastasis (Table 1). These data are consistent with the concept that the acquisition of a limited number of additional clonal changes is necessary to yield the final metastatic cell(s). Several groups have recently reported metastatic signatures in HNSCC, although most of these have been based on gene expression data from primary tumors only or cell lines (Chung et al., 2004, Cromer et al., 2004, Hunter et al., 2006, O'Donnell et al., 2005, Roepman et al., 2005, Roepman et al., 2006, Schmalbach et al., 2004).

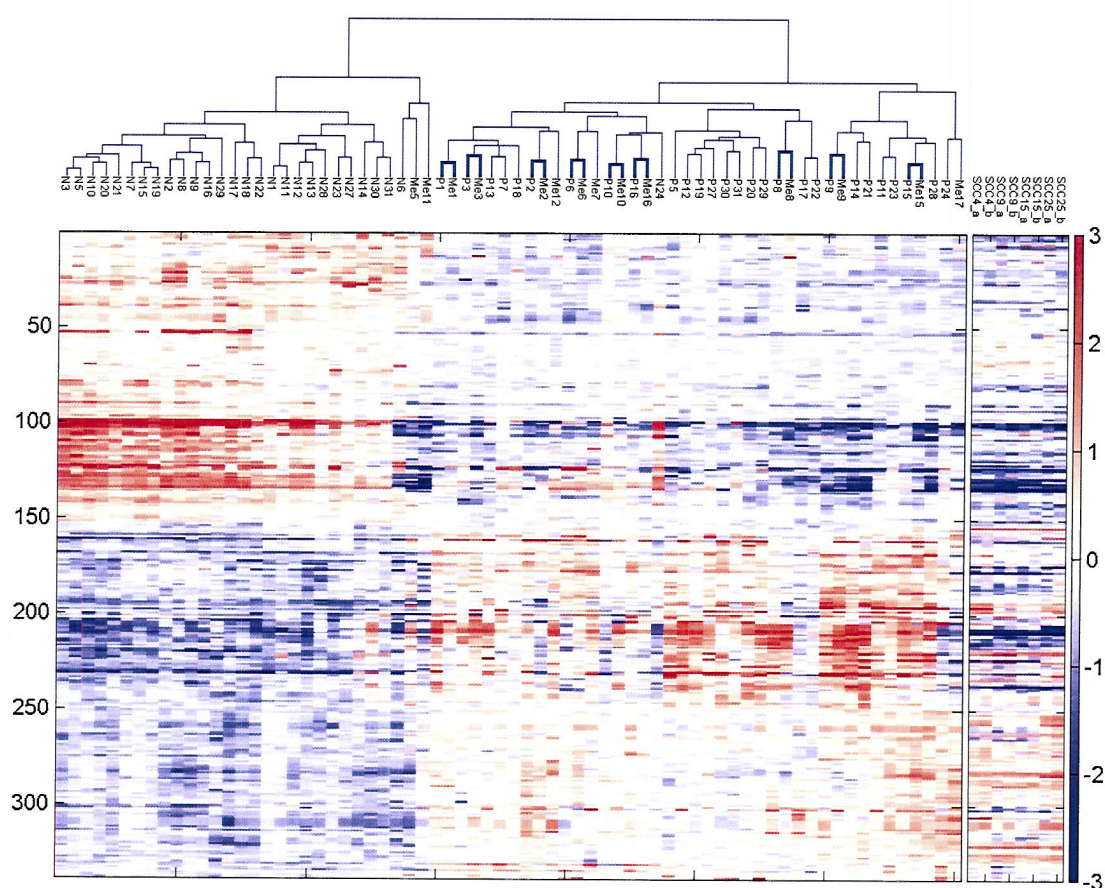


Figure 1. Two-way hierarchical cluster analysis of gene expression profiles generated on pseudo-probe set gene expression data. Hierarchical clustering of all 74 samples (cell lines to the side) from both chip types (a, HuGeneFL; b, U95Av2) using Euclidean distance and complete linkage applied to RMA quantifications of the 338 pseudo-probe sets passing the rank filter. Normal specimens cluster to the left, tumors to the right. Of particular interest is that most P (primary tumor) and M (metastatic lymph node) from the same patient show pairing (9 of 14, 64% highlighted by thicker lines). Two P samples obtained from the same patient before and after therapeutic treatment (P13 and P3) are also very near in the hierarchical samples cluster, suggesting a patient-specific tumor-signature. Results on cell lines for each individual chip type are effectively identical.

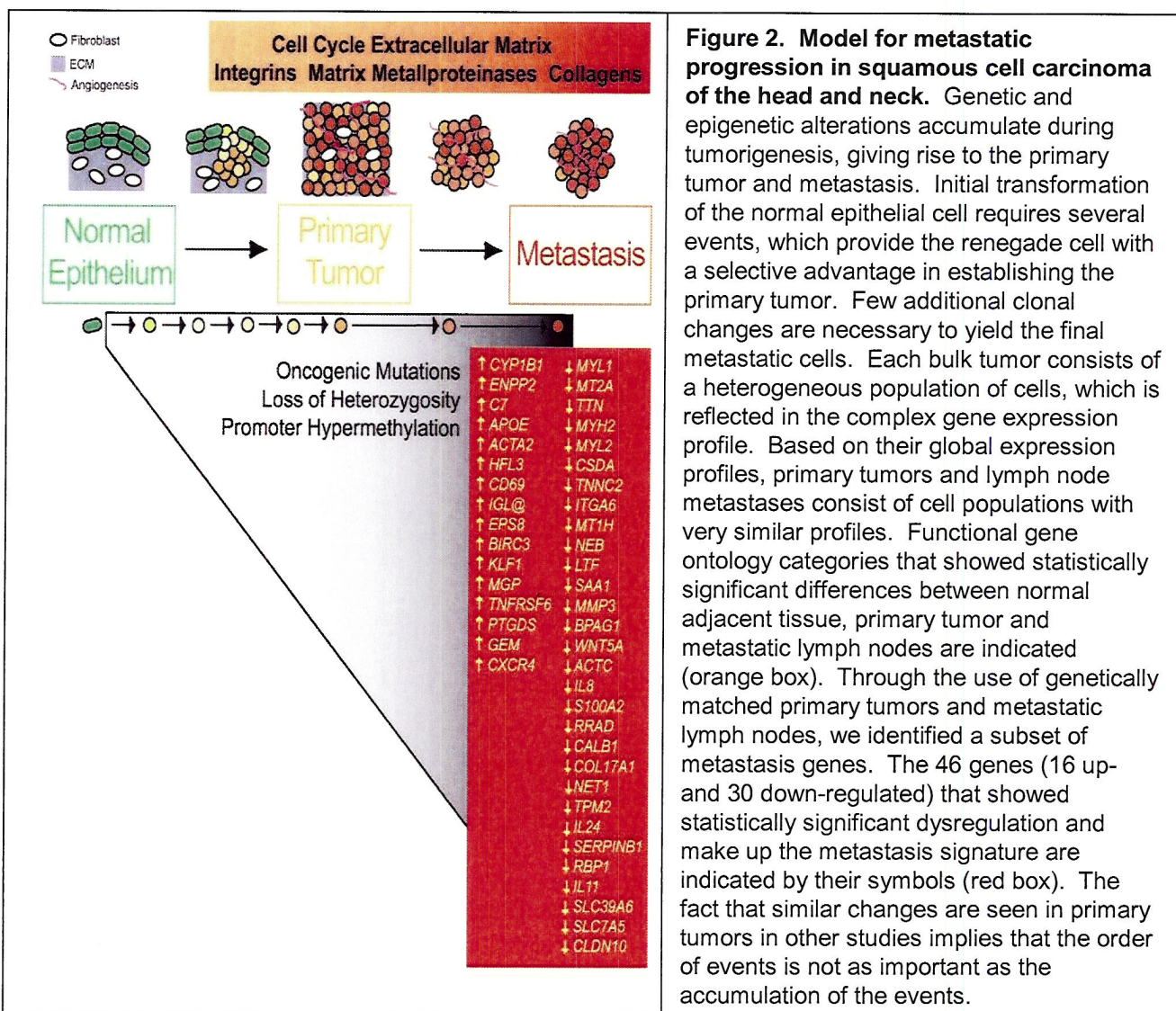
Table 1: HNSCC Metastasis Genes
16 Upregulated Genes

Hu6800 Probe ID	U95Av2 Probe ID	Gene Symbol	Title	Entrez Gene	Location	Average Positive Fold Change
U03688_at	859_at	CYP1B1	cytochrome P450, subfamily 1 (dioxin-inducible), polypeptide 1 (glaucoma 3, primary infantile)	1545	Chr:2p21	2.5564
U03688_at	40071_at	ENPP2	ectonucleotide pyrophosphatase/phosphodiesterase 2 (autotaxin)	5168	Chr:8q24.1	2.5166
L35594_at	41124_r_at	C7	complement component 7	1.6961		
L35594_at	41123_s_at	APOE	apolipoprotein E	730	Chr:5p13	1.6668
J03507_at	37394_at	ACTA2	actin, alpha 2, smooth muscle, aorta	348	Chr:19q13.2	1.884
M12579_at	608_at	HFL3	H factor (complement-like 3)	59	Chr:10q23.3	1.7824
X13839_at	36341_s_at	CD69	CD89 antigen (p60, early T-cell activation antigen)	3080	Chr:1q31-q32.1	1.6111
X64877_s_at	36341_s_at	IGL@	immunoglobulin lambda locus	969	Chr:12p13-p12	1.6062
Z30426_at	37645_at	EPS8	epidermal growth factor receptor pathway substrate 8	3535	Chr:22q11.1-q11.2	1.5928
X57809_s_at	31459_i_at	BIRC3	baculoviral IAP repeat-containing 3	2059	Chr:12q23-q24	1.5276
X57809_s_at	31344_at	KLF1	Kruppel-like factor 1 (thyroid)	330	Chr:11q22	1.5052
U12535_at	1467_at	MGP	matrix Gla protein	10661	Chr:19p13.13-p13.12	1.5052
U37546_s_at	1717_s_at	TNFRSF6	tumor necrosis factor receptor superfamily, member 6	4256	Chr:12p13.1-p12.3	1.5052
U65404_at	137_at	PTGDS	prostaglandin D2 synthase 21kDa (brain)	355	Chr:10q24.1	1.4919
X5331_at	36683_at	GEM	GTP binding protein overexpressed in skeletal muscle	5730	Chr:9q34.2-q34.3	1.638
X89101_s_at	1441_s_at	CXCR4	chemokine (C-X-C motif) receptor 4	2669	Chr:8q13-q21	1.5689
M9839_at	216_at			7852	Chr:2q21	1.5148
U10550_at	37279_at					
L06797_s_at	649_s_at					

30 Downregulated Genes

Hu6800 Probe ID	U95Av2 Probe ID	Gene Symbol	Title	Entrez Gene	Location	Average Negative Fold Change
M20642_s_at	40157_s_at	MYL1	myosin, light polypeptide 1, alkali; skeletal, fast	4632	Chr:2q33-q34	-4.2466
M20642_s_at	40158_r_at	MT2A	metallothionein 2A	4502	Chr:16q13	-4.5890
V00594_s_at	39081_at	TTN	titin	7273	Chr:2q24.3	-1.5118
V00594_at	39081_at	MYH2	myosin, heavy polypeptide 2, skeletal muscle, adult	4620	Chr:17p13.1	-3.2370
X90568_at	40795_at	MYL2	myosin, light polypeptide 2, regulatory, cardiac, slow	4633	Chr:12q23-q24.3	-2.9306
S73840_at	39101_at	CSDA	cold shock domain protein A	8531	Chr:12p13.1	-2.0088
X66141_at	36640_at	TNNC2	troponin C2, fast	7125	Chr:20q12-q13.11	-1.5510
M24069_at	39839_at	ITGA6	integrin, alpha 6	3655	Chr:2q31.1	-1.5346
M33772_s_at	41748_at	MT1H	metallothionein 1H	4496	Chr:16q13	-1.5339
X53586_rna1_at	33411_q_at	NEB	nebulin	4703	Chr:2q22	-2.9512
X53586_rna1_at	33410_at	LTF	lactotransferrin	4057	Chr:3q21-q23	-2.7714
X64177_f_at	39594_f_at	SAA1	serum amyloid A1	6288	Chr:11p15.1	-2.5386
U35637_s_at	38461_at	MMP3	matrix metalloproteinase 3 (stromelysin 1, progelatinase)	4314	Chr:11q22.3	-2.3024
X53961_at	37149_s_at	BPAG1	bulous pemphigoid antigen 1, 230/240kDa	667	Chr:6p12-p11	-2.3736
X51441_at	33272_at	WNT5A	wingless-type MMTV integration site family, member 5A	7474	Chr:3p21-p14	-2.2511
X51441_s_at	33272_at					-2.0523
X05232_at	437_at					-2.2151
M69225_at	40304_at					-1.5605
M69225_at	32782_r_at					
L20861_at	31852_at					
L20861_at	1669_at					

Our study derived the metastatic signature from a comparison between primary tumors and metastases. Although our metastatic signature was derived from and is specific to metastases, it shares genes in common, and even more strikingly, shares a similar set of biologic pathways and processes with previously published HNSCC metastatic signatures derived from primary tumors. This implies that while metastasis requires changes in expression of genes in many pathways/processes, the order and timing of these changes is less important, since our signature, derived from expression changes specific to metastases, matches other signatures derived from primary tumors. Through the incorporation of genetically matching tissue samples (normal adjacent tissue, primary tumor and cervical lymph node metastases), our experimental design enabled us to objectively address the unresolved issue of genetic heterogeneity between tumor and metastasis tissues from different patients in our analyses.. Based on our data, we have proposed a model for HNSCC metastasis that incorporates features derived from the primary tumor and metastases(Figure 2).



In addition, we have completed expression profiling on 8 retrospective matched tumor/normal (T/N) pairs of lung cancers, 5 adenocarcinomas and 3 SCCs, from a total of 22 NSCLC T/N pairs initially collected(14 of which had partial or complete degradation of RNA preventing analyses to be performed). Notwithstanding, the DNA extracted from the same samples was of sufficient quality for Aims 2 and 3 as described below.

Sample collection under the institutional protocol to bank specimens (LAB03-0320) was suspended temporarily last year (August 2, 2006) due to minor discrepancies in the informed consent process. Corrective action was submitted and approved to our IRB (September 19, 2006). Thus, the protocol was reopened and we are in the process of identifying additional suitable samples. We aim to have 50 NSCLC normal/tumor pairs profiled. Based on the limited expression profiling data currently in hand, it is too early to draw statistically meaningful conclusions for the lung cancer part of the study, or to perform meaningful comparisons with the HNSCC part of the study.

Aim 2 To DNA profile the same samples by complementing DNA approaches to stratify RNA expression profiles on the basis of their corresponding DNA profiles.

Update

DNA profiling of corresponding NSCLC tumors

To date, we have extracted DNA from 22 NSCLCs as mentioned above. Because we wish to correlate the DNA profiles with the RNA expression profiles, we are waiting until we get a more complete set of tumors for which a good quality of RNA is available so that these analyses can be carried out with as much overlap between the two sets of tumor samples as possible. In addition because there are now DNA copy number analysis tools available which will allow analysis of chromosome copy number and LOH using the same data set (from SNP chips), making the completion of this aim less labor intensive, we will be using this technology in place of the originally proposed SNP arrays. We have extensively tested this approach now on other available tumor samples in our lab and will use high-density oligonucleotide based SNP arrays (at least 500K SNPChip, Affymetrix, Santa Clara, CA).

Aim 3 To evaluate the contribution of promoter hypermethylation and transcriptional inactivation of known cancer genes subject to epigenetic silencing to cancer phenotype.

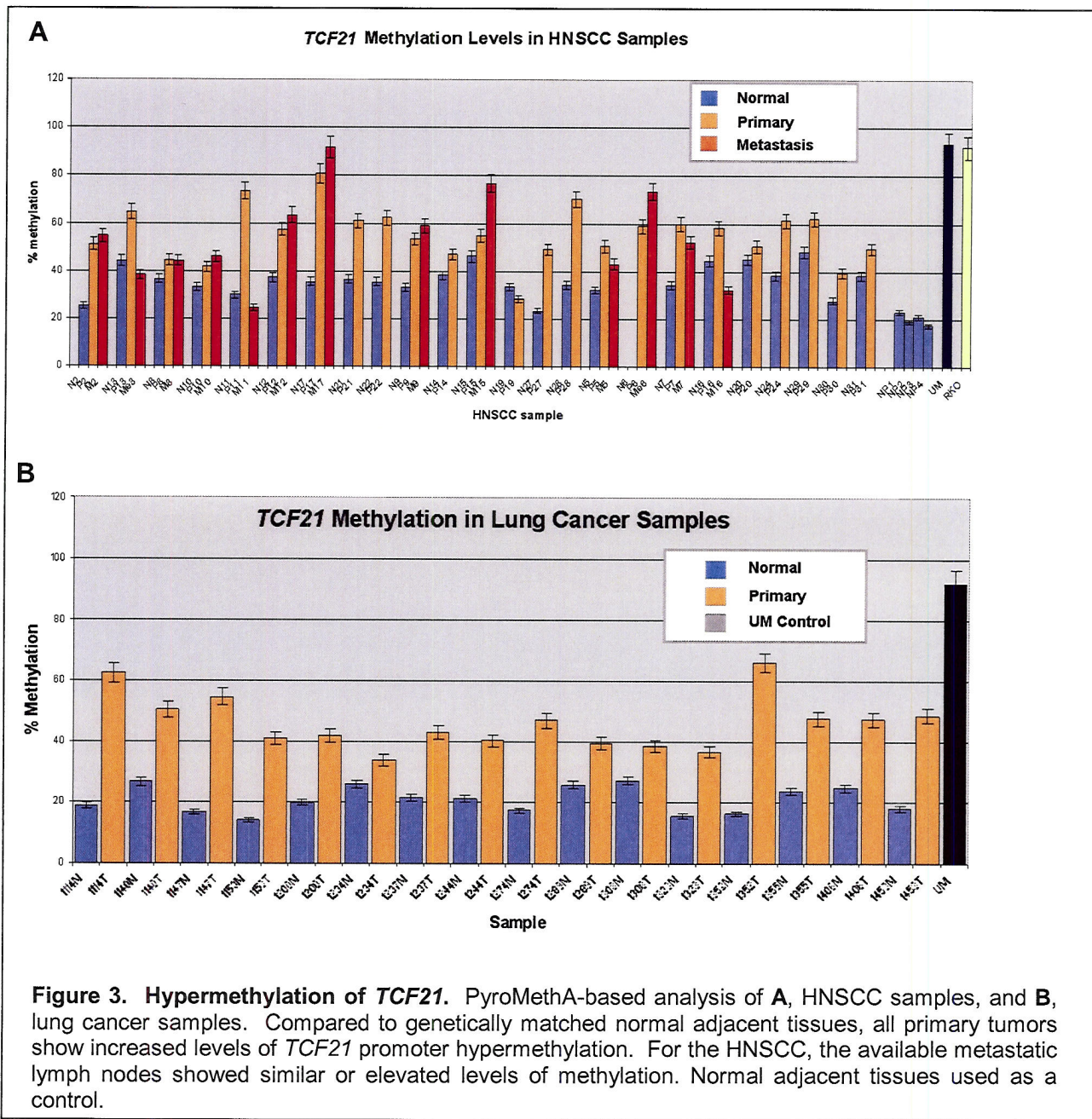
Update

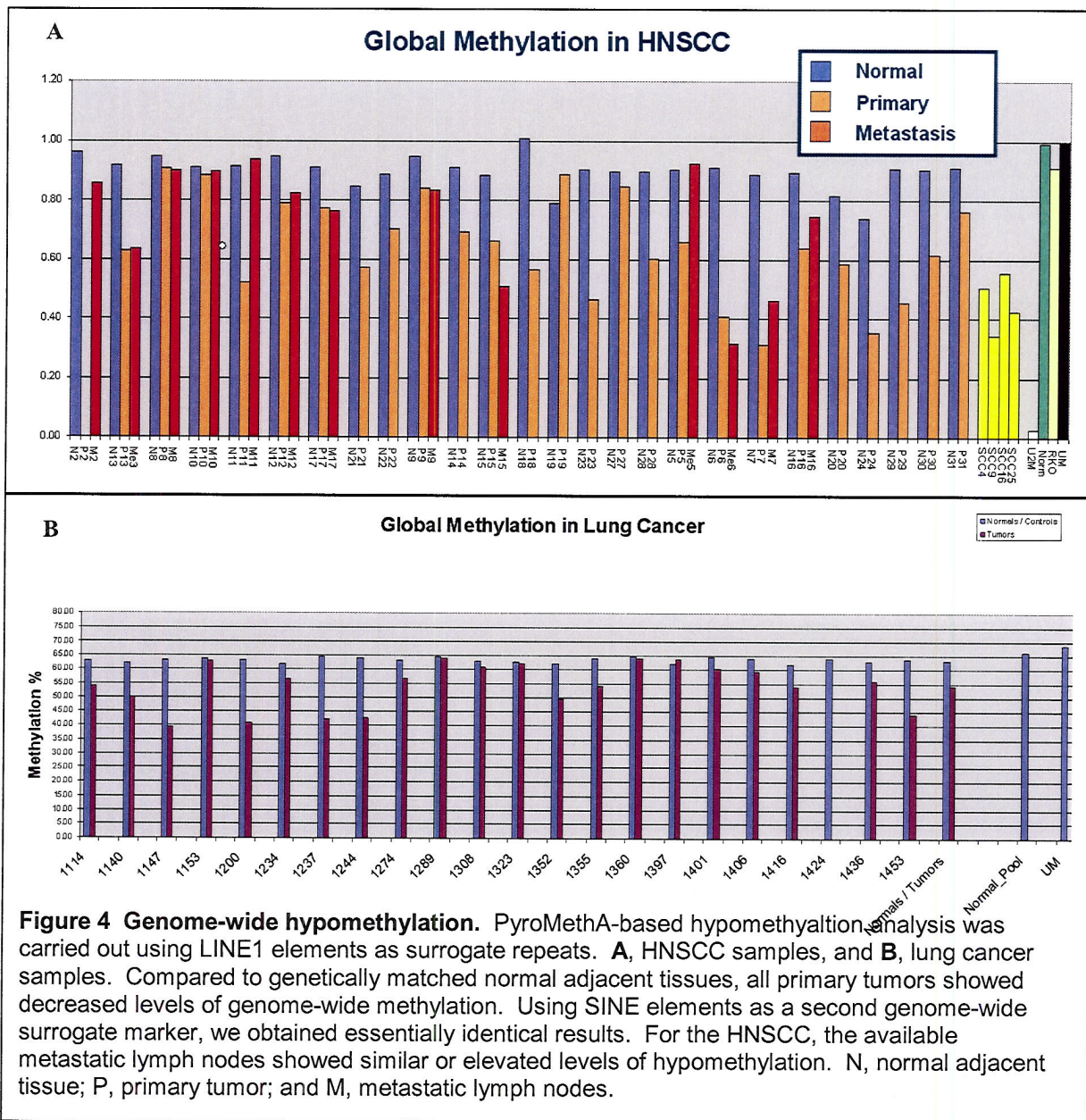
Methylation profiling of NSCLC tumors

To date, we have completed methylation profiling for 9 genes known (or suspected) to be methylated in head and neck and lung cancer (*APC*, *MLH1*, *RASSF1*, *MGMT*, *CDKN2A/p14* and *p16*, *ATM*, *GSTP1* and *TCF21*) on 24 pairs of matched HNSCC primary tumors and normal adjacent tissue, plus an additional matched 14 metastatic lymph nodes, and 22 NSCLCs and their matched normal samples. Varying frequencies of methylation (0% to 100% of samples) were observed. All 9 genes were hypermethylated in NSCLC. HNSCC and NSCLC showed similar levels of hypermethylation for 5 of 9 genes (56%; *CDKN2A/p14* and *p16*, *MGMT*, *RASSF1* and *TCF21*), while 4 of 9 genes (44%; *APC*, *ATM*, *GSTP1* and *MLH1*) were only hypermethylated in NSCLC. Interestingly, the level of hypermethylation was generally higher in the available HNSCC metastatic lymph nodes to the matching primary tumors. Of particular note, *TCF21* was hypermethylated in all HNSCC and NSCLC tumor samples (Figure 1A-B). More samples will be analyzed as they become available, and more genes will be analyzed as their methylation assays are developed. Ultimately, the expression levels of genes identified as differentially regulated from Aim 1 will be correlated with their corresponding DNA and methylation profiles.

Together with Dr. Ignacio Wistuba (Pathology Core), we are now performing *TCF21* protein immunohistochemical (IHC) analysis on lung cancer tumor specimens. *TCF21* was hypermethylated in HNSCC and NSCLC tumor samples described above. Two antibodies against *TCF21* protein (sc-15007, Santa Cruz Biotechnology, Santa Cruz, CA; and Ab-32981, Abcam, Cambridge, MA) have been obtained and are currently being optimized for IHC analysis

of formalin-fixed and paraffin-embedded (FFPE) tissues. A set of 57 NSCLC cell lines FFPE pellets is available for screening and validation of TCF21. To investigate the frequency and pattern of TCF21 protein expression in NSCLCs, we have obtained archival FFPE tissues from surgically resected lung cancer specimens containing tumor and adjacent normal tissues from 281 NSCLCs (172 adenocarcinomas and 109 squamous cell carcinomas). Tumors have been histologically examined and classified using the 2004 World Health Organization (WHO) classification. All cases have been placed in tissue microarrays (TMAs) using triplicate 1-mm diameter tissue cores per tumor specimen obtained from central, intermediate, and peripheral tumor areas. Detailed clinical and pathological information, including demographic, smoking history (never- and ever-smokers) and status (never, former, and current smokers), clinical and pathologic TNM staging, overall survival and time of recurrence, are available in all cases. Whole histology sections are also available to study the TCF21 expression distribution in tumor specimens and adjacent normal lung tissues.





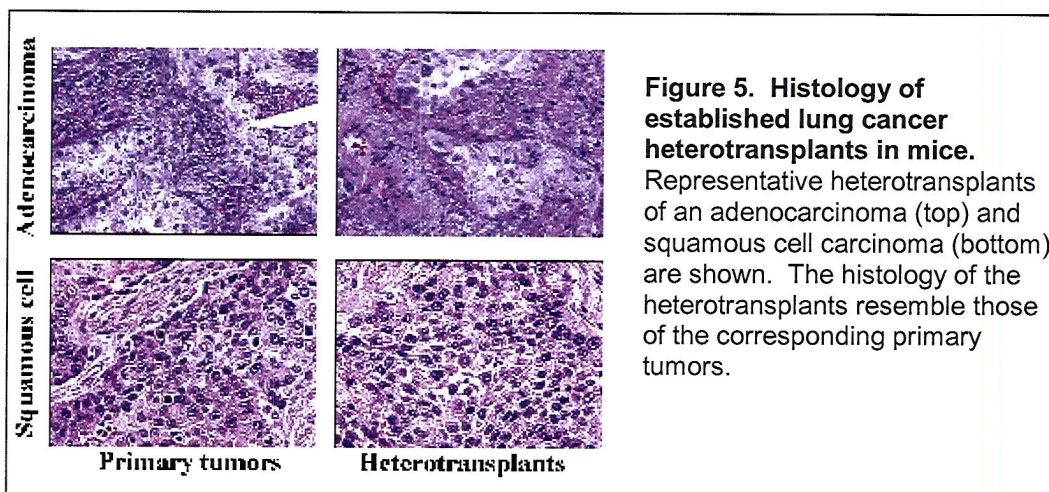
In addition to the gene-specific hypermethylation of cancer genes, we have also determined the level of genome-wide hypomethylation using corresponding PyroMethA-based assays developed for LINE1 (long interdispersed) and SINE (short interdispersed) repetitive elements (Krahe, unpublished). Using LINE1 (~600,000 copies in the human genome, or 17.3% of the human genome) and SINE (~1,200,000 copies in the human genome, or 10.7% of the human genome) repeats as surrogate genomic markers, we can interrogate ~28.0% of the human genome for levels of methylation. Similar to the level of hypermethylation for specific cancer genes, the level of hypomethylation was generally also higher in metastatic lymph nodes compared to their genetically matched primary tumors (Figure 4).

Aim 4 To determine protein signatures of erlotinib treatment in NSCLC and identify molecular predictors of response.

We proposed to establish 50 lung heterotransplant tumor mouse models and use the models to test the EGFR TKI (tyrosine kinase inhibitor) erlotinib to identify the molecular predictors of response to this targeted agent.

Update

Last year, we reported some difficulties in establishing heterotransplant tumor models. To address the issues, we made serial modifications to our process as follows: (1) reduction of the time between tumor harvest and tumor implantation by more efficient coordination between surgery, surgical pathology, and the tumor bank; (2) modification of the implantation procedures, including the use of Matrigel (BD Biosciences, San Jose, CA), to improve tumor survival; (3) recruitment of a new postdoctoral fellow dedicated to the project. With these efforts, we have successfully established 7 heterotransplant NSCLC models from 7 individual patients. Three of these models have been passaged for 3 times and are ready for the proposed experiments to evaluate therapeutic agents and for biomarker discovery. In collaboration with Dr. Wistuba, we have compared the histological features of the heterotransplant tumors developed in mice with the corresponding primary tumors, and found that the histology of the heterotransplants tumors mimics that of the primary tumors (Figure 5).



We will continue to establish additional heterotransplant tumor models as planned. Because of the potential utility of the models for new drug testing and biomarker discovery, the establishment and characterization of additional models will be a priority. We have begun to determine global gene expression profiles and will compare the profiles of the heterotransplant tumors and their corresponding primary tumors to identify any potential changes.

Aim 5 To determine a clinical utility of the molecular predictors.

Any biomarker developed must be tested in clinical trials to determine its sensitivity and specificity. In addition, the assay should also be tested to determine the minimum amount of tissue sample or body fluids required to be obtained in clinical practice. So far, the most sensitive and specific clinical tests are antibody-based assays.

Update

The test of clinical specimens proposed in this aim was planned for the latter stages of the proposal. Due to unforeseen delays with the gefitinib clinical trials, progress on this aim is delayed.

Key Research Accomplishments

- Conducted global expression analysis of a set of 29 HNSCC matched T/N pairs and an initial set of 8 lung adeno- and squamous cell carcinoma matched T/N pairs.
- Developed a model for metastatic progression in HNSCC from profiling data.
- Completed gene-specific hypermethylation analysis of 9 genes and genome-wide hypomethylation in all available HNSCC and NSCLC samples.
- Detected both aberrant hypermethylation and hypomethylation in metastatic lymph nodes and their genetically matched primary tumors.
- Established 7 heterotransplant primary NSCLC tumor models, which will allow us to evaluate target therapeutic agents and to initiate biomarker discovery experiments.

Reportable Outcomes

- Colella S, Richards KL, Baggerly KA, Tsavachidis S, Lang JC, Schuller DE, Krahe R. Expression Signature of Head and neck Cancer Metastasis. *Cancer* (submitted), 2007.

Conclusions and Future Work

Based on our methylation profiling, *TCF21* may be a good biomarker of early lung and head and neck cancer. With an established role in the epithelial-mesenchymal transition, *TCF21* may be important in predicting metastatic potential.

Although EGFR TKIs were novel agents at the time of the grant application, their biology and clinical implications have been extensively studied in the recent years including a number of studies using patients' biologic materials and data. Consequently, we believe that we should take advantage of the newly established heterotransplant tumor models to test novel concepts and new targeted agents or combinations thereof. Because of the importance of DNA methylation in lung tumorigenesis, we also propose to test demethylation agents such as decitabine, which was recently approved for patients with leukemia, and the combination of decitabine with histone deacetylase inhibitors, such as SAHA. Through these experiments, we can test the potential efficacy of combinations which are currently considered for clinical trials (has not yet been implemented), determine biological effects of the agents, and identify predictive biomarkers that will guide selection of patients for better treatment outcomes.

Revised Aim 4: To determine protein signatures of treatments of erlotinib and other therapeutic agents, alone or in combination, in NSCLC and identify molecular predictors of response.

Core B: Biostatistics & Data Management Core

(Core Director: J. Jack Lee, Ph.D.)

The Biostatistics and Data Management Core has continued to work with all IMPACT Projects in their research efforts, especially in the area of biostatistical support and consulting in the clinical trial design, implementation, and analysis of experimental results.

In addition to Dr. Lee, Core B recruited Dr. Guosheng Yin, Assistant Professor of Biostatistics, to work on various projects of IMPACT.

Specific Aims:

1. To ensure that the results of all projects are based on well-designed experiments and are appropriately interpreted by providing experimental design; sample size estimates; power calculations; and integrated, comprehensive analysis for each basic science, pre-clinical, and clinical study.
2. To develop a data management system that integrates clinical, pathological, and basic science data while providing data integrity through process tracking and quality control.
3. To provide statistical and data management support for genomic and imaging studies including microarray, proteomics, and molecular targeted imaging.
4. To develop and adapt innovative statistical methods pertinent to biomarker-integrated translational lung cancer studies.
5. To produce statistical reports for all projects.
6. To collaborate and assist all project investigators with the publication of scientific results.

Update

One major effort in the second year of funding is to continue providing statistical support in the design and revision of the clinical trial proposed in Project 1. We have continued to assist the Project PI in the revisions of the trial: "A Phase I/II Study of TARCEVA (erlotinib) in Combination with Chemoradiation in Patients with Stage III A/B Non-Small Cell Lung Cancer" (PI: Dr. Ritsuko R. Komaki) which has successfully undergone review by various regulatory agencies and awaits the final approval shortly.

In addition, we have provided the initial design and the revised design to a clinical trial proposed in the Developmental Research Project 1 (see DRP-1 below) named: "Treatment of Malignant Pleural Effusion with ZD6474 a Novel Vascular Endothelial Growth Factor Receptor (VEGFR) and Epidermal Growth Factor Receptor (EGFR) Tyrosine Kinase Inhibitor" (PI: Dr. Roy Herbst). We have interacted with study PI, CRC, IRB, and regulatory agencies to address critiques and provided revisions to change from a two-arm randomized study to a single-arm study compared to the set target obtained from historical control data. We are also involved with the design of Case Report Forms (CRFs) for these trials.

We have worked with Drs. Mao (Project 6) and Wistuba in the analysis of methylation data from lung cancer cases. In addition, we worked with Dr. Wistuba on three IMPACT research projects: Project 3, Tissue microarray study of GRP78, IL11R and EphA5 on 301 NSCLC patients; Projects 2 and 4, analysis of VEGFR and EGFR expression in 284 NSCLC patients, analysis of the data for EGF/EGFR expression in paired tissues of primary lung cancer and brain metastasis from 57 patients, and analysis of the expression data of fibroblast growth factor-2, receptors 1 and 2, and syndecan-1 in SCC and adenocarcinoma of the lung. Abstracts of the results for the latter two projects were submitted to the 2007 AACR meeting (Sun et al., 2007; Massarelli et al., 2007; Behren et al., 2007). We have also worked with Dr. Gelovani, Project 2, in evaluation of the statistical aspects for the clinical trials using novel imaging techniques.

Key Research Accomplishments

- Continued to provide statistical support in the clinical trial design and revision for Project 1 and DRP-1.
- Provided data analysis for Projects 2, 3, 6, and Pathology Core.

- Continued to work closely with the Project 4 PI (Dr. Reuben Lotan) on synergy studies of combination drug treatment in cell lines to determine whether the effect is synergistic, additive, or antagonistic.
- Generalized the currently available methods to allow different mode and magnitude of drug interaction to account for the possibility that the combination may produce synergistic effect in certain dose ranges but additive or antagonistic in other dose ranges. The magnitude of drug interaction can also vary from dose to dose.
- Developed two new statistical methods – one parametric generalized response surface model and one semi-parametric model, which allow more general interaction patterns for the drug interaction and relax the restrictions of the existing methods.
- Developed methods to construct the confidence interval for the interaction index.

Reportable Outcomes

Manuscripts published in peer-reviewed

- Kong, M. and Lee, J. J. A generalized response surface model with varying relative potency for assessing drug interaction. *Biometrics* 62 (1282): 986-95, 2006.

Manuscripts in review, revision, or submission

- Kong M, Lee JJ. A semiparametric model for assessing drug interaction. *Biometrics* (in revision), 2006.
- Lee JJ, Kong M. Confidence Interval of Interaction Index for Assessing Multiple Drug Interaction. *Statistics in Biopharmaceutical Research* (submitted), 2007.

Abstracts

- Massarelli E, Maria L, Silva P, Ozburn N, Feng L, Yin G, O'Reilly M, Hong WK, Herbst RS, Wistuba II. Correlation between VEGF/VEGFR2 and EGFR immunohistochemical protein expression in early stage non-small cell lung carcinoma. The 98th AACR Annual Meeting, abstract#: 5029, 2007.
- Sun M, Massarelli E, Feng L, Ozburn N, Yin G, Komaki R, Hong WK, Aldape KD, Wistuba II. Differential immunohistochemical expression pattern of HER family receptors and ligands is detected in primary lung cancers and corresponding brain metastases. The 98th AACR Annual Meeting, abstract #: 468, 2007.
- Behrens C, Lin H, Lee J, Hong WK, Wistuba II, Lotan R. Differential immunohistochemical expression patterns of fibroblast growth factor-2, receptors 1 and 2, and syndecan-1 in squamous cell carcinoma and adenocarcinoma of the lung. The 98th AACR Annual Meeting, 2007.

Conclusions

Core B continued to provide statistical and data management support for all research projects in the IMPACT study.

Core C: Pathology Core

(Director: Ignacio Wistuba, M.D.)

The IMPACT interdisciplinary research proposal for studying targeted therapy of lung cancers requires extensive histopathologic, immunohistochemical (IHC) and molecular studies of cell and tissues specimens, which are assisted, coordinated or performed by the Pathology Core. One of the most important roles of the Pathology Core is to coordinate and provide professional technical services for proper procurement, storage and use of human and animal tissues, as well as technical assistance for immunohistochemical analysis.

Aim 1 Develop and maintain repository of tissue, cell and serum specimens from patients with lung neoplasia requested by IMPACT research project PIs

Two groups of samples were proposed to be collected for the research projects: a) Prospectively, frozen and corresponding archival tumor and normal lung cancer patients undergoing surgery in our institution and patients enrolled in the clinical trials; b) Retrospectively, frozen and corresponding archival tumors and normal lung cancer patients' samples already banked in the Lung Cancer SPORE/MDACC Tissue Bank in which extensive clinical data, including smoking history and survival information is available.

Update

Project 1 – Drs. Ritsuko Komaki and Ray Meyn

- No specimens requested. Clinical trial has not started yet.

Project 2 – Drs. Juri Gelovani and Roy Herbst

- Retrospectively collected formalin-fixed and paraffin-embedded (FFPE) specimens from 284 NSCLC patients have been distributed and examined with Dr. Herbst's laboratory for IHC expression analysis of angiogenesis markers (VEGF/VEGFR) (see the Aim 4- Project 2 below).

- Retrospectively collected core biopsy and fine-needle aspiration (FNA) tissue and cell specimens (N=73) have been distributed for molecular biomarker analysis to predict response to EGFR TKIs in lung cancer patients (see the Aim 4- Project 2 below).

- Cross-body frozen tissue specimens have been processed and examined in the Pathology Core to obtain histology sections at thoracic level of mice injected with NSCLC cell lines (see the Aim 4- Project 2 below).

Project 3 – Drs. Renata Pasqualini and Wadih Arap

- We have identified retrospective FFPE specimens from 390 NSCLC cases in the M. D. Anderson Cancer Center Tissue Bank and distributed them to Dr. Pasqualini's laboratory.

- We have also examined GRP78, IL-11R and Eph5A markers expression by IHC in these specimens (see the Aim 4 - Project 3 below).

Project 4 – Dr. Reuben Lotan

- We identified retrospective FFPE specimens from 321 NSCLC cases in the M. D. Anderson Cancer Center Tissue Bank and distributed them to Dr. Lotan's laboratory.

- We have examined the expression of bFGF, receptors FGFR-1 and -2, and syndecan-1 using IHC (see the Aim 4 - Project 3 below). These data from these specimens was combined with that from 372 cases of normal bronchial epithelia and preneoplastic lesions, which were previously examined for the expression of the same set of IHC markers.

Project 5 – Drs. Fadlo Khuri and Shi-Yong Sun

- No specimens requested.

Project 6 – Drs. Ralf Krahe and Li Mao

- We have prospectively collected fresh NSCLC tumor tissue specimens (N=26) from the Pathology Frozen Room at M. D. Anderson and distributed them to Dr. Mao's laboratory to develop mouse tumor heterotransplant models. FFPE human tissue specimens from these cases have been also collected and banked in our Pathology Laboratory.

Aim 2 Develop innovative tissue and cell reagents from lung cancer patients for the investigation and validation of the molecular endpoints relevant to each component project.

The development of new tissue and cell reagents from lung cancer patients by this Core focuses on four different methodologies, three were described last year with progress updated here and one is new.

Update

1) *Tissue and cell pellets microarrays (TMA)*. The TMAs prepared last year (primary lung tumors, paired primary and brain metastasis NSCLC tumors, and cell lines pellets) have been utilized for IHC and fluorescent *in situ* hybridization (FISH) analyses (see Aim 4). A second generation of primary NSCLC TMAs is under construction containing all surgically resected tumors (N = 350) from the period Jan 1, 2003 to Dec 31, 2005. Also, the corresponding clinicopathologic data are being collected.

2) *Short-term cultures and cell lines of clinical lung tumor specimens*.

This work has not been initiated yet. The Pathology Core laboratory was moved to new facilities in December 2006, and we will be able to initiate this work this year.

3) *Lung cancer heterotransplants using clinical lung tumor samples*. In collaboration with Dr. Mao's lab (Project 6), we have collected fresh NSCLC (adenocarcinoma and squamous cell carcinoma histology) tumor specimens from 26 surgically resected tumors from the Pathology Frozen Room at M. D. Anderson to establish tumor heterotransplants in nude mice. Seven of such

heterotransplants have been established and tissue histopathological and IHC characterization is in progress (Figure 1).

4) *Pleural fluid specimens*. This year, through an agreement with M. D. Anderson Pulmonary Medicine Department, we have collected, processed and banked lung cancer pleural fluid specimens for preparation of cell smears, cell pellet FFPE blocks and histology sections, TMA cell pellets, frozen pellets and supernatants, and primary cell cultures. A laboratory-based research project has been recently submitted to the M. D. Anderson IRB for review and approval. These specimens will be important to examine molecular mechanisms involved in lung cancer pleural invasion. In the coming year, we plan to collect approximately 150 of these specimens, with a subset of paired primary tumor tissues and pleural fluid tumor cell pellets

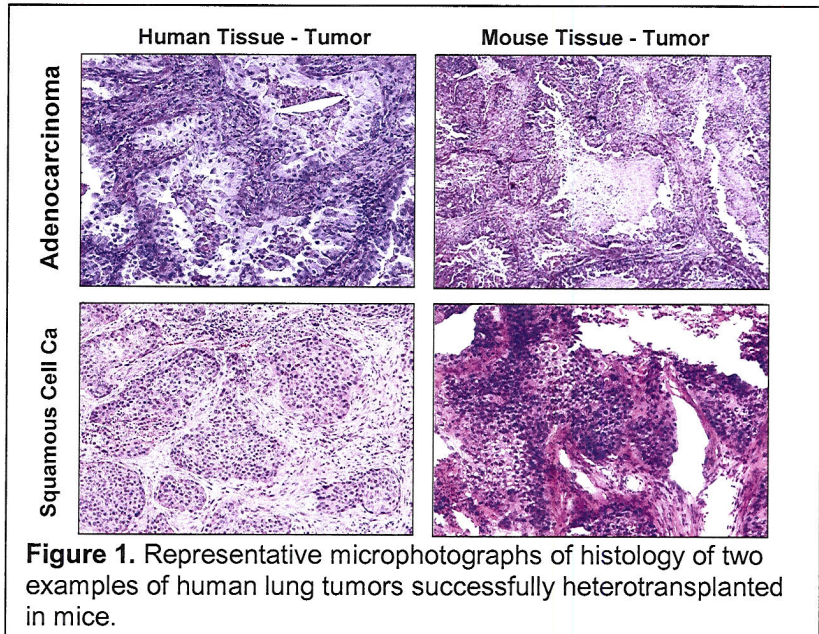


Figure 1. Representative microphotographs of histology of two examples of human lung tumors successfully heterotransplanted in mice.

Aim 3 Process human and animal cell and tissues for histopathological, immunohistochemical and molecular analyses, including tissue microdissection, as required by each component project.

Update

1) Tissue Processing. FFPE lung cancer tissues have been processed and distributed for Projects 2, 3, 4 and 6. Processing (cutting and H&E staining) for histology evaluation and sectioning for IHC has been performed in about 400 paraffin-embedded blocks from lung cancer, including TMA and whole tissue block specimens. Frozen lung cancer tissues and corresponding archival FFPE specimens have been processed and distributed for Project 6. Thoracic-level cross-body sections of mice injected with NSCLC cell lines have been prepared for histology and IHC analysis for Project 2. Tissue microdissection has not yet been requested by the research projects.

Aim 4 Perform and evaluate immunohistochemical analysis in human and animal cell and tissue specimens, as required by each component project.

Update

Collaboration with research projects

Examination of IHC markers in collaboration with IMPACT research projects is the most important activity of the Pathology Core during the second year, which has been performed by a Pathologist Post-doctoral Fellow (Ming Sun, M.D.) under the supervision of Dr. Wistuba.

Project 2. Three main tasks have been performed collaboratively in the Pathology Core.

1) Correlation of protein expression levels determined by IHC between VEGF/VEGFR2 and EGFR in early stage NSCLC. In collaboration with Drs. Roy Herbst and Juri Gelovani, we have performed a detailed analysis of the expression of Vascular Endothelial Growth Factor (VEGF) and its receptor (VEGFR) by IHC in a large number of NSCLC (N=284) using TMAs (Figure 2) to better understand the correlation between VEGFR and EGFR pathways expression. We have investigated the expression of VEGF-A, VEGF-R2, phosphorylated VEGF-R2 (p-VEGF-R2), EGFR and phosphorylated EGFR (p-EGFR). Correlations between VEGF-A, VEGFR2, p-VEGFR2 and clinicopathologic information and survival analysis were examined. In a subset of NSCLCs with adenocarcinoma histology, mutation status of *EGFR* and *KRAS* genes was correlated with IHC expression levels. Two hundred eighty-four surgically resected tumors, including 179 adenocarcinomas and 105 squamous cell carcinomas from patients with stage I-II-III A NSCLC were studied. A semi-quantitative analysis of nuclear, cytoplasmic and membranous localization was performed for each marker.

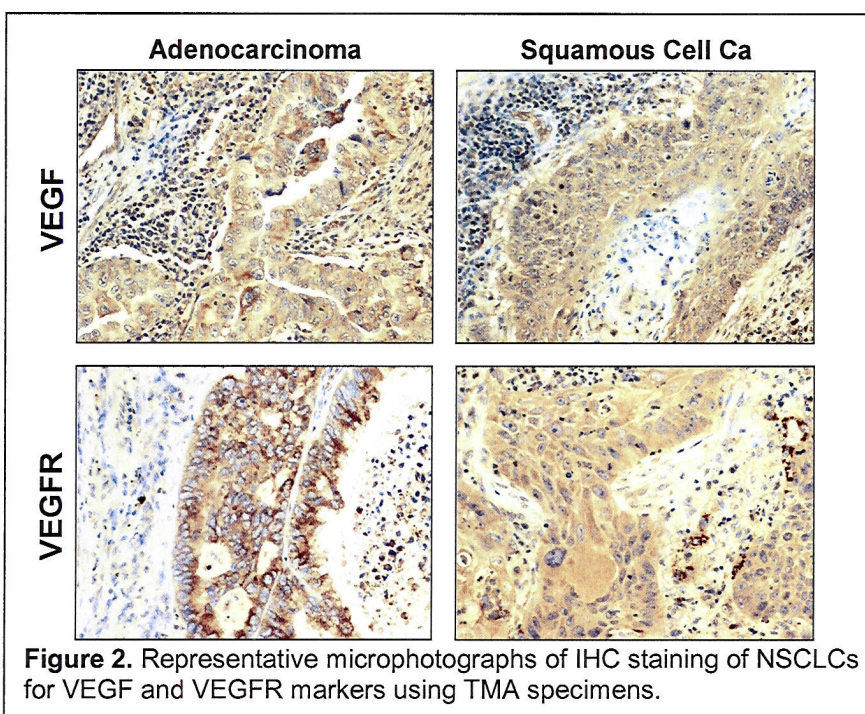


Figure 2. Representative microphotographs of IHC staining of NSCLCs for VEGF and VEGFR markers using TMA specimens.

Lung adenocarcinomas demonstrated higher levels of expression of cytoplasmic VEGF-A ($P = 0.0001$), membranous ($P = 0.005$) and cytoplasmic ($P = 0.03$) VEGF-R2, and membranous p-VEGF-R2 ($P = 0.0002$) compared to SCC. Lower VEGF-A ($P = 0.0009$) in membranous ($P = 0.01$) and cytoplasmic VEGF-R2 ($P = 0.02$) expression was statistically associated with non-smoking history. With a median follow up of 4.28 years, 91 deaths occurred. Independent of age, histology and stage, cytoplasmic p-VEGF-R2 expression was found to have a prognostic role for worse overall survival ($P = 0.01$, HR = 1.047, 95%CI = 1.01, 1.085). Of interest, significant increase of cytoplasmic and membranous p-EGFR expression was detected in tumors showing higher levels of cytoplasmic VEGF-A ($P = 0.01$ and $P = 0.0001$, respectively), VEGF-R2 ($P = 0.0001$ and $P = 0.0001$), and p-VEGF-R2 ($P = 0.0001$ and $P = 0.0003$). In the 15 *EGFR*-mutated cases a significant lower membranous VEGF-R2 expression was observed ($P = 0.02$). Higher membranous VEGF-R2 expression was observed in the 9 *KRAS* mutated cases, but this did not reach statistical significance.

Our findings indicate that the VEGFR and EGFR pathways are positively correlated in early stage NSCLC and expression of p-VEGF-R2 is an indicator of worse overall survival in stage I-IIIA NSCLC. These results will be presented in the 98th AACR Annual Meeting, 2007 (Massarelli et al., 2007).

2) KRAS Mutation is an Important Predictor of Resistance to Therapy with EGFR Tyrosine Kinase Inhibitors (TKI) in NSCLC. We have also examined a panel of molecular markers that could predict response to EGFR TKIs using retrospectively collected tissues. *EGFR* gene mutations and increased *EGFR* copy number have been associated with favorable response to EGFR TKIs in patients with NSCLC. In contrast, *KRAS* mutation has been shown to predict poor response to such therapy.

In addition, we have tested the utility of combinations of these three markers in predicting response and survival in patients with NSCLC treated with EGFR-TKIs. Patients with advanced NSCLC treated with EGFR-TKI with available archival tissue specimens were included. *EGFR* and *KRAS* mutations were analyzed using polymerase chain reaction (PCR)-based sequencing. *EGFR* copy number was analyzed using fluorescence *in situ* hybridization. Tumors with high polysomy or gene amplification were considered to have increased *EGFR* copy number.

The study included 73 patients, 59 of whom had all *EGFR* mutation and copy number, and *KRAS* mutation analyzed. *EGFR* mutation was detected in 7/71 patients (9.8%), increased *EGFR* copy number in 32/59 (54.2%), and *KRAS* mutation in 16/70 (22.8%). *EGFR* mutation ($P < 0.0001$) but not increased *EGFR* copy number ($P = 0.48$) correlated with favorable response. No survival benefit was detected in patients with either of these features. *KRAS* mutation correlated with progressive disease ($P = 0.04$) and shorter median time to progression ($P = 0.0025$) but not with survival. Patients with both *EGFR* mutation and increased *EGFR* copy number had a greater than 99.7% chance of objective response, whereas patients with *KRAS* mutation with or without increased *EGFR* copy number had a larger than 96.5% chance of disease progression.

We have concluded that *KRAS* mutation represents a marker of resistance of NSCLC to EGFR-TKIs and should be included in the panel of markers used to predict response to such therapy. A manuscript with these data has been recently submitted to *Clinical Cancer Research* and it is under review (Massarelli et al., 2007).

3) Histopathologic and immunohistochemical analysis of NSCLC xenograft mice models to investigate correlation between activated EGFR (pEGFR) expression and molecular imaging using NSCLC cell lines.

In collaboration with Dr. Gelovani, we have examined tumor histopathology and expression of EGFR and pEGFR Tyr1086 by IHC in cross body sections of mice injected with NSCLC tumor cells having mutant or wild-type *EGFR*. We have studied 10 mouse bearing tumors from 4 cell lines: PC14GL, H1975GL, H441GL and H3255GL. The cell lines H441GL and H3255GL have wild-type and mutant *EGFR*, respectively. Tumors in the thorax from cell lines H441GL and H3255GL were treated with EGFR TKI gefitinib. We also examined tumor histopathology and size. In addition, we examined the membrane and cytoplasmic expression of total and phosphorylated (Y1086) EGFR in tumors and normal lung. We detected hair follicle staining in the skin of the mice. Expression as determined by IHC was assessed for intensity (0, 1, 2, 3 and 4) and for extension (0-100%). A score was obtained by multiplying intensity and extension (range 0-400). We found that there was a reduction in the score and intensity of pEGFR membrane in all tumor specimens treated. Total levels of EGFR expression showed less reduction, with membrane reduction in H3255GL cell lines tumor treated at 24 hours and cytoplasmic reduction at 3 and 24 hours (for detailed data, please refer to the update for Project 2).

Project 3. In collaboration with Dr. Pasqualini (Project 3), we have performed a semi-quantitative analysis of membrane, cytoplasmic and nuclear expression of GRP78, IL11R and EphA5 markers by IHC in FFPE tissue obtained from surgically resected lung cancer specimens (Figure 3) and correlated those findings with clinicopathologic features of tumors and patients, including tumor histology, smoking history, TNM (tumor, node, metastasis) tumor stage, disease free and overall survival. The work started last year has been completed this year as summarized below.

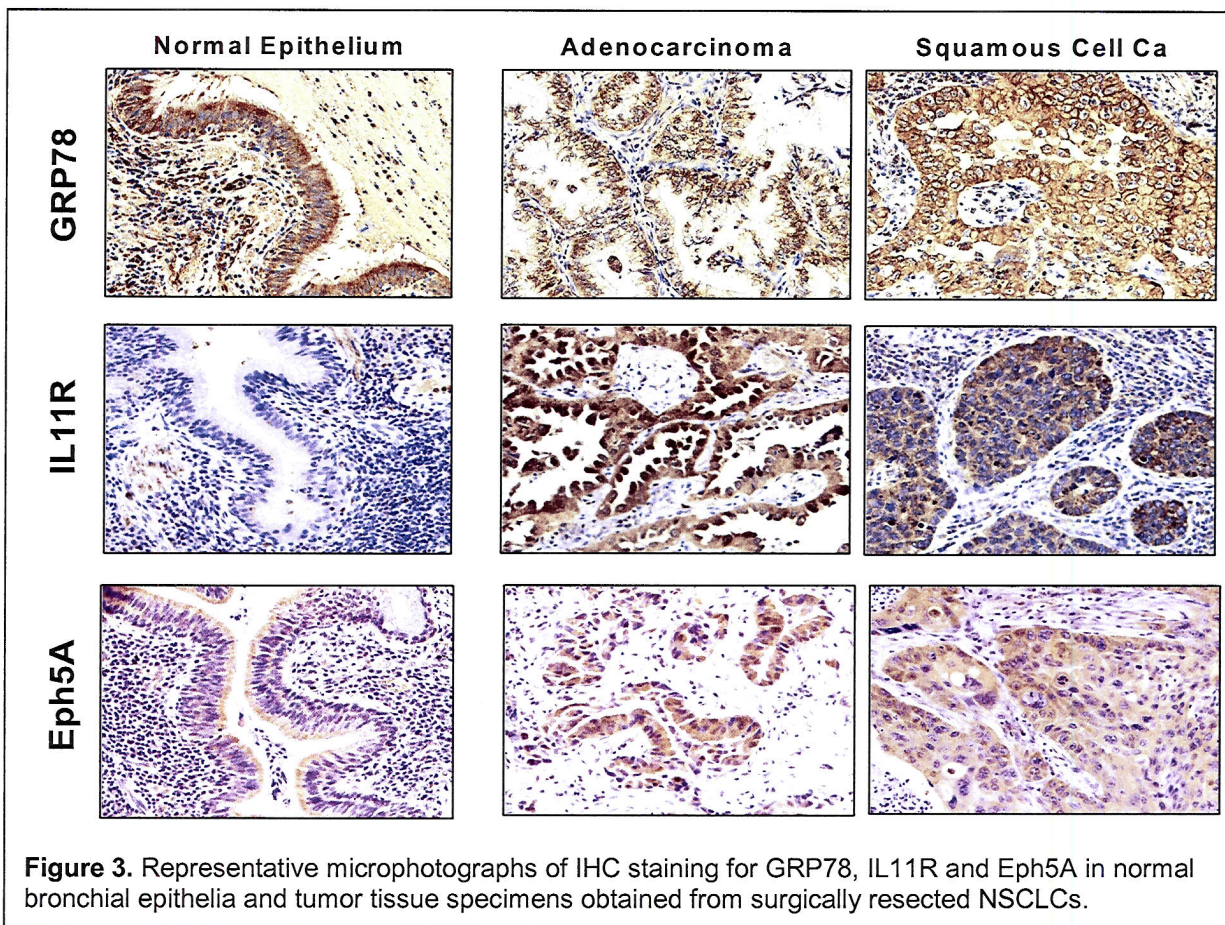


Figure 3. Representative microphotographs of IHC staining for GRP78, IL11R and Eph5A in normal bronchial epithelia and tumor tissue specimens obtained from surgically resected NSCLCs.

1) We first compared expression in histologically normal bronchial epithelia adjacent to tumors with tumor tissues obtained from 40 NSCLCs (20 squamous and 20 adenocarcinomas), and found that:

- The expression of GRP78 in the cytoplasm of tumor cells was lower than in cytoplasm of normal bronchial epithelia ($P = 0.06$).
- The expression of IL11R in the cytoplasm of tumor cells was higher than in cytoplasm of normal bronchial epithelia ($P = 0.003$).
- The expression of EphA5 in nucleus of tumor cells was higher than of the levels in normal bronchial epithelia ($P = 0.07$), and the EphA5 expression in the cytoplasm of tumor cells was not significantly different from that in cytoplasm of normal bronchial epithelia ($P = 0.45$).

2) We then examined the expression of GRP78, IL11R and EphA5 in lung cancer TMAs containing 301 NSCLCs (192 adenocarcinomas and 109 squamous cell carcinomas) and 26 SCLCs with annotated clinical data using IHC. We performed analysis of immunostaining using microscope evaluation by 2 independent observers, and consensus data were used for further analysis. Overall, high levels of GRP78, IL11R and EphA5 expression were detected in lung cancer tumor specimens. Significant differences in the expression of these markers were detected comparing both tumor types (Table 1): a) NSCLCs histologies, adenocarcinoma and SCC, demonstrated significantly higher levels of GRP78 expression in cytoplasm and membrane of tumor cells compared with SCLC; b) NSCLCs showed higher levels of cytoplasmic expression of IL11R, but lower levels of membrane expression; c) EphA5 expression was higher in NSCLC tumor cells compared with SCLC. For NSCLCs adenocarcinoma and squamous cell carcinoma histologies, a detailed analysis comparing GRP78, IL11R and EphA5 expression in tumor cells with patients' clinicopathologic features, including tumor histology, age, gender, smoking history, pathological TNM stage, disease free and overall survival, was performed. Significant differences in the expression of these markers were detected comparing both NSCLC histologies with adenocarcinomas demonstrating higher levels of cytoplasmic GRP78 ($P = 0.0003$) and cytoplasmic IL11R ($P < 0.0001$). In contrast, squamous cell carcinomas showed significantly higher expression for membrane GRP78 ($P = 0.003$) and EphA5 ($P = 0.002$). Only IL11R demonstrated correlation with smoking status, with tumors from patients that ever smoked had higher levels ($P = 0.005$) of cytoplasmic IL11R than never smokers. No correlation between marker expression and disease free and overall survival was detected.

Table 1. Expression of GRP78, IL11R and EphA5 in lung cancer TMA specimens.

Marker	Tumor Histology			Difference among histology groups (P-Value)
	Adenocarcinoma (n = 192)	Squamous (n = 109)	SCLC (n = 26)	
GRP78				
Cytoplasm Mean (SD)	210.2 (61.8)	182.8 (56.8)	119.0 (74.5)	<0.0001
Membrane N (%)	123 (70)	100 (93)	11 (52)	<0.0001
IL11R				
Cytoplasm Mean (SD)	133.8 (60.9)	116.4 (56.2)	109.7 (37.6)	0.02
Membrane N (%)	31 (18)	36 (33)	9 (50)	0.0008
EphA5				
Cytoplasm Mean (SD)	133.5 (50.6)	125.9 (43.4)	82.3 (40.5)	<0.0001
Membrane N (%)	54 (30)	65 (61)	2 (10)	<0.0001
Nucleus N (%)	125 (70)	78 (73)	20 (95)	0.02

Project 4. Differential expression patterns of bFGF, receptors FGFR-1 and -2, and syndecan-1 in NSCLC. In collaboration with Dr. Lotan (PI, Project 4) and Dr. Behrens (co-PI, Project 4), IHC analysis of bFGF and receptors FGFR-1 and -2 and heparan sulphate proteoglycan syndecan-1 (SDC-1) has been performed in 301 NSCLC specimens in TMAs (Figure 4), and investigated the simultaneous expression of all four markers in a large set of NSCLCs with annotated clinic and pathologic information.

We performed semi-quantitative IHC expression analysis of 196 lung adenocarcinomas (ADCA) and 125 SCC using formalin-fixed specimens in TMAs. FGF2, FGFR-1, and FGFR-2 were examined in tumor cells and SDC-1 in tumor (SDC-1T) and stromal (SDC-1S) cells.

Overall, we found high levels of expression of all markers in NSCLC. SCC expressed significantly higher levels of nuclear FGF2 ($P=0.01$), cytoplasmic FGFR-2 ($P = 0.006$), SDC-1T ($P < 0.0001$) and SDC-1S ($P < 0.0001$). ADCA expressed higher levels of nuclear FGFR-1 ($P < 0.0001$) and FGFR-2 ($P = 0.003$). Patient's clinical-pathologic data when correlated with expression of the markers showed different patterns of correlations in ADCA and SCC, especially for gender and smoking. In univariate analysis, females demonstrated higher levels of nuclear FGF2 ($P = 0.03$), nuclear FGFR-1 ($P = 0.019$) and SDC-1T ($P = 0.03$) than males in ADCA, while males had higher SDC-1T ($P = 0.02$) in SCC. Among ADCAs, smokers demonstrated higher levels of cytoplasmic FGFR-1 ($P = 0.04$) and SDC-1S ($P = 0.02$) and lower levels of nuclear FGFR-1 ($P = 0.002$) and FGFR-2 ($P = 0.04$). Among SCCs, smokers demonstrated higher nuclear FGFR-2 ($P = 0.02$). A complex pattern of marker correlations was detected: ADCA and SCC showed correlation between nucleus and cytoplasm for FGFR-2 ($P = 0.0005$) and between cytoplasms of FGF2 and FGFR-1 ($P < 0.03$) and FGFR-1 and FGFR-2 ($P < 0.0001$); only in ADCAs, nuclear FGFR-1 correlated with nuclear FGF2 and FGFR-2 ($P <$

0.0001 and 0.0003, respectively), and SDC-1T correlated with nuclear FGF2, FGFR-1 and FGFR-2 ($P = 0.04, 0.006$ and 0.02, respectively); in SCC, SDC-1T correlated with cytoplasmic FGF2 and FGFR-2 ($P = 0.002$ and 0.02, respectively) and nuclear FGFR-1 ($P = 0.05$). SDC-1S only showed correlation with SDC-1T in SCC ($P = 0.0002$).

We have concluded that FGF2, FGFRs and SDC-1 are frequently overexpressed in NSCLC, although different patterns of expression were detected in the two major forms of NSCLCs. Our findings suggest that FGF2 signaling pathway is frequently activated in NSCLC, but tumor characteristics must be considered to develop therapeutic strategies. These results will be presented in the 98th AACR Annual Meeting, 2007 (Behrens et al., 2007).

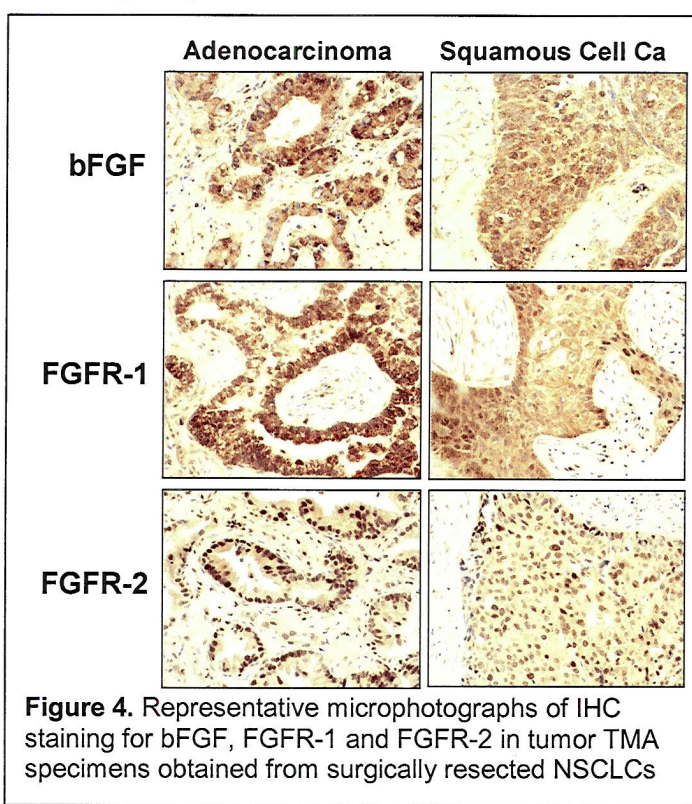


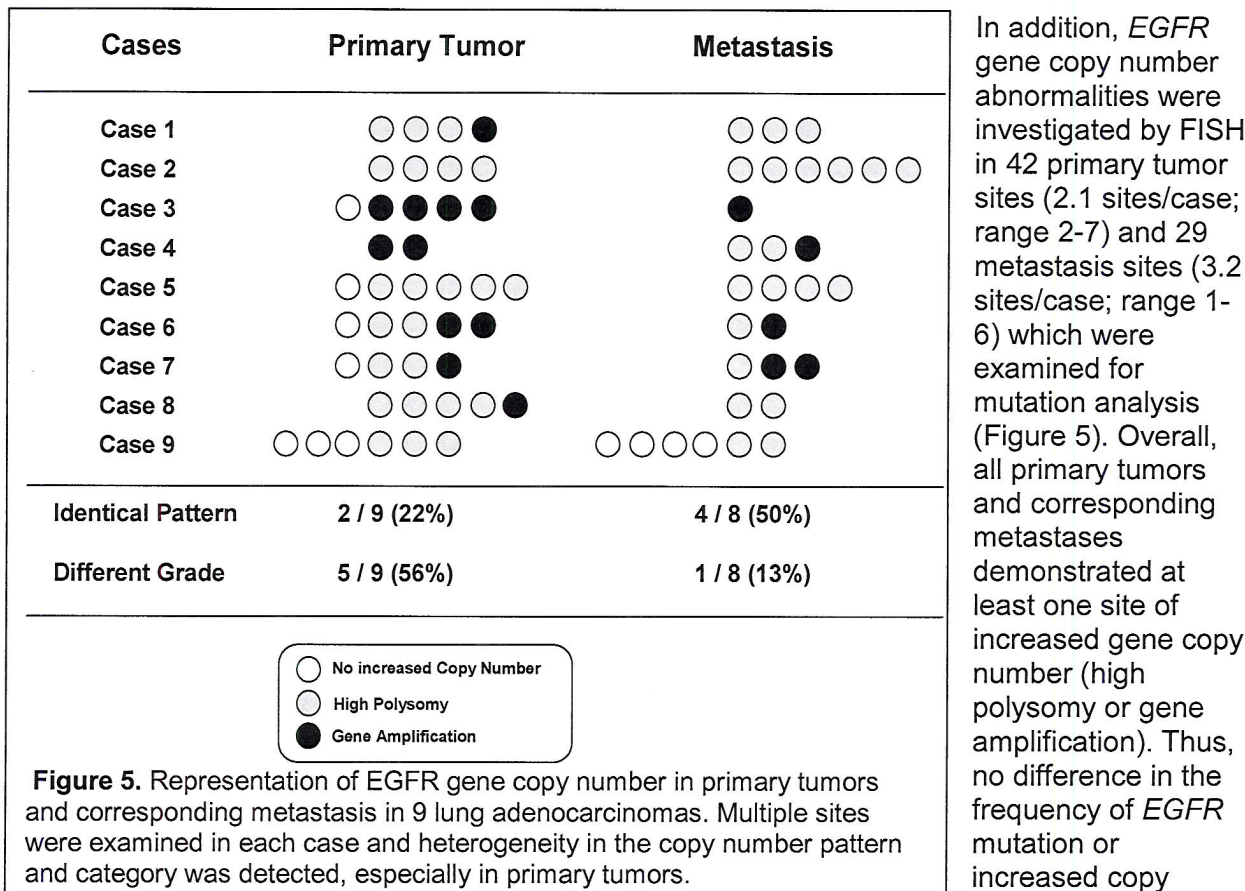
Figure 4. Representative microphotographs of IHC staining for bFGF, FGFR-1 and FGFR-2 in tumor TMA specimens obtained from surgically resected NSCLCs

Additional IMPACT research activities of the Pathology Core

In addition to the responsibilities described above, the Pathology Core has performed independent research activities to better characterize the *EGFR* molecular abnormalities: a) involved in the pathogenesis and progression of lung cancer, and b) to establish their role in the development of lung cancer brain metastasis. These results will be integrated into the ongoing research activities in the corresponding IMPACT research projects (Projects 1 and 2). As a result of this work, we are preparing a manuscript for submission to *Clinical Cancer Research* (Tang et al., 2007) and some results will be presented in the 98th AACR Annual Meeting, 2007 (Sun et al., 2007).

a) EGFR abnormalities in the progression of lung adenocarcinomas. Using a detailed molecular pathology mapping strategy, we investigated the frequency and characteristics of EGFR abnormalities (mutation, copy number and protein expression) in normal bronchial and bronchiolar epithelia field, primary tumors and corresponding lymph node metastases obtained from 24 lung adenocarcinoma specimens with *EGFR* mutation and compared the findings with similar samples obtained from 26 lung adenocarcinomas with wild-type *EGFR*.

We selected 9 lung adenocarcinomas with known EGFR mutations (5 cases for exon 19; 4 cases for exon 21) and with lymph node metastasis from which there was sufficient tissue to perform our mapping analysis. For mutation analysis of *EGFR* exons 19 and 21, precise tissue microdissection from non-contiguous primary tumoral foci (N = 59 sites; 6.5 sites/tumor; range 2-11) containing at least 1,000 cells was performed. Surprisingly, 4 of 9 tumors examined demonstrated mixed *EGFR* mutation patterns. Three primary tumor specimens demonstrated two types of exon 19 deletions: one case had 7 sites with the 15bp deletion 746-750, 4 sites had the 12bp deletion 748-751; one with 8 sites with 12bp deletion 748-751 and 1 site with 15bp deletion 746-750; and, one case with exon 19 deletion 15bp 746-750 in 8 sites and exon 21 L858R mutation in 1 site. The remaining case demonstrated 5 sites with exon 19 15bp deletion 746-750 and 2 sites with wild-type sites. *EGFR* mutation analysis of corresponding 30 lymph node metastasis sites from the 9 *EGFR* mutant cases (3.3 sites/case; range 1-6) revealed only one type of *EGFR* mutation detected in all tumor sites in each case, and the mutation detected was always present in at least one site of the corresponding primary tumor. Similarly to the corresponding primary tumor, one metastasis case demonstrated wild-type (2 sites) and *EGFR* mutant (1 site; exon 19, 15bp deletion 746-750) tumor sites. Our findings showed a relatively high level of heterogeneity for *EGFR* mutation, with several tumor cell clones having different pattern of mutation, in primary tumor specimens, but not in lymph node metastasis sites.



number was detected comparing primary tumors and metastases (Table 2). However, 5 (56%) primary tumors and 1 (11%) metastasis cases demonstrated at least one site without increased copy number (disomy in 1 primary tumor site; high trisomy in 1 metastasis site; and low polysomy in 7 primary and 3 metastasis tumor sites; *EGFR* copy number heterogeneity was higher in the primary tumor than in the corresponding metastasis cases. In 2 (22%) primary tumors and 4 (50%) metastases, identical *EGFR* copy abnormality was detected in all sites examined. In contrast, 5 (56%) primary tumors and only 1 (13%) metastasis case demonstrated a combination of not-increased and increased copy number sites.

A tumor site having positive expression of *EGFR* and p*EGFR* was detected by IHC in 16/24 (67%) and 7/15 (47%) of *EGFR* mutant primary adenocarcinoma cases, respectively. The protein expression of both markers was heterogeneous, especially for p*EGFR*. While *EGFR* was detected in 66/102 (65%; 4.25 sites/case examined) distinct sites, p*EGFR* was positive in 15/103 (15%; 4.29 sites/case examined) tumor sites (Table 2). In 9 *EGFR* mutant lung adenocarcinoma cases, both primary tumors and corresponding lymph node metastases were examined for *EGFR* and p*EGFR* expression by IHC. For both tumor locations combined, 96 distinct tumor sites were examined (N = 65 primary tumor sites, 7.2 sites/case; and N = 31 metastasis sites, 3.4 sites/case). Significantly higher levels of *EGFR* ($P = 0.0219$) and p*EGFR* ($P < 0.00001$) expression were detected in metastases (*EGFR* 27/31, 87%; p*EGFR* 21/31, 68%) compared to primary tumor sites (*EGFR* 42/65, 65%; p*EGFR* 13/52, 20%) (Table 3). Whereas no correlation between *EGFR* and p*EGFR* expression and *EGFR* copy number status by FISH was detected, the 14 tumor sites with wild-type *EGFR* sequence demonstrated slightly lower expression of *EGFR* (7/14, 50%) and p*EGFR* (5/14, 36%) compared to those with mutant *EGFR* (*EGFR* in 79% and p*EGFR* in 44%).

Table 2. Summary of *EGFR* abnormalities in the progression of lung adenocarcinoma (N = 9 cases)

Samples Sites	Gene Abnormalities		Protein Expression (IHC)	
	Mutation Positive	Increased Copy Number ¹	EGFR Positive ²	p <i>EGFR</i> Positive ¹
Primary Tumor	57/59 (97%)	34/42 (81%)	42/65 (65%) ³	13/52 (20%) ⁴
Metastasis	28/30 (93%)	25/29 (86%)	27/31 (87%) ³	21/31 (68%) ⁴

¹ High polysomy and gene amplification; ² Positive immunohistochemical (IHC) expression score >200 (range 0-400); ³ Primary tumor vs. metastasis $P = 0.02$; ⁴ Primary tumor vs. metastasis $P < 0.00001$

b) Differential immunohistochemical expression pattern of HER family receptors and ligands detected in primary lung cancers and corresponding brain metastases. The brain is one of the main metastatic sites for lung cancer patients and those metastases occur in about 50% of patients with NSCLC. Despite recent advances in lung cancer targeted therapy research, there is limited information on the molecular characteristics of lung cancer brain metastases and on markers that can predict their development. In NSCLC, the over-expression of HER family receptors and ligands has been involved in tumor pathogenesis and progression (Herbst et al., 2004), and some of those markers have been associated with the prediction of response to EGFR TKIs (Prudkin et al., 2006)).

We investigated the level of expression of 3 HER family receptors and 3 ligands in a series of primary NSCLCs and corresponding brain metastasis (N = 57 pairs) using IHC, and compared the level of expression of markers between primary tumors with (N = 57 cases) and without (N = 81 controls) brain metastases. Archival formalin-fixed tissues obtained from surgically resected primary tumors and metastases were placed in tissue microarrays and examined for expression of *EGFR*, phosphorylated-*EGFR* (p*EGFR*), Her2, Her3, phosphorylated-Her3 (p*Her3*), EGF, amphiregulin (AR) and TGF α using semi-quantitative IHC. All markers were examined at membranous (M), cytoplasmic (C) and nuclear (N) localization in tumor cells.

Statistically significant higher levels of N- ($P < 0.001$) and M-AR ($P = 0.06$), M-pHer3 ($P = 0.001$), and M- and C-pEGFR ($P < 0.001$) were found in brain metastases compared to corresponding primary tumor tissues. In contrast, brain metastases showed lower levels ($P = 0.018$) of C-TGF α expression than primary tumors. Interestingly, in multivariate analysis the expression of M-pHer3 in primary tumors correlated ($P = 0.02$, HR 1.02, 95%CI=1.003-1.043) with shorter time to brain metastases development. Primary lung tumors with brain metastases showed statistically significant higher expression of C- and M-EGF ($P < 0.0001$) and C-Her2 ($P = 0.003$) compared to primary tumors without such metastasis. In contrast, M-AR, C-, M- and N-pHer3, M-EGFR, M- and C-pEGFR markers showed statistically significant higher levels of expression in primary tumors without brain metastases.

Our data indicate differential expression pattern of HER family receptors and ligands in lung cancer and corresponding brain metastases, with AR, pHer3 and pEGFR being significantly over-expressed in metastasis sites. A complex pattern of expression of HER family receptors and ligands differentiate primary NSCLC tumors with and without brain metastases. We conclude that brain metastasis sites must be examined for molecular target expression to better predict the response to targeted therapy in lung cancer patients. These results will be presented in the 98th AACR Annual Meeting (Sun et al., 2007).

Key research accomplishments

- Developed a repository of lung cancer tissue specimens, including TMAs, to be utilized for research projects.
- Assisted with the development of a series of lung cancer heterotransplants in mice in collaboration with Project 6.
- Utilized NSCLC primary tumors and brain metastasis TMA specimens for IHC analysis and other *in situ* techniques.
- Characterized the expression of angiogenic markers (VEGF/VEGFR and bFGF/receptors) in NSCLC and correlated with clinicopathologic features and EGFR pathway.
- In collaboration with Project 2, identified KRAS gene mutation as a negative predictive factor for response to EGFR TKI using clinical specimens and characterization of EGFR abnormalities and HER family proteins expression in the progression and metastasis of NSCLC.

Reportable outcomes

Manuscripts published in peer-reviewed journals

- Massarelli E, Varella-Garcia M, Tang X, Xavier AC, Ozburn N, Liu DD, Bekele BN, Herbst RS, Wistuba II. KRAS Mutation is an Important Predictor of Resistance to Therapy with Epidermal Growth Factor Receptor Tyrosine Kinase Inhibitors in Non-Small Cell Lung Cancer. *Clin Cancer Res* (in press), 2007.

Abstracts

- Massarelli E, Maria L, Silva P, Ozburn N, Feng L, Yin G, O'Reilly M, Hong WK, Herbst RS, Wistuba II. Correlation between VEGF/VEGFR2 and EGFR immunohistochemical protein expression in early stage non-small cell lung carcinoma. The 98th AACR Annual Meeting, abstract #: 5029, 2007.
- Sun M, Massarelli E, Feng L, Ozburn N, Yin G, Komaki R, Hong WK, Aldape KD, Wistuba II. Differential immunohistochemical expression pattern of HER family receptors and ligands is detected in primary lung cancers and corresponding brain metastases. The 98th AACR Annual Meeting, abstract #: 468, 2007.

- Behrens C, Lin H, Lee J, Hong WK, Wistuba II, Lotan R. Differential immunohistochemical expression patterns of fibroblast growth factor-2, receptors 1 and 2, and syndecan-1 in squamous cell carcinoma and adenocarcinoma of the lung. The 98th AACR Annual Meeting, abstract #: 6412, 2007.

Manuscripts in Review or Preparation

- Tang X, Varella-Garcia M, Xavier AC, Massarelli E, Ozburn N, Moran C, Wistuba II. EGFR Abnormalities in the Pathogenesis and Progression of Lung Adenocarcinomas. Manuscript (in preparation), 2007.

Conclusions

The Pathology Core has assisted and collaborated actively with several research projects by performing multiple histopathological, immunohistochemical and molecular studies in a large series of lung cancer tissue specimens. Several abstracts have been presented in international meetings and manuscripts are in press or in preparation for submission. In addition, the Pathology Core has managed to conduct specific research activities, which fully integrate with several IMPACT research projects. The Pathology Core has successfully fulfilled the goals proposed in the second grant year.

Core D: Imaging Core: Provide Imaging Support for IMPACT Projects

(PI and co-PI: Juri Gelovani, M.D., Ph.D.; Chun Li, Ph.D.)

In the first grant year, the Imaging Core provided support for IMPACT projects 2, 3, and 4 as previously detailed. This year, Projects 2 and 4 were main focus.

Update

Project 2. Molecular imaging of EGFR expression and activity in targeted therapy of lung cancer. The Imaging Core has synthesized a precursor of JGAP5 that was then radiolabeled with isotopes ¹³¹I and ¹²⁴I, and developed and optimized the radiolabeling procedures for routine synthesis of ¹³¹I- and ¹²⁴I-JGAP5 (Figure 1). It is noteworthy that the compound JGAP-5 was selected because it was highly soluble in water and was expected to have less hepatobiliary clearance and, as a result, have a longer half-life of plasma circulation.

Towards the end of this funding period, the Imaging Core initiated the development and evaluation of the last set of IPQA derivatives with a hydrophilic side chain on the 7-position of quinazoline moiety (Figure 2).



Figure 1. Structure of the novel lead candidate JGAP5 with improved water solubility.

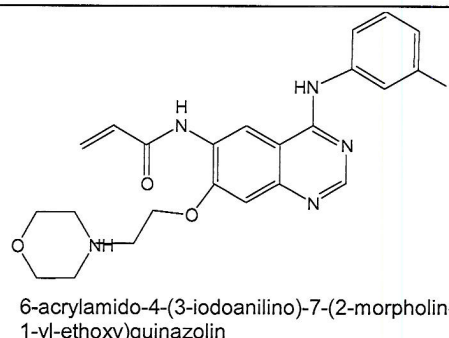


Figure 2. A representative chemical structure of the 3rd generation of EGFR kinase specific ¹²⁴I-labeled radiotracers with improved water solubility.

Project 4. Inhibition of bFGF signaling for lung cancer therapy. Imaging Core has developed A549 cells expressing GFP-Luciferase (GL) dual-modality reporter gene for imaging of tumor fluorescence (FLI) and bioluminescence (BLI). The expression of the GL reporter gene in A549GL cells was assessed by FACS (GFP positive cells were selected by sorting) and by BLI imaging with IVIS200 system (Xenogen, Hopkinton, MA) 2–5 minutes after addition of D-luciferin (Biosynth, Int., Naperville, IL) substrate at 150 μ g/mL in medium to each well.

Subsequently, the A549GL cells were provided to Dr. Reuben Lotan (PI of Project 4) to conduct *in vitro* and *in vivo* animal studies as mentioned in the update for Project 4. Once the animal study begins, the Imaging Core will monitor the tumor growth rate and responses to therapy with BLI following administration of D-luciferin at 150 mg/kg in PBS by i.p. injection.

Key Research Accomplishments

- Produced novel IPQA derivative JGAP5 radiolabeled with ^{124}I and ^{131}I for PET and *in vitro* uptake studies for Project 2.
- Performed all multi-modality imaging (and autoradiography) studies in mice with orthotopic models of different NSCLC cells using ^{124}I -JGAP5 (EGFR expression/activity), ^{18}F -FMAU (1-(2'-fluoro-2'-deoxy-d-arabinofuranosyl)-5-methyluracil; proliferative activity), and ^{18}F -FDG (2-[fluorine-18]fluoro-2-deoxy-D-glucose; glucose metabolism) for Project 2.
- Installed an automated radiosynthesis module TraceLab-FN (GE Healthcare, Milwaukee, WI) and established a routine CGMP grade synthesis of ^{18}F -FLT (3'deoxy-3'-[^{18}F]fluorothymidine) and ^{18}F -FMAU for PET/CT imaging of tumor proliferative activity, which can be applied for the assessment of early responses to therapy in preclinical and in upcoming clinical trials.,
- Maintained SOPs and performed QC/QA procedures for routine synthesis of ^{111}In -DTPA (diethylenetriaminepentaacetic) -PEG (polyethylene glycol)-AnnexinV for SPECT (single photon emission computed tomography)/CT imaging in Project 1.
- Performed routine synthesis of [^{18}F]FEAU (2'-fluoro-2'-deoxyarabinofuranosyl-5-ethyluracil) for Project 3.
- Maintained synthesis and ^{111}In / ^{64}Cu radiolabeling of GRP78-specific cyclic nanopeptide CGRRAGGSC for imaging studies in Project III for imaging studies with ^{64}Cu -DOTA-CGRRAGGSC PET/CT in animals for Project 3.

Reportable Outcomes

None at this time.

Conclusions

The Imaging Core continues to provide imaging support requested by the PIs of IMPACT research projects, in addition to synthesizing more optimal IPQA derivatives.

DRP-1: Treatment of Malignant Pleural Effusion with ZD6474, a Novel VEGFR and EGFR TK Inhibitor

(PI and co-PI: Roy Herbst, M.D., Ph.D., Carlos Jimenez, M.D.)

Aim 1 To determine clinical effects of ZD6474.

Aim 2 To investigate biological correlates.

Aim 3 To investigate radiographic correlates.

Aim 4 To assess quality of life.

Update

In September 2006, Dr. Amir Onn, the former principal investigator (PI), left M. D. Anderson to return to his home country. Dr. Roy Herbst, the former co-PI, was thus assigned to be the PI of the trial. Approval documents by the IRB are attached in Appendix F – DRP-1- Memo of PI change and IRB approval letter.

As reported last year, after AstraZeneca approved the revised protocol, we then submitted it to our Clinical Research Committee (CRC) for review on February 21, 2006, and subsequently to our IRB and the DoD. The protocol was approved by our IRB on August 08, 2006, and by the DoD on August 16, 2006. On October 13, 2006, the clinical trial was activated for study enrollment.

To date, 16 patients have been screened for enrollment. However, no patients have been consented for study participation. The most significant reasons for the current low accrual are: 1) Concerns by both physicians and patients about randomization to the placebo arm for 10 weeks without treatment, and 2) Eligibility criteria that may cause some difficulty in successful recruitment for a given patient population. After careful review of the protocol and consultation with the clinical research team, the study investigators and the study statistician decided to modify the study design and broaden the eligibility criteria in an effort to reach its accrual goal and achieve the study objectives. The modifications are as follows:

1. The study design will be revised from a randomized, double-blind, placebo-controlled study to a single arm, open-label study to evaluate the efficacy of ZD6474 on the management of pleural effusion in NSCLC patients. The primary objective, duration of study treatment, target patient population, and safety monitoring procedures remain the same as in the current approved study design. The expected treatment effect of ZD6474 – a 50% reduction in the medium time to catheter removal compared to without treatment – remains the same as well. The revised design is a 15 month study which requires enrollment of 25 patients in 13 months plus an additional 70 days of follow up. These goals are feasible and we expect to complete the study in the grant funding period.
2. The eligibility criteria will be modified from allowing no prior malignancy within the last five years to within the last two years and originally INR ≥1.5 and PTT ≥ 30 to INR ≥ 2.5 only, removing the term no evidence of coagulopathy, and adding patients with blood diathesis in exclusion criteria.
3. Remove the dynamic contrast CT measurements since these studies are quite costly and take a great deal of time for the patients and do not constitute the primary endpoint.

We have recently completed the revisions and are prepared to submit for HSRRB, AstraZeneca, and MDACC IRB review and approval. If appropriate, we would like to request an administrative review of the protocol amendment with the hope of re-opening the study as soon as possible. A final approved protocol, informed consent, and the approval letter will be included in next year's report.

Key Research Accomplishments

- The original protocol was approved and the trial was opened.
- The amended protocol has been submitted to AstraZeneca and our IRB for review and approval.
- 16 patients were screened for enrollment under the original protocol.

Reportable Outcomes

None at this time.

Conclusions

No conclusion can be reached up to this point.

DRP-2: TALK - Teens and Young Adults Acquiring Lung Cancer Knowledge

(PI: Alexander V. Prokhorov, M. D., Ph.D.)

Ninety percent of lung cancer cases in adults are the direct result of smoking. In children and young adults, tobacco use remains a major public health problem in spite of the recent declines in smoking prevalence among children and adolescents. Over the past 2-3 decades, numerous factors of smoking initiation among adolescents have been thoroughly investigated. A considerable volume of literature is currently available providing important clues with respect to designing tobacco prevention and cessation programs among youth.

Focusing on this major public health problem of tobacco use among young individuals and the lack of in-depth knowledge of lung cancer issues, Project TALK was conceived and funded as a smoking cessation/prevention pilot project for culturally diverse high-risk young populations that include school drop-outs, economically disadvantaged, and underserved. Using modern technologies, the Departments of Behavioral Science and Thoracic/Head & Neck Medical Oncology have joined their efforts to conduct this developmental project under the leadership of Dr. Alexander V. Prokhorov. The project will assist in making major advances in lung cancer education and prevention among youth. The major goal for Project TALK is to produce a CD-ROM-based education/behavior change for teenagers and young adults (15-24 years of age).

We have thus been devoting our effort in 4 tasks as described in the Statement of Work based on the project timeline:

Task 1. **Develop intervention program.** Focus groups will be held with adolescents and young adults to ensure we are capturing the essence of the program, using the right messages, and employing the appealing video and animated characters. (Years 1-2)

Task 2. **Develop and beta-test CD-ROM.** This includes the design of the animation, illustrations, scripts and accompanying videos. (Years 1-2)

Task 3. **Implement program in agreed upon locations and recruit young adults to participate in the study.** (Years 3-4)

Task 4. **Collect and analyze data.** (Year 3-4)

Years 01-02 have been devoted to intervention program conceptualization and development. Beginning in March 2007 (Year 03), the program will be tested among an ethnically diverse

sample of youth to evaluate its feasibility and impact. In this annual report, TALK development procedures and graphic products are provided.

Update

In the second program year, exciting new paths were included, which resulted in an even more promising smoking prevention/cessation tool. The Project TALK team met weekly to discuss the design of the project, its timeline, and multiple time sensitive tasks ensuring a quality interactive “gaming” product.

The design of the game’s Graphic User Interface (GUI) involved several steps. The first aspect of Project TALK was built based on theoretical underpinnings finalized during Year 01. Three different interfaces, the Amazing Race, Extreme Health Rescue, and Psy-Ops (Psychological Operations) were conceived. Prototypes of all three were built and TALK personnel chose one, Psy-Ops. These images were presented with the Year 01 report. Scripts relating to the graphic game elements were written and were also included in last year’s report too, therefore, will not be included here.

During Year 02, Project TALK staff, Alexander V. Prokhorov, M.D, Ph.D., Ellen R. Gritz, Ph.D., Mario Luca, M.S., Nancy Stancic Luca, Ph.D., Kentya Ford, Dr. PH., Julie John, in cooperation with the contracted *Radiant Create Group*, continued to develop the program. Keeping to the TALK timeline, the first focus group was held on March 27, 2006. The concept was presented and tested with 2 focus groups (a total of 8 students) at the University of Houston’s Health Center. Four questions were asked and discussed:

- 1) Was the game approach appropriate?
- 2) How can we improve the program?
- 3) What do you think of the Avatar and Program Guide? Are they tailored to represent different race/ethnic groups?
- 4) Would a smoker complete the program and what motivates a smoker to quit?

The first focus group subjects expressed that the program is appropriate for middle and high school students. Subjects thought that more realistic medical and emotional aspects of tobacco use needed to be added, and they suggested that the ethnicity of Avatars should be broadened (e.g., one student noticed that White and Asian characters were not shown). Students also felt that the smoking in the movies segment was a needed component. Finally, they said that 15-24 year-olds may already know the information but the information can be given in a more real and emotional way. For a full report on the focus group see the Appendix G - TALK-1.

A second focus group session with a minority population was held on April 28, 2006. Its purpose was to test the usability of the program, observe any problems with navigation, and to offer more feedback to staff for program enhancement. During this focus group, participants worked through the game for 30 minutes without any instruction from the Project TALK staff and were then interviewed by staff about their opinions and enthusiasm for the game. All users reported that they liked the animation and game style. They also indicated that it was appropriate for their age and appealed to them. The male participants were excited by the prospect of seeing a surgery performed. Regarding usability, participants suggested more orientation instructions, additional pop-up hints when users get stuck, and bonus item messages must appear on the game screen. For a full report on this focus group see the Appendix G - TALK-1 - Focus groups.

In addition, during this year, two new members joined the research team: Drs. Joel Dunnington (Associate Professor, Diagnostic Radiology) and Garrett Walsh (Professor, Thoracic & Cardiovascular Surgery). Both are medical professionals at M. D. Anderson and are proactive

tobacco control advocates. They offered and shared their knowledge. Dr. Dunnington provided tobacco facts that were included and recruited celebrities who were victims of second hand smoke who agreed to give a videotaped statement to also be included in the game. Dr. Walsh has reviewed the program and assisted with audiovisual materials pertinent to lung cancer surgery. With the two expert collaborators' advice and material, and the focus group participant responses, the look of the game was transformed. Fortunately, the original four mapping tracks for each type of smoker (stage introduction, physical, emotional/mental and social) were maintained, only the theme (setting) changed from a community setting to hospital *Healthscare General*. The TALK program is now named "*Escape with Your Life*." The media map spreadsheet describing each hospital room and its stage of production, was created for *Hospital Healthscare* and can be found in Appendix H - TALK-2 - Development, as can tobacco facts used as pop-up messages encountered by the user. New scripts relating for the 19 hospital rooms were written and can be found in the Appendix I - TALK-3 - Script. TALK screen captures, including the new hospital rooms, can be seen in Appendix H - TALK-2 - Development.

With the changes to the look of the game, we conducted the final focus group testing the usability of the new version with students at the 5th Ward Enrichment Center in Houston. This focus group occurred on January 30, 2007. Four teens participated and were given a set of representative tasks to complete within the game. The teens were all male, 17 years old, and high school students. Mr. Jeffery McLaughlin from Radiant Creative Group and Mr. Mario Luca from M. D. Anderson observed the teens' interaction with the game interface. At the end of the trial, the teens were asked to rate the difficulty of the tasks as well as provide qualitative feedback about the game itself. All four participating subjects rated this task "Not Difficult." General observations made by the staff noted that three of the four test subjects were enthusiastic about the educational game and enjoyed the experience. Two subjects in particular continued playing after being told they were finished and could leave. Minor refinements to the interface will improve usability considerably. For a full report on this focus group see Focus Group in Appendix I - TALK-3 - Script.

TALK Deployment Location: To ensure that the target population would be accessed for project TALK, Dr. Alexander V. Prokhorov met with Dr. Lovell Jones, Director of Health Disparities Research at M. D. Anderson to discuss possible game operating venues. Dr. Jones suggested several potential locations. We contacted them and decided to work with Sharpstown Mall, billed as Houston's Premiere Urban Mall. The mall is open Monday through Saturday from 10 a.m. to 9 p.m. and from noon to 6 p.m. on Sundays. A general agreement has been signed and submitted to Mr. Robert Nguyen, the General Manager, and his assistant Nina Daniels of Sharpstown Mall. They have secured a location in a high traffic area for our project beginning the third week of March 2007.

Key Research Accomplishments

- The intervention tool is nearly completed and will be fully ready for testing according to the study timeline.
- All educational modules are in place.
- The CD-ROM-based program has undergone the first round of beta testing and all the glitches and problems have been removed.
- TALK deployment location (Houston's Sharpstown Mall) has been selected.

Reportable Outcomes

Presentations of Project TALK

- Prokhorov AV. ASPIRE: Smoking prevention & cessation programs for youths using computer technology. Seminar presentation to members of the M. D. Anderson

Ambassadors. The University of Texas M. D. Anderson Cancer Center, Cancer Prevention Building Conference Room, Tuesday, October 3, 2006.

- Prokhorov AV. Challenges & Successes in Persuading Youth to Adopt Tobacco Free Lifestyles. Julie Rogers "Gift of Life" Program, Montagne Center, Lamar University, Beaumont, Texas, October 5, 2006.
- Prokhorov AV. Should Our Consortium Advocate Smokeless Tobacco Instead of Cigarettes? A Debate with Discussion. American Academy of Pediatrics Tobacco Consortium Meeting, Renaissance Hotel, Schaumburg, Illinois, December 14, 2006.
- Prokhorov, AV. Invited Panelist, Smoking Cessation and Prevention in Youth. President's Cancel Panel Meeting on *Promoting Healthy Lifestyles to Reduce the Risk of Cancer*. University of Mississippi Medical Canter, Jackson, Mississippi, February 12, 2007.

Conclusions

Project TALK is successfully developing according to the timeline. It produced an innovative, highly informative, and easy-to-navigate videogame, which was enthusiastically accepted by young individuals involved in the pre-testing activities. The investigative team is ready to move to the evaluation phase of the study for which community venues have been identified and their support and cooperation secured.

Career Developmental Project (CDP1)

Identification of Membrane Proteins in Bronchial Epithelia Cells as Biomarkers of Early Detection for Lung Cancer

(PI: Shin-Myung Kang, M.D.)

Lung cancer is the leading cause of cancer deaths, and its incidence is rising. In the United States, 174,470 new cases of lung cancer and 162,460 deaths from lung cancer were estimated for this disease were expected in 2006. Early detection of the malignant lesion leads to an improved 5-year survival rate after surgical resection. Unfortunately, most patients are diagnosed in later stages, which is due to the limit of current standard detection screening tools. Furthermore, population screening tools, such as sputum cytology and chest X-ray, have failed to show reduced lung cancer mortality after surgical resection. Therefore, advanced screening tools are needed urgently to detect lung cancer at an early stage to improve control of such deadly lung cancer.

Dr. Shin-Myung Kang has strong clinical background in a field of the evaluation and diagnosis of lung cancer and pulmonary medicine. He has participated in the translational research at the Molecular Pathology Laboratory. He has been working on a research topic analyzing *EGFR* mutations in lung adenocarcinomas using PCR-SSCP (polymerase chain reaction - Single Strand Conformational Polymorphism) methods and its clinical application and reported the results to *CANCER*, entitled "Identical *EGFR* mutations in adenocarcinomatous and squamous cell carcinomatous components of adenosquamous carcinoma of the lung". He also published an article entitled 'Identification of tumor suppressor loci on the long arm of chromosome 5 in pulmonary large cell neuroendocrine carcinoma' in *CHEST*. The data suggested the presence of at least four tumor suppressor loci on chromosome 5q through microsatellite and loss of heterozygosity analysis. For his work, Dr. Kang was awarded the Young Investigator Award at *CHEST* 2004.

For this Career Development Award, Dr. Kang will participate in research to develop new biomarkers for early detection of lung cancer that will extend his expertise and interests. The immediate goal of this study is to identify membrane proteins associated with premalignant squamous metaplasia. To accomplish this goal, the following specific Aims will be pursued:

Aim 1. To isolate membrane proteins uniquely expressed on the surface of squamous metaplasia using organotypically cultured bronchial epithelial cells. Membrane proteins will be isolated from squamous metaplastic bronchial epithelial cells and compared with that of normal mucociliary bronchial epithelial cells by 2-dimensional polyacrylamide gel electrophoresis.

Aim 2. To identify differentially represented proteins using proteomics. Using HPLC-tandem Mass Spectrometer in collaboration with the Proteomics Core facility in our institute, we will sequence and determine the specific identity of the proteins isolated in Aim 1.

Aim 3. To verify the differentially represented proteins using PCR, Western blotting, and immunocytochemistry. Further verification will be done by real-time PCR, Western blotting, and immunohistochemical staining of the putative biomarkers on lung cancer specimens in tissue microarrays in collaboration with the Pathology Core.

KEY RESEARCH ACCOMPLISHMENTS

Project 1: Targeting epidermal growth factor receptor signaling to enhance response of lung cancer to therapeutic radiation.

- Finalized the revision of the clinical protocol, Tarceva (erlotinib) informed consent, and the IND application, and await the final approvals by the DoD, IRB, and FDA, and the drug contract to be signed.
- Extended our model systems to include an additional NSCLC cell line, H460, and showed that it is radiosensitized by erlotinib.
- Demonstrated that erlotinib suppresses the radiation-induced activation of the EGFR.
- Demonstrated using two new assays, the neutral comet assay and pulsed field gel electrophoresis, that gefitinib suppresses the repair of radiation-induced DNA double strand breaks.
- Demonstrated that sorafenib suppresses activation of vascular endothelial growth factor receptor and platelet derived growth factor receptor in NSCLC cells.
- The animal protocol for xenograft model was prepared and approved.

Project 2: Molecular imaging of EGFR expression and activity in targeted therapy of lung cancer

- Demonstrated that the xenograft human NSCLC tumors accumulated significantly higher levels of $[^{124}\text{I}]$ JGAP5 compared to $[^{124}\text{I}]$ mIPQA measured by PET imaging studies, although the uptake and retention of JGAP5 *in vitro* in the human NSCLC cell lines with increased EGFR tyrosine kinase activity and high sensitivity to therapy with gefitinib was almost similar to those of $[^{124}\text{I}]$ mIPQA. This result was found to be due to the differential hepatobiliary clearance and water solubility properties of the compounds
- Demonstrated that the accumulation of $[^{124}\text{I}]$ JGAP5 was significantly decreased by pre-treatment of the mice with gefitinib as compared to non-treated animals, and the response was more sensitive than with $[^{124}\text{I}]$ -mIPQA.
- Demonstrated the feasibility of PET imaging with $[^{124}\text{I}]$ -JGAP5 for prediction of tumor responsiveness to therapy with EGFR TKIs.

- Observed the accumulation of [¹²⁴I]-JGAP5 in normal tissue structures expressing highly active EGFRs (i.e., hair follicle cells) that are currently used as surrogate biomarkers of EGFR activity/inhibition, providing additional proof of the approach to imaging EGFR tyrosine kinase activity with [¹²⁴I]-JGAP5.

Project 3: Targeted peptide-based systemic delivery of therapeutic and imaging agents to lung tumors

- Found that EphA5 mediated the cell internalization of the ephrin-mimic peptides (CSGIGSGGC and CRFESSGGC).
- Found that CSGIGSGGC and CRFESSGGC increased the proliferation and/or survival of lung cancer cells expressing the EphA5 receptor
- Detected the high levels of GRP78, IL11R and EphA5 expression in lung cancer tumor specimens
- Found that NSCLC adenocarcinomas had higher levels of cytoplasmic GRP78 ($P = 0.0003$) and cytoplasmic IL11R ($P < 0.0001$) than NSCLC squamous cell carcinoma. In contrast, squamous cell carcinomas showed significantly higher expression for membrane GRP78 ($P = 0.003$) and EphA5 ($P = 0.002$).
- Demonstrated that only the cytoplasmic IL11R expression in tumors had significant correlation with smoking status ($P = 0.005$), and no correlation of markers expression with disease free and overall survivals was detected.

Project 4: Inhibition of bFGF Signaling for Lung Cancer Therapy

- Established that some luciferase transfected NSCLC cell lines are sensitive and others are resistant to bFGF.
- Performed the first exhaustive analysis of the different bFGF signaling components (the growth factor, its receptors and the associated accessory molecule syndecan) in premalignant and malignant lung tissues using TMAs.

Project 5: Targeting mTOR and Ras signaling pathways for lung cancer therapy

- Demonstrated that long-term treatment with a mTOR inhibitor in human NSCLC cells still increased Akt activity while inhibiting mTOR-riktor activity.
- Demonstrated that Akt activation during mTOR-targeted therapy was associated with acquired rapamycin resistance, thus providing a strong scientific rationale for combining mTOR inhibitors with agents that inhibits Akt activation such as a PI3K inhibitor in the clinical treatment of lung cancer.
- Demonstrated that rapamycin-resistant cell line was fully sensitive to PI3K inhibitors, suggesting a more rational treatment strategy targeting mTOR-signaling pathway through intermittent utilization of an mTOR inhibitor and a PI3K inhibitor to avoid the development of rapamycin resistance.
- Demonstrated that co-targeting of mTOR and MEK/ERK signaling pathways exhibited enhanced growth-inhibitory effect of NSCLC cells.
- The Phase IB trial of RAD001 in patients with operable non-small cell lung cancer (NSCLC) was activated on February 06, 2007.

Project 6: Identification and Evaluation of Molecular Markers in Non-Small Cell Lung Cancer (NSCLC)

- Conducted global expression analysis of a set of 29 HNSCC matched T/N pairs and an initial set of 8 lung adeno- and squamous cell carcinoma matched T/N pairs.
- Developed a model for metastatic progression in HNSCC from profiling data.
- Completed gene-specific hypermethylation analysis of 9 genes and genome-wide hypomethylation in all available HNSCC and NSCLC samples.

- Detected both aberrant hypermethylation and hypomethylation in metastatic lymph nodes and their genetically matched primary tumors.
- Established 7 heterotransplant primary NSCLC tumor models, which will allow us to evaluate target therapeutic agents and to initiate biomarker discovery experiments

Core B: Biostatistics & Data Management Core

- Continued to provide statistical support in the clinical trial design and revision for Project 1 and DRP-1.
- Provided data analysis for Projects 2, 3, 6, and Pathology Core.
- Continued to work closely with the Project 4 PI (Dr. Reuben Lotan) on synergy studies of combination drug treatment in cell lines to determine whether the effect is synergistic, additive, or antagonistic.
- Generalized the currently available methods to allow different mode and magnitude of drug interaction to account for the possibility that the combination may produce synergistic effect in certain dose ranges but additive or antagonistic in other dose ranges. The magnitude of drug interaction can also vary from dose to dose.
- Developed methods to construct the confidence interval for the interaction index.

Core C: Pathology Core

- Developed a repository of lung cancer tissue specimens, including TMAs, to be utilized for research projects.
- Assisted with the development of a series of lung cancer heterotransplants in mice in collaboration with Project 6.
- Utilized NSCLC primary tumors and brain metastasis TMAs specimens for IHC analysis and other *in situ* techniques.
- Characterized the expression of angiogenic markers (VEGF/VEGFR and bFGF/receptors) in NSCLC and correlated with clinicopathologic features and EGFR pathway.
- In collaboration with Project 2, identified KRAS gene mutation as a negative predictor factor for response to EGFR TKI using clinical specimens and characterization of EGFR abnormalities and HER family proteins expression in the progression and metastasis of NSCLC.

Core D: Imaging Core

- Produced novel IPQA derivative JGAP5 radiolabeled with ^{124}I and ^{131}I for PET and *in vitro* uptake studies for Project 2.
- Performed all multi-modality imaging (and autoradiography) studies in mice with orthotopic models of different NSCLC cells using ^{124}I -JGAP5 (EGFR expression/activity), ^{18}F -FMAU (proliferative activity), and ^{18}F -FDG (glucose metabolism) in Project 2.
- Installed an automated radiosynthesis module TraceLab-FN (GE Healthcare, Milwaukee, WI) and established a routine CGMP grade synthesis of ^{18}F -FLT and ^{18}F -FMAU for PET/CT imaging of tumor proliferative activity, which can be applied for the assessment of early responses to therapy in preclinical and in upcoming clinical trials.
- Maintained SOPs and performed QC/QA procedures for routine synthesis of ^{111}In -DTPA-PEG-AnnexinV for SPECT/CT imaging in Project 1.
- Performed routine synthesis of $[^{18}\text{F}]$ FEAU for Project 3.
- Maintained synthesis and ^{111}In / ^{64}Cu radiolabeling of GRP78-specific cyclic nanopeptide CGRRAGGSC for imaging studies in Project III for imaging studies with ^{64}Cu -DOTA-CGRRAGGSC PET/CT in animals for Project 3.

DRP-1: Treatment of Malignant Pleural Effusion with ZD6474, a Novel VEGFR and EGFR TK Inhibitor

- The original protocol was approved and the trial was opened.
- The amended protocol has been submitted to AstraZeneca and our IRB for review and approval.
- 16 patients were screened for enrollment under the original protocol.

DRP-2: TALK - Teens and Young Adults Acquiring Lung Cancer Knowledge

- The intervention tool is nearly completed and will be fully ready for testing according to the study timeline.
- All educational modules are in place.
- The CD-ROM-based program has undergone the first round of beta testing and all the glitches and problems have been removed.
- TALK deployment location (Houston's Sharpstown Mall) was selected.

REPORTABLE OUTCOMES

Manuscripts published in peer-reviewed Journals

- Kong M, Lee JJ. A generalized response surface model with varying relative potency for assessing drug interaction. *Biometrics* 62 (1282): 986-95, 2006.
- Massarelli E, Varella-Garcia M, Tang X, Xavier AC, Ozburn N, Liu DD, Bekele BN, Herbst RS, Wistuba II. KRAS Mutation is an Important Predictor of Resistance to Therapy with Epidermal Growth Factor Receptor Tyrosine Kinase Inhibitors in Non-Small Cell Lung Cancer. *Clin Cancer Res* (in press), 2007.
- Souza GR, Levin CS, Hajitou A, Pasqualini R, Arap W, Miller JH. "In Vivo Detection of Gold-imidazole Self-assembly Complexes: NIR-SERS Signal Reporters", *Anal Chem* 78:6232-6237, 2006.
- Trepel M, Arap W, Pasqualini R. Selection, isolation, and identification of targeting peptides for ligand-directed gene delivery. In: *Gene Transfer: A Laboratory Manual*, New York: Cold Spring Harbor Laboratory Press. Ch. 30:359-369, 2007.

Manuscripts in review, revision, or preparation

- Colella S, Richards KL, Baggerly KA, Tsavachidis S, Lang JC, Schuller DE, Krahe R. Expression Signature of Head and neck Cancer Metastasis. *Cancer* (submitted), 2007.
- Kong M, Lee JJ. A semiparametric model for assessing drug interaction. *Biometrics* (in revision), 2006.
- Lee JJ, Kong M. Confidence Interval of Interaction Index for Assessing Multiple Drug Interaction. *Statistics in Biopharmaceutical Research* (submitted), 2007.
- Tang X, Varella-Garcia M, Xavier AC, Massarelli E, Ozburn N, Moran C, Wistuba II. EGFR Abnormalities in the Pathogenesis and Progression of Lung Adenocarcinomas. (Manuscript in preparation), 2007.
- Wang X, Yue P, Fu H, Khuri, Sun S-Y. Prolonged treatment with mTOR inhibitors increases Akt phosphorylation, which is associated with development of rapamycin resistance, despite inhibition of mTOR complex 2 in human lung cancer cells. *Clin Cancer Res* (in revision), 2007.

Abstracts

- Behrens C, Lin H, Lee J, Hong WK, Wistuba II, Lotan R. Differential immunohistochemical expression patterns of fibroblast growth factor-2, receptors 1 and 2, and syndecan-1 in

squamous cell carcinoma and adenocarcinoma of the lung. The 98th AACR Annual Meeting, abstract #: 6412, 2007.

- Colin Brooks, Toshimistu Tanaka, Anupama Munshi, Jenny Liu, Nathan Wang, Marvette Hobbs, Raymond Meyn. Targeting EGFR signaling to enhance response of non-small lung cancer cells to radiation. The 98th AACR annual meeting, abstract #: 4154, 2007.
- Massarelli E, Maria L, Silva P, Ozburn N, Feng L, Yin G, O'Reilly M, Hong WK, Herbst RS, Wistuba II. Correlation between VEGF/VEGFR2 and EGFR immunohistochemical protein expression in early stage non-small cell lung carcinoma. The 98th AACR Annual Meeting, abstract #: 5029, 2007.
- Nishii R, Mukhopadhyay U, Soghomonyan S, Volgin A, Alauddin MM, Gelovani J. PET with ¹⁸F-FDG and ¹⁸F-FMAU in the assessment of early response to EGFR-targeted therapy in mice bearing human NSCLC xenografts with different EGFR mutations. Proceedings of the 53rd Annual Meeting of the Society for Nuclear Medicine, June 3-7, San Diego, CA.
- Nishii R, Pal A, Soghomonyan S, Balatoni J, Mushkudiani I, Yeh HH, Mukhopadhyay U, Volgin A, Shavrin A, Maxwell D, Tong W, Alauddin M, Bornmann W, Gelovani J. Molecular Imaging of Different EGFR Kinase Mutant NSCLC Carcinomas with [¹²⁴I]-mIPQA and [¹²⁴I]-JGAP5 PET for Prediction of Responsiveness to EGFR Kinase Inhibitors. Proceedings of the 4th Annual Meeting of the Society of Molecular Imaging, Kona, Hawaii. September 1-4, 2006.
- Sun M, Massarelli E, Feng L, Ozburn N, Yin G, Komaki R, Hong WK, Aldape KD, Wistuba II. Differential immunohistochemical expression pattern of HER family receptors and ligands is detected in primary lung cancers and corresponding brain metastases. The 98th AACR Annual Meeting, abstract #: 468, 2007.

Presentations of Project TALK

- Prokhorov AV. ASPIRE: Smoking prevention & cessation programs for youths using computer technology. Seminar presentation to members of the M. D. Anderson Ambassadors. The University of Texas M. D. Anderson Cancer Center, Cancer Prevention Building Conference Room, Tuesday, October 3, 2006.
- Prokhorov AV. Challenges & Successes in Persuading Youth to Adopt Tobacco Free Lifestyles. Julie Rogers "Gift of Life" Program, Montagne Center, Lamar University, Beaumont, Texas, October 5, 2006.
- Prokhorov AV. Should Our Consortium Advocate Smokeless Tobacco Instead of Cigarettes? A Debate with Discussion. American Academy of Pediatrics Tobacco Consortium Meeting, Renaissance Hotel, Schaumburg, Illinois, December 14, 2006.
- Prokhorov, AV. Invited Panelist, Smoking Cessation and Prevention in Youth. President's Cancel Panel Meeting on *Promoting Healthy Lifestyles to Reduce the Risk of Cancer*. University of Mississippi Medical Canter, Jackson, Mississippi, February 12, 2007.

Project-Generated Grants

- Awarded NIH R01 research grant entitled "Enhancing mTOR-targeted Cancer Therapy" in 2006. Principal Investigator: Shi-Yong Sun, Ph.D.

CONCLUSIONS

For the second year of the grant period, the research projects have been progressing as originally proposed in the grant with minor recommended changes in Projects 5 and 6 stated in the revised Statement of Work and detailed in the body of the report. Two clinical trials are opened, and one is in the final review stages with approval, activation, and recruitment of patients expected soon.

This year, we have 4 publications, including 1 in *Clinical Cancer Research*, and 1 in *Biometrics*, and 5 abstracts, 3 of which will be presented at 2007 AACR Annual meeting. In addition, we have successfully been awarded a NCI R01 grant based on data generated from Project 5. Finally, we have generated 2 programs for biostatistics which have been made freely available to the public.

In summary, the individual projects of IMPACT can conclude below:

Project 1: Using the additional cell lines, we now confirm that gefitinib and erlotinib, at clinically achievable concentrations, sensitize NSCLC cell lines to radiation. This apparently small sensitization in cell lines with a single dose and exposure is expected to translate into significant clinical benefit. Using 4 independent assays, we have shown that gefitinib radiosensitizes NSCLC cells by suppressing the cellular capacity for repairing radiation-induced DSBs.

Project 2: Based on the progress at this point, we conclude that imaging with pharmacokinetically optimized more water-soluble [¹²⁴I]-JGAP5 (as compared to [¹²⁴I]-mIPQA derivatives) should allow for identification of tumors with increased EGFR signaling. However, this series of compounds still remains suboptimal for the clinical use and we believe that a further decrease in lipophilicity of the series of IPQA-based compounds will result in additional improvement of AUC and the magnitude of the radiotracer accumulation in tumors vs lung.

Project 3: We determined that EphA5 protein overexpression in lung cancer cells in light of candidate ephrin mimics (GGS peptides) targeting these cells provides an original evidence for EphA5 being a lung cancer marker.

Project 4: Our findings of frequent activation and different expression patterns of the FGF signaling components in the two major forms of NSCLCs, adenocarcinomas and squamous cell carcinomas, suggest that individual tumor characteristics must be considered to develop individualized therapeutic strategies. Also the differential sensitivity of NSCLC cell lines *in vitro* to mitogenic effects of bFGF will allow us to interpret the effects of bFGF signaling inhibitors *in vivo*. For example, if we couldn't find that an inhibitor exhibiting anti tumor effects *in vivo* affected a cell line directly *in vitro*, we would explore the possibility that the *in vivo* effect might be due to targeting host endothelial cells instead of the tumor cells.

Project 5: Targeting the mTOR axis appears to be a promising strategy against lung cancer. Given the nature of the complexity of lung cancer signaling pathways including mTOR signaling, it is essential to understand the biology of lung cancer and the action mechanism of the interested therapeutics in order to efficiently treat lung cancer through application of mechanism-driven therapeutic regimens. Thus, our effort in pursuing mTOR-targeted lung cancer therapy is scientifically rational.

Project 6: Based on our methylation profiling, *TCF21* may be a good biomarker of early lung and head and neck cancer. With an established role in the epithelial-mesenchymal transition, *TCF21* may be important in predicting metastatic potential.

Biostatistics Core: Core B continued to provide statistical and data management support for all research projects in the IMPACT study and created new tools and methods in statistical analysis.

Pathology Core: The Pathology Core has assisted and collaborated actively with several research projects by performing multiple histopathological, immunohistochemical and molecular studies in a large series of lung cancer tissue specimens. Several abstracts have been

presented in international meetings and manuscripts are in press or in preparation for submission. In addition, the Pathology Core has conducted specific research activities, which fully integrate into several of the IMPACT research projects. The Pathology Core has successfully fulfilled the goals proposed for the second grant year.

Imaging Core: The Imaging Core continues to provide imaging support requested from the PIs of IMPACT research projects in addition to synthesizing more optimal IPQA derivatives.

DRP-1: No conclusion can be reached up to this point. However, important revisions have been made to the protocol which will enhance the ability to complete this study in a timely manner.

DRP-2: Project TALK is successfully developing according to the timeline. It produced an innovative, highly informative, and easy-to-navigate videogame, which was enthusiastically accepted by young individuals involved in the pre-testing activities. The investigative team is ready to move to the evaluation phase of the study for which community venues have been identified and their support and cooperation secured.

REFERENCES

Arap MA, Lahdenranta J, Mintz PJ, Hajitou A, Sarkis AS, Arap W, Pasqualini R. Cell surface expression of the stress response chaperone GRP78 enables tumor targeting by circulating ligands. *Cancer Cell* 6(3): 275-284, 2004.

Behrens C, Wistuba II, Feng L, Jack Lee JJ, Hong WK, Lotan R. Expression of fibroblast growth factor and its receptors in premalignant and malignant human lung tissues. *AACR Meeting Abstracts*: #1350, 2006.

Chung CH, Parker JS, Karaca G, Wu J, Funkhouser W K, Moore D, Butterfoss D, Xiang D, Zanation A, Yin X, Shockley WW, Weissler MC, Dressler LG, Shores CG, Yarbrough WG, Perou CM. Molecular classification of head and neck squamous cell carcinomas using patterns of gene expression. *Cancer Cell* 5: 489-500, 2004.

Cromer A, Carles A, Millon R, Ganguli G, Chalmel F, Lemaire F, Young J, Dembele D, Thibault C, Muller D, Poch O, Abecassis J, and Waslylk B. Identification of genes associated with tumorigenesis and metastatic potential of hypopharyngeal cancer by microarray analysis. *Oncogene* 23: 2484-2498, 2004.

Demetri GD, von Mehren M, Blanke CD, et al. Efficacy and safety of imatinib mesylate in advanced gastrointestinal stromal tumors. *N Engl J Med* 347(7):472-80, 2002.

Druker BJ, Sawyers CL, Kantarjian H, et al. Activity of a specific inhibitor of the BCR-ABL tyrosine kinase in the blast crisis of chronic myeloid leukemia and acute lymphoblastic leukemia with the Philadelphia chromosome. *N Engl J Med* 344:1038-42, 2001.

Druker BJ, Talpaz M, Resta DJ, et al. Efficacy and safety of a specific inhibitor of the BCR-ABL tyrosine kinase in chronic myeloid leukemia. *N Engl J Med* 344:1031-7, 2001.

Druker BJ. Imatinib as a paradigm of targeted therapies. *Adv Cancer Res* 91:1-30, 2004.

Giaccone G, Herbst RS, Manegold C, Scagliotti G, Rosell R, Miller V, Natale R, Schiller J, von Pawel J, Pluzanska A, Gatzemeier U, Grous J, Ochs J, Averbuch S, Wolf M, Rennie P, Fandi A, Johnson DH. A phase III clinical trial of gefitinib ('Iressa', ZD1839), and EGFR inhibitor, in combination with gemcitabine and cisplatin in advanced non-small-cell lung cancer (INTACT 1). *J Clin Oncol* 22(5):777-84, 2004.

Hajitou A, Trepel M, Lilley CE, Soghomonyan S, Alauddin MM, Marini FC 3rd, Restel BH, Ozawa MG, Moya CA, Rangel R, Sun Y, Zaoui K, Schmidt M, von Kalle C, Weitzman MD,

Gelovani JG, Pasqualini R, Arap W. A hybrid vector for ligand-directed tumor targeting and molecular imaging. *Cell* 125(2): 385-98, 2006.

Herbst RS, Bunn PA, Jr. Targeting the epidermal growth factor receptor in non-small cell lung cancer. *Clin Cancer Res* 9:5813-24, 2003.

Herbst RS, Giaccone G, Schiller J, Natale R, Miller V, Manegold C, Scagliotti G, Rosell R, Oliiff I, Reeves J, Wolf M, Krebs A, Averbuch S, Ochs J, Grous J, Fandi A, Johnson DH: Gefitinib ('Iressa', ZD1839) in combination with paclitaxel and carboplatin in chemotherapy-naive patients with advanced non-small-cell lung cancer: Results from a phase III clinical trial (INTACT 2). *J Clin Oncol* 22(5):785-94, 2004.

Herbst RS, Maddox AM, Rothenberg ML, Small EJ, Rubin EH, Baselga J, Rojo F, Hong WK, Swaisland H, Averbuch SD, Ochs J, LoRusso PM: Selective oral epidermal growth factor receptor tyrosine kinase inhibitor ZD1839 is generally well-tolerated and has activity in non-small-cell lung cancer and other solid tumors: results of a phase I trial. *J Clin Oncol* 20:3815-25, 2002.

Herbst RS. Review of epidermal growth factor receptor biology. *Int J Radiat Oncol Biol Phys* 59: 21-26, 2004.

Howell A, Cuzick J, Baum M et al. Results of the ATAC (Arimidex, Tamoxifen, Alone or in Combination) trial after completion of 5 years' adjuvant treatment for breast cancer. *Lancet* 365:60-2, 2005.

Hunter KD, Thurlow JK, Fleming J, Drake PJ, Vass JK, Kalna G, Higham DJ, Herzyk P, Macdonald DG, Parkinson EK, Harrison PR. Divergent routes to oral cancer. *Cancer Res* 66: 7405-7413, 2006.

Hurwitz H, Fehrenbacher L, Cartwright T, et al. Bevacizumab (a monoclonal antibody to vascular endothelial growth factor) prolongs survival in first-line colorectal cancer (CRC): Results of a phase III trial of bevacizumab in combination with bolus IFL (irinotecan, 5-fluorouracil, leucovorin) as first-line therapy in subjects with metastatic CRC. *PASCO* 21: Abs #3646, 2003.

Kris MG, Natale RB, Herbst RS, Lynch TJ, Jr., Prager D, Belani CP, Schiller JH, Kelly K, Spiridonidis H, Sandler A, Albain KS, Cella D, Wolf MK, Averbuch SD, Ochs JJ, Kay AC: Efficacy of gefitinib, an inhibitor of the epidermal growth factor receptor tyrosine kinase, in symptomatic patients with non-small cell lung cancer: a randomized trial. *JAMA* 290:2149-58, 2003.

Nishikawa T, Munshi A., Story MD, Ismail S, Stevens C, Chada S, Meyn RE. Adenoviral-mediated *mda7* expression suppresses DNA repair capacity and radiosensitizes non-small lung cancer cells. *Oncogene* 23:7125-31, 2004.

O'Donnell RK, Kupferman M, Wei SJ, Singhal S, Weber R, O'Malley B, Cheng Y, Putt M, Feldman M, Ziobor B, Muschel RJ. Gene expression signature predicts lymphatic metastasis in squamous cell carcinoma of the oral cavity. *Oncogene* 24: 1244-1251, 2005.

Prudkin L, Wistuba II. Epidermal growth factor receptor abnormalities in lung cancer. Pathogenetic and clinical implications. *Ann Diagn Pathol*, 10: 306-15, 2006.

Rahmani M, Davis EM, Bauer C, Dent P, Grant S. Apoptosis induced by the kinase inhibitor BAY 43-9006 in human leukemia cells involves down-regulation of Mcl-1 through inhibition of translation. *J Biol Chem* 280(42):35, 217-27, 2005.

Roepman P, de Jager A, Groot Koerkamp MJ, Kummer JA, Slootweg PJ, Holstege FC. Maintenance of head and neck tumor gene expression profiles upon lymph node metastasis. *Cancer Res* 66: 11110-11114, 2006.

Roepman P, Wessels LF, Kettelarij N, Kemmeren P, Miles AJ, Lijnzaad P, Tilanus MG, Koole R, Hordijk GJ, van der Vliet PC, Reinders MJ, Slootweg PJ, Holstege FC. An expression profile for diagnosis of lymph node metastases from primary head and neck squamous cell carcinomas. *Nat Genet* 37: 182-186, 2005.

Sarbassov DD, Ali SM, Sengupta S, Sheen JH, Hsu PP, Gagley AF, Markhard AL, Sabatini DM. Prolonged rapamycin treatment inhibits mTORC2 assembly and Akt/PKB. *Mol Cell* 22(2):159-68. 2006.

Schmalbach CE, Chepeha DB, Giordano TJ, Rubin MA, Teknos TN, Bradford CR, Wolf GT, Kuick R, Misek DE, Trask DK, Hanash S. Molecular profiling and the identification of genes associated with metastatic oral cavity/pharynx squamous cell carcinoma. *Arch Otolaryngol Head Neck Surg* 130: 295-302, 2004.

Sun S-Y, Rosenberg LM, Wang X, Zhou Z, Yue P, Fu H, Khuri FR. Activation of Akt and eIF4E survival pathways by rapamycin-mediated mTOR inhibition. *Cancer Res (Priority Report)* 65:7052-8, 2005.

Tsao MS, Sakurada , Cutz JC, Zhu CQ, Shepherd FA et al. Erlotinib in lung cancer - molecular and clinical predictors of outcome. *N Engl J Med* 353(2):133-44, 2005.

Vos MD, Ellis CA, Elam C, Ulku AS, Taylor BJ, Clark GJ. RASSF2 is a novel K-Ras-specific effector and potential tumor suppressor. *J Biol Chem* 278: 28045-51, 2003.

Zurita AJ, Troncoso P, Cardó-Vila M, Logothetis CJ, Pasqualini R, Arap W. Combinatorial screenings in patients: the interleukin-11 receptor alpha as a candidate target in the progression of human prostate cancer. *Cancer Res* 64: 435-39, 2004.

APPENDICES

APPENDIX A



Deborah Andrade To: <towilliams@mdanderson.org>
<andrade.deborah@gene.com> cc: <rkomaki@mdanderson.org>
12/22/2006 08:57 AM Subject: FW: Dr. Ritsuko Komaki

Hi Toni:

I got you phone message the other day.

Good news is that Genentech considers the protocol approved, and I will be sending in the revised protocol for our records. With that said, Josh Wahkahquah contacted me a few weeks ago telling me he is the contact in terms of contracting. I have since put our ops group in touch with him, so they have already begun the process. You may want to contact Josh for additional info.

Genentech will be closed after today until Jan 2nd. I am on vacation already, but wanted to send you a quick note to let you know the process is moving forward. I will be in touch once I return from the holiday with more follow-up.

Happy Holidays.

Debbie

Deborah Andrade, MS, PhD
Medical Science Liaison, HER Family
Cell: 214-803-9768

From: jd wahkah@mdanderson.org [mailto:jd wahkah@mdanderson.org]

Sent: Wednesday, December 06, 2006 11:44 AM

To: andrade.deborah@gene.com

Subject: Dr. Ritsuko Komaki

Hello Deborah,

Here is my contact info. Thank you for your help.

JOSH WAHKAHQUAH • Research Administration Analyst

PHONE: 713.563.3895 • FAX: 713.794.4535

JDWahkah@mdanderson.org

THE UNIVERSITY OF TEXAS • M. D. ANDERSON CANCER CENTER
LEGAL SERVICES – Unit 176

1100 Holcombe Blvd., Suite HMB 7.060.03, Houston, Texas 77030-4009

APPENDIX B

(Handwritten signature)

Lydia G. Jackson To: Ray Meyn/MDACC@MDACC
02/20/2006 02:10 PM cc: Rosie M. Handy/MDACC@MDACC, Ray
Meyn/MDACC@MDACC, Glynda B.
Quinn/MDACC@MDACC
Subject: e-ACUF Generic Memo from IACUC, Re:
01-06-00431



Office of Research Administration
Unit 176
phone 713-563-3888
Fax 713-794-4535

Office of Research Administration

02/20/2006

To: Ray Meyn/MDACC
Copy: Rosie M. Handy/MDACC
From: Lydia G. Jackson/MDACC

ACUF ID #: 01-06-00431
Version: 01
Subject: e-ACUF Generic Memo from IACUC, Re: 01-06-00431

PROTOCOL STATUS: APPROVED AND ACTIVATED

Title: Radiosensitization of Human Tumor Xenografts by the Small Molecule, Epidermal Growth Factor Receptor Inhibitor, Gefitinib and Tarceva

Meeting Date: January 17, 2006
Approval Date: February 20, 2006
Expiration Date: February 2009

Number of animals approved: 420

The IACUC has reviewed and approved the above animal protocol. The Office of Research Administration has activated the protocol for use. For information concerning this protocol, please contact your appropriate IACUC Coordinator.

Sincerely,

Lydia G. Jackson
02/20/2006 02:10:06 PM

**Animal Care and Use Form
University of Texas M. D. Anderson Cancer Center**

ACUF Protocol # 01-06-00431

(Temporary Identification Number: AM-45CU-1029A)

Have you had a previously IACUC approved ACUF on this work? Yes No

I. Investigator and Proposal

A. Principal Investigator: Ray Meyn

PI Title: Professor

PI Phone: 713 792-3424

PI Department: Experimental Radiation Oncology

PI Fax: 713 794-5369

PI Unit: 066

B. Contact Person: Glynda B. Quinn

Contact Title: Senior Administrative Assistant

Contact Phone: 713 792-3424

C. Study Location: Houston

D. Document Details

Version: 02

Version Status: Working Copy 02/20/2006

Save Status: Saved in "(Re)Submittable" format

E. Proposal Title:

Radiosensitization of Human Tumor Xenografts by the Small Molecule, Epidermal Growth Factor Receptor Inhibitor, Gefitinib and Tarceva

F. Describe the goal(s) of this research project in lay terms:

To enhance the cell killing effect of ionizing radiation using the EGFR inhibitors, Gefitinib and Tarceva. We hypothesize that these inhibitors will synergistically interact with radiation to enhance the radiosensitivity of human tumor xenografts.

G. Who will perform experimental manipulations on the animals?

1. Anupama Munshi; Ph.D.; Assistant Professor; YEARS EXPERIENCE WITH SPECIES:

10/Training form on file; Will administer anesthesia

2. Venugopal Radjendirane; Ph.D; Research Scientist; YEARS EXPERIENCE WITH SPECIES:

3/Training form on file; Will administer anesthesia

3. Rajagopal Ramesh; Ph.D.; Associate Professor; YEARS EXPERIENCE WITH SPECIES:

11yrs/Training form on file; Will administer anesthesia

Will Any personnel need training or assistance in surgical procedures, Yes No
aseptic technique or postsurgical care?

H. List All Collaborators (include all individuals other than those directly involved with the animal Manipulations)

- 1. Susan L. Tucker; Department of Biostatistics and Mathematics; CONTRIBUTION TO PROJECT: Biostatistician**
- 2. Howard D. Thames; Biostatistics and Mathematics; CONTRIBUTION TO PROJECT: Biostatistician**

I. Do the studies proposed within this ACUF involve the use of industry-sponsored research?
(e.g. sponsored research agreements with pharmaceutical or biotechnology companies)

Yes No

II. Animal Model

Description of Animals

A. Species: Mouse

Select as applicable:

Of Genus mus
 These animals were bred for use in research.

B. Stock/Strain: Balb/c Nude

Trans/KO Gene:

Do any of these strains develop unique pathological conditions?

Yes No Unknown

C. Sex: Both

D. Age: 6-8 weeks

E. Weight: 15-20gm

F. Why is it necessary to use animals in this project?

Preclinical information from animal models is necessary before proceeding to clinical trials

The growth of tumors *in vivo* is necessary in order to mimic as closely as possible the responses seen in humans to similar treatments. The use of mice will provide the data that cannot be obtained using *in vitro* models.

G. Why is this species used?

The immunocompromised mouse is ideal for reproducible generation of tumors composed of human cancer cell lines. The formation and manipulation of these tumors are critical for the goals of this research.

H. Total number of animals requested over a three year period.

Note: ACUFs are approved for a 3 year period.

Number to be purchased:	420
Number to be bred on site:	0
Current Inventory of animals from previous protocol:	0
Total Number Request:	420

I. Why is this number of animals required?

The number of mice is required in order to demonstrate reproducibility and generate statistically significant data. We will evaluate the effects of Gefitinib and Tarceva using 3 different human tumor cell lines, with 70 mice used for each cell line. My colleagues from Experimental Radiation Oncology, Dr. Luka Milas and Kathy Mason, and my colleagues from Biomathematics, Drs. Howard Thames and Susan Tucker, have been working together along with me for many years to design, conduct, and analyze tumor growth delay following the combination of drugs and irradiation in mouse models. Between the 5 of us, we have approximately 175 years of experience with experiments identical to those proposed here (albeit with different drugs). This empirical experience indicates that 10 mice per group is optimal. Can fewer mice per group be used? Sure. We have used as few as 5 mice per group and gotten away with it when the effects are big. With the drugs proposed here, we are not sure what degree of radiosensitization will be achieved. Thus, using 10 mice per group will assure that we will be able to detect small but clinically significant differences in growth delay amongst the different treatment arms with appropriate

statistical power. Briefly, we measure the volume of each tumor every other day and record this information. When the experiment is completed, we calculate the time for each tumor to reach a specific volume (usually something between 800 and 1200 mm³) and average this time period for the group of ten mice. This average time (+/- standard deviation) can be compared with the control groups to calculate the increased delay in tumor growth over the controls. The statistical significance of this difference is also calculated using the appropriate test recommended by our statistician colleagues (Drs. Thames and Tucker) and the difference is considered significant if $p < 0.05$.

In our studies we will compare the times to tumor regrowth to a specified threshold tumor size in groups of mice treated with drug + radiation versus either drug or radiation alone. A typical tumor regrowth time in one of these control treatment groups is 40 days, with a range of about 30-50 days.

For the purposes of sample size calculations, we assume that the tumor regrowth times in the control group are distributed lognormally with a mean of 40 days and a standard deviation of 5 days. We assume that the tumor regrowth times in the experimental arm (drug + radiation) are also distributed lognormally, and have the same coefficient of variation as in the control group. We wish to be able to detect an increase in mean tumor regrowth time of 25% over the control group, i.e. a mean tumor regrowth time of 50 days. Occasionally (up to about 20% of mice), there is no tumor take, leading to censored tumor regrowth times. Therefore, we compare the regrowth times in the control group vs the experimental group using the generalized Wilcoxon test.

Numerical simulations were performed to estimate the sample size required for 90% power of detecting a difference in mean tumor regrowth times of 40 versus 50 days under the assumptions laid out above. The simulations indicated that with 10 mice per dose group, the statistical power is 96% to a difference at a significance level of $P = 0.05$. Allowing for lack of tumor take in up to 20% of the mice per group (i.e., 2 mice per group), the power is 89%. Therefore we expect that 10 mice per group will provide adequate statistical power to detect the target differences in treatment groups that we set out to identify.

We have consulted with Dr. Susan Tucker and she will use the generalized Wilcoxon test, to allow for the possibility of animals with censored time-to-event data, as the statistical method to analyze our data from this study.

J. Can in vitro systems or other approaches, e.g. mathematical models, be used to reduce the number of animals in this project? Yes No

Why can other methods not be used to minimize the number of animals used?

We have carefully designed the study to use the smallest number of mice necessary to answer the scientific questions posed.

III. Animal Housing and Nutrition

A. Type of Animal Facility:

Conventional - SPF:

SPF animals that need to move between the animal room and other facilities (i.e. imaging equipment or irradiators).

Biohazard:

animals receiving carcinogens or infectious microbes or are involved in recombinant DNA work

B. Animals will be housed:

Bates-Freeman Building:

floors 8 and 3 (germ free) and floor 1 (conventional, barrier, biohazard)

C. Primary animal enclosures housing(cage, run, stall, pasture)

SPF:

SCID, nude and germ free rodents, virus anti-body free rodents (micro isolator cages)

D. Animal Feed

Autoclavable:

rodents in SPF barriers

E. Drinking Water

RO Autoclaved:

SPF rodents, others as required.

IV. Agents Used In Animal

HAZARDOUS AGENTS: include carcinogenic chemicals, antineoplastic drugs, infectious microbial agents, viral agents, toxins, recombinant DNA. Do not include anesthetics or routine antibiotics

Note: Grants, programs, projects, etc., involving the use of hazardous agents are reviewed by the Institutional Biosafety Committee. Contact the Office of Research Administration (713-563-3879) to determine the appropriate method of approval for pilot projects involving hazardous agents' use in animals.

Note: In your flow chart(s), please include an informational description (e.g. dosage, routes of administration, frequency, durations of exposure, etc.) of agents to be used in this research protocol.

For Approval-Pending Agents: No Animal Manipulation may begin before IRB approval is granted and a copy of your Authorization is provided to the Office of Research Administration.

A. Will Hazardous Agents Be Used? Yes No

1. Indicate Hazardous Agents to be used below:

Hazardous Agents must be reviewed by the Institutional Biosafety Committee (IBC).

Submit a copy of your approval letter to the IACUC Office (required for approval)
Please update your IBC to include this protocol Number

Chemical Agents:

1. Gefitinib (Iressa, ZD1839) -- IBC Approval #: Pending. Submitted to IBC for approval -- *not yet submitted to the IBC

2. Tarceva -- IBC Approval #: Pending. Submitted to IBC for approval -- *not yet submitted to the IBC

B. Will Human or Animal tissues or cells be injected or transplanted as part of this study?

Yes No

Will Cells or Tissue be genetically modified before use in animals? Yes No

Animal Tissues or Cells Types:

1. Type: Human tumor cells; Species of origin: Human Non small cell lung cancer cells H1299, A549, H358; Source: ATCC; Cell line has not been MAP tested

C. Will Radioactive Agents Be Used? Yes No

D. Will External Radiation be administered to animals? Yes No

Radiation Type: Cobalt

Provide Dose and Schedule:

Single dose of 5-15 Gy

E. Will Non-Hazardous Experimental Agents be used? Yes No

F. During administration of any of the above agents, animals will be:

- Anesthetized/Unconscious**
- Unanesthetized/Conscious**

V. Experimental Procedures

A. Type of Restraint

1. Will restraint of animal be necessary? Yes No

Answer "Yes" if using any degree of restraint. The housing of animals in standard cages is not deemed restraint.

Indicate type of restraint, and the maximum time any one animal would be restrained within a 24 hour period.

Restraint Type:	Duration:	Dosage Information:
<input checked="" type="checkbox"/> Manual	Less than 5 minutes	
<input checked="" type="checkbox"/> Chemical	Less than 15 minutes	60mg/kg IP

2. Will paralytic drugs be used without associated general anesthetic? Yes No

B. Anesthesia

If Anesthetics/analgesics/sedatives are used, include complete dosage information.

NOTE: This information should also be provided in Flow Sheet, Section VII, for each experimental group.

1. Will anesthesia be used for any reason? Yes No

Anesthetic	Dose	Route
1) Nembutal	60mg/kg	IP
2)		
3)		
4)		
5)		

2. Indicate what methods will be used to monitor anesthetic depth

Measure Respiratory Rate

Measure Corneal and Pedal Reflexes

3. Building and Room Number where animal(s) will be anesthetized: DVMS Building: Tan Zone
Room Number TB 3927

C. Analgesia

Note: For information about the regulations/policies concerning the use of analgesia, please consult the IACUC's Analgesia Standard Operating Procedure.

1a. Moribund animals must be euthanized-In the event that an animal associated with this protocol experiences pain or suffering (e.g. after major survival surgery), analgesics will be given.

Euthanized

2. Will you use other techniques to minimize experimental pain or distress? Yes No

D. Surgery

1. Will there be any surgical manipulations of these animals? Yes No

IACUC's Analgesia Standard Operating Procedure

E. Sample collection from living animals

1. Will you be collecting tissues from animals? Yes No

F. Other Information

1. Will adjuvant be used? Yes No

<http://utm-int01a.mdacc.tmc.edu/dept/prot/orahomepage.nsf/IACUC%20Manual>

2. Will food and/or water be restricted for reasons other than a normal fast (<= to 12 hrs) associated with surgery/anesthesia? If Yes, please provide the reason and length of time food and/or water will be restricted. Yes No

<http://utm-int01a.mdacc.tmc.edu/dept/prot/orahomepage.nsf/IACUC%20Manual>

3. Will the mouse ascites method be used for monoclonal antibody (MAB) production?
 Yes No

<http://utm-int01a.mdacc.tmc.edu/dept/prot/orahomepage.nsf/IACUC%20Manual>

4. Will any animal manipulations not previously mentioned be performed? Yes No

5. Are there any postmortem procedures? Yes No

Please describe the procedures:

Subcutaneous tumors will be removed postmortem and analyzed for cell morphology, gene expression, immunohistochemistry and apoptosis using TUNEL assay

6. Will animals be removed from the DVMS/DVS facilities for any experimental procedure?
 Yes No

G. Monitoring of Animals

1. Describe any physical or physiological impairment of animals resulting from experimental manipulations (e.g., MTD50, neoplasia). If tumor(s) exist, state the maximum size, burden, and length of time the tumor will be present. Scientific justification must be provided if requesting total tumor burdens greater than 1.5cm diameter in mice and 2.0cm diameter in rats.

The IACUC policy on tumor burdens in animals is available on the IACUC Website at:
<http://utm-int01a.mdacc.tmc.edu/dept/prot/orahomepage.nsf/IACUC%20Manual>

Mice will be administered (by oral gavaging) gefitinib alone, tarceva alone or solvent alone, when tumor reaches a size of 100mm³. After 2 weeks of daily oral dosing, the tumors will be locally irradiated on day 15. The duration of growth delay to reach a size of 1.5cm will then be obtained (10-40 days). Animals will be sacrificed when the tumor diameter exceeds 1.5cm.

2. Describe monitoring procedure/schedule, including weekends and holidays, for morbid and moribund animals.*

Animals will be monitored daily, including weekends and holidays, for healthy activity levels and presence of morbidity criteria. Tumor diameter will be measured every other day. Moribund animals will be euthanized within 24hr

3. Describe criteria to determine morbidity, and the point at which moribund animals will receive euthanasia.*

Cachexia, inability to obtain food or water, lethargic movements, hunched posture, excessive tumor volume (when tumor diameter exceeds 1.5cm), ulcerated tumor and shallow breathing. Any of these constitute criteria for euthanasia.

***NOTE:** All investigators are expected to continue to monitor animals at least daily, including weekends and holidays. Morbid is defined as affected with disease or illness; moribund is defined as being in the state of dying.

H. Euthanasia

Include age and euthanasia method for unused rodent pups, if applicable.
(Ether and chloroform are not approved agents for euthanasia because of potential flammable, toxic and carcinogenic hazards)

Note: The use of hypothermia to induce anesthesia in rodent pups < 6 days old requires the use of an acceptable method of euthanasia and must be scientifically justified.
If applicable, please include justification below:

1. Indicate the method(s) to be used:

C02

2. Will death be used as an endpoint? Yes No

<http://utm-int01a.mdacc.tmc.edu/dept/prot/orahomepage.nsf/IACUC%20Manual>

VI. Flow Sheet



ANIMAL PROTOCOL-Gefitinibrevised.c

FLOW SHEET

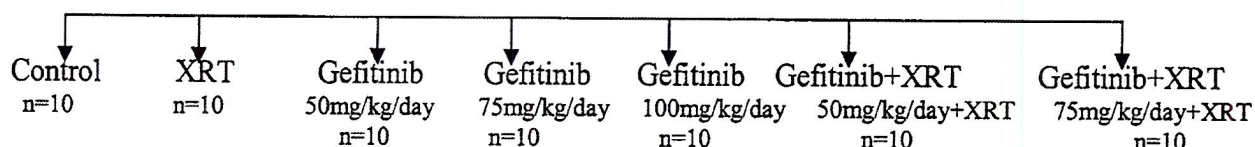
Flow Sheet

Radiosensitization of human tumor xenograft by the small molecule EGFR inhibitor, Gefitinib

420 mice, male/female, Balb/c, Nu/Nu, 6-8 weeks: 10 mice in each of the groups for each cell line to be tested

2×10^6 human tumor cells* injected SQ into right hind legs in 0.1 ml volume, sterile techniques, tumor size measured every day

Gefitinib treatment of xenograft tumors at approximately 100 mm^3
Oral administration of Gefitinib daily for 2 weeks



Control mice receive only vehicle and no radiation

Mice in the Gefitinib alone group receive no irradiation (10 mice per group for each of the three doses to be used – 50mg/kg, 75mg/kg, 100mg/kg delivered by oral gavaging in a maximum volume of 0.1ml).

10 mice in the XRT alone group are treated with ionizing radiation to the leg, 60Co, 5-10 minutes, 5Gy. Mice immobilized with surgical tape, localized irradiation delivered to leg that bears tumor only. Rest of body shielded with lead block using irradiation jig. Anesthesia – Nembutal (60mg/kg IP)

Mice in the combination group receive irradiation on day 11 as described above (24 hrs after the last of oral dose of Gefitinib)

3-dimensional volume measurements every other day to assess tumor re-growth delay. Endpoint is tumor re-growth to 1.5 cm which is anticipated to take between 10-40 days depending on the tumor type, radiation dose and dose of Gefitinib used. Mice will be monitored daily for signs of distress including cachexia, hunched posture, lethargy, inability to obtain food or water, shallow breathing.

When tumor diameter exceeds 1.5 cm or any criteria of moribund status are identified, mice will be euthanized by CO2. Postmortem necropsy and excision of subcutaneous tumor, followed by histologic exam. Tumor will be analyzed for morphology, gene expression and immunohistochemical changes.

- Similar strategy will be followed for the EGFR inhibitor, Tarceva
- Human tumor cells include the following lines: A549, H1299, H358
- All cell lines are available through ATCC.

VII. Addenda

VIII. Funding Sources

Source	Status
Other	Active
Specify: DOD	

Investigators are responsible for budgeting sufficient funds for animal purchase and maintenance.
Information on the current maintenance charges is available on the DVMS Intranet Website.

IX. Investigator's Assurance Statement

Principal Investigator:

I accept and will conform to all Federal and State laws and guidelines, and all institutional policies and procedures concerning the care and use of animals in research, teaching, or testing. I also assure that I and all persons named on this form will complete the institutional animal care and use training program and submit documentation before working with animals. I understand that I have a responsibility to notify in writing the Institutional Animal Care and Use Committee of any changes in the proposed project or personnel, relative to this application, prior to proceeding with any animal use, and will provide an annual project status report.

Principal Investigator Signature: _____

Principal Investigator Name: Ray Meyn Date: _____

Chairman/Division Head:

I have reviewed this request for animal care and use and have found the proposed research to be scientifically meritorious.

Chairman/Division Head

Signature: _____

Chairman/Division Head Name: James D. Cox

Date: _____

APPENDIX C

Appendix C
Revised Statements of Work

Project 1 **Targeting Ras-Raf-Mek-ERK signaling to enhance response of lung cancer to therapeutic radiation. (No change)**

- Task 1. Conduct clinical trial in patients with NSCLC using the combination of Iressa and radiation. (Years 1-4)
- Task 2. Conduct studies characterizing signaling pathways of EGFR activation in NSCLC cell lines and correlative studies (Years 1-4)
- Task 3. Test ability of EGFR inhibitors to suppress DNA repair, restore apoptosis and radiosensitize NSCLC cells (Years 1-4)
- Task 4. Test for additive radiosensitizing effect on NSCLC targeting both EGFR and signaling pathways (Years 1-4)
- Task 5. Test strategies developed in aims 2-4 in xenograft tumor model (Years 1-4)

Project 2 **Molecular imaging of EGFR expression and activity in targeted therapy of lung cancer. (No change)**

- Task 1. Synthesize novel pharmacokinetically optimized ¹²⁴I and ¹⁸F-labeled IPQA derivatives for PET imaging of EGFR kinase activity and conduct in vitro radiotracer accumulation studies in tumor cells expressing different levels of EGFR activity. (Years 1-2)
- Task 2. Assess the biodistribution (PK/PD) and tumor targeting by novel ¹²⁴I and ¹⁸F-labeled EGFR kinase-specific IPQA derivatives using microPET in animals with orthotopic models of lung cancer; compare in vivo radiotracer uptake/retention with phospho-EGFR levels measured in situ. Select the most promising ¹²⁴I or ¹⁸F-labeled IPQA derivative for further studies. (Years 1-3)
- Task 3. Using selected ¹²⁴I or ¹⁸F-labeled IPQA derivative, to conduct pre-clinical studies in animals with orthotopic models of lung cancer xenografts with different levels of EGFR expression/activity, and to assess the value of PET imaging as the inclusion criterion for therapy by EGFR inhibitors as well as for monitoring the efficacy of treatment with EGFR-targeted drugs. (Year 3)
- Task 4. Perform pilot clinical PET imaging studies with the optimized ¹²⁴I or ¹⁸F-labeled IPQA derivative under the RDRC guidelines in patients with NSCLC undergoing adjuvant therapy before tumor resection or biopsy. Compare PET image-based measures of EGFR activity with immunohistochemical measures of phospho-EGFR in situ. (Year 4)

Project 3 **Targeting Ras-Raf-Mek-ERK signaling to enhance response of lung cancer to therapeutic radiation. (No change)**

- Task 1. Select peptides targeting primary and metastatic tumors in lung cancer patients. (Years 1-2)
- Task 2. Validate receptors for targeting human lung cancer. (Years 1-3)
- Task 3. Design tools for molecular imaging of lung tumors. (Years 1-4)

Project 4 **Inhibition of bFGF Signaling for Lung Cancer Therapy. (No change)**

- Task 1. Determine the effects of bFGF on in vitro growth, survival, motility, invasion and angiogenesis of NSCLC cells and endothelial cells. (Years 1-2)
- Task 2. Evaluate the potency of inhibitors of bFGF binding to receptor in inhibition of the effects of bFGF and evaluate the effects of these inhibitors in combination with paclitaxel on in vitro growth and survival of tumor cells. (Years 2-3)
- Task 3. Evaluate anti-tumor activity of the most effective inhibitor identified in Specific Aim 2 when used alone and in combination with paclitaxel in an orthotopic lung cancer model using luciferase-

expressing NSCLC cells for in vivo bioluminescence imaging of tumor growth and response to treatment. (Years 3-4)

Extended

Task 4.

Investigate the expression of bFGF signaling components (bFGF, FGFR-1, FGFR-2, heparan sulfate, syndecan-1, and FGFR-3) by IHC staining of the tissue microarrays (TMAs), and correlate the IHC expression of bFGF/bFGFRs between tumor and non-malignant epithelial cells with angiogenesis.

Project 5

Targeting mTOR and Ras signaling pathways for lung cancer therapy. (New change)

Task 1. Conduct experiments to determine whether CCI-779 inhibits the growth of human NSCLC cells via G1 growth arrest or induction of apoptosis, and to identify the molecular determinants of CCI-779 sensitivity. (Year 1)

Task 2. Conduct experiments to determine whether the effect of CCI-779 on the growth of human NSCLC cells is enhanced in the presence of a PI3K inhibitor or a MAPK inhibitor. (Years 2-3)

Task 3. Conduct experiments to determine whether restoration of the Ras-dependent death-signaling pathway enhances the growth inhibitory effect of CCI-779 in human NSCLC cells. (Years 3-4)

Task 4. Conduct a pilot clinical biochemical induction trial to investigate the effect of CCI-779 in operable NSCLC patients and identify molecular determinants of CCI-779 sensitivity and prognosis. (Years 1-4)

Modified Tasks (replace CCI-779 in original Tasks 1-4 with RAD001):

Task 1. Determine whether mTOR inhibitor (RAD001) inhibits the growth of human NSCLC cells via G1 growth arrest or induction of apoptosis, and to identify the molecular determinants of mTOR inhibitor sensitivity

Task 2. Determine whether effects of mTOR inhibitor (RAD001) on the growth of human NSCLC cells is enhanced in the presence of a PI3K inhibitor or a MAPK inhibitor

*Task 3. Determine whether restoration of the Ras-dependent death-signaling pathway enhances the growth inhibitory effect of RAD001 in human NSCLC cells

Revised to: Evaluate the efficacies of the combinations of rapamycin with LY294002 or U0126 in nude mice models of lung cancer xenografts *in vivo*.

Task 4. Conduct a pilot clinical biochemical induction trial to investigate the effect of RAD001 in operable NSCLC patients and identify molecular determinants of RAD001 sensitivity and prognosis.

Project 6

Identification of Novel Biomarkers and Therapeutic Targets in Aerodigestive Cancers (new change)

Task 1. Expression profile before- and after-treatment NSCLC and head and neck squamous cell carcinoma (HNSCC) patient samples and cell lines by DNA microarray technology. (Years 1-2)

Task 2. DNA profile samples by complementing DNA approaches to stratify RNA expression profiles on the basis of their corresponding DNA profiles. (Years 1-4)

Task 3. Evaluate the contribution of promoter hypermethylation and transcriptional inactivation of known cancer genes subject to epigenetic silencing to cancer phenotype. (Years 1-4)

Extended Task from Aims 1- 3:

Determine the *EGFR* mutation status of the NSCLC tumors from series of patients to stratify patients based on *EGFR* mutation status and characterize NSCLC tumors of patients (usually nonsmokers) with and without *EGFR* mutations of the same histology. To this end, we plan to enroll at least 15 patients in each group.

Task 4. Determine protein signatures of Iressa treatment in NSCLC and to identify molecular predictors of treatment response. (Years 1-4)
Task 5. Determine a clinical utility of the molecular predictors. (43-60 month)

Modified Tasks 4- 5 (replace Iressa with Tarceva):

Task 4: Determine protein signatures of tarceva treatment in NSCLC and identify molecular predictors of response.
Revised to: Determine protein signatures of treatments of erlotinib and other therapeutic agents, alone or in combination, in NSCLC and identify molecular predictors of response.
Task 5: To determine a clinical utility of the molecular predictors for tarceva treatment.

Developmental Research Project #1

The goal of this project is to better understand the biology of VEGF/VPF in vascular permeability and pleural effusion formation to improve therapy of malignant pleural effusion in lung cancer patient. We propose a clinical trial and study management of malignant pleural effusion with small molecule ZD6474, a VEGFR tyrosine kinase inhibitor. (Years 1-3)

Task 1. Increase time to insertion of indwelling pleural catheter (Denver ® catheter) from 3.5 weeks, which is the common practice in our clinic, to 7 weeks.
Task 2. Study expression of VEGF, IL-6, IL-8, bFGF, LDH, protein, pH in serum and pleural effusion.
Study expression of VEGFR, EGFR and activated receptors on tumor cells collected from effusion.
Task 3. Measure level of circulating endothelial cells and circulating endothelial progenitor cells in serum and pleural effusion.
Task 4. Evaluate rate of fluid re-accumulation with chest roentgenograms.
Evaluate drug effect on tumor burden with chest CTs.
Evaluate drug effect on vascular permeability with dynamic contrast enhanced chest CTs.
Task 5. Evaluate drug effect on quality of life and shortness of breath using standard questionnaires.

Developmental Research Project #2

We propose Project TALK (Teens and Young Adults Acquiring Lung Cancer Knowledge), a highly innovative program using modern computer technologies. The Departments of Behavioral Science and Thoracic/Head & Neck Medical Oncology will jointly conduct this pilot project. It will assist in making major advances in lung cancer education and prevention among youth. Project TALK will produce a CD-ROM-based education/behavior change for teenagers and young adults. It will be designed to dramatically reduce tobacco use among the target population. Thus, this project will address a critical component of the BESCT Lung Cancer Program – prevention of lung cancer via smoking control in youth.

Task 1. Develop intervention program. Focus groups will be held with adolescents and young adults to ensure we are capturing the essence of the program, using the right messages, and employing the appealing video and animated characters. (Years 1-2)
Task 2. Develop and beta-test CD-ROM. This includes the design of the animation, illustrations, scripts and accompanying videos. (Years 1-2)
Task 3. Implement program in agreed upon locations and recruit young adults to participate in the study. (Years 3-4)
Task 4. Collect/analyze data. (Year 4)

Career Development Program

The Career Development Program is designed to provide training and guidance for academic physician-scientists, clinician-investigators and laboratory-based scientists who wish to dedicate their efforts to translational research in the area of diagnosis, prevention and treatment of lung cancer.

In order to meet this goal, the specific objectives of the Career Development Program are the following:

- Task 1. Recruit and train physicians, scientists and senior post-doctoral fellows to become outstanding translational investigators in the field of lung cancer. (Years 1-2)
- Task 2. Educate awardees in the basic principles of cancer biology, at both the molecular and cellular level, with an emphasis on translational science. (Years 1-2)
- Task 3. Provide a firm foundation for awardees in the specific area of lung cancer biology, laboratory, clinical and epidemiologic evaluation. (Years 1-2)
- Task 4. Guide awardees through the development process of becoming effective lung cancer translational researchers. (Years 1-2)

APPENDIX D

EMORY UNIVERSITY

Institutional Animal Care and Use Committee
1256 Briarcliff Road, NE Room 213-N
Emory University, Briarcliff Campus
Atlanta, Georgia 30306
Phone: 404-712-0734 Fax: 404-727-8452
Email: IACUC@emory.edu
Web Site: (Case Sensitive) <http://www.emory.edu/IACUC>

October 6, 2006

Shi-Yong Sun PhD
WCI: - Winship Cancer Institute
1365-B Clifton Road
Suite B5111

RE: **NOTIFICATION OF ANNUAL CONTINUATION APPROVAL**

PI: Shi-Yong Sun PhD (shi-yong_sun@emoryhealthcare.org)
IACUC ID: 181-2005
TITLE: Enhancing mTOR targeted cancer therapies

This approval will be valid as of 11/30/2006 through 11/30/2007.

Your on-going research proposal referenced above has been approved by the Institutional Animal Care and Use Committee. Approval is contingent upon your agreement to abide by the policies and procedures of Emory University with regard to the use of animals in research.

Our records indicate funding by the following:

NIH - NAT INSTITUTES OF HEALTH
Department of Defense

You have permission to continue to use:		<u>Species Name</u>	<u>Species Class</u>	<u>Species Qty</u>
	Mouse		E	790
	Mouse		E	380

The USDA requires annual renewal of research projects using animals and PHS policy requires a new IACUC application every three years before animal use approval can be extended. Both must be reviewed and approved by the IACUC prior to the anniversary or expiration date of this study. Emory's Animal Welfare Assurance Number is A3180-01.

If there are additions or changes to this protocol, you must submit a 'Request to Modify' form for approval. The form can be obtained from the IACUC web site: <http://www.emory.edu/IACUC> .

All inquiries and correspondence concerning this protocol must include the above referenced IACUC number, the name of the principal investigator and the full title of the study.

If you have any questions, feel free to contact the IACUC office.

Sincerely,



Samuel Speck, Ph.D.
IACUC Chair

cc: Emory's Office of Sponsored Programs (OSP)
Emory's Department of Animal Resources (DAR)
Department Chair

APPLICATION FOR THE USE OF ANIMAL SUBJECTS IN RESEARCH, TEACHING AND TRAINING
Institutional Animal Care and Use Committee of Emory University

REvised

1256 Briarcliff Rd., Bldg. A, Room 421-S
 Atlanta, GA 30322

<http://www.emory.edu/IACUC>
 Email: IACUC@emory.edu

Office: 404-727-6786
 Fax: 404-727-8452

FOR OFFICE USE ONLY

Date Received: **10/25/05**
 Biohazard: Yes No

Reviewers: Yes No
 Radiac: Yes No

APPROVED

IACUC # **181-2025**
 Date Approved: **10-26-05**
 Enrichment Waiver: Yes No

PROVIDE A COPY OF THE RELEVANT GRANT APPLICATION(S), OR A RESEARCH PROPOSAL FOLLOWING OUTLINE OF THE UNIVERSITY RESEARCH COMMITTEE. (URC guidelines at <http://www.urc.emory.edu/>). However, do not refer reviewers to original grant application instead of responding the questions below. Feel free to add more space as required to adequately address each point.

A. BASIC INFORMATION

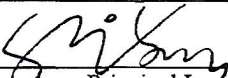
1. Title of Proposal	Enhancing mTOR Targeted Cancer Therapies		
2. Funding Agency/Source	NIH or DoD		
3. Anticipated Start Date	10-01-05		
4. Category	<input checked="" type="checkbox"/> Research	<input type="checkbox"/> Teaching/Training	
5. Type	<input checked="" type="checkbox"/> New	<input type="checkbox"/> Re-Submission	<input type="checkbox"/> 3Yr Renewal
(If Applicable) Previous IACUC #			

6. **Veterinary Care and Consultation:** You are required to obtain a written consultation from an Emory University attending veterinarian in the planning stage of the project before submission of the application to the IACUC. Contact the Division of Animal resources (vet_cons@dar.emory.edu, 404-727-3248) or Yerkes Research Center (Non-human primate contact Elizabeth Strobert, DVM, eliz@rmy.emory.edu, 404-727-7772; Rodent contact Denyse Levesque, DVM, denysel@rmy.emory.edu, 404-727-8101) as appropriate, to arrange for the consultation. If animals are to be used at both Emory and Yerkes, then a consultation should be obtained from each. This form must be submitted to the Veterinarian on or before the last Wednesday of the month.

Name of veterinarian consulted:	Curtis W. Schondelmeyer, DVM	Date consult requested:	07/25/05
---------------------------------	---------------------------------	-------------------------	----------

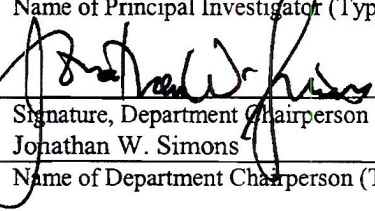
7. **Environmental Enrichment Consultation:** A written consultation from Mollie Bloomsmith, the Yerkes Environmental Enrichment Coordinator (mblooms@rmy.emory.edu or 404-727-8809), is required for protocols involving non-human primates (see Section O of this form). This form must be submitted to the Enrichment Coordinator on or before the last Wednesday of the month or it will not be evaluated until the following month

8. **Certification:** I will comply with the procedures described in the NIH Guide for the Care and Use of Laboratory Animals (National Academy of Sciences, 1996), with PHS policy, the Animal Welfare Act (regulations can be viewed at <http://www.emory.edu/IACUC>), applicable University policies, and Standard Operating Procedures as described by the DAR and IACUC. I acknowledge responsibility for this project and assure that the faculty, staff and students who participate in it are qualified (or will be adequately trained) to conduct it in a humane manner.


 Signature, Principal Investigator

Shi-Yong Sun

Name of Principal Investigator (Typed)


 Signature, Department Chairperson

Johathan W. Simons

Name of Department Chairperson (Typed)


 Date

Hematology and Oncology

Department


 Date

APPLICATION FOR THE USE OF ANIMAL SUBJECTS IN RESEARCH, TEACHING AND TRAINING
Institutional Animal Care and Use Committee of Emory University

1256 Briarcliff Rd., Bldg. A, Room 421-S
Atlanta, GA 30322

<http://www.emory.edu/IACUC>
Email: IACUC@emory.edu

Office: 404-727-6786
Fax: 404-727-8452

B. STUDY OBJECTIVES:

Using easily understandable **LAY TERMS**, briefly describe the objectives and the specific aims of the study. Describe the relevance of the study to advancing scientific knowledge and/or the benefits of the study to human and/or animal health. *(Note: A scientific abstract from grant application using highly technical terms is NOT acceptable. Use simple terms and define all abbreviations.)*

→ Targeted cancer therapies represent a major advance in our fight against cancer. However, it has been increasingly recognized that dysregulated survival mechanisms not only contribute to tumorigenesis, but also induce resistance to therapies, thus decreasing their treatment efficacy. The long-term goal of our research is to develop novel and efficacious therapeutic regimens for the treatment of human lung cancer based on our mechanistic studies on cancer biology. The current protocol aims specifically at enhancing the efficacy of the mammalian target of rapamycin (mTOR)-targeted therapies against lung cancer. Rapamycin and its derivatives (e.g., RAD001) that specifically inhibit mTOR are now being actively tested either alone or in combination with other drugs in phase I-II oncology clinical trials. Recent studies have revealed an intricate regulatory network that controls the mTOR axis (4), thus providing a critical mechanistic basis for the mTOR-targeted cancer therapy. It has been established in many cell types that the PI-3 kinase (PI3K)/Akt pathway functions upstream of mTOR and activates mTOR signaling. However, our results in human lung cancer cells revealed that mTOR inhibitors not only inhibit mTOR signaling, but also rapidly induces the activation of the PI3K/Akt survival pathway. Moreover, an mTOR inhibitor in combination with a PI3K inhibitor synergistically inhibited the growth of lung cancer cells in cell culture systems. In this protocol, we will validate our in vitro findings by testing the anticancer effect of an mTOR inhibitor in combination with an agent that inhibits PI3K or Akt activity in a mouse lung xenograft model. By accomplishing the studies in this protocol, we may develop novel mechanism-based combinations to enhance mTOR-targeted cancer therapy.

C. RESEARCH DUPLICATION:

You are required by law to provide assurance that the proposed research does not unnecessarily duplicate previous work. A thorough computer assisted search of the literature provides the best evidence of the lack of duplication. Thus, the IACUC recommends that you perform a search and list the date, period covered, keywords and the database(s) searched. Keep copies of the results in your files. (If you need help with developing a computer search, call the University Health Sciences Center Library (404-727-5813) for assistance). The personal knowledge of the principal investigator may be accepted if his or her experience and expertise as leader in the field can be adequately demonstrated by such activities as serving as a regular member of a study section for federal and non-federal funding agencies, as editor of relevant journals, or as organizer of national or international meetings. See <http://www.emory.edu/WHSCL/animalwelfare.html>

Does this research duplicate previous work? No Yes

If no, provide the following information:

Date of Search:	07-20-05	Keywords:	Rapamycin, RAD001, Perifosine, LY294002, Tarceva, U0126, 17-AAG, xenografts, lung cancer
Period Covered:	1960-2005	Database(s) searched:	PubMed

If yes, provide justification for this study.



D. RESEARCH PROCEDURES: (Complete this section for each individual species. If more than one species is used, please use **Procedure.DOC** at http://www.emory.edu/IACUC/general_forms.php for additional copies of this page.)

SPECIES: Mouse (nude mouse)

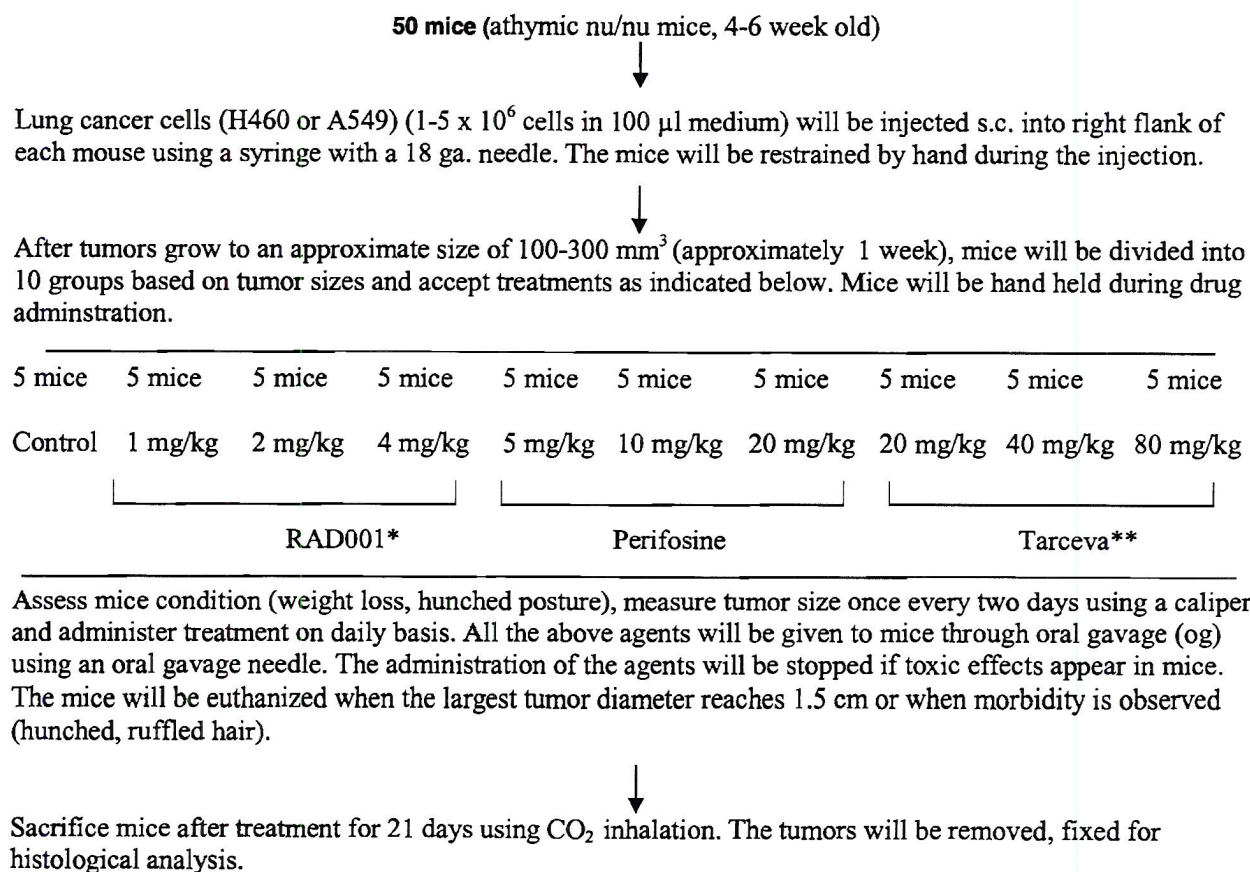
1. Provide a complete description of the proposed use of animals. Outline the study design, including the number of animals in experimental and control groups. A diagram or chart may be helpful to explain complex designs. Describe all procedures on the animals and how often they will be done. Surgery should be described here only as it relates to the study design. Specific details on surgery, anesthesia for surgery, and postoperative care are requested in section H.

→ This protocol is designed to determine whether an mTOR inhibitor combined with an agent that inhibits the PI3K/Akt survival pathway exhibits enhanced effect on the growth of human lung cancer in mouse xenograft models. To successfully assess the enhanced antitumor effects of the proposed combination as well as save animals and time, we need to determine the sub-optimal doses (e.g., IC_{30} - IC_{40}) for each single agent with small numbers of mice. Following this experiment, we will conduct formal experiments to determine the effects of a mTOR inhibitor combined with different agents, respectively, on the growth of lung xenografts. These experiments will be done in two xenograft models. The detailed protocols for these experiments are shown in flow charts as follows:

Experiment #1: To determine the sub-optimal doses for each single agent with small numbers of mice.

Since there are several agents being tested in this experiment, we divided it as three small-scale experiments as follows:

Experiments #1a



* If RAD001 is not available for animal experiment, we will alternatively use rapamycin since both agents work through same mechanism.

** If Tarceva is not available, we will alternatively use Iressa, another EGFR inhibitor with similar action mechanism as Tarceva.

References for the dosages and administrative routes of the tested agents

1. Boffa DJ, Luan F, Thomas D, Yang H, Sharma VK, Lagman M, Suthanthiran M. Rapamycin inhibits the growth and metastatic progression of non-small cell lung cancer. *Clin Cancer Res.* 2004; 10:293-300.
2. Eshleman JS, Carlson BL, Mladek AC, Kastner BD, Shide KL, Sarkaria JN. Inhibition of the mammalian target of rapamycin sensitizes U87 xenografts to fractionated radiation therapy. *Cancer Res.* 2002; 62:7291-7.
3. Ng SS, Tsao MS, Nicklee T, Hedley DW. Effects of the epidermal growth factor receptor inhibitor OSI-774, Tarceva, on downstream signaling pathways and apoptosis in human pancreatic adenocarcinoma. *Mol Cancer Ther.* 2002;1:777-83.
4. Dai Q, Ling YH, Lia M, Zou YY, Kroog G, Iwata KK, Perez-Soler R. Enhanced sensitivity to the HER1/epidermal growth factor receptor tyrosine kinase inhibitor erlotinib hydrochloride in chemotherapy-resistant tumor cell lines. *Clin Cancer Res.* 2005;11:1572-8.
5. Hilgard P, Klenner T, Stekar J, Nossner G, Kutscher B, Engel J. D-21266, a new heterocyclic alkylphospholipid with antitumour activity. *Eur J Cancer.* 1997;33:442-6.
6. Vink SR, Schellens JH, van Blitterswijk WJ, Verheij M. Tumor and normal tissue pharmacokinetics of perifosine, an oral anti-cancer alkylphospholipid. *Invest New Drugs.* 2005;23:279-86.

Experiments #1b

50 mice (athymic nu/nu mice, 4-6 week old)

Lung cancer cells (H460 or A549) ($1-5 \times 10^6$ cells in 100 μ l medium) will be injected s.c. into right flank of each mouse using a syringe with a 18 ga. needle. The mice will be restrained by hand during the injection.

After tumors grow to an approximate size of 100-300 mm³ (approximately 1 week), mice will be divided into 10 groups based on tumor sizes and accept treatments as indicated below. Mice will be hand held during drug administration.

Assess mice condition (weight loss, hunched posture), measure tumor size once every two days using a caliper, and administer treatment on daily basis. All the above agents will be given to mice intraperitoneally (ip) using a 26G5/8 needle. The administration of the agents will be stopped if toxic effects appear in mice. The mice will be euthanized when the largest tumor diameter reaches 1.5 cm or when morbidity is observed (hunched, ruffled hair).

Sacrifice mice after treatment for 21 days using CO₂ inhalation. The tumors will be removed, fixed for histological analysis.

**** If a prodrug for LY294002 named SF1126 (from Semafore Pharmaceutical, Indianapolis, Indiana) is available, we will alternatively use SF1126 in the experiments because it has better PK properties.

Notes:

- 1) If necessary, we need to repeat some of the treatments. Therefore, we need totally 150 mice for this experiment.
- 2) Based on the above experiments, we will choose doses, which cause approximately 30-40% tumor regression, for each individual agent and use these doses in the subsequent experiment (Experiment #2).

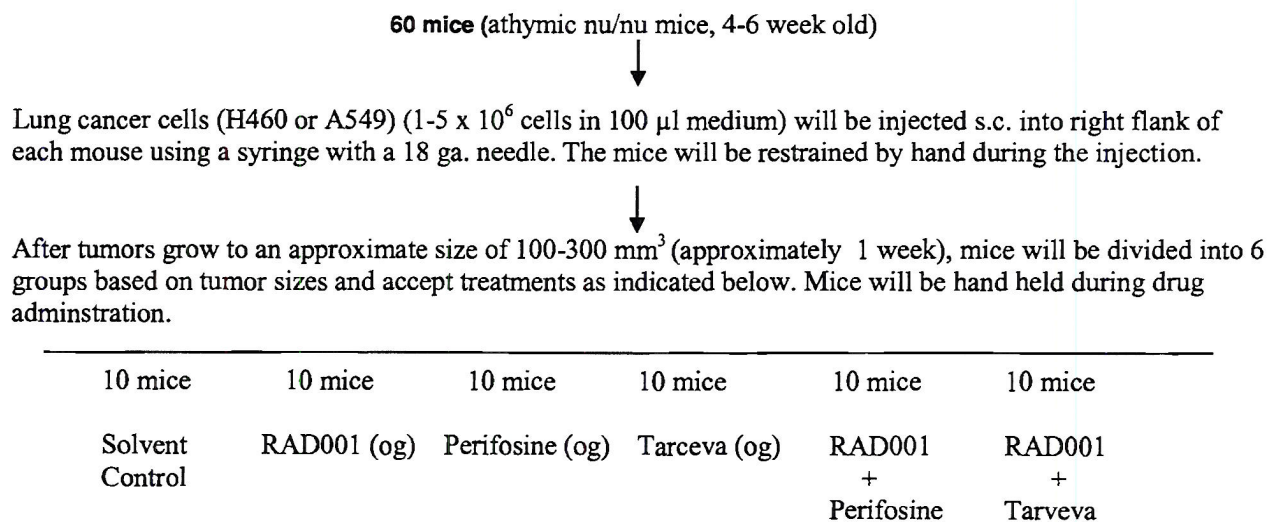
References for the dosages and administrative routes of the tested agents

1. 1Hu L, Hofmann J, Lu Y, Mills GB, Jaffe RB. Inhibition of phosphatidylinositol 3'-kinase increases efficacy of paclitaxel in in vitro and in vivo ovarian cancer models. *Cancer Res* 2002; 62:1087-92.
2. Fan QW, Specht KM, Zhang C, Goldenberg DD, Shokat KM, Weiss WA. Combinatorial efficacy achieved through two-point blockade within a signaling pathway-a chemical genetic approach. *Cancer Res*. 2003; 63:8930-8.
3. Horiuchi H, Kawamata H, Fujimori T, Kuroda Y. A MEK inhibitor (U0126) prolongs survival in nude mice bearing human gallbladder cancer cells with K-ras mutation: analysis in a novel orthotopic inoculation model. *Int J Oncol*. 2003;23:957-63.
4. Uchida D, Begum NM, Tomizuka Y, Bando T, Almofti A, Yoshida H, Sato M. Acquisition of lymph node, but not distant metastatic potentials, by the overexpression of CXCR4 in human oral squamous cell carcinoma. *Lab Invest*. 2004;84:1538-46.
5. Yin X, Zhang H, Burrows F, Zhang L, Shores CG. Potent activity of a novel dimeric heat shock protein 90 inhibitor against head and neck squamous cell carcinoma in vitro and in vivo. *Clin Cancer Res*. 2005;11:3889-96.
6. Solit DB, Zheng FF, Drobnyak M, Munster PN, Higgins B, Verbel D, Heller G, Tong W, Cordon-Cardo C, Agus DB, Scher HI, Rosen N. 17-Allylamino-17-demethoxygeldanamycin induces the degradation of androgen receptor and HER-2/neu and inhibits the growth of prostate cancer xenografts. *Clin Cancer Res*. 2002;8:986-93.

Experiment #2: To determine the effects of a mTOR inhibitor (Rapamycin or RAD001) combined with each of the above agents on the growth of lung xenografts

There are several combinations being tested in this experiment. To better handle the experiment, we will conduct three experiments to achieve our research goal as follows:

Experiment #2a:



The sub-optimal doses determined from Experiment #1 will be used in this experiment.

Assess mice condition (weight loss, hunched posture), measure tumor size once every two days using a caliper, and administer treatment on daily basis. The administration of the agents will be stopped if toxic effects appear in mice. The mice will be euthanized when the largest tumor diameter reaches 1.5 cm or when morbidity is observed (hunched, ruffled hair).

Sacrifice mice after treatment for 21 days using CO₂ inhalation. The tumors will be removed, fixed for histological analysis.

Experiment #2b:

60 mice (athymic nu/nu mice, 4-6 week old)

Lung cancer cells (H460 or A549) (1-5 x 10⁶ cells in 100 µl medium) will be injected s.c. into right flank of each mouse using a syringe with a 18 ga. needle. The mice will be restrained by hand during the injection.

After tumors grow to an approximate size of 100-300 mm³ (approximately 1 week), mice will be divided into 6 groups based on tumor sizes and accept treatments as indicated below. Mice will be hand held during drug administration.

10 mice	10 mice	10 mice	10 mice	10 mice	10 mice
Solvent Control	RAD001 (og)	LY294002 (ip)	U0126 (ip)	RAD001 + LY294002	RAD001 + U0126

The sub-optimal doses determined from Experiment #1 will be used in this experiment.

Assess mice condition (weight loss, hunched posture), measure tumor size once every two days using a caliper, and administer treatment on daily basis. The administration of the agents will be stopped if toxic effects appear in mice. The mice will be euthanized when the largest tumor diameter reaches 1.5 cm or when morbidity is observed (hunched, ruffled hair).

Sacrifice mice after treatment for 21 days using CO₂ inhalation. The tumors will be removed, fixed for histological analysis.

Experiment #2c:

40 mice (athymic nu/nu mice, 4-6 week old)

Lung cancer cells (H460 or A549) (1-5 x 10⁶ cells in 100 µl medium) will be injected s.c. into right flank of each mouse using a syringe with a 18 ga. needle. The mice will be restrained by hand during the injection.

After tumors grow to an approximate size of 100-300 mm³ (approximately 1 week), mice will be divided into 4 groups based on tumor sizes and accept treatments as indicated below. Mice will be hand held during drug administration.

10 mice	10 mice	10 mice	10 mice
---------	---------	---------	---------

Solvent
Control

RAD001 (og) 17-AAG (ip)

RAD001
+
17-AAG

The sub-optimal doses determined from Experiment #1 will be used in this experiment.

Assess mice condition (weight loss, hunched posture), measure tumor size once every two days using a caliper, and administer treatment on daily basis. The administration of the agents will be stopped if toxic effects appear in mice. The mice will be euthanized when the largest tumor diameter reaches 1.5 cm or when morbidity is observed (hunched, ruffled hair).



Sacrifice mice after treatment for 21 days using CO₂ inhalation. The tumors will be removed, fixed for histological analysis.

Notes:

- 1) This experiment will be conducted using two lung xenograft models (e.g., H460 and A549), which need 320 mice. We may repeat the experiment once. Therefore, we need a total of 640 mice for this experiment.

2. Indicate where these procedures will be performed:					
Facility:	Winship Cancer Institute	Bldg:	Clinic Bldg B	Room:	B3315
3. Indicate where animals will be housed:					
Facility:	Winship Cancer Institute	Bldg:	Clinic Bldg B	Room:	B3115
4. Describe special animal husbandry requirements:					
a. Caging or housing:	Sterile cages				
b. Diets:	Standard				
c. Environment:	standard				
d. Care:	standard				
5. Will any live animals be removed from the animal facilities:			<input checked="" type="checkbox"/> No	<input type="checkbox"/> Yes - please provide the following:	
a. How will they be transported:					
b. The location where they will be taken:	Bldg:		Room:		
c. How long they will be held outside the animal facility:					
d. Will live animals be returned to animal facilities:					

E. ANIMAL SPECIES AND NUMBERS TO BE USED FOR THESE STUDIES:

1. **Classification by stress level:** This classification system is required by the Animal Welfare Act. It is only a reporting mechanism and does not alter IACUC or veterinary oversight. Issues of assessment and minimization of pain and distress are addressed in other sections throughout the protocol form.

Class B. Animals bred, conditioned, or held for use in teaching, testing, experiments, research, or surgery but not yet needed for such purposes.

Species	Year 1	Year 2	Year 3	Total

Class C. Non-Painful/Non-Stressful: Animals upon which teaching, research, experiments, or tests will be conducted involving no pain, distress, or use of pain-relieving drugs. (routine procedures causing only slight or momentary discomfort such as: venipuncture, injections, and the use of non-inflammatory adjuvants)

Species	Year 1	Year 2	Year 3	Total

Class D. Painful/Stressful WITH Analgesia/Anesthesia/Tranquilizers: Animals upon which experiments, teaching, research, surgery, or tests will be conducted involving accompanying pain or distress to the animals and for which appropriate anesthetic, analgesic, or tranquilizing drugs will be used.

Species	Year 1	Year 2	Year 3	Total

Class E. Painful/Stressful WITHOUT Pain or Stress Relieving Measures: Animals upon which teaching, experiments, research, surgery or tests will be conducted involving accompanying pain or distress to the animals and for which the use of appropriate anesthetic, analgesic, or tranquilizing drugs would have adversely affected the procedures, results, or interpretation of the teaching, research, experiments, surgery, or test.

Species	Year 1	Year 2	Year 3	Total
Nude mice				790

2. **Lack of non-painful, non-stressful alternatives:** If any animals are listed in class D or E in question E1 above, the Principal Investigator is required by law to document that alternatives to procedures that may cause pain or distress to animals have been considered. The USDA and Public Health Service support the three R's (Replace, Reduce, and Refine) as guidelines for the choice of species and number of animals to be used. (See instructions for USDA Policy at <http://www.aphis.usda.gov/ac/policy/policy12.html>).

a. The USDA considers a computer-assisted literature search to be the best method to check for non-painful, non-stressful alternatives. Thus, the IACUC recommends that you perform a search and list the date, period covered, keywords and the database(s) searched. Available sites can be found below at <http://altweb.jhsph.edu/> and <http://www.iacuc.org/>. (Keep copies of the search results in your files.) You may provide an alternative strategy that describes the methods and sources used to determine that no alternatives were available to the painful or distressful procedure. (See the USDA's "closer look at Policy No. 12" at <http://warp.nal.usda.gov:80/awic/newsletters/v9n3/9n3dehav.htm> and The USDA's text of Policy No. 12 at <http://www.aphis.usda.gov/ac/policy/policy12.html>)

Date of Search:	07-20-05	Keywords:	Tumor xenografts and animal testing alternatives,
Period Covered:	1970-2005	Database(s) searched:	http://www.altwebsearch.org/search.htm , Agricola



b. Are less painful or stressful alternatives available?

Yes

No

c. If YES, justify why they are not going to be used.



3. Rationale for Animal Use: Provide a clear and logical thought process explaining the choice of species and the number of animals to be used. Statistical methods should be described where possible.

a. Species.

→ We must use nude mice for our studies because this is the only experimental system that can provide assessment of the ability of the tested agents to inhibit cancer growth *in vivo*. Inhibition of cancer growth studied using cell lines in culture is limiting because tumor growth *in vivo* is a complex process involving three dimensional growth and interactions between tumor cells and normal cells (i.e., stromal and normal epithelial cells) as well as angiogenesis; these activities occur only under *in vivo* conditions. Athymic mice used in this protocol allow the growth of human cells *in vivo* because of their suppressed immune system.

b. Number of animals.

→ In this protocol, we have two experiments. The first one will determine the sub-optimal doses for each individual agent, which will be used in the second experiment. In this way, we will warrant the success in evaluating the enhancing antitumor effects of the tested combinations. In addition, this will reduce mice numbers and save time. Therefore, we need 20 groups x 5 mice per group =100 mice. We need an additional 50 mice to repeat some treatment in case we fail to get sub-optimal doses. For experiment #1, we need a total of 150 mice. For the experiment #1, we have three studies that involve 16 groups of treatments. To achieve our goal, we need 16 groups x 10 mice/group x two models x two repeats = 640 mice in total. In this way, we can achieve statistical significance in assessing the enhanced effects of the combinations vs. single agent alone and generate reproducible results. This also includes consideration of other attritions such as no tumor development and animal sickness. We expect 8-10 mice/group left in the end of experiment. For this protocol, we need a total of 790 mice.

4. Annual Report of Stress Level E Procedures: Emory University must submit an annual report to the United States Department of Agriculture describing the use of any animals (other than rats, mice, birds, and amphibians) that are classified in stress level E above. Briefly describe, in lay terms, all procedures on such animals that are listed in stress level E above. State why pain or distress relieving measures cannot be used (your summary will be included in the annual report to the USDA).

→ In this protocol, mice may experience minor stress due to injection (og, ip, and sc) and tumor burden. Therefore, it is not necessary to use any pain or distress relieving measures, which themselves may cause additional stresses, during the procedures.

F. MONITORING ANIMALS FOR WELL BEING, PREVENTION AND REDUCTION OF DISTRESS INCLUDING SURGERY:

1. Describe the anticipated pain or distress for animals listed in stress levels D and E from section E1:

→ In this protocol, anticipated pain of mice may come from i.p. or s.c. injection. At the late stage, there may be some distress associated with tumor growth, which will be monitored and the mice will be sacrificed if the tumor

volumes are too big (>1.5 cm diameter). It is also possible that agents used may have potential toxicity that may be a source of pain or discomfort. Since the dosage of each agent is sub-optimal and has been used in published literatures, the drug toxicities may occur, but with very low likelihood. We will watch drug toxicities very closely.

2. Describe how pain or distress will be monitored:

→ Pain or distress will be monitored visually, which includes hunched posture, weight loss, lethargy, tumor size, ulceration at tumor site, etc.

3. List who will monitor or observe animals:

→ The animal will be monitored daily for undue stress, or complications of tumor burden or treatment by the individuals responsible for performing the experiments. These individuals are people who were listed in section Q and their credentials were also on file.

4. Indicate schedule of monitoring:

→ Animals will be monitored daily including weekends and holidays. Signs of respiratory distress, loss of weight and size of primary tumor are noted.

5. For animals in stress levels D, describe the interventions and/or the dose, frequency and type of analgesic drugs or tranquilizers to be administered if pain or distress occurs:

→

6. For animals in stress levels D and E studies that may result in debilitation (such as infectious diseases or toxicity testing), describe specific criteria at which animals should be euthanized to prevent undue pain or distress:

→ Animal will be monitored visually for signs of lethargy or changes in appearance. Loss of 25% body weight (not including tumor weight), and large diameter of tumor size ≥ 1.5 cm are all indicators of morbidity. These mice will be sacrificed within 24 hours. The body weight of each mouse will be recorded twice per week during the study. The weight will be compared with the body weight of the same mouse at the beginning of the experiment. We will assure that IACUC endpoints will be followed.

G. EUTHANASIA:

Whether or not euthanasia is planned as part of the study, indicate the method to be used should it be required. Include the agent and dose for each species. Euthanasia methods must be in accord with methods approved by the AVMA Panel on Euthanasia available at

<http://www.emory.edu/WHSC/MED/DAR/resource.htm> Justification to do otherwise must be provided here.

Emory endpoint guidelines will be used unless otherwise specified by the investigator in Section F. 6.

Species	Method	Agent	Dose	Comments
Mouse	Carbon dioxide	CO ₂	Inhalation	Compressed source. The chamber to be used will not be precharged with CO ₂ .

H. SURGERY, SURGICAL ANESTHESIA, POST-OPERATIVE CARE: (Complete this section for each individual species. If more than one species is used, please use **Surgery.DOC** at http://www.emory.edu/IACUC/general_forms.php for additional copies of this page.)

SPECIES:	
1. Describe each surgical procedure to be used. Indicate the number of animals used for each surgical procedure and the number of procedures to be performed each year.	

→N/A

2. Surgical anesthesia and analgesia			
	Drug	Dose/Frequency	Route
Pre-anesthesia			
Maintenance Anesthesia			
Paralytic Agents			
Post-operative Analgesia			

3. Will animals be allowed to recover from anesthesia?	Yes <input type="checkbox"/>	No <input type="checkbox"/>
4. Describe how depth of anesthesia will be determined and monitored:		

→N/A

5. If the answer to #3 is YES, will more than one major survival surgery be conducted on each animal?	Yes <input type="checkbox"/>	No <input type="checkbox"/>
6. If the answer to #5 is YES, how many		
7. Provide scientific justification for more than one major, survival surgery on each animal:		

→N/A

8. Site of operating room	Facility		Bldg		Room	
9. Site of recovery room	Facility		Bldg		Room	
10. Describe the postoperative care						
a. First 24 hours:						
b. Second 24 hours						
c. Thereafter:						
11. Person responsible for postoperative care		Name:		Phone:		
12. Name of surgeon		Name:		Phone:		

I. ANIMAL TRAINING:

Describe goals of and methods to be used to train animals. Include frequency and duration of training sessions as well as positive and negative stimuli.

→N/A

J. PHYSICAL OR PHARMACOLOGICAL RESTRAINT OF ANIMALS:

Describe methods, frequency and duration of physical restraint (other than routine caging and handling) or chemical (sedation or anesthesia) restraints. Complete this section for each individual species. If more than one species is used, please use **Restraint.DOC** at http://www.emory.edu/IACUC/general_forms.php for additional copies of this page.

1. Describe each non-surgical procedure to be used. Indicate the number of animals used for each non-surgical procedure and the number of procedures to be performed each year.

→N/A

2. For each species, fill out table to describe the treatments to be used in experimental procedures (other than surgery described in section H).

Restraint	Drug	Dose/Frequency	Route
Chemical			
Sedation			
Anesthesia			
Site where procedures will be carried out	Facility:	Bldg	Room

3. Describe post-treatment care, including how animals will be monitored during recovery from treatment.

→N/A

K. TISSUE COLLECTION: (List all blood, body fluid and tissues to be collected).

Species	Fluid/Tissue	Amount	Frequency	Site/Method	postmortem Harvest (Y/N)
Mouse	Xenografted human tumor	Whole tumor tissue	After sacrificing mice	Freeze and fixed	yes

L. ADMINISTRATION OF TISSUE, FLUID, SUBSTANCE: List all materials (drug, special diet, gas, vehicle, adjuvant, cells, carcinogen, etc.) except chemicals, anesthetics, analgesics and paralytics that are listed in Sections F, H, or J.

1. Describe all agents to be administered to animals:

Species	Agent	Route	Dose (mg/kg, gm or ml)	Frequency	Possible Complications
Mouse	RAD001 (or rapamycin)	og	1-4 mk/kg	daily	No complication at current doses
	LY294002	ip	10-40 mg/kg	daily	No complication at current doses
	Perifosine	og	5-20 mg/kg	daily	No complication at current doses
	Tarceva	og	20-80 mk/kg	daily	No complication at current doses
	U0126	ip	4-12 mg/kg	daily	No complication at current doses
	17-AAG	ip	25-100 mg/kg	daily	No complication at current doses
	A549 cells	sc	1-5x10 ⁶ /mouse	once	Form tumor or xenograft
	H460 cells	sc	1-5x10 ⁶ /mouse	once	Form tumor or xenograft

2. The use of Complete Freund's Adjuvant requires adherence to the Emory University recommendation for Complete Freund's Adjuvant (see <http://www.emory.edu/IACUC>).

a. Will Freund's complete adjuvant be administered to animals? If NO, skip to number L3.	Yes <input type="checkbox"/> No <input checked="" type="checkbox"/>
b. If yes, state that the guidelines will be followed or describe and justify any deviation from this policy below.	

→N/A

3. Tumors, tissues, cells, and cell lines can be infected with pathogens that may cause disease in humans or other animals. Therefore, IACUC applications will be approved for the use of these materials only if they were derived from: mice obtained from commercial vendors; or mice that have cleared quarantine and are housed at Emory University; or if they have been shown to be free of infectious agents, or if animals receiving untested materials are housed under strict quarantine.

a. Will tumors, tissues or tissue culture cell lines be administered to living animals? If NO, skip to number 4.	Yes <input checked="" type="checkbox"/> No <input type="checkbox"/>
b. Will these materials derived from mice obtained from approved, commercial vendors or mice that were cleared through quarantine and housed at Emory University?	Yes <input checked="" type="checkbox"/> No <input type="checkbox"/>
i. If yes, skip to number 4.	
ii. If no, have these materials been tested to show that they are pathogen-free? (See http://www.emory.edu/WHSC/MED/IACUC for a table of existing MAP test results)	Yes <input type="checkbox"/> No <input type="checkbox"/>
iii. If yes, provide the documentation.	

iv. If no, contact a veterinarian at your location (see page 1 A5) to arrange for appropriate testing.
v. If no, and no testing is to be done, section M must be completed.



4. Emory University requires adherence to the OLAW policies concerning the Production of Monoclonal Antibodies Using Mouse Ascites Method. Please refer to the policy at http://grants.nih.gov/grants/olaw/references/dc98-01.htm
--

Will monoclonal antibodies be produced using the Ascites method?	Yes <input type="checkbox"/>	No <input checked="" type="checkbox"/>
--	------------------------------	--

If NO, go to section M. If YES, use of the Ascites Method must be justified here.



M. FOR USE OF INFECTIOUS AGENTS, TOXINS, OR HAZARDOUS CHEMICALS IN LIVE ANIMALS LIST:
--

1. Agent	N/A
2. Date of Bio-Safety Committee Approval	

N. FOR USE OF RADIOISOTOPES IN LIVE ANIMALS LIST:
--

1. Labeled Compound	N/A
2. Radioisotope	N/A
3. Dose per animal	N/A
4. Date of Radiation Safety Committee Approval	N/a

O. ENVIRONMENTAL ENHANCEMENT FOR NON-HUMAN PRIMATES: (If Non-Human Primates are used, Complete this section for each individual species. If more than one species is used, please use Environmental.DOC at http://www.emory.edu/IACUC/general_forms.php for additional copies of this page.)

1. a. Are non-human primates to be used?	Yes <input type="checkbox"/>	No <input checked="" type="checkbox"/>
b. If no, proceed to section P	Name of Species:	
c. If yes, answer all items in section O2.		

2. HOUSING CATEGORIES: (Each category below MUST be checked either Yes or No.) If animals are to be housed under different conditions at different times during the protocol indicate all categories that apply. Please do NOT select additional housing categories to accommodate the possibility of social incompatibility, transient post-operative care, or clinical complications. These are issues related to clinical management rather than your experimental protocol.

Yes <input type="checkbox"/> No <input type="checkbox"/>	Group housing – three or more non-human primates housed together in an enclosure. This housing category is considered optimal for all age classes of animals but particularly encouraged for infants and young juveniles as well as all chimpanzees. No justification of this housing category is required.
Yes <input type="checkbox"/> No <input type="checkbox"/>	<p>Pair housing – two non-human primates housed together in an enclosure. The specific type of pairing may be selected below. If pairing is selected but not the type, the default is “any compatible animal.” It is important to note that only animals with the same virus strains (if known) or within the same arm of a study will be paired. This setting is <u>particularly</u> encouraged for infants and young juveniles, as well as all chimpanzees, when group housing is not feasible. No justification of this housing category is required. The specific type of pairing may be selected.</p> <p>same sex <input type="checkbox"/> same age <input type="checkbox"/> same sex and same age <input type="checkbox"/> mother-offspring <input type="checkbox"/></p>
Yes <input type="checkbox"/> No <input type="checkbox"/>	<p>Protected contact housing – two non-human primates housed in adjacent cages separated by a partition that permits social contact. This setting is encouraged for subjects who would otherwise be single housed due to differences in diets between individuals, or due to frequent removal from primary housing for testing. This setting also reduces the risks of injury to surgical sites and experimental appliances. The specific type of pairing may be selected. <u>This housing option MUST be scientifically justified.</u> Explanations must be explicit. Statements such as “the research or the science requires separate housing,” without substantive justification will not be accepted.</p> <p>same sex <input type="checkbox"/> same age <input type="checkbox"/> same sex and same age <input type="checkbox"/></p> <p>Scientific justification for protected contact housing is as follows:</p>

→

Yes <input type="checkbox"/> No <input type="checkbox"/>	<p>Single housing – A non-human primate housed alone but with visual, auditory, and olfactory contact with others of the same or compatible species. While this is not an optimal means of providing any social access, it is understood that it may be necessary due to the nature of the research. <u>Investigators requesting this type of housing MUST provide justification.</u> Explanations must be explicit. Statements such as “the research or the science requires separate housing,” without substantive justification will not be accepted. This housing option is particularly discouraged for infants and young juveniles due to its persistent effects on development.</p> <p>Scientific justification for single housing is as follows:</p>
--	--

→

Yes <input type="checkbox"/> No <input type="checkbox"/>	<p>Isolation housing – a non-human primate housed without visual, auditory, and olfactory contact with others of the same or compatible species. <u>Investigators requesting this type of housing MUST provide justification.</u> Explanations must be explicit. Statements such as “the research or the science requires separate housing,” without substantive justification will not be accepted. This housing option is particularly discouraged for infants and young juveniles due to its persistent effects on development.</p> <p>Scientific justification for isolation housing is as follows:</p>
--	---

3. ENRICHMENT CATEGORIES: (Each category below MUST be checked either Yes or No.)	
Yes <input type="checkbox"/> No <input type="checkbox"/>	Standard Enrichment – These techniques are appropriate for the vast majority of research projects. All categories listed below comprise the standard enrichment protocol. <ul style="list-style-type: none"> ▪ Objects to manipulate in cage, including durable objects and paper ▪ Cage complexities such as perches or swings ▪ Varied food supplements such as fruits, vegetables, or seeds ▪ Foraging or task-oriented feeding method ▪ Human interaction by caregiver and research staff <p>The implementation of each category is tailored to the species of the animals as dictated by the Animal Welfare Act and outlined in the Emory University Policy on Environmental Enhancement. In addition, the Animal Welfare Act stipulates that animals showing signs of being in psychological distress through behavior or appearance must receive special attention, which may include additional enrichment devices, alterations to room configurations, and/or clinical intervention.</p>
Yes <input type="checkbox"/> No <input type="checkbox"/>	Restricted Enrichment – If any of the above enhancements are not compatible with the proposed research, describe each exception and provide justification. Note that study subjects cannot be exempted from all enrichment categories at any one time.
	Scientific justification for restricted enrichment is as follows:

→

4. SPECIAL ENRICHMENT CATEGORIES: (Each category below MUST be checked either Yes or No.)	
Yes <input type="checkbox"/> No <input type="checkbox"/>	Infants and young juveniles (which receive social enrichment, human interaction, food, and enrichment objects appropriate to the various ages).
Yes <input type="checkbox"/> No <input type="checkbox"/>	Those used in research requiring restricted activity (which must receive special attention through the entire restraint period and at least one continuous hour of unrestricted activity if the period of constraint is over 12 hours).
Yes <input type="checkbox"/> No <input type="checkbox"/>	Individuals housed without the ability to see and hear others of the same or compatible species (which receive increased human attention, supplementary food treats and foraging tasks, videotape viewing, and/or addition cage enrichment).
Yes <input type="checkbox"/> No <input type="checkbox"/>	Great apes weighing over 110 lbs. (which are housed in appropriately sized cages, usually indoor/outdoor units; food and enrichment devices are also scaled to meet the needs of these animals).

P. EXERCISE FOR DOGS:

Unless otherwise approved, all dogs will be provided exercise according to Emory University Policy. If this is not compatible with the proposed research, state exceptions required and provide justification.

→N/A

Q. PERSONNEL:

Credentials must be on file at the IACUC office. Please indicate if they are on file. If they are not on file, please complete the Credentials form and attach to the application http://www.emory.edu/IACUC/general_forms.php.

1. List ALL Personnel that will work on this Protocol/Project. Indicate whether credential forms are on file or attached:

Name	Campus Address	Office Phone	Office Fax	Email	Emory Emp ID	Attached OR on File
Shi-Yong Sun	1365-C Clifton Rd, Suite C3088	404-778-2170	404-778-5520	shi-yong_sun@emory.org		On file
Xuerong Wang	1365-C-Clifton Rd., C3060	404-778-2268	404-778-5520	xwang35@emory.edu		Attached
Ping Yue	1365-C-Clifton Rd., C3060	404-778-2268	404-778-5520	pyue@emory.edu		Attached
Heath Acuff	1365-C-Clifton Rd., C3060	8-2268	8-5520	hacuff@emory.edu		Attached

2. List the personnel who serve as EMERGENCY Contacts

Name	Home Phone	Office Phone	Email	Pager
Shi-Yong Sun	404-210-9353	404-778-2170	shi-yong_sun@emory.org	
Xuerong Wang	404-329-0231	404-778-2268	xwang35@emory.edu	

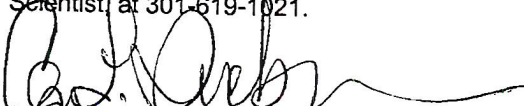
APPENDIX E

Duchesneau, Caryn L Ms USAMRMC

From: Duchesneau, Caryn L Ms USAMRMC
Sent: Monday, January 15, 2007 8:25 PM
To: 'Fadlo Khuri'
Cc: Izwellin@mdanderson.org; cbrunelli@mdanderson.org; whong@mdanderson.org; judie.wells@emoryhealthcare.org; leah.holloway@emoryhealthcare.org; Rice, Stephen L USAMRAA; Bennett, Jodi H Ms USAMRMC; Brosch, Laura R COL USAMRMC; Duchesneau, Caryn L Ms USAMRMC; Wilberding, Julie A Dr USAMRMC; Ziehm, Amanda K Ms AMDEX A-13247.5 Protocol Approval (Proposal Number 04100001, Award Number W81XWH-05-0027)

SUBJECT: Protocol, "Phase IB Study of RAD-001 in Patients With Operable Non-Small Cell Lung Cancer (NSCLC)." Submitted by Fadlo R. Khuri, M.D., Winship Cancer Institute, Emory University School of Medicine, Atlanta, Georgia, in Support of the Proposal, "IMPACT: Imaging and Molecular Markers for Patients With Lung Cancer: Approaches With Molecular Targets, Complementary/Innovative Treatments and Therapeutic Modalities," Submitted by Waun Ki Hong, M.D., University of Texas, M.D. Anderson Cancer Center, Houston, Texas, IND # 73,094, Winship Cancer Institute Project # WCI1017-04, Proposal Log Number 04100001, Award Number W81XWH-05-2-0027, HRPO Log Number A-13247.5

1. The revised protocol (version dated 5 September 2006), informed consent form (version dated 15 September 2006), and supporting documents have been reviewed and found to comply with the recommendations made at the 9 August 2006 meeting of the Human Subjects Research Review Board (HSRRB). Documentation of the Emory University School of Medicine Winship Cancer Center Institute Institutional Review Board (IRB) review and approval of this version of the protocol and consent form were received by the United States Army Medical Research and Materiel Command (USAMRMC) Office of Research Protections (ORP), Human Research Protection Office (HRPO) on 19 December 2006.
2. There are no outstanding human subjects' protection issues to be resolved. This greater than minimal risk protocol is approved by the USAMRMC HSRRB for the enrollment of up to 60 subjects at the Emory University School of Medicine Winship Cancer Institute.
3. In accordance with 32 Code of Federal Regulations 219, a continuing review must be completed at least annually. According to our records for continued approval of the protocol, the next continuing review report must be reviewed and approved by the Emory University School of Medicine Winship Cancer Institute IRB no later than 27 January 2007. These approvals should be submitted to the U.S. Army Medical Research and Materiel Command, Office of Research Protections, 504 Scott Street, Fort Detrick, Maryland 21702-5012, as soon as the approval becomes available. Should the protocol not receive approval of continuation by its anniversary date, all study activity including subject enrollment, data collection and/or data analysis must be discontinued.
4. Any protocol modifications (including, but not limited to, changes in the principal investigator, the use of human subjects or the data there from, inclusion/exclusion criteria, number of subjects to be enrolled, study sites or procedures) must be submitted as a written amendment for HSRRB review and approval prior to implementing the changes. Documentation that the Emory University School of Medicine Winship Cancer Institute IRB reviewed and approved the modifications must also be submitted.
5. All unanticipated problems involving risks to subjects or others, serious adverse events, and all subject deaths must be reported promptly to the HSRRB.
6. Any deviation to the subject protocol that affects the safety or rights of the subject and/or the integrity of the study data must be promptly reported to the HSRRB.
7. Further information regarding this review can be obtained by calling Amanda Ziehm, Human Subjects Protection Scientist, at 301-619-1021.


CARYN L. DUCHESNEAU, CIP
Chief Human Subjects Protection Review
Human Research Protection Office
Office of Research Protections
U.S. Army Medical Research and Materiel Command

Note: The official copy of this approval is housed with the protocol file at the Office of Research Protections, Human Research Protection Office, 504 Scott Street, Fort Detrick, Maryland 21702. Signed copies will be provided upon request.

Note: Do not construe this correspondence as approval for any contract funding. Only the Contracting Officer or Grants Officer can authorize expenditure of funds. It is recommended that you contact the appropriate contract specialist or contracting officer regarding the expenditure of funds for your project.

APPENDIX F

THE UNIVERSITY OF TEXAS
MD ANDERSON
CANCER CENTER

Office of Protocol Research

Institutional Review Board (IRB)
Unit 198
Phone 713-792-2933
Fax 713-794-4589

To: Roy S. Herbst 10/13/2006
From: Denise Olson
CC: Alisha Thierry, Mellanie J. Price
MDACC Protocol ID #: 2005-0929
Protocol Title: Treatment of Malignant Pleural Effusion with ZD6474,
a Novel Vascular Endothelial Growth Factor Receptor (VEGFR)
and Epidermal Growth factor Receptor (EGFR) Tyrosine Kinase Inhibitor
Version: 06
Subject: Administrative IRB Approval -- Protocol 2005-0929

On Friday, 10/13/2006, the Institutional Review Board (IRB) 1 chair or designee reviewed and approved your revision dated 09/22/2006 for Protocol 2005-0929

These Pages Include:

- Protocol Body -- Document header Date: 09/20/2006
- Abstract Page -- Document header Date: 09/20/2006
- Informed Consent(s) -- Document header Date: 09/20/2006
- Signature>Title Page -- Document header Date: 09/20/2006
- Co-Chair(s) Page -- Document header Date: 09/20/2006
- Collaborator(s) Page -- Document header Date: 09/20/2006

Revision included the following changes:

Changed Study Chair, Previous Collaborator now Study Co-Chair, Included COI information in the informed consent.

The revision can now be implemented. Please inform the appropriate individuals in your department or section and the collaborators of these changes.

Please Note: This approval does not alter or otherwise change the continuing review date of this protocol.

This protocol has not yet been activated

In the event of any questions or concerns, please contact the sender of this message at (713) 792-2933.

Denise Olson 10/13/2006 01:59:59 PM

This is a representation of an electronic record that was signed electronically and
below is the manifestation of that electronic signature:

Denise Olson
10/13/2006 01:59:47 PM

IRB 1 Chair Designee
FWA #: IRB 1 IRB00000121

THE UNIVERSITY OF TEXAS
MD ANDERSON
CANCER CENTER

To: IRB 9/22/2006 11:27:20 AM
From: Mellanie J. Price
CC: Amir Onn, Roy Herbst, Christine M. Alden, Brenda Coldman, Alisha Thierry, James W. Luca, Faye D. Martin, Jeanne R. Riddle, Denise Olson, Carlos A. Jimenez
Protocol Name: Treatment of Malignant Pleural Effusion with ZD6474, a Novel Vascular Endothelial Growth Factor Receptor (VEGFR) and Epidermal Growth factor Receptor (EGFR) Tyrosine Kinase Inhibitor
MDACC Protocol ID #: 2005-0929
Version: 06
Subject: Resubmission Cover Letter - Protocol 2005-0929

The above protocol is being resubmitted to the Office of Protocol Research (IRB).

Please indicate below the reason for re-submission.

IRB meeting contingencies
 IRB continuing review contingencies
 IRB revision contingencies
 Response/Acceptance of edited informed consent
 Other revisions/amendments

Please indicate below the documents which have been revised.

Protocol Waiver(s)
 Abstract Co-Chair(s) Page
 Appendices Collaborator(s) Page
 Informed Consent Signature / Title page

»»» Revised Text # 1

Document: Signature Page

Section:

Paragraph:

Page:

Old Text (if applicable): Amir Onn

New Text: Roy Herbst

Scientific Rationale: The PI for this study has been changed from "Amir Onn" to "Roy Herbst".

»»» Revised Text # 2
Document: Protocol Page

Section: Study Chair

Paragraph:

Page:

Old Text (if applicable): **Amir Onn**

New Text: **Roy Herbst**

Scientific Rationale: The PI for this study has been changed from "Amir Onn" to "Roy Herbst".

»»» Revised Text # 3
Document: Co-Chair Page

Section: Co-Chair Page

Paragraph:

Page:

Old Text (if applicable): **Roy Herbst**

New Text: **Carlos Jimenez**

Scientific Rationale: The PI for this study is now "Roy Herbst" and "Carlos Jimenez" is now the study co-chair.

»»» Revised Text # 4
Document: Protocol

Section: **7.1 Investigator Contact Information**

Paragraph:

Page:

Old Text (if applicable):

Principal Investigator:
Amir Onn, MD
University of Texas M.D. Anderson Cancer Center
1515 Holcombe Blvd., Unit 403
Houston, TX 77030
Phone: 713-563-6707
Fax: 713-794-4922
Email: amironn@mdanderson.org

Co-Principal Investigators:

~~Roy Herbst, MD, PhD~~
~~University of Texas M.D. Anderson Cancer Center~~
~~1515 Holcombe Blvd., Unit 432~~
~~Houston, TX 77030~~
~~Phone: 713-792-6363~~
~~Fax: 713-796-8655~~
~~e-mail: rherbst@mdanderson.org~~

New: Text:

Principal Investigator:
Roy Herbst, MD, PhD
University of Texas M.D. Anderson Cancer Center
1515 Holcombe Blvd., Unit 432
Houston, TX 77030
Phone: 713-792-6363
Fax: 713-792-1220
e-mail: rherbst@mdanderson.org

Co-Principal Investigators:

David J. Stewart, M.D.
University of Texas M.D. Anderson Cancer Center
1515 Holcombe Blvd., Unit 432
Houston, TX 77030
Phone: 713-792-6363
Fax: 713-792-1220
e-mail: dstewart@mdanderson.org

Scientific Rationale: Updated Contact information to change "Amir Onn" to "Roy Herbst" and updated text for current phone information.

»»» Revised Text # 5
Document: Protocol

Section: 10.14 Roles and Responsibilities of Key Study Personnel

Paragraph: 1-3

Page:

Old Text (if applicable):

Dr. Amir Onn will serve as the Study Chairman for this protocol at M. D. Anderson Cancer Center. He will assume primary responsibility for the study.

Dr. Roy Herbst will serve as Study Co-Chairman of this protocol at M. D. Anderson Cancer Center. He will coordinate and supervise all aspects of the clinical trial, supervise the biological correlate studies, and the preparation of results for presentations and publication.

Dr. David Stewart will serve as a Study Co-Chairman of this protocol at M. D. Anderson Cancer Center. He will coordinate and supervise all aspects of the clinical trial, and preparation of results for presentations and publication.

Dr. Carlos Jimenez will assist with pleural procedures for patients enrolled in the clinical trial at M. D. Anderson Cancer Center.

New Text:

Dr. Roy Herbst will serve as Study Chairman of this protocol at M. D. Anderson Cancer Center. He will coordinate and supervise all aspects of the clinical trial, supervise the biological correlate studies, and the preparation of results for presentations and publication. **He will assume primary responsibility for the study.**

Dr. David Stewart will serve as a Study Co-Chairman of this protocol at M. D. Anderson Cancer Center. He will coordinate and supervise all aspects of the clinical trial, and preparation of results for presentations and publication.

Dr. Carlos Jimenez will serve as a Study Co-Chairman of this protocol at M. D. Anderson Cancer Center. He will assist with pleural procedures for patients enrolled in the clinical trial at M. D. Anderson Cancer Center.

Scientific Rationale: Updated text to removed Dr. Amir Onn as the Study Chairman and change Dr. Carlos Jimenez as the Study Co-Chairman.

»»» Revised Text # 6

Document: Collaborator's Page

Section: Collaborator(s): Pulmonary Medicine

Paragraph:

Page:

Old Text (if applicable): ~~Carlos A. Jimenez~~

New Text: None.

Scientific Rationale: Carlos Jimenez is now listed on the study Co-Chair Page and has been removed from the collaborator's page.

»»» Revised Text # 7

Document: Informed Consent

Section: **Study Chair:**

Paragraph:

Page:

Old Text (if applicable): ~~Amir Onn~~

New Text: **Roy Herbst**

Scientific Rationale: The PI for this study has been changed from "Amir Onn" to "Roy Herbst".

»»» Revised Text # 8

Document: Informed Consent

Section: 11.

Paragraph:

Page:

Old Text (if applicable): I may contact the study chair for this study, Dr. ~~Amir Onn~~ at 713-792-6363 or the Chairman of the Institutional Review Board (IRB) at 713-792-2933 with any questions that have to do with this study or my rights as a study participant.

New Text: I may contact the study chair for this study, Dr. **Roy Herbst** at 713-792-6363 or the Chairman of the Institutional Review Board (IRB) at 713-792-2933 with any questions that have to do with this study or my rights as a study participant.

Scientific Rationale: Updated text to reflect Dr. Roy Herbst is the study chair.

»»» Revised Text # 9

Document: Informed Consent

Section: 16.

Paragraph: #2, Sentence #4

Page:

Old Text (if applicable): If you have any questions about this medical care, talk to the principal investigator for this study, Dr. ~~Amir Onn~~ at 713-792-6238.

New Text: If you have any questions about this medical care, talk to the principal investigator for this study, Dr. **Roy Herbst** at 713-792-6363.

Scientific Rationale: Updated text to change "Amir Onn" to "Roy Herbst" as the principal investigator.

»»» Revised Text # 10

Document: Abstract

Section: Protocol Monitoring

Paragraph:

Page:

Old Text (if applicable): ~~Amir Onn~~

New Text: **Roy Herbst**

Scientific Rationale: Updated text to change "Amir Onn" to "Roy Herbst" to the person responsible for protocol monitoring.

»»» Revised Text # 11

Document: Abstract

Section: **Prior Protocol at M.D. Anderson:**

Paragraph:

Page:

Old Text (if applicable): N/A

New Text: 2005-0873

Scientific Rationale: Updated text to reflect current clinical trial that accrued patients for the new study
PI.

»»» Revised Text # 12

Document: Informed Consent

Section: #8

Paragraph: Text following paragraph #1

Page:

Old Text (if applicable): No previous text.

New Text:

<u>Investigator Name</u>	<u>Type of Interest</u>
--------------------------	-------------------------

**Dr. Roy Herbst (Study Chair) is a compensated Scientific/Advisory Board Member
for AstraZeneca Pharmaceuticals, a sponsor for this study.**

Scientific Rationale: Updated text to disclose Study Chair's compensation information with
AstraZeneca Pharmaceuticals (study supporter).

Edit History:

Mellanie J. Price 9/22/2006 -- Sent

Mellanie J. Price 09/22/2006 -- Edited

Mellanie J. Price 9/20/2006 -- Sent

Mellanie J. Price 09/20/2006 -- Edited

Mellanie J. Price 09/19/2006 -- Created

APPENDIX G

Appendix G

TALK Focus Group Reports

First “TALK” Focus Group (3/27/2006)

Location: University of Houston, Health Center

Groups: #1 (6 in first session, 2 in second)

Staff Members Present: Kentya Ford, Mario Luca, Julie John, Jeffery McLaughlin

Q: Is the game approach appropriate?

Student responses:

- Maybe appropriate for middle and high school students, but may not be effective for college students because the program is a little cartoonish.
- Program characters are too slow
- Maybe too cartoonish for even a 15 year old
- Program targets younger generation (maybe add more action for older generation)
- Use print material, in addition to the game

Q. How to improve the program? What would you like to see?

Student responses:

- Maybe add more action to cater to an older generation
- Older generation might be affected with more of an emotional appeal
- Suggest to use real characters rather than cartoon characters
- Add more realistic medical and emotional aspects of tobacco use

Q. What do you think of the Avatar and Program Guide? Are they tailored to represent different race/ethnic groups?

Student responses:

- Add more diversity for males
- Program characters are too slow
- Suggest to broaden the ethnicity of Avatars (for ex., one student noticed that White and Asian characters were not shown)
- “one of the characters made me feel like he was a pot smokers rather than a tobacco smokers. It was amusing to see but I would take well to advice given by this character” (he is not a role model).

Q. Would a smoker complete the program? What motives a smoker to quit?

Student responses:

- Include information about peer pressure (**we had a discussion of this but I did not get all of the notes)
- Smoking in the movies (for example, one of the participants said, "when I see smoking in the movies, it makes me want to smoke. *two of the participants even left the theater while the movie was still playing to smoke a cigarette outside.

What do you think of the program concept?

Student responses:

- As far as concepts are concerned, a 15-24 year old may already know the information; make the information more real and emotional
- Suggest targeting the topic of smoking as being associated with sex appeal and being mature and sophisticated.
- Add statistics to make the information more relevant
- Do not add statistics because this is of no concern to me
- Set the computer so the program gives information regarding the immediate consequences of smoking. (**The student said that we are in a quick world. She prefers to see information that is quickly available and provides information on how smoking can harm her at this stage in her life (not long-term). Also, she recommends tailoring the messages to different levels of smokers, this way the information is more appropriate for the audience.

***Were there any surprises during the session?

Second “TALK” Focus Group (April 28, 2006)

General comments

- All users reported that they liked the animation and game style, all users indicated it was appropriate and appealing to them.
- In follow-up sessions, users reported statistics and information they had learned via the quizzes.
- Some users, primarily males, were excited by the prospect of seeing surgery
- Most users reported that some of the information contained in the program repeated things they had already learned in health classes

Observations of usability issues

- need orientation instructions (what's the point of the game, which keys to use, how to move around etc)
- need additional pop-up hints when users get stuck (timed hints that appear if user doesn't take the correct action after a certain amount of time).
- Bonus item messages must appear on game screen, users don't read all of the messages that appear in the right hand bar.
- No one clicked on the items in inventory when taking the quiz. This “information container” aspect of game play is lost on users.
- Use of arrow keys seems to be problematic for some users. Solution is to implement the point-to-box navigation system.

Final “TALK” Focus Group (Jan 30th, 2006)

Project Talk – Results of Round 1 Usability Testing

We conducted the first round of usability testing at the 5th Ward Enrichment Center on Jan 30th, 2006. Four teens were given a set of representative tasks to complete within the game. The teens were all male, 17 years old, and three were seniors while one was a sophomore. Jeffery McLaughlin and Mario Luca observed the teen’s interaction with the game interface, and the teens were asked to rate the difficulty of the tasks as well as provide qualitative feedback about the game itself.

Task One : Start the game.

- Click the button that says “Proceed”
- Answer the demographic questions (Age, Gender, Ethnicity)
- Build an avatar
- Answer the set of questions about your smoking behavior. Remember, you’re pretending that you are a smoker who wants to quit, and you’ve recently made an attempt to quit.
- Pick a FEMALE guide character

Ratings offered: NOT DIFFICULT, SOMEWHAT DIFFICULT, VERY DIFFICULT

All four test subjects rated this task “Not Difficult”

Observations:

- two subjects did not intuitively understand that you could click on left/right arrows to change avatar appearance in the avatar builder.

Task Two: Complete first room.

- Listen to the guides instructions and complete each task that the guide describes. Note that you can use the mouse instead of a touch screen.
- Go to the Elevator

All four test subjects rated this task “Not Difficult”

Observations:

- two subjects tried to click on the elevator itself in order to move there.
- All had brief initial learning period before they understood how to indicate a destination for the avatar

Task Three: Find a hidden item

- Navigate to the Research Room
- Find one hidden item

All four test subjects rated this task “Not Difficult”

Observations:

- Two subjects immediately identified the glowing TV as a destination
- All subjects immediately began active search for bonus items and all subjects picked up all bonus items
- On initial elevator screen, one subject initially clicked on the room label rather than the green button.

Task Four: Find hidden items

- Navigate to the Examination Room
- Find three hidden items

All four test subjects rated this task “Not Difficult”

Observations:

- All subjects immediately identified “TV” item
- All subjects had some initial difficulty navigating doors (wanted to click doors themselves)
- All subjects immediately began active search for bonus items and all subjects picked up all bonus items
- All subjects found all three media pieces within a reasonable amount of time

Task Five: Talk to a character

- Navigate to the Psyche Ward
- Talk to all five characters in this room

Two test subjects rated this task “Not Difficult” two subjects rated the task “Somewhat Difficult”

Observations:

- All subjects had trouble identifying “visited” characters
- Some subjects had trouble “catching” a character to initiate an interaction

Task Six: Find a key

- Navigate around the hospital and find one key

One test subject rated this task “Not Difficult”, three subjects rated the task “Somewhat Difficult”

Observations:

- Subjects reported that they wanted to “see” the keys which are currently hidden.
- All subjects solved the key search within a reasonable amount of time
- Subjects reported that the directions from room to room were easy to follow.

General Observations:

- Three of the four test subjects were enthusiastic about the game and enjoyed playing it. Two subjects in particular stayed in front of the machines and continued playing after being told we were done and that they could leave.
- Minor refinements to the interface will improve usability considerably.

APPENDIX H

Appendix H: Media Map and Screen Shots

TALK: Media Map

SM	Description	Notes	Dependencies	Next Task	Production
STAG	Data Collection and Staging				
	DEMOGRAPHIC QUESTIONS				COMPLET
	AVATAR BUILDER				COMPLET
	STAGING QUESTIONS				COMPLET
	GUIDE SELECTOR				COMPLET
GAME ENGINE					
	ADDITIONAL CHARACTER ART				COMPLET
	IMPLEMENT CONFIGURABLE DIFFICULTY				COMPLET
	IMPLEMENT BUG TRACKER SOFTWARE				COMPLET
	IMPLEMENT "CHARACTER DROPS OBJECT" FEATURE	-	-	-	FEATURE DROPPED
ADMI	DEBUG AND TEST				IN PROGR
	Admissions Room	User orientation and game instructions			
	GUIDE MESSAGES FOR ALL STAGES	Game instructions and tailored intro			COMPLET
ELEV	Elevator	Access to individual rooms, access is limited by staging questions but may change depending on user's progress through the various rooms			
	GUIDE MESSAGES	On first elevator entry, guide gives instruction			COMPLET
	GUIDE MESSAGES	If player chooses locked room, guide gives feedback			COMPLET
RADI	Radiology	Medium and long term smoking risks Ingredients in cigarettes			
	GUIDE MESSAGES	Room Orientation			COMPLET
	radiology 1	MD Anderson - X-ray image + narration			COMPLET
	radiology 2	MD Anderson - X-ray image + narration			COMPLET
	radiology 3	MD Anderson - X-ray image + narration			COMPLET
	radiology 4	MD Anderson - X-ray image + narration			COMPLET
PATI	Radiology Doctor Character	Doctor Dialog		ADD HINT	IN PROGR
PATI	Patient Records	Smoking effects: statistics			
	GUIDE MESSAGES	Room Orientation			COMPLET
	dossier 1	MD Anderson - picture + story behind illness and surgery/outcome			COMPLET
	dossier 2	MD Anderson - picture + story behind illness and surgery/outcome			COMPLET
	dossier 3	MD Anderson - picture + story behind illness and surgery/outcome			COMPLET

	dossier 4	MD Anderson - picture + story behind illness and surgery/outcome			COMPLET
	Patient Records Room Ghost	Ghost modal dialog		ADD HINT	IN PROGR
EXAM	Examination Room	Physiology of Addiction			
	GUIDE MESSAGES	Room Orientation			COMPLET
	EVALUATION	Evaluate user's level of addiction + provide tailored response			COMPLET
	ANIMATION	Physiology of addiction (nicotine's effect on the brain and heart)			COMPLET
	ANIMATION	Effects of Nicotine cessation on the body			COMPLET
SURG	Surgery	Long term health risks			
	GUIDE MESSAGES	Room Orientation			COMPLET
	VIDEO	MD Anderson - Thoracic surgery video - describe reality of thoracic surgery	MD Anderson Video shoot	Edit surgery video + add Garret Walsh voice-over	IN PROGR
WAST	Waste Disposal Room	Environmental effects of smoking			
	GUIDE MESSAGES	Room Orientation			COMPLET
	ANIMATION	Environment "Newscast"			COMPLET
	WAST1	What's in a cigarette (hazardous chemicals and protective gear concept)			COMPLET
	WAST2	What's in a cigarette (hazardous chemicals and protective gear concept)			COMPLET
	WAST3	What's in a cigarette (hazardous chemicals and protective gear concept)			COMPLET
	WAST4	What's in a cigarette (hazardous chemicals and protective gear concept)			COMPLET
	WAST DISPOSAL ROBOT	MODAL DIALOG		ADD HINT	IN PROGR
RECO	Recovery Room	Long term smoking risks			
	GUIDE MESSAGES	Room Orientation			COMPLET
	RECO1	MD Anderson - First hand patient accounts of cancer survival (talking head)	MDAnderson patients	Locate patient volunteers to record	IN PROGR
	RECO2	MD Anderson - First hand patient accounts of cancer survival (talking head)	MDAnderson patients	Locate patient volunteers to record	IN PROGR
	Recover Room Doctor	MODAL DIALOG		ADD HINT	IN PROGR

ROOF	Rooftop	Social risks			
	GUIDE MESSAGES	Room Orientation			COMPLET
	CHARACTER 1	Video from ASPIRE		Locate and edit video clip	IN PROGR
	CHARACTER 2	Video from ASPIRE		Locate and edit video clip	IN PROGR
	CHARACTER 3	Video from ASPIRE		Locate and edit video clip	IN PROGR
	CHARACTER 4	Video from ASPIRE		Locate and edit video clip	IN PROGR
	CHARACTER 5	Video from ASPIRE		Locate and edit video clip	IN PROGR
	ANIMATION	Game win animation			COMPLET
ACCO	Accounting	Economic cost of smoking			
	GUIDE MESSAGES	Room Orientation			COMPLET
	INTERACTIVE ACTIVITY	Cost calculator (personal)		Programming	COMPLET
	INTERACTIVE ACTIVITY	Cost calculator (health costs to public)		Programming	IN PROGR screen lay complete, programmi to be comp
	Mister Big Tobacco	MODAL DIALOG		ADD HINT	IN PROGR
PHAR	Pharmacy	Tobacco Chemistry			
	GUIDE MESSAGES	Room Orientation			COMPLET
	INFO SCREEN	Pharmacotherapy options			COMPLET
	INFO SCREEN	Pharmacotherapy options			COMPLET
	INFO SCREEN	Pharmacotherapy options			COMPLET
	INFO SCREEN	Pharmacotherapy options			COMPLET
	INFO SCREEN	Pharmacotherapy options			COMPLET
	INFO SCREEN	Pharmacotherapy options			COMPLET
	INFO SCREEN	Pharmacotherapy options			COMPLET
RESE	Research	Practical quit techniques: Recognize, Remember and React			
	GUIDE MESSAGES	Room Orientation			COMPLET
	ANIMATION	Recognize Remember React intro (Mad Scientist)			COMPLET
	INTERACTIVE ACTIVITY	Refusal Skills Activity	-	-	MOVED TO

EMER	Emergency Room	Practical quitting techniques: Dealing with Temptation			
	GUIDE MESSAGES	Room Orientation			COMPLET
	Bonus Item	bottle of water		Lay out screen	IN PROGR
	Bonus Item	cell phone		Lay out screen	IN PROGR
	Bonus Item	toothbrush		Lay out screen	IN PROGR
	Bonus Item	running shoes		Lay out screen	IN PROGR
	Bonus Item	banana		Lay out screen	IN PROGR
	Bonus Item	cough drops		Lay out screen	IN PROGR
	Bonus Item	yoga mat		Lay out screen	IN PROGR
	Nurse	MODAL DIALOG		ADD HINT	IN PROGR
NURS	Nurses Lounge	Practical quitting techniques: Chill Chat Change			
	GUIDE MESSAGES	Room Orientation			COMPLET
	ANIMATION	Describe Chill Chat Change approach to dealing with stress			COMPLET
RECR	Recreation Room	Alternatives to smoking			
	GUIDE MESSAGES	Room Orientation			COMPLET
	Rec Room Resident 1	Skateboarder		Lay out screen	IN PROGR
	Rec Room Resident 2	DJ		Lay out screen	IN PROGR
	Rec Room Resident 3	BMX Guy		Lay out screen	IN PROGR
	Rec Room Resident 4	Surfer		Lay out screen	IN PROGR
	Rec Room Resident 5	Video Game Player		Lay out screen	IN PROGR
	Rec Room Resident 6	Kickboxer		Lay out screen	IN PROGR
	Rec Room Resident 7	Painter		Lay out screen	IN PROGR
COUN	Patient Counseling	Positive Reinforcement			
	GUIDE MESSAGES	Room Orientation			COMPLET
	ANIMATION	Social Support Network			COMPLET
PSYC	Psyche Ward	Negative Affect			
	GUIDE MESSAGES	Room Orientation			COMPLET

	Zombie 1	Practice Recognize Remember and React			COMPLET
	Zombie 2	Practice Recognize Remember and React			COMPLET
	Zombie 3	Practice Recognize Remember and React			COMPLET
	Zombie 4	Practice Recognize Remember and React			COMPLET
	Zombie 5	Practice Recognize Remember and React			COMPLET
THEA	Theater	Correct smoking in the movies perceptions			
	GUIDE MESSAGES	Room Orientation			COMPLET
	Animation	"Hollywood up in Smoke" uses redrawn stills from famous movies		Voice-over recorded, animation in progress	IN PROGR
LEGA	Legal Department	Advocacy			
	GUIDE MESSAGES	Room Orientation			COMPLET
	INTERACTIVE ACTIVITY	Advocacy activity - describe and practice advocacy skills		Voice-over recorded, animation in progress	IN PROGR
DELI	Delivery Room	Smoking and Pregnancy			
	GUIDE MESSAGES	Room Orientation			COMPLET
	delivery 1	MDAnderson - image + story of babies born to smoking mothers (available)			COMPLET
	delivery 2	MDAnderson - image + story of babies born to smoking mothers (available)			COMPLET
	delivery 3	MDAnderson - image + story of babies born to smoking mothers (available)			COMPLET
	delivery 4	MDAnderson - image + story of babies born to smoking mothers (available)			COMPLET
SECU	Security	Short Term Smoking Risks			
	GUIDE MESSAGES	Room Orientation			COMPLET
	security 1	Database animation pt1			COMPLET
	security 2	Database animation pt2			COMPLET
	security 3	Database animation pt3			COMPLET
BOIL	Boiler Room	Red Herring			
	Robot	MODAL DIALOG		ADD HINT	IN PROGR

Tell us all about **YOURSELF**

AGE

17

GENDER

Male

ETHNICITY

Caucasian

Build your **AVATAR**

USE THE YELLOW ARROWS TO SELECT



NEXT

Answer a few short **QUESTIONS**

Do you currently smoke?

YES

NO

Do you plan to quit in the
next 6 months?

YES

NO

OK!

SELECT YOUR GUIDE

You'll need a guide to navigate this world.
Click one of the guides below to select.



Elevator



head to the elevator.

Now head to the elevator and start exploring.

Select a room that you would like to explore. Green room numbers mean that the room is open, red room numbers mean that the room is closed.

TALK: Records Room with Ghosts

SCORE: 20
KEYS FOUND
3
2
1
HELP QUIT
???
Select a room that you would like to explore. Green room numbers mean that the room is open, red room numbers mean that the room is closed.
Select another room you would like to explore.
Select another room you would like to explore.

TALK: Nursery



SCORE: 20
KEYS FOUND

3
2
1

HELP QUIT

??? ▲ ▾

head to the elevator.

Now head to the elevator and start exploring.

Select a room that you would like to explore. Green room numbers mean that the room is open, red room numbers mean that the room is closed.

TALK: Surgery



TALK: Helicopter

SCORE: 20
KEYS FOUND

3
2
1

HELP QUIT

???

Now head to the elevator and start exploring.

Select a room that you would like to explore. Green room numbers mean that the room is open, red room numbers mean that the room is closed.

Select another room you would like to explore.

APPENDIX I

Appendix I: Complete TALK Scripts

Intro Story

Escape With Your Life

VO: Dark and sinister forces are at work. You may not even be aware they exist. But they are everywhere. And they have years of experience targeting people just like you.

Your mission is to expose these villains and bring the truth to light.

Soon, you'll be engaged in an epic battle of good vs. evil, fact vs. fiction, and life vs. death.

You will be tested, but will you be strong enough to survive?

There's no turning back. It's time to Escape With Your Life.

Escape With Your Life

Escape Animation Script

1) Smoker Who Doesn't Want to Quit

Guide: So you're ready to escape? And leave all this? I thought we were pals! Go see if the helicopter pilot can help you out.

(Interaction with pilot at gate)

Once in air:

Pilot: Just so you know, not everyone escapes from the Memorial HealthScare System alive. You're lucky, but a lot of smokers who don't want to quit aren't. I hope you remembered what you learned today -- like how to recognize your smoking triggers, develop your refusal skills, and change your behavior...and your thinking. I bet you won't be able to forget some of those pictures and videos of the terrible and often fatal effects of smoking on your body. But that's what happens when you continue to take in toxic chemicals with every cigarette you smoke. And how about all that money you're throwing away on a powerful addiction? Maybe you changed your mind, and you're now ready to quit. I'm proud to say you've got the tools to succeed...and lots of support all around you. One more thing: you never know....you might end up in this hospital again. People like you are always welcome!

Face of Mr. Big Tobacco fills screen:

MBT: You may have gotten away this time, but this isn't over. I'll do my best to make sure we meet again! BWA HA HA HA HA HA!

2) Smoker Who Does Want to Quit

Guide: So you're ready to escape? And leave all this? I thought we were pals! Go see if the helicopter pilot can help you out.

(Interaction with pilot at gate)

Pilot: Just so you know, not everyone escapes from the Memorial HealthScare System alive. You're lucky, but I can't promise you that quitting is going to be easy. What I do know is that you have all the information and skills you'll need to be successful. I hope you remembered what you learned today -- like how to recognize your smoking triggers, develop your refusal skills, and change your behavior...and your thinking. I bet you won't be able to forget some of those pictures and videos of the terrible and often fatal effects of smoking on your body. But that's what happens when you continue to take in toxic chemicals with every cigarette you smoke. And how about all that money you were throwing away? Now that you're ready to quit, you can put all that knowledge into action...and get support from other non-smokers, friends, family, teachers, counselors and your doctor. I'm proud to say you've got the tools to succeed. One more thing: you never know....you might end up in this hospital again. People like you are always welcome!

Face of Mr. Big Tobacco fills screen:

MBT: You may have gotten away this time, but this isn't over. I'll do my best to make sure we meet again! BWA HA HA HA HA HA HA!

3) Nonsmoker Thinking About Starting

Guide: So you're ready to escape? And leave all this? I thought we were pals! Go see if the helicopter pilot can help you out.

(interaction with pilot at gate)

Pilot: Just so you know, not everyone escapes from the Memorial HealthScare System alive. You're lucky, but if you're still thinking about starting smoking, your luck's going to run out one of these days. I hope you remembered what you learned -- like how to recognize smoking triggers, develop your refusal skills, and react in positive ways that don't involve smoking. I bet you won't be able to forget some of those pictures and videos of the terrible and often fatal effects of smoking on your body. But that's what happens when you continue to take in toxic chemicals with every cigarette you smoke. I hope you've changed your mind about starting smoking...it's just not a good choice. You're not in this alone, though -- you've got lots of support all around you: other non-smokers, friends, family, teachers, counselors and your doctor. One more thing: you never know....you might end up in this hospital again. People like you are always

welcome!

Face of Mr. Big Tobacco fills screen:

MBT: You may have gotten away this time, but this isn't over. I'll do my best to make sure we meet again! BWA HA HA HA HA HA HA!

4) Nonsmoker Not Thinking About Starting

Guide: So you're ready to escape? And leave all this? I thought we were pals! Go see if the helicopter pilot can help you out.

(interaction with pilot at gate)

Pilot: Just so you know, not everyone escapes from the Memorial HealthScare System alive. You're lucky, but you've been on the right track since you got here. NOT starting smoking is the best choice you can make for your future. I hope you remembered what you learned today about the serious health, social and financial effects of tobacco on smokers and on those around them. I'm proud to say you've got the tools to be a great advocate for not smoking...and all the tools you'll need to help others out when they need support. One more thing: you never know....you might end up in this hospital again. People like you are always welcome!

Face of Mr. Big Tobacco fills screen:

MBT: You may have gotten away this time, but this isn't over. I'll do my best to make sure we meet again! BWA HA HA HA HA HA HA!

ROOM: Admissions – Welcome and explain gameplay

Visual: Player finds himself in hospital admissions area. Unoccupied nurse's desk, chairs filled with a variety of characters. An elevator is on the far wall.

S1 Scenario

VO: Welcome to St. Euthanasius Hospital – a place filled with bloody operations, psycho zombies, toxic waste and mad scientists. Your mission is to get out of here alive!

It looks like you're a smoker who doesn't want to quit. OK, you may have your reasons for that. But maybe this game will help change your mind.

S2 Scenario

VO: Welcome to St. Euthanasius Hospital – a place filled with bloody operations, psycho zombies, toxic waste and mad scientists. Your mission to get out of here alive!

It looks like you're a smoker who wants to quit. That's great! You'll find a lot of information here to help you.

NS1 Scenario

VO: Welcome to St. Euthanasius Hospital – a place filled with bloody operations, psycho zombies, toxic waste and mad scientists. Your mission is to get out of here alive!

It looks like you're a non-smoker who's thinking about starting smoking. Are you sure? That's a big decision that can affect your whole life. Pay close attention to some of the things you're about to see.

NS2 Scenario

VO: Welcome to St. Euthanasius Hospital – a place filled with bloody operations, psycho zombies, toxic waste and mad scientists. Your mission is to get out of here alive!

It looks like you're a non-smoker who doesn't want to start smoking. You should really be proud of yourself.

All Scenarios

You have to find THREE KEYS that will allow you to leave the hospital.

It's easy to get around in this hospital. Use the touch screen and touch the floor of the room to make your character move to a new location. Try it now.

As you move through the hospital, you'll choose what rooms you want to visit. Some rooms will contain special hidden items, so search carefully! By picking up bonuses and finding hidden items, you'll increase your strength, knowledge and endurance. Try it out! Pick up the red heart in the middle of this room.

It's up to you to decide where you want to go, but as your guide I'll always be by your side to lend a hand. So, are you up to the challenge? Get on the elevator and let's get started.

ROOM: Surgery/Operating Room – Long Term Effects

S1 Stage: Key One Path

Guide: Got your x-rays? Good, because you're going to need them to get into the

Operating Room. If you don't have your x-rays, you'll have to go find them in another room.

Instructions: When player approaches the door to the operating room (and if he has collected x-rays), the door slides open and he can view the surgery video.

Guide: So, how do you think you'll look and feel after years of smoking? I hope better than this guy! I think they cut him wide open. I can't look! But you'll have to if you we're going to get out of this place and back on the elevator.

Visual: Player moves toward operating table, triggering a popup screen of surgery video.

Guide: Remember, you have to watch the **WHOLE** thing.

Visual: Player watches explicit open-heart surgery video.

Guide: OK, show's over. Let's go! Back on the elevator.

Room: Examination Room – Physiology of Addiction

For S1 and S2 Scenarios

Three separate media sections:

- 1) Player's level of physical addiction
- 2) What nicotine does to the body and psychologically
- 3) What withdrawal is like/symptoms

Visual: Player and guide enter examination room. There are three curtained off room areas. In addition to the standard exam room furnishings, one has a monitor, one has a medical skeleton and one has medical posters.

Room One: When player approaches, a video screen pops up.

Visual: Mad scientist face appears on screen.

VO: Yeah, I know, I'm supposed to be in the lab, but I'm working a second job in the exam room. Let's go inside your brain and see how addicted you are to tobacco. What power does the evil weed have over you???

(multiple choice test. Based on answers, player gets tailored response)

How many cigarettes a day do you smoke?

- 1) more than 26 (2)
- 2) About 16-25 (1)
- 3) About 1-15 (0)
- 4) Less than 1 (0)

Do you inhale?

- 1) Always (2)
- 2) quite often (1)
- 3) seldom (1)
- 4) never (0)

How soon after you wake up to you have your first cigarette?

- 1) within the first 30 minutes (1)
- 2) more than 30 minutes after waking but before noon (0)
- 3) in the afternoon (0)
- 4) in the evening (0)

Which cigarette would you have to give up most?

- 1) 1st in the morning (1)
- 2) any before noon (0)
- 3) any before afternoon (0)
- 4) any in evening (0)

Do you find it hard to keep from smoking in places where you're not allowed to smoke?

- 1) Yes, very difficult (1)
- 2) Yes, somewhat difficult (1)
- 3) No, not usually (0)
- 4) No, not all all (0)

Do you smoke if you are so sick that you are in bed most of the day?

- 1) yes, always (1)
- 2) yes, quite often (1)
- 3) no, not usually (0)
- 4) no, never (0)

Do you smoke more in the first two hours of the day than you do during the rest of the day?

- 1) Yes (1)
- 2) No (0)

How soon after you wake up do you crave your first cigarette?

- 1) within the first 30 minutes (1)
- 2) more than 30 minutes after waking but before noon (0)
- 3) in the afternoon (0)
- 4) in the evening (0)

Tailored response:

(If score is under 3) "Rats. Looks like you're stronger than I thought. You're probably not addicted to cigarettes. This is good news and will make quitting much easier.

(If score is 3-5) "Very interesting. It looks like you are moderately addicted and may have some withdrawal symptoms when you try to quit. It shouldn't hurt too much.

(If score is 5-10) "Well, lookee here. Bad news! It seems that you have quite a few symptoms of addiction and will probably have some withdrawal symptoms – irritability, headaches, anxiety. You may feel like you're going CRAZY. I know just how you feel."

Room Two: Curtained exam room with medical skeleton. This is where player learns about how nicotine works on the body and causes addiction.

Visual: When player walks in, skeleton starts talking.

Skeleton: Hey buddy, got a light? I'm DYING for a cigarette. Ha ha ha ha
<<Cough, cough, cough, rattle>>

Do you ever feel that way? I used to smoke because it made me feel good – and nicotine is as addictive as cocaine and heroin!.

(as he continues talking in voiceover, different parts of his body become the visual focus)

SFX: ticking clock

Visual: path of smoke from mouth to lungs to blood to heart to brain.

VO: When you inhale, it only takes eight seconds for nicotine to make its way through your body – from your lungs to the blood to your heart and finally, your brain.

Visual: Close up on skull/brain

VO: Once in your brain, nicotine triggers chemicals that make you concentrate better, improve your mood, or make you feel good. Sounds nice, huh? It is, but after smoking for a while, you need more and more nicotine to get the same feeling.

Visual: Back on face, talking

VO: Before long, you feel like you HAVE TO smoke just to feel normal. If you don't smoke, you feel bad. You start actually saying, "I NEED a cigarette." That's

when you're hooked. In fact, one-third to **half** of cigarette smokers eventually become addicted and may have withdrawal symptoms. Here's what's important: If the good feelings are your body's reaction to the poison in nicotine, the bad feelings that may come with withdrawal are signs of your body **healing**. So feeling bad is actually good.

Room Three: Symptoms of Withdrawal

Visual: Curtained exam room with books, posters, etc. Guy lying on gurney.

VO: So, how's it feel when you quit smoking? Depending on how addicted you are, it can feel pretty bad. You might experience some of these symptoms.

Visual: body on gurney with specific areas/symptoms highlighted as VO continues.

VO:

- Irritability – this seems to get really bad at about 48 hours after quitting and goes away as your body chemistry re-adjusts itself
- Nervousness – deep breathing and meditation can help fight this.
- Drowsiness – you may feel tired and dizzy. That's OK. Get more rest!
- Hunger/weight gain – don't start eating everything in sight; eat healthy
- Cravings for nicotine – it can take 10 days to two weeks before your mind and body are used to functioning without nicotine

VO: Remember, these are signs that your body is healing. So don't give up. You'll feel better in the long run.

(Review activity)

Room: Nurses Lounge/Practical Quitting Techniques – Chill, chat, change

S2 Scenario

Guide: Let's take a break in the lounge. I wonder what the nurses are up to? Go check it out.

Visual: Player and guide enter nurses lounge, where a bunch of them are sitting around watching TV. When player moves near the TV, a screen pops up, featuring a game show like Family Feud.

SFX: Loud game show music

Announcer: It's time to play CHILL, CHAT AND CHANGE!!!! And here's your host...the one and only Chuck Charleston!

Chuck: Good evening teams, and welcome to the show. As you know it's Smoking Week on the program, and you're going to be asked questions about

temptations. We asked 100 people the following questions and you've got to guess their answers. Top five answers are on the board.

Visual: Players face off at podium

Chuck: Chilling out is one way to react to temptations. Instead of smoking, what are the most popular ways to chill out?

SFX: Player buzzes in

Visual: Closeup on game board

Player 1: Umm...meditation?

Chuck: Meditation. Survey says?

Visual: Top line of game board flips over: MEDITATION 50

Chuck: Correct! You have control of the board. What's another way to chill out?

Player 1: How about... exercise?

Visual: Third line of game board flips over: EXERCISE 15

Chuck: Great answer!! Want to keep playing?

Player 1: OK, how about writing in a diary?

Chuck: Survey says?

Visual: Second line on game board flips over: DIARY WRITING 20

Chuck: Only two answers left. Let's make it interesting....how about you try to guess both?

Player 1: OK, OK, let me see...I'm going to go with music and deep breathing!

Visual: Lines four and five flip over, with MUSIC and DEEP BREATHING as answers.

Chuck: Amazing!! A clean sweep! Congratulations! Player Two, the pressure's on. Are you ready for a challenge?

Player 2: Bring it, Chuck!!!

Chuck: Here's how the second round goes. You have five seconds to write down who you would chat with when you want to resist temptation. And....go!

Visual: Players, heads down, write their lists.

Chuck: Time's up, folks. Please turn over your cards.

Visual: Closeup on the two lists. One has:

Parents
Friends
Teachers
Pastor
Psychic Friends Network

The other has:

My mom
A counselor
My barber
My friends
A doctor

Chuck: WOW! It's close, but I don't think we can count Psychic Friends. Sorry, player one. You've both got the right idea. Just pick a person you can trust, set a time and then ask questions. Always be open and honest.

SFX: Game show warning music

Chuck: Final round. And this is about changing your thinking. Maybe "negativity" is holding you back, hmm? Buzz in to fill in the blanks:

Chuck: If you want to succeed, set realistic...

Player 1: Expectations?

Chuck: Correct! Just do your....

Player 2: Best?

Chuck: Exactly! Don't be too "blank" on yourself.

Player 2: Hard!

Chuck: Great answer. Maybe you have to "blank" your thinking.

Player 1: Change!

Chuck: Yessssss! Last one, and this is for the game. Always turn a negative into a....

Player 2: A Positive!

Chuck: You win! And remember: we all win when we use these strategies. Good night everyone, and thanks for joining us on CHILL CHAT AND CHANGE!

Guide: I love that show. Were you paying attention? Let's see.

Multiple Choice Game Activity. Player checks off correct answers.

- 1) What are some ways to chill?
 - a. Exercise
 - b. Meditation
 - c. Worrying
 - d. Journal Writing
 - e. Binge eating
 - f. Listening to music

- 2) Who's a good person to chat with?
 - a. Parent
 - b. Zombie
 - c. Friend
 - d. Teacher
 - e. Complete stranger
 - f. Counselor

- 3) What are some ways to change your thinking?
 - a. Turn negative thoughts into positive ones
 - b. Ignore problems and hope they'll go away
 - c. Stop being so hard on yourself
 - d. Set realistic expectations
 - e. Give up before you even try
 - f. Just do your best

Guide: So, you were paying attention. I hope you remember all this as you're trying to quit. This stuff works. Back on the elevator!

Patient Counseling – Positive Reinforcement

S2 Scenario

Visual: patient counseling room with people (counselors) sitting at desks. Player visits each desk and receives a positive message. He can be rewarded with a trophy, ribbon, etc. (this object can also be tied to a "key").

Guide: That's great that you want to quit smoking. But if you're going to succeed, you've got to think positively. You can do it! See if anyone wants to help you out.

Player visits the desks/counselors, and receives the following messages:

"You're starting to feel better and look better, and you sure do smell better."

"Keep up the good work."

"Why don't you use the money you're saving by not buying cigarettes and go buy something you want?"

"Quitting smoking is the most important thing you can do to protect your health."

"You're making the right choice! Stick with it and you'll succeed."

"Keep telling yourself, 'I am a non-smoker.' Because it's the truth!"

"Practice saying, 'No thank you, I don't smoke!' when someone offers you a cigarette."

"Food tastes better, so go have a healthy snack."

"Your social life is going to improve!"

After player has visited all areas, he returns to elevator.

Guide: A positive attitude is the key to success. Speaking of keys, I hope you got your trophy. If not, you'll have to go back and get it. You have to take it to XXXX if you want to get your key. Let's go.

REVIEW ACTIVITY

Project TALK: Pharmacy Pharmacotherapy Options

Guide: When you're ready to quit, there are a variety of drugs and medicines that can help you succeed. To find the best one – or combination – that's right for you, you should talk to your doctor or pharmacist. Remember there are no guarantees, and you must follow the specific instructions for each. Take a look at what's out there, and how they work. All the information is on the workstations. Check it out.

Station 1:

Name: Zyban

Description: a prescription medication designed to in a pill form that does NOT contain nicotine

Usage: Treatment begins while the patient is still smoking and continues for 7 to 12 weeks after the quit date
Where to get it: From your doctor.

Station 2:

Name: Chantix

Description: A new tablet recently approved by the FDA that does NOT contain nicotine.

Usage: Treatment begins one week before your quit date and continues for up to 12 weeks.

Where to get it: From your doctor.

Station 3:

Name: Nicotine Gum (Nicorette, for example)

Description: A gum that delivers nicotine to the brain quickly, but not as quickly as smoking does.

Usage : Chew it and then park it between your gum and cheek. Reduce the number of pieces you chew over time and stop using after three weeks.

Where to get it: Over the counter, any drug store or pharmacy.

Station 4:

Name: Nicotine Patch

Description: Similar to adhesive bandages, it comes in different shapes and sizes and releases a constant amount of nicotine to the body.

Usage: Wear the patch all day and it reduces the effects of smoking withdrawal symptoms.

Where to get it: Over the counter, any drug store or pharmacy.

Station 5:

Name: Nicotine Nasal Spray

Description: A prescription medication in a pump bottle for the most heavily addicted smokers.

Usage: Nicotine is sprayed into the nose and rapidly absorbed through the nasal membranes. It reaches the bloodstream faster than any other nicotine-replacement product.

Where to get it: From your doctor.

Station 6:

Name: Nicotine Inhaler

Description: A plastic cylinder that looks like a cigarette that delivers nicotine when you puff on it.

Usage: It delivers nicotine into the mouth, not the lungs, and enters the body more slowly than in cigarettes. It helps reduce cravings.

Where to get it: From your doctor.

Station 7:

Name: Nicotine Lozenge

Description: A prescription nicotine-replacement medication taken orally that reduces withdrawal effects.

Usage: Place the lozenge in your mouth and suck on it until it is completely dissolved. Most effective when used in combination with a supervised stop-smoking program.

Where to get it: From your doctor.

Guide: You've got a lot of medical options to help you quit. You should talk to your doctor or pharmacist to see which one is right for you. But now it's time to go. First, let's see what you learned.

Room: Psych Ward/Mood triggers

Visual: Player and guide enter Psych Ward, at which point room sign falls off, revealing the name "Psycho Ward." Zombies are milling about, chain smoking.

Guide: Well, well, well, the old zombie room fake out. They look harmless enough, except for all that <<cough, cough>> smoke. Are they crazy?? Go talk to them.

Visual: Player moves around room and interacts with zombies. As player approaches each, he asks, "why are you still smoking?" or "what makes you want to smoke?"

Player: Why are you still smoking?

Zombie 1: I'm really stressed out. I'm CRAZY for a cigarette.

Player: Why are you still smoking?

Zombie 2: I suck at sports. I always get picked last. I mean, I know I'm a "zombie" and all, but still..."

Player: Why are you still smoking?

Zombie 3: I thought this girl zombie wanted to go out with me, but she really just wanted to eat my brain. I mean it's the story of my life.

Player: What makes you want to smoke?

Zombie 4: School is real hard. I study, do my homework, ask for extra help and still I can't make good grades.

Player: What makes you want to smoke?

Zombie 5: All I do is fight with my family – about what I wear, who my friends are, where to bury the bodies, etc. Sometimes I just light up to freak them out.

-- When player is done interacting, he goes to the elevator --

Guide: For a bunch of zombies, they're not too brain-dead. Like they said, there are a lot of reasons people smoke. So it's important to remember why you don't want to smoke – and react by finding something else to do...like taking this quiz. Psych!

(review activity)

ROOM: Delivery/Nursery – Smoking and Pregnancy/Infertility
S1 Stage: Key Two Path

Guide: What happens when you mix smoking with pregnancy? See what you can find out. You're also going to have to find a folder that will let you go into other rooms.

(When player approaches different beds, or the incubator, or oxygen tent, etc., the following popup messages and/or videos are triggered)

“This baby doesn't weigh what he should because his mother smoked during her pregnancy.”

“This baby was born too soon because her mother smokes.”

“This baby will have health problems his whole life because his mother didn't quit smoking.”

“This baby can't breathe on her own because her lungs don't work right.”

“This baby is at risk for cerebral palsy and mental retardation.”

“This baby is healthy because his mother doesn't smoke.”

“This baby is going to develop asthma and other breathing problems.”

“This baby is going to die from Sudden Infant Death Syndrome in a few months.”

“Second-hand smoke has caused this baby's many health problems.”

Pop-Up Videos

WOMEN:

When a pregnant woman smokes, she's going to hurt her baby. But, if she stops smoking by the end of the first three months of her pregnancy, she probably won't have a low-birthweight baby. Even if she stops smoking in the final three months, this can help her baby's growth.

Also, women who smoke may have more trouble getting pregnant than nonsmokers, but if they quit, it gets much easier.

MEN:

If you want to be a father, you probably want to quit smoking. Smoking can damage blood vessels throughout the body, including those that carry blood to the penis. This can make it difficult to get or maintain an erection. That's called impotence. Not a good thing.

KIDS:

Kids whose parents smoke around them can have a lot of health problems. Secondhand smoke exposure can cause asthma, ear infections, even Sudden Infant Death Syndrome.

After checking all the cribs and viewing media, pop-up screen instructs player, "Here is the baby's file. Take it to Patient Records."

Guide: Babies and smoking don't mix. Smoking creates unhealthy, underweight babies who are at risk for lots of diseases and health complications. Even after they're born, kids who have parents who smoke around them also get asthma, ear infections and other problems. Let's see what you learned.

REVIEW ACTIVITY

Room: Radiology – Medium and Long-term smoking risks

S1 Stage: Key One Path

Guide: Welcome to Radiology. If you've got your pass card, you're going to be able to look inside the bodies of some smokers and see some pretty gross stuff. Check out all the lightboxes and you'll get your next set of instructions. If you don't have your pass card, you'll have to go back and check in with security.

Lightbox 1: X-ray of lung tumor

When player approaches, screen pops up showing lung tumor. X-ray is marked "Lung Cancer."

V/0: "Smoking causes lung cancer. This patient has developed a tumor in his lung and it needs to be removed. Lung cancer spreads early, and is difficult to treat."

Lightbox 2: PET Scan

When player approaches, screen pops up showing a PET scan of a body that reveals bladder and/or cervical cancer. Scan is marked "Cancer in other parts of the body."

V/O: "Smoking can cause cancer in other parts of the body besides the lungs. This patient's lung cancer has metastasized and spread to other vital organs, including the bladder and liver."

Lightbox 3: Angiogram

When player approaches, screen pops up showing video capture (or video?) of an angiogram. Video/still is marked "Heart Disease."

V/O: "This procedure is called an angiogram. Doctors go inside your arteries to look at damage to your blood vessels and heart. This patient has been diagnosed with severe heart disease and will have a heart attack if it's not treated."

Lightbox 4: CAT Scan

When player approaches, screen pops up showing CAT Scan of a head that reveals mouth and/or throat cancer. Scan is marked "Mouth Cancer."

V/O: "This scan shows a patient who has developed cancer of their mouth from years of smoking. It looks like part of his jaw is going to have to be removed if he's going to survive. With the tongue, partially removed, it is difficult to eat and talk.

After viewing all the lightboxes, the player receives a pop-up message. "Now you have your own set of x-rays. Take them to surgery and you can check out the operating room."

Guide: Before you get going, we need to see what you learned about the risks to your body from years of smoking. Take this short review.

REVIEW ACTIVITY

ROOM: Patient Records – Smoking Effects/Statistics

S1 Stage: Key Two Path

(Player must have picked up folder in delivery room in order to explore the records room. If not, when he approaches door to room with box that must be picked up, he receives the pop-up message "You'll need a folder from the delivery room if you want to get in here."

Guide: Here we are...Patient Records. A lot of people have come through this place. And many of them haven't gotten out alive. Why? They smoked. About 438,000 Americans die every year from diseases caused by smoking. And the ones that survive after surgery? Their lives sometimes aren't so great either. Check it out:

Dossier 1: Picture of disfigured face

V/O: I smoked ever since I was a kid. I never thought anything bad would happen to me, like lung cancer or a heart attack. But what I got...mouth cancer...might even be worse. I had surgery, and they had to take out part of my jaw. Yeah, I survived, but I can't even look in the mirror.

Dossier 2: Picture of black lung with tumors

V/O: Lung cancer...that was something I thought other people got. People who smoked two or three packs a day for sixty years, not just a pack a day for a pretty young guy like me. But at least they caught it early before it spread to the rest of my body. Of course, they had to cut me open and take out part of my lung. I don't have the energy I used to, or the strength. But I'm alive.

Dossier 3: Picture of amputated leg

V/O: I thought when I had a heart bypass that I was in the clear, so why not keep smoking? Bad idea. Smoking un-does the surgery by weakening the arteries. But I couldn't stop smoking. So the only thing the doctor could do is amputate my leg. Yeah, it's hard to get around. It's going to be worse if they cut off the other one.

Dossier 4: Picture of open heart surgery

V/O: I smoked a lot. But I don't anymore. I had to have a triple bypass because my arteries were so blocked that I was going to have a heart attack. They cracked my chest with a saw and the surgeons had to take part of a vein out of my leg to create new vessels to get blood to my heart. It took three months for my chest to heal.

After viewing the records, player can access the room with the box. When they approach the box, pop up message instructs: "Take this to the BioHazard room and get rid of it."

Guide: That was bad, huh? Smoking hurts a lot of people in a lot of painful ways, and not just on the inside. Losing part of your face or your leg? Not pretty. Let's see what you learned.

REVIEW ACTIVITY

Recreation Room in Extreme Lifestyle/Alternatives to smoking

(This is the rec room of the hospital, with athletes milling about, sports equipment, posters, games, etc. Objects such as a skateboard, goggles, boxing gloves, a helmet and elbow pads can be collected by player as he moves around room. When player approaches athletes, popup screen displays question and answer.)

Guide: Hey, how about taking a break? These guys and girls get their thrills from extreme sports – and not from smoking. And instead of ruining their health with cigarettes, they're having fun, staying fit and looking good. What do they like? Go find out.

Player interacts with people in the room, asking them questions”

Player: What do you do instead of smoking?

Male Skateboarder: I skate, dude. I've got a slammin' kickflip.

Player: What do you do instead of smoking?

Female BMX Biker: BMX is rad, rookie. Totally sweet.

Player: How come you don't smoke?

Male Surfer: I'm too busy catching waves. They were epic today.

Player: What do you do instead of smoking?

Female Kickboxer: I'm a kickboxer. I stay in shape and get to beat the crap out of things.

Player: What do you for fun instead of smoking?

Male Snowboarder: I'm a snowboarder! Want to see me bust a huge air?

After player interacts with all characters and collects objects, guide's voice breaks in.

Guide: Hey, if you want to be cool, you don't have to smoke. Why not get your thrills from extreme sports? Have you watched the XGames lately? Now THAT's cool. Find something you like and make it your own. But now it's time to go. Back to the elevator.

Room: TVRoom/Theater – Correct perceptions about smoking in the movies

All Scenarios

Visual: Darkened theater with movie screen. As player comes in, screen comes to life. This screen will play a footage from Hollywood movies with characters smoking, but will be given a “pop-up video” treatment. (This can be accomplished

by taking a series of movie clips and stringing them together to form a trailer for a fictional movie called “Hollywood Up In Smoke.)

For example, depending on what footage is available, the commentary could be:

“She doesn’t really smoke.”

“He’s faking it. That’s why he’s an actor.”

“I read in Celebrity Star that he’s hates smoking in real life.”

“Nice product placement!”

“You’d think everyone smokes from watching this. But they don’t”

“Look! She isn’t inhaling.”

“I don’t think she could run and beat up guys like that if she was a smoker.”

“I thought smoking was against the law in California bars.”

“Only 20-25% of Americans are smokers, but in 75% of PG movies and 90% of R movies, the characters smoke.

Review Activity

Room: Accounting – Economic Cost of Smoking Incorporating all comments to date

(This is the accounting office of the hospital, with desks, ledgers, desks, green-shaded “banker’s lamps, and an adding machine that enlarges into a financial cost calculator when player approaches. The desks have nameplates on them that say “House Insurance,” “Health Insurance” and “Employment.” When player approaches each of these desks, he receives a message related to costs.)

S1 Scenario

Guide: Smoking doesn’t just hurt your body – it hurts your wallet, too. What are you spending on your addiction? Probably more than you think! Check out this room and you’ll see that it really adds up.

Desk 1: House Insurance

Message: Smokers pay more for house insurance, because they’re more likely to have fires.

Desk 2: Health Insurance

Message: Smokers pay hundreds of dollars more per year for health insurance than non-smokers.

Desk 3: Employment

Message: Smoking can cost you your job. There are more than 6,000 companies in the U.S that refuse to hire smokers, and the number keeps going up.

Cost Calculator:

When player approaches adding machine, lights and bells go off. Screen pops up. This is the cost calculator. Player enters how much they smoke, what they pay for cigarettes. This figure will tell them what they're spending a month, year, etc.

V/O: Hey big spender! How much are cigarettes costing you? It's time to find out!

V/O Questions:

- 1) How much do you smoke a day?
- 2) What do you pay for cigarettes?

Calculator spits out receipt.

V/O: Now THAT's a lot of money up in smoke!

After player completes cost calculators, he gets a receipt.

Guide: More than you thought, huh? That's not even taking into account what you'll spend on dry cleaning and higher insurance costs. Smoking might even cost you your job.

Got your receipt? If not, you'll have to go back and calculate again. Take it to the Recovery Room and you'll see what the real costs of smoking are.

(review activity)

Room: Research Lab/Practical Quitting Techniques

S2 Scenario

Visual: Elevator doors open and player and guide are in the lab. This is your stereotypical "mad scientist's" laboratory, with test tubes and beakers fizzing, monitors buzzing, random jars, etc. There is a monitor in the room with the words "secret formula" on the screen.

Guide: This looks....interesting. I wonder what they're making here. Why don't you go see?

Visual: Player moves around lab, equipment fizzes and pops. When he walks up to the monitor, it triggers a pop-up screen. "Secret Formula" becomes "Secret Formula for Quitting."

Mad scientist's face appears on screen.

Scientist: Sorry, I've stepped away from my lab for a moment. Please leave a message after the tone. Bwahaaaahaaaahahaha, just kidding. (sigh) OK, so you want to quit. It's not rocket science. Call me crazy, but this simple formula really works. If you don't watch the whole thing, I may turn you into a zombie.

Visual: The words "recognize, remember and react" appear on screen.

Visual: Quick cuts (illustrations) of people in situations where they might be exposed to smoking.

VO: First, **recognize** situations where you might be tempted.

- 1) At a party – guy offering a cigarette. "Hey, have a smoke."
- 2) Group of people at bowling alley – girl offers. "Everybody's smoking. Come on!"
- 3) Behind the school – girl offers. "Hey have a cigarette and hang out."

VO: Then, **remember** why you want to quit.

- 1) A guy with a bat. "I want a sneaker contract."
- 2) A goth girl. "I'm tired of being unhealthy. So, so, so tired."
- 3) A nerd guy. "It never made me popular anyway."
- 4) A cheerleader. "I don't want to – mess up my – B-O-D-Y!"

VO: Now, here are ways to **react**.

Text and VO: choose to Ignore..

Visual: Guy in headphones yelling, "I'm sorry, did you say something?!?!?!"

Text and VO: Try humor.

Visual: Extremely tall girl saying, "Nah, I don't want to stunt my growth."

Text and VO: Ask for support.

Visual: Woman saying, "Hey I'm trying to quit, OK? Why can't you support me? Whose side are you on?"

Text and VO: Make positive plans.

Visual: Gang-style kid saying, embarrassed, "Sorry, I, um...I have ballroom dancing class."

Text and VO: Get smart.

Visual: Nerd saying, "Let me analyze this. I don't think I'll be more popular with the ladies if I stink, I can't breathe and I can't perform in the bedroom. Just a theory."

Text and VO: Change the subject.

Visual: Jock saying, "You see that game last night? Wanna arm wrestle?"

Scientist: OK, you watched the whole thing. No zombie for you. You're free to go.

REVIEW ACTIVITY

Room: Rooftop/Social Risks

Visual: Hospital rooftop, avatars milling about, a "lifeFlight" type helicopter is on the roof with a person standing outside its door. Player needs a friend AND a key to be able to get on the helicopter. If he approaches the helicopter without a friend or key, guard says, "Sorry, you can't take a ride without the right key. Go back to XXX (room where it can be found)."

S1 Scenario

Guide: So, how about we take a break? Maybe you'd like to go for a ride in the helicopter. Find a friend to go with you.

Visual: Player approaches other avatars to seek out friend. Pop up dialogue bubbles contain text.

Player: Want to go on a helicopter ride with me?

Avatar: I don't think so. You smell like a chimney and I don't think you respect yourself.

Player: Hey, want to go up in the helicopter with me?

Avatar: Maybe. Do you have an extra cigarette?

Player: Hey, want to go up in the helicopter with me?

Avatar: I might. But don't smoke around me. I don't want to smell like an ashtray.

Player: How about going on a helicopter ride with me?

Avatar: No way – I'm trying to quit smoking and I think you're a bad influence.

Player: Hey, want to take a helicopter ride with me?

Avatar: If you're gonna be smoking, I think I'll pass.

Player: Hey, want to take a helicopter ride with me?

Avatar: OK, I've got nothing else going on.

Visual: Player interacts with all avatars. Eventually he finds a suitable friend.

Now that player has friend (and ideally, the key), he can approach the helicopter for a ride.

Guard: Welcome. How about a tour of the city?

(Video screen pops up with pilot's voiceover):

Pilot: Hey...you're a smoker! Well, in this city, most every place you can see for miles around (show landscape/buildings in quick cuts) is now non-smoking. Parks, Schools, Malls, Hospitals, Sports Arenas, Bars and Restaurants – you can't smoke anyplace anymore. It's not just here – all over the world, public spaces are going smoke-free. Pretty soon the only place you'll be able to smoke is your own house. Now that's going to limit your social life!

Video ends.

Player goes back to elevator.

(Review activity/quiz on social risks of smoking)

ROOM: Security – Short and Medium Term Health Risks

S1 Stage: Key One Path

Visual: Hospital security office, monitors and blinking devices arranged throughout. When the player approaches it, it activates a pop-up screen that plays animations about the short-term effects of smoking.

S1 Scenario

Guide: In the security office, they watch what everyone's doing. Because you're a smoker who doesn't want to quit, you're doing something pretty dangerous. But you'll see that when you view the security tapes. Check them out.

Monitor #1

Visual: Girl talking to guy at the mall. Guy is dressed like stereotypical suburban "rapper."

Brian: Hey Veronica, you're looking fine. Want to hear me rap?

Veronica: (cringing) No thanks, Brian. I'm busy.

Brian: (rapping) Me too, yeah it's true, do you... <<cough, cough, cough>>. Want to go outside and smoke?

Visual: He smiles, showing yellow teeth and gum disease.

Veronica: Gross! How long have you been smoking? And already, you've got yellow teeth, filthy gums and a nasty cough. And that breath! No thanks.

Brian: That's cold.

Monitor #2

Visual: Jeff, a young guy, is looking in the mirror, fixing his hair, humming, smoking a cigarette, thinking he's pretty hot. He's dressed like a typical teenager. His friend Jon stands next to him.

Jon: What are you doing?

Jeff: (distracted). Um, what? I'm just checking to see if I've still got it...

Jon: Yeah, you've got it all right. You've got grey hair and you're starting to get wrinkles, dude. Maybe it's time to lay off the smokes.

Visual: You see his face. Jeff looks much older than his age.

Jeff: (singing) You are so beautiful....to me.

Monitor #3

Visual: Two girls, Erica and Sarah, are sitting at a Starbucks-type place.

Erica: Oh, I love your new bag. Can I see it?

Visual: Sarah hands over bag. Erica stares at Sarah's fingers, which are yellow and stained.

Erica: Gross, Sarah, your fingers are all stained from smoking!

Visual: Sarah sits on her hands.

Erica: How are you ever going to hook up with a guy with hands like that? And another thing...it can make you infertile. Don't you want babies some day? And, you know if a guy smokes, he might be sterile not be able to "perform" anyway.

Sarah: I wonder where my triple decaf non-fat light whip extra hot latte is?

Monitor #4

Visual: Alex, a guy in his mid-twenties, talking to Carla, his girlfriend. They're sitting on a couch watching TV.

Alex: Have you seen my smokes?

Carla: (Sighs) I threw them out.

Alex: You did what? I want a cigarette. I need one. I deserve one!

Carla: You're an addict, you know that?

Alex: Yeah, I know. I'll quit. Someday. But not right now. I can't.

Carla: Well, then don't do it around me.

Alex: OK, that's cool....(pauses for a few seconds, watching TV, then gets up quickly and leaves.) Later!

Monitor #5

Visual: Two guys, Mike and Adam, doing homework. One is studying while the other is playing the guitar and smoking a cigarette.

Mike: Could you put that out please? It's gross and it's stinking up the room.

Adam: I'm an *artist*. Cigarettes help me create.

Mike: They're not helping you, fool. Don't you ever think about lung cancer or heart disease? Tobacco kills more people than alcohol, murder, cocaine, heroin and AIDS combined.

Adam: That's really sad. Maybe I'll write a song about that.

Mike. Just put it out. Please.

Adam: (singing) "Tobacco, so beautiful, so dangerous, a puff of pleasure, the kiss of death..."

--- After viewing all the tapes, the player can pick up the security card, which is indicated by a large red arrow over it. When the player gets the card, a pop-up message reads: "Congratulations! You've now got the pass card. It can open some doors for you. You might want to try it out in the Radiology Lab."

Guide: You've seen the damage that smoking can do to you in just a few short months – gum disease, wrinkles, even sex problems. It's not pretty. Let's see what you learned.

REVIEW ACTIVITY

ROOM: Waste Disposal-BioHazard/Environmental Effects

S1 Stage: Key Two Path

(Player needs a box of patient records to access the interior room that holds the key. If he does not have them, he gets the pop-up message: "You can't get in here without a box of patient records."

Guide: You know that if you keep on smoking, it's going to make you sick, miserable and poor. What you may not know is that it can damage the environment and people around you, too. Check out the waste disposal area and see what I mean.

TV AREA

As player approaches TV area, screen pops up playing newsmagazine program about the environmental effects of smoking.

Visual: Player moves toward TV, and screen pops up. It's an investigative newsmagazine show. (this will be an animation)

AnnCr: Tonight on 60 Seconds, we take a look at the real story of tobacco. Cigarettes are harmless, right? Smoking doesn't hurt anyone...or does it? Tobacco companies want us to believe the world's a better, more fun place when we're all puffing away. (Lowers voice) I want to warn you, folks, this is some pretty nasty footage. We go now to Danger McGillicuddy, in the field.

Visual: Field reporter beside a river.

Reporter: Thanks, Dan. I'm standing here at the river, which as you can see is polluted with cigarette butts (Visual: dead ducks and plants). Smoking kills again! They say cigarettes even too toxic for landfills! Alice?

Visual: Field reporter leaving a bar/restaurant, with a big cloud of smoke rolling out behind her.

Reporter: <<Cough, cough>> Thanks, Ron. We tried to have a nice dinner in the NON-smoking section of this restaurant, but when anyone is smoking, we ALL feel the effects of second-hand smoke. Having a smoking section in a restaurant is like having a peeing section in a swimming pool! (pause) The employees have it WORSE. Night after night, breathing in OTHER people's smoke. A dangerous situation indeed! Clint?

Visual: Field reporter outside a burning house.

Reporter: Good evening everyone. Yes, it's yet another avoidable fire, again caused by someone smoking in bed... Fires due to careless smoking kill thousands of people, including many children, every year.

ANNCR: And now for an emergency weather bulletin. Today's air quality is, well, terrible. Lots of pollution out there. When you smoke in a polluted environment, you do even more damage to your health.

It's worse than I thought, folks. Thanks for watching. From all of us here at 60 Seconds, good night, and good health.

DUMPSTER AREA:

Visual: Hazardous waste dumpsters with "radioactive" symbols on them and signs reading "Protective Gear Required". When player approaches the dumpster/bin area, he receives the following voice over message:

VO: Tobacco smoke contains over 4,000 different chemicals. At least 43 are known to cause cancers in humans. You wouldn't touch these poisons with your bare hands, but when you smoke you inhale them directly into your delicate lungs.

Now, when player approaches each labeled dumpster, its symbol starts glowing and then a pop-up screen with animation delivers information:

- Bin 1: Arsenic (this is rat poison) – show hazmat suit
- Bin 2: Carbon Monoxide (this is what comes out of your car's exhaust pipe) – show gas mask
- Bin 3: Nicotine – (a very poisonous chemical used as an insecticide) – show protective gloves and boots
- Bin 4: Hydrogen Cyanide (this is what they give you in the gas chamber to kill you) – show gas mask
- Bin 5: Polonium –210 (this is radioactive material, dangerous nuclear waste) – SFX: meltdown alarm. Show nuclear plant suit.

Guide: When you smoke, you're putting poison in your body and hurting the environment. Do you want to be a chemical dump? Let's see what you learned.

REVIEW ACTIVITY

APPENDIX J

DIFFERENTIAL IMMUNOHISTOCHEMICAL EXPRESSION PATTERNS OF FIBROBLAST GROWTH FACTOR-2, RECEPTORS 1 AND 2, AND SYNDÉCAN-1 IN SQUAMOUS CELL CARCINOMA AND ADENOCARCINOMA OF THE LUNG.

Carmen Behrens¹, Heather Lin², J. Jack Lee², Waun Ki Hong¹, Ignacio I. Wistuba^{1,3} and Reuben Lotan¹. Departments of ¹Thoracic/Head and Neck Medical Oncology, ²Biostatistics, and ³Pathology, UT MD Anderson Cancer Center, Houston, TX 77030

Fibroblast growth factor-2 (FGF2), its transmembrane tyrosine kinase receptors 1 and 2 (FGFR1 and FGFR2), and heparan sulphate proteoglycan syndecan-1 (SDC-1) are involved in angiogenesis. All of these proteins are increased in non-small cell lung cancer (NSCLC). However, the simultaneous expression of all four markers in a large set of NSCLCs with annotated clinic and pathologic information has not been investigated so far. Therefore, we performed semi-quantitative immunohistochemical (IHC) expression analysis of 196 lung adenocarcinomas (ADCA) and 125 squamous cell carcinomas (SCC) using formalin-fixed specimens in tissue microarrays. FGF2, FGFR1, FGFR2 were examined in tumor cells and SDC-1 in tumor (SDC-1T) and stromal (SDC-1S) cells. Overall, we found high levels of expression of all markers in NSCLC. SCC expressed significantly higher levels of nuclear FGF2 ($P=0.01$), cytoplasmic FGFR2 ($P=0.006$), SDC-1T ($P<0.0001$) and SDC-1S ($P<0.0001$). ADCA expressed higher levels of nuclear FGFR1 ($P<0.0001$) and FGFR2 ($P=0.003$). Patient's clinical-pathologic data when correlated with IHC expressions of the markers showed different patterns of correlations in ADCA and SCC, especially for gender and smoking. In univariate analysis, in ADCA, females demonstrated higher levels of nuclear FGF2 ($P=0.03$), nuclear FGFR1 ($P=0.019$) and SDC-1T ($P=0.03$) than males, while in SCC males had higher SDC-1T ($P=0.02$). Among ADCAs, smokers demonstrated higher levels of cytoplasmic FGFR1 ($P=0.04$) and SDC-1S ($P=0.02$) and lower levels of nuclear FGFR1 ($P=0.002$) and FGFR2 ($P=0.04$). Among SCCs, smokers demonstrated higher nuclear FGFR2 ($P=0.02$). A complex pattern of marker correlations was detected: ADCA and SCC showed correlation between nucleus and cytoplasm for FGFR2 ($P=0.0005$) and between cytoplasms of FGF2 and FGFR1 ($P<0.03$) and FGFR1 and FGFR2 ($P<0.0001$); only in ADCAs nuclear FGFR1 correlated with nuclear FGF2 and FGFR2 ($P<0.0001$ and 0.0003, respectively), and SDC-1T correlated with nuclear FGF2, FGFR1 and FGFR2 ($P=0.04$, 0.006 and 0.02, respectively); in SCC, SDC-1T correlated with cytoplasmic FGF2 and FGFR2 ($P=0.002$ and 0.02, respectively) and nuclear FGFR1 ($P=0.05$). SDC-1S only showed correlation with SDC-1T in SCC ($P=0.0002$). We conclude that FGF2, FGFRs and SDC-1 are frequently overexpressed in NSCLC, although different patterns of expression were detected in the two major forms of NSCLCs. Our findings suggest that FGF2 signaling pathway is frequently activated in NSCLC, but tumor characteristics must be considered to develop therapeutic strategies. (Supported by Grant W81XWH-05-2-0027).

Targeting EGFR signaling to enhance response of non-small cell lung cancer cells to radiation

Colin S. Brooks, Toshimistu Tanaka, Anupama Munshi, Jenny Liu, Nathan Wang, Marvette Hobbs, Raymond E. Meyn. Department of Experimental Radiation Oncology, The University of Texas M.D. Anderson Cancer Center, Houston, TX 77030.

In spite of significant technical advances including IMRT and chemoradiation, locally advanced lung cancer continues to have a dismal prognosis as many patients' tumors appear to be resistant to radiation therapy. The need to improve the result of radiation therapy presents an opportunity to evaluate molecular targeting strategies for sensitizing NSCLC to radiation. It is well established that EGFR is constitutively activated in many human, non-small cell lung cancers (NSCLC) and that this activation correlates with a radioresistant phenotype. Thus, the response of NSCLC to radiation may be improved through the use of inhibitors of EGFR signaling. Several novel agents that target various steps in this pathway are currently available for testing this hypothesis.

In the present study, we report the effects of Tarceva (Erlotinib, OSI-774), a selective EGFR tyrosine kinase inhibitor, and C225 (Erbitux, Cetuximab) a monoclonal antibody to the EGF receptor, on the radiation sensitivity of three NSCLC cell lines, A549, H460 and H1299, that express moderate to high levels of the EGFR. Clonogenic cell survival assays showed that Tarceva significantly radiosensitized all three NSCLC cell lines, substantially reducing the surviving fraction at 2 Gy (SF2). Pre-treatment with 5 μ M Tarceva for 24 hr enhanced tumor cell radiosensitivity with the survival factor at 2Gy (SF2) being reduced from 61.5%, 78% and 56% in vehicle-treated to 37.9%, 56% and 52% in Tarceva-treated A549, H460 and H1299 cells respectively. Similarly, pre-treatment with 30nM C225 for 1 hr radiosensitized both H1299 and A549 cells with SF2 being reduced from 72% and 44.2% in vehicle-treated to 54.9% and 16% in C225 treated A549 and H1299 cells respectively. Both agents had a radioprotective effect on normal human lung fibroblasts. We examined potential mechanisms that may contribute to the enhanced radiation response induced by Tarceva and C225. Dose-dependent decreases in pEGFR were evident following treatment with Tarceva and C225 in H1299 cells. C225 blocked constitutive and radiation-induced activation of pERK in A549 cells possibly correlating with its radiosensitizing effects. Overall, our results suggest that both Tarceva and C225 synergistically interact with radiation and enhance the radioresponse of human NSCLC cells. A detailed investigation of the mechanism is ongoing. The insight gained from the analyses of these molecular mechanisms will be very useful in future research examining the combination of molecular targeted agents such as Tarceva and C225 and ionizing radiation. The study was supported by the Department of Defense grant IMPACT W81XWH-06-1-0303.

A Generalized Response Surface Model with Varying Relative Potency for Assessing Drug Interaction

Maiying Kong and J. Jack Lee*

Department of Biostatistics and Applied Mathematics, University of Texas, M. D. Anderson Cancer Center,
Unit 447, 1515 Holcombe Boulevard, Houston, Texas 77030, U.S.A.

*email: jjlee@mdanderson.org

SUMMARY. When multiple drugs are administered simultaneously, investigators are often interested in assessing whether the drug combinations are synergistic, additive, or antagonistic. Based on the Loewe additivity reference model, many existing response surface models require constant relative potency and some of them use a single parameter to capture synergy, additivity, or antagonism. However, the assumption of constant relative potency is too restrictive, and these models using a single parameter to capture drug interaction are inadequate to describe the phenomenon when synergy, additivity, and antagonism are interspersed in different regions of drug combinations. We propose a generalized response surface model with a function of doses instead of one single parameter to identify and quantify departure from additivity. The proposed model can incorporate varying relative potencies among multiple drugs as well. Examples and simulations are given to demonstrate that the proposed model is effective in capturing different patterns of drug interaction.

KEY WORDS: Additivity; Antagonism; Dose-response curve; Dose-response surface; Interaction index; Loewe additivity model; Synergy.

1. Introduction

Studies of interactions among biologically active agents, such as drugs, carcinogens, or environmental pollutants, have become increasingly important in many branches of biomedical research (Suhnel, 1998). An effective and accurate evaluation of drug interaction for *in vitro* and/or *in vivo* studies can help to determine whether a combination therapy should be further investigated in clinical trials.

The literature supports the notion that the Loewe additivity model can be considered as the “gold standard” to define drug interactions (Berenbaum, 1989; Greco, Bravo, and Parsons, 1995). Based on the Loewe additivity model, we focus on applying the response surface method (RSM) to study drug interaction. The RSM, which involves an estimation of the $(n + 1)$ -dimensional response surface in n drug combinations, can take all of the information present in the full dose-effect data set for n drugs to give a complete picture of drug interactions over all possible drug combinations. In addition, the RSM can be used to determine the optimal combination therapy. Many examples of the RSM (e.g., Finney, 1971; Greco, Park, and Rustum, 1990; Plummer and Short, 1990) used a single parameter to capture synergy, additivity, or antagonism. These approaches are valid if only either synergy, additivity, or antagonism exists throughout the whole surface. They are inadequate to describe the presence of pockets of local synergy or local antagonism when they are interspersed in different regions of drug combinations. White et al. (2004) proposed a nonlinear mixture response surface approach based on the assumption that the combination doses

at each fixed ratio follow the median effect model (Chou and Talalay, 1984), and the parameters in the median effect model are assumed to be polynomials of the ratio. The resulting models capture synergy, additivity, or antagonism exclusively based on the 50% maximal effect isoboles. However, at a fixed ratio, the combination doses of two drugs do not necessarily yield the same mode of drug interactions as that at 50% maximal effect. For example, Savelev et al. (2003) showed that the combinations of 1,8-cineole and α -pinene at the fixed ratio 11:1 are synergistic for higher combination doses and additive for lower combination doses. To address this issue, we propose a generalized response surface (GRS) model for two drugs. Instead of using one single parameter, we construct a function of the doses of two drugs to capture synergy, additivity, and antagonism without assuming any fixed patterns of drug interactions. The model contains a rich class of dose-response relationships and allows the drug interaction patterns to be determined by the observed data.

Before we proceed, let us recall a widely used model that provides a dose-response curve for a single agent: Chou and Talalay’s (1984) median effect equation,

$$E = \frac{\left(\frac{d}{D_m}\right)^m}{1 + \left(\frac{d}{D_m}\right)^m}. \quad (1)$$

Here d is the dose of a drug, D_m is the median effective dose of a drug, and m is a slope parameter depicting the shape

of the dose-response curve. All these dose-response curves can be rewritten as Y , a monotone function of E , having a linear relationship with $\log d$. For example, the median effect equation has the form

$$Y = \log \frac{E}{1-E} = m(\log d - \log D_m). \quad (2)$$

All the families described by Suhnel (1998), excluding the Weibull family, can take such form by establishing a linear relationship between a monotone transformation of E and $\log d$. Tallarida (2000, Chapter 2) pointed out that, in many settings, the data points in the mid range (say between 20% and 80% of the maximum effect) typically display a nearly linear trend between the response and the $\log d$ when responses are measured on a continuous scale. For quantal response data, Finney (1971) and Govindarajulu (2001) pointed out that the probit- or logistic-transformed response usually exhibits a linear relationship with $\log d$. Consequently, we assume that the response or transformed response follows a linear function of $\log d$ for each of the two drugs when acting alone. Without loss of generality, we denote the dose-response curve as $Y = \beta_0 + \beta_1 \log d$.

Suhnel (1998) explicitly derived the combined additive effect of two drugs under the Loewe additivity model and made the assumption that the slopes β_1 are the same for both drugs. Finney (1971) proposed an additivity model for two drugs as $Y = \beta_0 + \beta_1 \log(d_1 + \rho d_2)$ for the combination dose (d_1, d_2) , where ρ is the relative potency of drug 2 versus drug 1 and is assumed to be a constant. The constant ρ again implies that the two dose-response curves have the same slope. To construct a generalized model, we would first loosen the parallel assumption by allowing a varying relative potency. Next, we propose the use of a quadratic function of two doses instead of one single parameter to depict different patterns of drug interactions. The proposed model can be considered as a generalization of Finney's model (1971) and the model derived by Plummer and Short (1990). We will describe our proposed model in Section 2, relate this new model to isoboles and interaction indices in Section 3, state how to make inference on drug combinations in Section 4, and give simulations and examples to illustrate how the new approach performs in Section 5. The last section is devoted to discussion.

2. Derivation of the Generalized Response Surface Model

Recall the Loewe additivity model (Loewe and Muischnek, 1926; Berenbaum, 1989; Greco et al., 1995)

$$\frac{d_1}{D_{y,1}} + \frac{d_2}{D_{y,2}} = 1, \quad (3)$$

where d_1, d_2 are doses of drug 1 and drug 2 in the mixture eliciting an effect y , and $D_{y,1}$ and $D_{y,2}$ are the respective single-agent doses of drug 1 and drug 2 that elicit the effect y . One can obtain the predicted additive effect based on the Loewe additivity model providing that the dose-effect curves for each of the two drugs are known. Suppose that the dose-effect curves are $F_1(D_1)$ for drug 1 and $F_2(D_2)$ for drug 2, then the predicted effect, say y , can be obtained by solving equation (3) after replacing $D_{y,1}$ by $F_1^{-1}(y)$ and $D_{y,2}$ by $F_2^{-1}(y)$, where F_i^{-1} is the inverse function of F_i ($i = 1, 2$). If the observed effect

at (d_1, d_2) is more than or less than the predicted effect, the combination dose (d_1, d_2) is correspondingly synergistic or antagonistic.

Note that the above additive equation (3) can be rewritten as

$$d_1 + d_2 \frac{D_{y,1}}{D_{y,2}} = D_{y,1}. \quad (4)$$

Denote $\frac{D_{y,1}}{D_{y,2}}$ as $\rho(y)$, which is the relative potency of drug 2 versus drug 1, meaning that 1 unit of drug 2 has the same effect as $\rho(y)$ units of drug 1. Grabovsky and Tallarida (2004) addressed the issue that the relative potency may vary. The nonparallel dose-effect curves introduced by Suhnel (1998) can also be interpreted as the varying relative potency. When the relative potency varies, finding a method to transform the combination dose (d_1, d_2) into the equivalent doses of drug 1 or drug 2 requires careful investigation. In the following derivation, we uphold the Loewe additivity model regardless of the shape of the dose-effect curve associated with each single drug. We expound the interpretation of the varying relative potency, its correct usage, and the relationship of various quantities in equation (4) in the Appendix. From the Appendix, it follows that the additive y -isobole is a straight line \overline{PQ} , which connects $P = (D_{y,1}, 0)$ and $Q = (0, D_{y,2})$ (Figure 1, panel A). Each drug combination (d_1, d_2) on the y -isobole shares the same relative potency $\rho(y)$, and its equivalent amount dose is $d_1 + \rho(y)d_2$ in terms of drug 1, or $\rho(y)^{-1}d_1 + d_2$ in terms of drug 2. On the other hand, the combination doses on different additive isoboles may have different relative potencies as shown in Figure 1, panel B.

In this article, we construct a GRS model which incorporates the varying relative potency. We assume that the log(dose)-response curves are linear. Without loss of generality, the model derivation begins with the assumptions of a constant relative potency and a log(dose)-effect curve for drug 1:

$$Y_1 = \beta_0 + \beta_1 \log D_{Y_1,1}. \quad (5)$$

Subsequently, the predicted additive effect of the combination can be written as $Y = \beta_0 + \beta_1 \log(d_1 + \rho d_2)$, where ρ is a constant relative potency parameter. In order to capture synergy, additivity, or antagonism, Finney (1971, Section 11.5) suggested a model of the form

$$Y = \beta_0 + \beta_1 \log(d_1 + \rho d_2 + \kappa(d_1 \rho d_2)^{\frac{1}{2}}). \quad (6)$$

Here the additional term $(d_1 \rho d_2)^{\frac{1}{2}}$ is the geometric mean of d_1 and ρd_2 , and κ is the synergy-antagonism parameter with $\kappa = 0$ corresponding to additivity, $\kappa > 0$ to synergy, and $\kappa < 0$ to antagonism.

Plummer and Short (1990) extended model (6) to a case in which the relative potency ρ may be varying while keeping the same formulation as (6). Let us assume that the log(dose)-effect curve for drug 2 is

$$Y_2 = \alpha_0 + \alpha_1 \log D_{Y_2,2}. \quad (7)$$

The question is: what form should the relative potency take under the log(dose)-effect curves (5) for drug 1 and (7) for drug 2? Let $Y_1 = Y_2 = y$, we have $\beta_0 + \beta_1 \log D_{y,1} = \alpha_0 + \alpha_1 \log D_{y,2}$. Then, $\beta_1 \log \frac{D_{y,1}}{D_{y,2}} = \alpha_0 - \beta_0 + (\alpha_1 - \beta_1) \log D_{y,2}$.

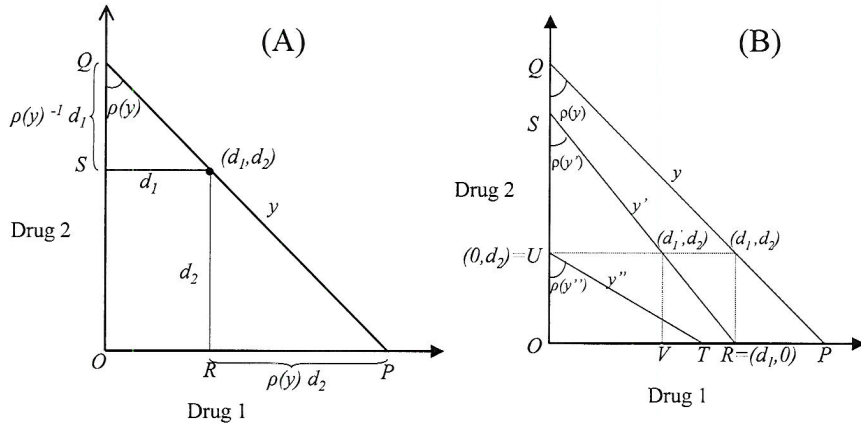


Figure 1. Relative potency and equivalent doses. \overline{PQ} is an additive isobole, $P = (D_{y,1}, 0)$, $Q = (0, D_{y,2})$. The relative potency of drug 2 versus drug 1 is defined as $\rho(y) = \frac{D_{y,1}}{D_{y,2}}$. Under additive assumption the effect at (d_1, d_2) is the same as the effect of drug 1 alone at $d_1 + \rho(y)d_2$, and also the same as the effect of drug 2 alone at $\rho(y)^{-1}d_1 + d_2$ (panel A). Panel B shows that given drug 2 at dose d_2 , its equivalent drug 1 dose may change when different amounts of drug 1 are added. Here $y = F_1(D_{y,1}) = F_2(D_{y,2})$, $y' = F_1(d_1)$, and $y'' = F_2(d_2)$. The equivalent amount of drug 1 doses of d_2 at combination doses (d_1, d_2) , (d'_1, d_2) , and $(0, d_2)$ are $\rho(y)d_2$ ($= \text{length}(\overline{RP})$), $\rho(y')d_2$ ($= \text{length}(\overline{VR})$), and $\rho(y'')d_2$ ($= \text{length}(\overline{OT})$), respectively.

Thus, the relative potency can be written as $\rho(y) = \frac{D_{y,1}}{D_{y,2}} = \exp\left(\frac{\alpha_0 - \beta_0}{\beta_1} + \frac{\alpha_1 - \beta_1}{\beta_1} \log D_{y,2}\right)$. Introducing two parameters $\gamma_1 (= \frac{\alpha_0 - \beta_0}{\beta_1})$ and $\gamma_2 (= \frac{\alpha_1 - \beta_1}{\beta_1})$, we can write

$$\rho(y) = \exp(\gamma_1 + \gamma_2 \log D_{y,2}). \quad (8)$$

Here $D_{y,2}$ is the amount of the drugs in terms of drug 2, that is, $D_{y,2} = \rho(y)^{-1}d_1 + d_2$, which produces the same effect as the combination (d_1, d_2) under the additive assumption. Note that given one of the two, $D_{y,2}$ and y are uniquely determined, so we may suppress y to obtain the relative potency at combination dose (d_1, d_2) by solving $\rho = \exp(\gamma_1 + \gamma_2 \log D_2)$ subject to $D_2 = \rho^{-1}d_1 + d_2$.

Plummer and Short's model incorporates the varying relative potency. However, the model is inadequate to describe the phenomena when synergy and antagonism are interspersed in different regions of the drug combinations. To overcome this limitation, we propose the GRS model of the following form,

$$Y = \beta_0 + \beta_1 \log(d_1 + \rho d_2 + f(d_1, d_2; \gamma, \kappa)(d_1 \rho d_2)^{\frac{1}{2}}) \quad (9)$$

using $f(d_1, d_2; \gamma, \kappa)$ to capture local synergy, local additivity, or local antagonism. In this article we take

$$\begin{aligned} f(d_1, d_2; \gamma, \kappa) &= \kappa_0 + \kappa_1 d_1^{\frac{1}{2}} + \kappa_2 (\rho d_2)^{\frac{1}{2}} + \kappa_3 d_1 \\ &\quad + \kappa_4 \rho d_2 + \kappa_5 (d_1 \rho d_2)^{\frac{1}{2}}, \end{aligned} \quad (10)$$

where f is a function of d_1 and d_2 with parameters γ 's capturing the varying relative potency ρ as described above and κ 's being the coefficients of the quadratic function.

Our main considerations for using the term $f(d_1, d_2; \gamma, \kappa)(d_1 \rho d_2)^{\frac{1}{2}}$ are: (i) the marginal dose-effect curves are easily obtained and are impacted as little as possible by this extra term, and (ii) the function f can have enough flexibility to capture the departure from the predicted additivity effect, $\beta_0 + \beta_1 \log(d_1 + \rho d_2)$. For the first consideration, we used the factor $(d_1 \rho d_2)^{\frac{1}{2}}$, and for the

second consideration, we adopted the complete quadratic form of $d_1^{\frac{1}{2}}$ and $(\rho d_2)^{\frac{1}{2}}$ for $f(d_1, d_2; \gamma, \kappa)$. Extensive search and simulations show that the proposed model parameterization is reasonable and appropriate. One caveat is that the current parameterization may contain more parameters than necessary; therefore, model selection procedures need to be developed.

The following equations demonstrate how the GRS model captures different patterns of drug interaction: for each fixed effect level y , setting $d_2 = 0$ in (9), we obtain $D_{y,1} = \exp\left(\frac{y - \beta_0}{\beta_1}\right)$; setting $d_1 = 0$, we obtain $D_{y,2} = \rho^{-1} \exp\left(\frac{y - \beta_0}{\beta_1}\right)$; and the combination dose (d_1, d_2) satisfies $\exp\left(\frac{y - \beta_0}{\beta_1}\right) = d_1 + \rho d_2 + f(d_1, d_2; \gamma, \kappa)(d_1 \rho d_2)^{\frac{1}{2}}$. Dividing both sides by $\exp\left(\frac{y - \beta_0}{\beta_1}\right)$ and rearranging the equality, the interaction index, $\frac{d_1}{D_{y,1}} + \frac{d_2}{D_{y,2}}$, could be written as

Interaction index

$$\begin{aligned} &= \frac{d_1}{D_{y,1}} + \frac{d_2}{D_{y,2}} = \frac{d_1}{\exp\left(\frac{y - \beta_0}{\beta_1}\right)} + \frac{d_2}{\rho^{-1} \exp\left(\frac{y - \beta_0}{\beta_1}\right)} \\ &= 1 - \frac{f(d_1, d_2; \gamma, \kappa)(d_1 \rho d_2)^{\frac{1}{2}}}{\exp\left(\frac{y - \beta_0}{\beta_1}\right)} \\ &= \left[1 + \frac{f(d_1, d_2; \gamma, \kappa)(d_1 \rho d_2)^{\frac{1}{2}}}{d_1 + \rho d_2} \right]^{-1}. \end{aligned} \quad (11)$$

From (11), the polynomial function $f(d_1, d_2; \gamma, \kappa)$ being greater than, equal to, or less than 0 corresponds to the interaction index being less than, equal to, or greater than 1, and consequently, this combination is synergistic, additive, or antagonistic, respectively.

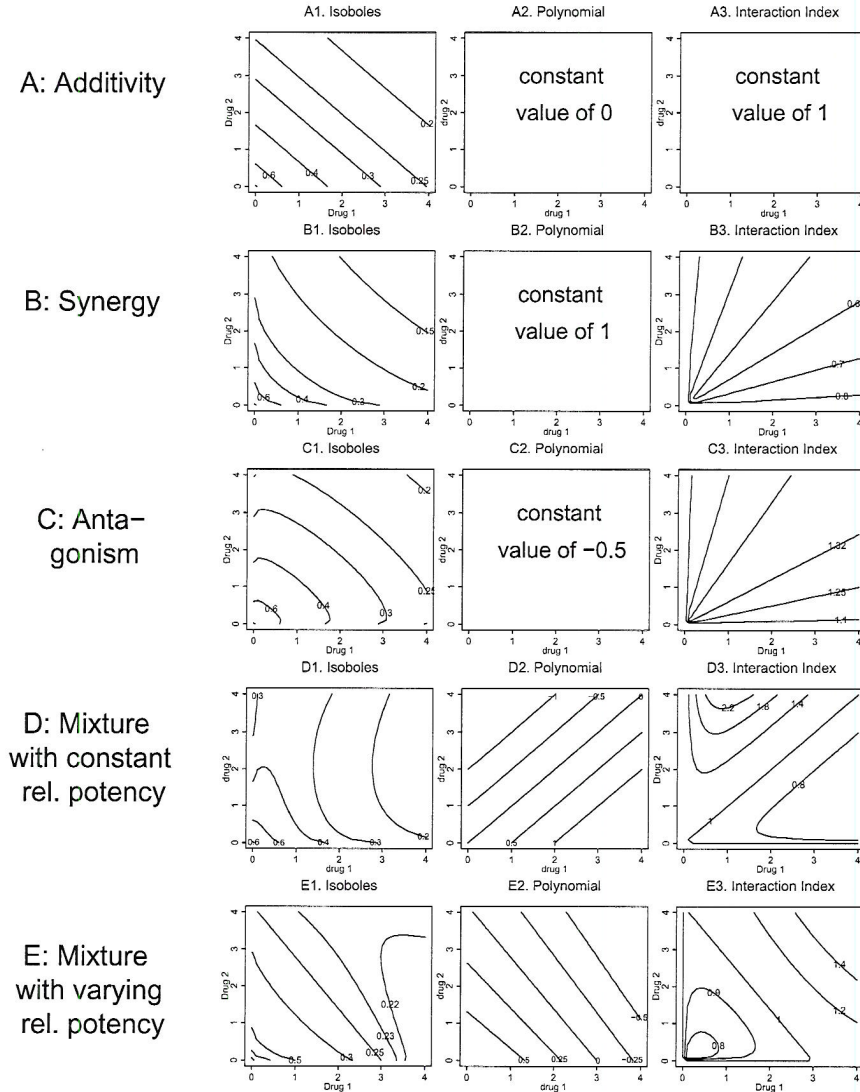


Figure 2. Contour plots of the response surfaces (i.e., isoboles), contour plots of the polynomial function $f(d_1, d_2; \gamma, \kappa)$, and contour plots of the interaction indices under different parameters. For all panels, $\beta_0 = 0$, $\beta_1 = -1$. For panels A, B, and C, $\kappa_0 = 0, 1$, and -0.5 , respectively, while $\gamma_1 = \gamma_2 = 0$, $\kappa_i = 0$ for $i = 1, \dots, 5$. Parameters in panel D are the same as in panel A except $\kappa_3 = 0.5$ and $\kappa_4 = -0.5$. In panel E we set $\gamma_1 = 0.1$, $\gamma_2 = -0.4$, $\kappa_0 = 0.9$, $\kappa_3 = \kappa_4 = -0.3$, and $\kappa_1 = \kappa_2 = \kappa_5 = 0$.

3. Relating the GRS Model to Isoboles and Interaction Indices

Recall that an isobole consists of all the drug combinations which elicit the same effect y . So, each curve in the contour plot of the response surface (9) can be viewed as an isobole. To better understand the proposed GRS model, we examine the relationship between the contour plots of the response surface, the polynomial function, and the interaction index. Chou and Talalay's (1984) median effect equation (2) is used to model the dose–effect curve for each single drug. We begin by taking the simplest case that the two dose–effect curves are the same with the slope being -1 and the median effective dose being 1 , which yields $\beta_0 = \gamma_1 = \gamma_2 = 0$, $\beta_1 = -1$, and $\rho = 1$. In this special case the relative potency is constant, and the model

conforms to equation (6). This model can be represented in the GRS model (9) by taking $\kappa_i = 0$ ($i = 1, \dots, 5$) with different values of κ_0 in $f(d_1, d_2; \gamma, \kappa)$. In Figure 2, panels A, B, and C illustrate the cases for $\kappa_0 = 0, 1, -0.5$, respectively. In panel A, the contour plot of the response surface shows that the isoboles are straight lines (subpanel A1); $f(d_1, d_2; \gamma, \kappa)$ is a constant at 0 (subpanel A2); and the interaction index is a constant at 1 (subpanel A3). All three subpanels indicate that the combination doses are additive. In panel B, the contour plot of the response surface shows that the isoboles are concave down (subpanel B1); $f(d_1, d_2; \gamma, \kappa)$ is a constant at 1 (subpanel B2); and the interaction indices are less than 1 (subpanel B3). All three subpanels indicate that the combination doses are synergistic. Similarly, subpanel C1 shows that the

isoboles are concave up, subpanel C2 shows $f(d_1, d_2; \gamma, \kappa) = -0.5$, and subpanel C3 shows that the interaction indices are greater than 1, indicating that the combination doses are antagonistic. These special cases of our proposed model with $\kappa_i = 0$ ($i = 1, \dots, 5$) use a single parameter κ_0 to capture synergy, additivity, or antagonism and they reduce to Finney's model and Plummer and Short's model. Beyond these three special cases, the proposed model can be used more broadly, in particular when synergy and antagonism appear in different combination doses. We construct a case in panel D by setting $\kappa_0 = \kappa_1 = \kappa_2 = 0$, $\kappa_3 = 0.5$, $\kappa_4 = -0.5$, and $\kappa_5 = 0$, that is, $f(d_1, d_2; \gamma, \kappa) = 0.5d_1 - 0.5d_2$. The contour plot of the response surface is shown in subpanel D1. The contour plot of the polynomial function forms straight lines at a 45° angle (subpanel D2). The diagonal line $0.5d_1 - 0.5d_2 = 0$ separates the space into two parts. In the area below this 45° diagonal line, the polynomial is positive and the interaction index is less than 1 (subpanel D3), indicating that the combination doses in this area are synergistic. On the other hand, in the area above this 45° diagonal line, the polynomial is negative and the interaction index is greater than 1, indicating that the combination doses in this area are antagonistic. Furthermore, to show the varying relative potency, we set $\gamma_1 = 0.1$, $\gamma_2 = -0.4$ with $\kappa_0 = 0.9$, $\kappa_3 = -0.3$, and $\kappa_4 = -0.3$ (panel E). The isobole with effect level 0.25 is a straight line (subpanel E1), the corresponding polynomial is a constant at 0 (subpanel E2), and the interaction index is a constant at 1 (subpanel E3), indicating that all the combination doses on this line are additive. The isoboles with effect levels greater than 0.25 are concave down, the corresponding polynomial is positive, and the interaction index is less than 1, indicating that the combination doses in these regions are synergistic. In contrast, the isoboles with effect levels less than 0.25 are concave up, the corresponding polynomial is negative, and the interaction index is greater than 1, indicating that the combination doses in the other areas are antagonistic.

4. Statistical Consideration of the GRS Model

First we may consider whether the new model (9)-(10) provides a significant improvement of Plummer and Short's model by testing $H_0: \kappa_1 = \kappa_2 = \kappa_3 = \kappa_4 = \kappa_5 = 0$ against $H_1: \kappa_i \neq 0$ for any i ($i = 1, \dots, 5$) using the F -statistics (Gallant, 1987):

$$F = \frac{(RSS_{P-S} - RSS_{full})/q}{RSS_{full}/(n-p)} \quad (12)$$

with $q = 5$ and $n - p$ degrees of freedom. Here n is the number of observations and $p = 10$ is the number of parameters in model (9)-(10). RSS_{full} is the residual sum of squares of our GRS model, and RSS_{P-S} is the residual sum of squares of Plummer and Short's model. Rejecting H_0 suggests that Plummer and Short's model does not provide adequate fit to the data. On the other hand, failing to reject H_0 suggests that Plummer and Short's model is sufficient and there is no need to add more terms to the model. Note that the F -test requires that the responses on Y -scale are normally distributed. One should check the normality assumption, for example, applying the Q-Q plot to the residuals to examine whether the assumption is reasonable. If not, proper transformation should be sought.

The true model may include only a few terms in the GRS model (9)-(10). To avoid overparameterization, we remove the unnecessary terms by using the Akaike information criterion (AIC) (Venables and Ripley, 2002) and a backward elimination procedure. For the backward elimination procedure, a constraint is added that no lower-order terms can be removed until after the corresponding higher-order terms are removed. Here, $AIC = -2 \times \text{maximized log likelihood} + 2p$, which can be written as $AIC = n\log(RSS/n) + 2p + C(n)$ under the normality assumption for the response Y . For a data set, the number of observations, n , remains constant, so, comparing AIC values under different parameterization is the same as comparing the sum of the first two terms, which is referred to as AIC later. To remove the unnecessary terms, we first fit the full model, calculate AIC, and then remove the parameter with the smallest absolute t -value among γ , β , and the higher-order terms of κ 's in f if the parameter has a p -value greater than the level of significance α , say, $\alpha = 0.10$ (Hocking, 1976). We repeat the procedure, refit the reduced model, calculate the AIC for the reduced model, and check the t -values until either all the remaining parameters among γ , β , and the higher-order terms κ 's in f have p -values smaller than α or when the AIC value increases.

As described in Section 3, the different patterns of drug interactions could be detected by observing the sign and magnitude of the polynomial function $f(d_1, d_2; \gamma, \kappa)$. Because the parameters γ and κ in the polynomial are estimated, their asymptotic properties follow the standard results from a nonlinear regression. For each combination dose (d_1, d_2) , the variance of the estimated polynomial $f(d_1, d_2; \gamma, \kappa)$ can be approximated by $\widehat{\text{Var}}_f = (\frac{\partial f}{\partial(\gamma, \kappa)})' \Sigma (\frac{\partial f}{\partial(\gamma, \kappa)})|_{(\gamma, \kappa) = (\hat{\gamma}, \hat{\kappa})}$, where

$$\begin{aligned} \frac{\partial f}{\partial(\gamma, \kappa)} &= \left(\frac{\partial f}{\partial\gamma_1}, \frac{\partial f}{\partial\gamma_2}, \frac{\partial f}{\partial\kappa_0}, \frac{\partial f}{\partial\kappa_1}, \frac{\partial f}{\partial\kappa_2}, \frac{\partial f}{\partial\kappa_3}, \frac{\partial f}{\partial\kappa_4}, \frac{\partial f}{\partial\kappa_5} \right)' \\ &= \left(\frac{\partial f}{\partial\rho} \frac{\partial\rho}{\partial\gamma_1}, \frac{\partial f}{\partial\rho} \frac{\partial\rho}{\partial\gamma_2}, 1, d_1^{\frac{1}{2}}, (\rho d_2)^{\frac{1}{2}}, d_1, \rho d_2, (d_1 \rho d_2)^{\frac{1}{2}} \right)' \end{aligned}$$

with $\frac{\partial f}{\partial\rho} = \frac{1}{2}\kappa_2(\frac{d_2}{\rho})^{\frac{1}{2}} + \kappa_4 d_2 + \frac{1}{2}\kappa_5(\frac{d_1 d_2}{\rho})^{\frac{1}{2}}, \frac{\partial\rho}{\partial\gamma_1} = \frac{\rho^2(d_2 + d_1 \rho^{-1})}{\rho(d_2 + d_1 \rho^{-1}) + \gamma_2 d_1},$ and $\frac{\partial\rho}{\partial\gamma_2} = \frac{\rho^2(d_2 + d_1 \rho^{-1})}{\rho(d_2 + d_1 \rho^{-1}) + \gamma_2 d_1} \log(d_2 + d_1 \rho^{-1})$. Σ is the estimated covariance matrix of the parameters ($\gamma_1, \gamma_2, \kappa_0, \kappa_1, \kappa_2, \kappa_3, \kappa_4, \kappa_5$). Thus, we may construct $(1 - \alpha) \times 100\%$ lower and upper confidence surfaces for $f(d_1, d_2; \gamma, \kappa)$:

$$f_{l,u}(d_1, d_2) = \hat{f}(d_1, d_2) \mp t_{\frac{\alpha}{2}, n-p} \sqrt{\widehat{\text{Var}}_f(d_1, d_2)},$$

where $t_{\frac{\alpha}{2}, n-p}$ is the upper $\frac{\alpha}{2}$ percentile of a t -distribution with $n - p$ degrees of freedom. The intercepts of the lower and upper confidence surfaces of $f(d_1, d_2; \gamma, \kappa)$ with the dose plane form a bound which embraces the curve $f(d_1, d_2; \gamma, \kappa) = 0$. The combination doses beyond the bound with positive polynomial values are synergistic. Conversely, the combination doses beyond the other side of the bound with negative polynomial values are antagonistic. Inside the bound, the drug combinations are considered additive because the responses are not significantly different from the predicted effect based on the additive model. When the final model is a subset of the full model, a similar approach can be used to construct the confidence bound for $f(d_1, d_2; \gamma, \kappa) = 0$ in the final model.

Table 1
Simulation results from fitting the full model and the true model with $\sigma = 0.1$

Parameters	True value	Set 1						Set 2					
		Full model			True model			Full model			True model		
		Est.	SE	CR	Est.	SE	CR	Est.	SE	CR	Est.	SE	CR
β_0	0	0.002	0.044	0.950				0	0.002	0.043	0.957		
β_1	-1	-0.999	0.034	0.951	-1.000	0.020	0.954	-1.0	-0.999	0.033	0.956	-0.999	0.031
γ_1	0	0.002	0.062	0.957				0.1	0.102	0.062	0.958	0.100	0.041
γ_2	0	0.002	0.046	0.952				-0.3	-0.299	0.040	0.955	-0.299	0.038
κ_0	0	0.003	0.324	0.946				0.9	0.901	0.553	0.953	0.900	0.138
κ_1	0	-0.001	0.478	0.956				0	0.018	0.577	0.952		
κ_2	0	0.004	0.499	0.942				0	0	0.850	0.948		
κ_3	0.5	0.515	0.227	0.946	0.502	0.049	0.944	-0.3	-0.298	0.195	0.958	-0.298	0.047
κ_4	-0.5	-0.500	0.188	0.933	-0.500	0.022	0.963	-0.3	-0.293	0.366	0.958	-0.297	0.063
κ_5	0	-0.013	0.236	0.953				0	-0.017	0.312	0.950		

Est. = parameter estimate; SE = standard error; CR = coverage rate.

In medical research and its applications, the inferences should be made considering both clinical and statistical significance. Although the above inferences on synergy and antagonism are primarily based on statistical significance, the importance of clinical significance, that is, the magnitude of drug interaction to be considered clinically meaningful, should also be considered. Chou and Hayball (1996) recommended that the synergy, antagonism, and additivity at a combination dose should be made based on whether interaction index at this combination is less than 0.9, greater than 1.1, or in between. Our method provides a more rigorous way to assess statistical significance and also provides a venue for gauging the magnitude of clinical significance.

5. Simulation and Data Analysis

5.1 Simulation

We performed simulation studies to examine the finite-sample properties of the estimates of the proposed model. We took two sets of parameters, as shown in Figure 2, panel D (set 1) and panel E (set 2). The corresponding response surface models are

$$\begin{aligned} \text{Set 1: } Y &= \log \frac{E}{1-E} \\ &= -\log(d_1 + d_2 + (0.5d_1 - 0.5d_2)(d_1d_2)^{\frac{1}{2}}) + \epsilon \end{aligned}$$

and

$$\begin{aligned} \text{Set 2: } Y &= \log \frac{E}{1-E} \\ &= -\log(d_1 + \rho d_2) \\ &\quad + (0.9 - 0.3d_1 - 0.3\rho d_2)(d_1\rho d_2)^{\frac{1}{2}} + \epsilon \end{aligned}$$

with $\rho = \exp(0.1 - 0.3 \log D_2)$, where $\epsilon \sim N(0, \sigma^2)$. For each model we generated 1000 random samples with $\sigma = 0.1$, and d_1 and d_2 taking values among $(0, 0.1, 0.5, 1, 2, 4)$. The sample size in each simulation run was $6 \times 6 = 36$. We fitted each random sample to the full model and then the true model (i.e., only fitting the nonzero parameters), and obtained the estimated parameters and their corresponding standard errors

(SE). For each parameter, we constructed the 95% confidence interval and observed whether the true parameter lies in the confidence interval. We report the averages of the estimated parameters, SE, and the coverage rate of the confidence intervals for the 1000 random samples in Table 1. We conclude that (1) the parameters are very well estimated; (2) the coverage rates are close to the nominal 95% coverage; (3) in the full model, the standard errors of β_0 , β_1 , γ_1 , and γ_2 are close to half of $\sigma (= 0.1)$, while the SE of κ_i ($i = 0, \dots, 5$) are two- to eightfold of σ . In the true model, the standard errors for β 's, γ 's, and κ 's are all with similar magnitude, ranging from 0.020 to 0.063 with an exception of κ_0 in set 2 (SE = 0.138). These facts reflect that including unnecessary parameters increases the uncertainty of estimating all parameters, especially those in the quadratic function f . Therefore, it is important to develop an appropriate procedure to remove unnecessary parameters. A parsimonious model can increase the accuracy of the estimated parameters; hence, it provides a better estimator for the dose-response relationship.

We also performed simulated case studies to examine whether the estimation and the backward elimination procedure described in Section 4 can recover the true dose-response function, that is, all the zero parameters are removed, the 95% confidence bounds for $f = 0$ have proper coverage rates, and the contours of the fitted response surfaces are similar to the underlying response surface. These simulations showed that the estimation and the backward elimination procedure work well (data not shown).

5.2 Data Analysis

We analyzed data sets from cell lines in a study conducted by Dr. Reuben Lotan and his colleagues at M. D. Anderson Cancer Center. The study aimed to evaluate the efficacy of combination therapy with two novel agents, SCH66336 and 4-HPR, in a number of squamous cell carcinoma cell lines (unpublished data). Cell lines of human squamous cell carcinoma were treated with SCH66336 and 4-HPR separately and in combination. After 6 hours, the proportions of surviving cells were calculated. To illustrate, we present the results for the cell line UMSCC22B, after treating with SCH66336 at

Table 2

Fractions of cells surviving (UMSCC22B) treated by single and combination doses of SCH66336 and 4-HPR

SCH66336 dose (μM)	4-HPR dose (μM)				
	0	0.1	0.5	1	2
0	1	0.7666	0.5833	0.5706	0.4934
0.1	0.6701	0.6539	0.4767	0.5171	0.3923
0.5	0.6289	0.6005	0.4919	0.4625	0.3402
1	0.5577	0.5102	0.4541	0.3551	0.2851
2	0.455	0.4203	0.3441	0.3082	0.2341
4	0.3755	0.3196	0.2978	0.2502	0.1578

doses ranging from 0 to 4 μM and 4-HPR at doses ranging from 0 to 2 μM , alone and in combination, respectively. The corresponding fractions of cells surviving at each combination dose are shown in Table 2.

We analyzed these data sets using different methods. We calculated the interaction indices and their associated confidence intervals at the combination doses at the fixed ratio 1:1 by first fitting the respective dose–effect curves for SCH66336 and 4-HPR. We concluded that the combination doses (0.1, 0.1) and (0.5, 0.5) are additive, and the combination doses (1, 1) and (2, 2) are synergistic. The contour plot of the raw data is shown in Figure 3, panel A. Based on Plummer and Short's

model, the combinations are synergistic ($\hat{\kappa} = 2.146$ with $\text{SE} = 1.102$). The contour plot, interaction indices, and residual plot of the fitted response surface of Plummer and Short's model are shown in Figure 3, panels B1, B2, and B3, respectively. The contour plot in panel B1 differs from the raw data contour plot in panel A. We fitted the data to our proposed full model, and found that the contour plot of the fitted response surface (panel C1) is more similar to the raw data contour plot. The contour plot of the polynomial function $f(d_1, d_2; \gamma, \kappa)$ is shown in panel C2, where the dotted curve is the upper boundary of the 95% confidence bound for $f(d_1, d_2; \gamma, \kappa) = 0$, and the lower boundary is below the illustrated region. The combination doses above the dotted line are synergistic. Panel C3 shows the contour plot of the interaction indices, and panel C4 shows the residual plot of the full model. We used the aforementioned backward elimination procedure with an order constraint to remove γ_2 , κ_4 , and β_0 sequentially, and the corresponding AIC values were -106.28 , -106.39 , and -106.72 , respectively. The backward elimination procedure stopped when AIC increased. The results of the final model are shown in panels D1–D4. Panel D2 shows that the combination doses above the confidence bound are synergistic, inside the bound are additive, and below the bound are antagonistic. The residual plots show that the full model (panel C4) and the final model (panel D4) provide better fit for the data than Plummer and Short's model

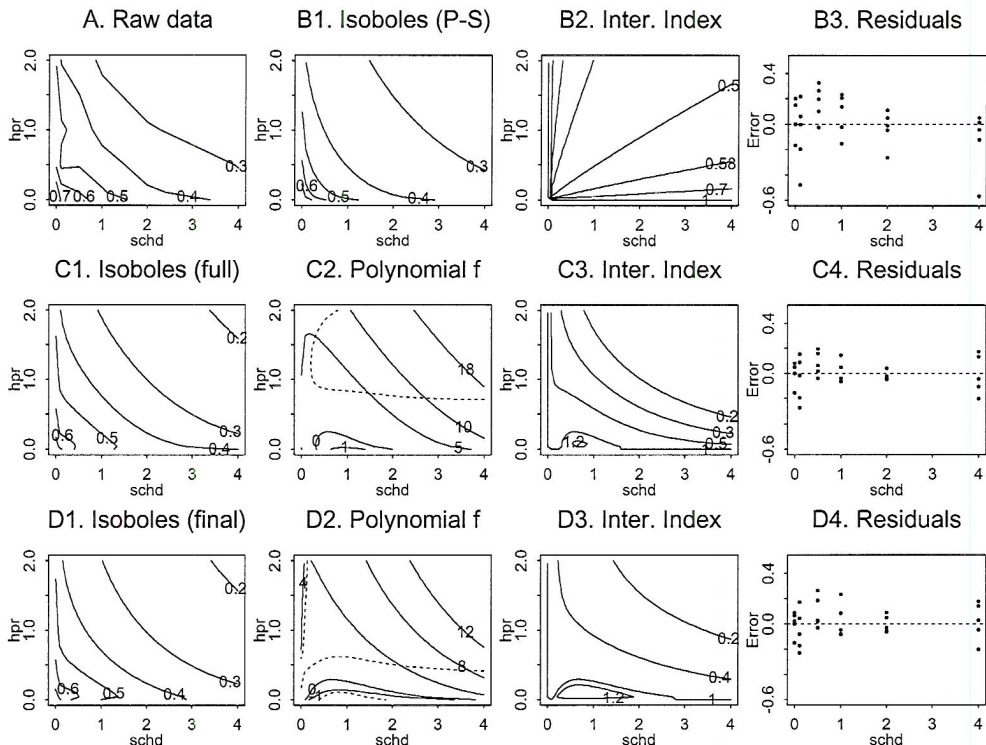


Figure 3. Results for cell line UMSCC22B: panel A is the contour plot of the raw data; panels B1–B3 show the results from Plummer and Short's model; panels C1–C4 show the results from the proposed full model; panels D1–D4 show the results from the final model. The dotted line in panel C2 is the upper boundary of the 95% confidence bound for $f(d_1, d_2; \gamma, \kappa) = 0$, and the lower boundary is out of the dose range. The two dotted lines in panel D2 are the two boundaries of a 95% confidence bound for $f(d_1, d_2; \gamma, \kappa) = 0$.

Table 3
The estimated parameters and their standard errors of different models for the data set shown in Table 2

		β_0	β_1	γ_1	γ_2	κ_0	κ_1	κ_2	κ_3	κ_4	κ_5	RSE
P-S model	Est.	0.099	-0.473	-0.083	0.120	2.146						0.227
	SE	0.093	0.062	0.292	0.259	1.102						
Full model	Est.	0.088	-0.354	-0.339	0.148	5.735	-14.104	-5.539	7.114	5.283	7.021	0.143
	SE	0.064	0.046	0.289	0.242	3.510	6.668	8.230	3.743	6.593	5.446	
Final model	Est.		-0.384	-0.575		3.220	-12.368	1.195	5.492		8.250	0.143
	SE		0.035	0.212		2.268	5.169	3.672	2.682		5.126	

P-S model = Plummer and Short's model; Est. = parameter estimate; SE = standard error; RSE = residual standard error.

(panel B3). The results from the final model are consistent with the results achieved by directly calculating the interaction indices and their associated confidence intervals.

In this example, $\text{RSS}_{\text{P-S}} = 1.238$, $\text{RSS}_{\text{full}} = 0.390$, and $n = 29$ (the model automatically assumed the fraction of cell survival being 1 at the combination dose $d_1 = d_2 = 0$ and this observation did not participate in the calculation). The Q-Q plots (not shown) indicated that the normality holds for the responses on Y -scale, therefore the F -test can be carried out. The F -statistic was 8.250 with degrees of freedom (5, 19), corresponding to $p < 0.003$. Hence, we rejected H_0 at $\alpha = 0.05$, that is, the new model (9)-(10) provides a significant improvement of Plummer and Short's model. The estimated parameters and their standard errors for Plummer and Short's model, the full model, and the final model are listed in Table 3. The residual standard error (RSE), which is an estimate of σ , is shown in the last column in Table 3 for each model. Figure 3 and Table 3 indicate that the final model fits the data as well as the full model, and the precisions on parameter estimation in the final model were improved over the full model. We conclude that the proposed model and procedure work well for this data set.

6. Discussion and Further Extension

One important contribution of this article is that the proposed model can incorporate varying relative potency. Although varying relative potency has been investigated by Tallarida (2000) and Grabovsky and Tallarida (2004), their interpretations resulted in inconsistent predicted additive effects for combination doses (Jonker et al., 2005). In the Appendix, we expound a method to correctly incorporate varying relative potency to predict the additive effect based on the Loewe additivity model. Using the proposed varying relative potency formulation, one can extend the additive response surface for k ($k \geq 2$) drug combinations as follows:

$$Y = \beta_0 + \beta_1 \log(d_1 + \rho_2 d_2 + \cdots + \rho_k d_k), \quad (13)$$

where $\rho_i = \exp(\gamma_{i0} + \gamma_{i1} \log D_1)$ ($i = 2, \dots, k$) is the relative potency of drug i versus drug 1, and D_1 is the amount of drug 1 having an equivalent effect to that of the combination (d_1, \dots, d_k) under the additive assumption. D_1 can be obtained by solving the following equation:

$$d_1 + \rho_2 d_2 + \cdots + \rho_k d_k = D_1.$$

Here γ_{i0} and γ_{i1} are uniquely determined by the two dose-effect curves for drug 1 and drug i ($i = 2, \dots, k$). The additive response surface model constructed this way is consistent with the Loewe additivity model.

In this article, we assume that the effect or transformed effect has a linear relationship with $\log d$. Although a broad class of dose-effect models satisfies this assumption, there are still some exceptions. One important exception is that the logit transform of the effect has a linear relationship with the dose, say $\log \frac{E}{1-E} = \alpha_0 + \alpha_1 d$. In that case, the relative potency for the two drugs is constant, and the additive response for the two drugs can be predicted by $\log \frac{E}{1-E} = \alpha_0 + \alpha_1 d_1 + \alpha_2 d_2$ (Carter et al., 1988). One can still use a quadratic function of d_1 and d_2 to detect different patterns of drug interactions by adding the product of the quadratic function and $(d_1 d_2)^{\frac{1}{2}}$ to the above model.

Suhnel (1990) used bivariate splines to fit dose-response data. The determination of drug interaction was based on the visualization of whether the contours of the response surface (i.e., isoboles) were concave up or concave down. The approach did not give any summary measure on drug interaction. Kelly and Rice (1990) used a monotone spline-based procedure to fit marginal dose-response curves first, then predicted the additive effect of the combination dose based on the Loewe additivity model. Extrapolation beyond the observed dose range is dangerous in this spline-based approach and, therefore, this approach has limited usage. Tan et al. (2003) proposed an optimal experimental design in the sense that it reduces the variability in modeling synergy while allocating the doses to minimize the sample size and to extract maximum information on the joint action of the compounds. The method uses a nonparametric function to detect drug interactions. Semiparametric approaches, as the format (9) or the format given by Tan et al. (2003), which combine parametric marginal dose-response curves with a nonparametric function to detect different patterns of drug interaction, provide logical extension to the current model and are appropriate topics for future research.

ACKNOWLEDGEMENTS

This research was supported in part by grants from the National Cancer Institute CA16672, CA97007, and CA91844, and the Department of Defense W81XWH-04-1-0142 and W81XWH-05-2-0027. The authors are thankful to the reviewers for their constructive comments, to Dr Reuben Lotan for providing the data, and to Lee Ann Chastain for editorial assistance.

REFERENCES

Berenbaum, M. C. (1989). What is synergy? *Pharmacological Reviews* **41**, 93–141.

Carter, W. H., Jr., Gennings, C., Staniswalis, J. G., Cambell, E. D., and White, K. L., Jr. (1988). A statistical approach to the construction and analysis of isobolograms. *Journal of American College Toxicology* **7**, 963–973.

Chou, T. C. and Hayball, M. (1996). *CalcuSyn for Windows: Multiple-Drug Dose-Effect Analyzer and Manual*. Cambridge, U.K.: Biosoft.

Chou, T. C. and Talalay, P. (1984). Quantitative analysis of dose-effect relationships: The combined effects of multiple drugs or enzyme inhibitors. *Advances in Enzyme Regulation* **22**, 27–55.

Finney, D. J. (1971). *Probit Analysis*. Cambridge, U.K.: Cambridge University Press.

Gallant, A. R. (1987). *Nonlinear Statistical Models*. New York: Wiley.

Govindarajulu, Z. (2001). *Statistical Techniques in Bioassay*. Basel: Karger.

Grabovsky, Y. and Tallarida, R. J. (2004). Isobolographic analysis for combinations of a full and partial agonist: Curved isoboles. *Journal of Pharmacology and Experimental Therapeutics* **310**, 981–986.

Greco, W. R., Park, H. S., and Rustum, Y. M. (1990). Application of a new approach for the quantitation of drug synergy to the combination of cis-diamminedichloroplatinum and 1- β -D-arabinofuranosylcytosine. *Cancer Research* **50**, 5318–5327.

Greco, W. R., Bravo, G., and Parsons, J. C. (1995). The search of synergy: A critical review from a response surface perspective. *Pharmacological Reviews* **47**, 331–385.

Hocking, R. R. (1976). The analysis and selection of variables in linear regression. *Biometrics* **32**, 1–49.

Jonker, D. M., Visser, S. A. G., Van der Graaf, P. H., Voskuyl, R. A., and Danhof, M. (2005). Towards a mechanism-based analysis of pharmacodynamic drug-drug interactions in vivo. *Pharmacology and Therapeutics* **106**, 1–18.

Kelly, C. and Rice, J. (1990). Monotone smoothing with application to dose-response curves and the assessment of synergism. *Biometrics* **46**, 1071–1085.

Loewe, S. and Muischnek, H. (1926). Effect of combinations: Mathematical basis of problem. *Archives of Experimental Pathology and Pharmacology* **11**, 313–326.

Plummer, J. L. and Short, T. G. (1990). Statistical modeling of the effects of drug combinations. *Journal of Pharmacological Methods* **23**, 297–309.

Savelev, S., Okello, E., Perry, N. S. L., Wilkins, R. M., and Perry, E. K. (2003). Synergistic and antagonistic interactions of anticholinesterase terpenoids in *Salvia lavandulaefolia* essential oil. *Pharmacology, Biochemistry and Behavior* **75**, 661–668.

Suhnel, J. (1990). Evaluation of synergism or antagonism for the combined action of antiviral agents. *Antiviral Research* **13**, 23–40.

Suhnel, J. (1998). Parallel dose-response curves in combination experiments. *Bulletin of Mathematical Biology* **60**, 197–213.

Tallarida, R. J. (2000). *Drug Synergy and Dose-Effect Data Analysis*. Boca Raton, Florida: Chapman Hall/CRC Press.

Tan, M., Fang, H., Tian, G., and Houghton, P. J. (2003). Experimental design and sample size determination for testing synergism in drug combination studies based on uniform measures. *Statistics in Medicine* **22**, 2091–2100.

Venables, W. N. and Ripley, B. D. (2002). *Modern Applied Statistics with S*, 4th edition. New York: Springer-Verlag.

White, D. B., Faessel, H. M., Slocum, H. K., Khinkis, L., and Greco, W. R. (2004). Nonlinear response surface and mixture experiment methodologies applied to the study of synergy. *Biometrical Journal* **46**, 56–71.

Received July 2005. Revised February 2006.

Accepted February 2006.

APPENDIX

Varying Relative Potency and Its Application

Figure 1, panel A shows that for each fixed effect y , as long as the dose-effect curves for each drug are known, $D_{y,1}$ and $D_{y,2}$ will be known and fixed, thus the relative potency defined by $\frac{D_{y,1}}{D_{y,2}}$ is fixed. Any combination dose (d_1, d_2) on the line \overline{PQ} connecting $P = (D_{y,1}, 0)$ and $Q = (0, D_{y,2})$ has the same relative potency, and d_2 units of drug 2 is equivalent to $\rho(y)d_2$ units of drug 1. Therefore the combination dose (d_1, d_2) is equivalent to $d_1 + \rho(y)d_2$ units of drug 1, which is exactly $D_{y,1}$, and the predicted effect is $F_1(d_1 + \rho(y)d_2)$, which is $F_1(D_{y,1})$. Similarly, for any combination dose (d_1, d_2) on the line \overline{PQ} , d_1 units of drug 1 is equivalent to $\rho(y)^{-1}d_1$ units of drug 2, thus the combination dose (d_1, d_2) is equivalent to $\rho(y)^{-1}d_1 + d_2$ units of drug 2, which is $D_{y,2}$. Consequently, the predicted effect is $F_2(\rho^{-1}(y)d_1 + d_2)$, that is, $F_2(D_{y,2})$. Hence, the predicted effect either by $F_1(d_1 + \rho(y)d_2)$ or by $F_2(\rho(y)^{-1}d_1 + d_2)$ is the same.

We then pay special attention to the fact that, for a given dose d_2 of drug 2, its equivalent amount of drug 1 may be different depending on the existing amount of drug 1 due to a varying relative potency. For example, suppose from the two marginal dose-effect curves we learn that the effects of drug 1 at doses $D_{y,1}$, d_1 , and $D_{y'',1}$ are the same as the effects of drug 2 at doses $D_{y,2}$, $D_{y',2}$, and d_2 , respectively. When two drugs are used, the three corresponding additive isoboles (Figure 1, panel B) are \overline{PQ} connecting $P = (D_{y,1}, 0)$ and $Q = (0, D_{y,2})$, \overline{RS} connecting $R = (d_1, 0)$ and $S = (0, D_{y',2})$, and \overline{TU} connecting $T = (D_{y'',1}, 0)$ and $U = (0, d_2)$. All the combinations on \overline{PQ} share the relative potency $\rho(y)$, all the combinations on \overline{RS} share the relative potency $\rho(y')$, and all the combinations on \overline{TU} share the relative potency $\rho(y'')$. Thus, in terms of drug 1 the equivalent dose of d_2 in the combinations (d_1, d_2) , (d'_1, d_2) , and $(0, d_2)$ will be $\rho(y)d_2$, $\rho(y')d_2$, and $\rho(y'')d_2$, which can be illustrated by the length of \overline{RP} , \overline{VR} , and \overline{OT} , respectively. Here $y = F_1(D_{y,1}) = F_2(D_{y,2})$, $y' = F_1(d_1)$, and $y'' = F_2(d_2)$. Grabovsky and Tallarida (2004) proposed a model to

incorporate the varying relative potency, but they interpret the relative potency as $\rho(y'')$ at all three combinations, namely, (d_1, d_2) , (d'_1, d_2) , and $(0, d_2)$. Consequently, the equivalent amount of drug 1 will be the dose of drug 1 plus $\rho(y'')d_2$ no matter the dose of drug 1. Their interpretation may result in two inconsistent additive effects, say $F_1(d_1 + \rho(y'')d_2)$ and

$F_2(\rho(y')^{-1}d_1 + d_2)$ (Jonker et al., 2005), and curved additive isoboles (Grabovsky and Tallarida, 2004). Therefore, their approach is questionable. On the other hand, when combinations of two drugs are additive with varying relative potency, our formulation shows straight line isoboles, which are consistent with the Loewe additivity model.

Correlation between VEGF/VEGFR2 and EGFR immunohistochemical protein expression in early stage non-small cell lung carcinoma.

Erminia Massarelli, Maria L. Prudkin Silva, Natalie Ozburn, Lei Feng, Guoshen Yin, Michael O'Reilly, Waun Ki Hong, Roy S. Herbst, Ignacio I. Wistuba

Several lines of evidence indicate that activation of Vascular Endothelial Growth Factor Receptor (VEGFR) and Epidermal Growth Factor Receptor (EGFR) pathways are critical for non-small cell lung cancer (NSCLC) development, growth and progression. Despite the availability of new biological compounds targeting both signaling pathways in NSCLC, data about the co-expression of these two pathways in a large cohort of NSCLC tumor samples are not available. To better understand the correlation between VEGFR and EGFR pathways expression, we investigated in a large series of surgically resected NSCLC tumor tissues placed in tissue microarrays the tumor immunohistochemical (IHC) protein expression of: VEGF-A, VEGF-R2, p-VEGF-R2 (phosphorylated VEGF-R2), EGFR and p-EGFR (phosphorylated EGFR). Correlations between VEGF-A, VEGFR2, p-VEGFR2 and clinicopathologic information and survival analysis were examined. In a subset of NSCLCs with adenocarcinoma histology, mutation status of EGFR and KRAS genes was correlated with IHC expression. Two hundred eighty-four surgically resected tumors, including 179 adenocarcinomas and 105 squamous cell carcinomas from patients with stage I-II-IIIA NSCLC were studied. A semi-quantitative analysis of nuclear, cytoplasmic and membranous localization of IHC expression was performed for each marker. Lung adenocarcinomas demonstrated higher expression of cytoplasmic VEGF-A ($p=0.0001$), membranous ($p=0.005$) and cytoplasmic ($p=0.03$) VEGF-R2, and membranous p-VEGF-R2 ($p=0.0002$) compared to squamous cell carcinomas. Lower VEGF-A ($p=0.0009$), membranous ($p=0.01$) and cytoplasmic VEGF-R2 ($p=0.02$) expression was statistically associated with non-smoking history. With a median follow up of 4.28 years, 91 deaths occurred. Independent of age, histology and stage, cytoplasmic p-VEGF-R2 expression was found to have a prognostic role for worse overall survival ($p=0.01$, HR=1.047, 95%CI=1.01, 1.085). Of interest, significant increase of cytoplasmic and membranous p-EGFR expression was detected in tumors showing higher levels of cytoplasmic VEGF-A ($p=0.01$ and $p=0.0001$, respectively), VEGF-R2 ($p=0.0001$ and $p=0.0001$), and p-VEGF-R2 ($p=0.0001$ and $p=0.0003$). In the 15 EGFR-mutated cases a significant lower membranous VEGF-R2 expression was observed ($p=0.02$). Higher membranous VEGF-R2 expression was observed in the 9 KRAS mutated cases, but this did not reach statistical significance. In summary, our findings indicate that VEGFR and EGFR pathways are positively correlated in early stage NSCLC and IHC expression of p-VEGF-R2 is an indicator of worse overall survival in stage I-IIIA NSCLC.

(Grant IMPACT W81XWH-05-0027).

KRAS Mutation is an Important Predictor of Resistance to Therapy with Epidermal Growth Factor Receptor Tyrosine Kinase Inhibitors in Non-Small Cell Lung Cancer

Erminia Massarelli¹, Marileila Varella-Garcia⁴, Ximing Tang¹, Ana C. Xavier⁴, Natalie C. Ozburn¹, Diane D. Liu², Benjamin N. Bekele², Roy S. Herbst¹, and Ignacio I. Wistuba^{1,3}

From the Departments of ¹Thoracic/Head and Neck Medical Oncology, ²Biostatistics and Applied Mathematics, and ³Pathology, The University of Texas M. D. Anderson Cancer Center, Houston, TX; ⁴University of Colorado Health Sciences Center, Cancer Center, Aurora, CO.

Supported in part by US Department of Defense grant W81XWH-05-2-0027 and Cecily and Robert Harris Foundation National Cancer Institute Cancer Center Support Grant CA-16672.

Correspondence to: Ignacio I. Wistuba, Department of Pathology–Unit 85, M. D. Anderson Cancer Center, 1515 Holcombe Blvd., Houston TX 77030-4009. Tel: (713) 563-9184; Fax: (713) 563-1848. E-mail: iiwistuba@mdanderson.org

Short title: *KRAS Mutation as Predictor of Resistance to EGFR-TKI therapy in NSCLC*

Keywords: *KRAS* mutation, *EGFR* FISH, lung cancer, *EGFR* tyrosine kinase inhibitor, *EGFR* mutation.

ABSTRACT

Purpose

EGFR gene mutations and increased *EGFR* copy number have been associated with favorable response to epidermal growth factor receptor (EGFR) tyrosine kinase inhibitors (EGFR-TKIs) in patients with non-small-cell lung cancer (NSCLC). In contrast, *KRAS* mutation has been shown to predict poor response to such therapy. We tested the utility of combinations of these three markers in predicting response and survival in patients with NSCLC treated with EGFR-TKIs.

Experimental Design

Patients with advanced NSCLC treated with EGFR-TKI with available archival tissue specimens were included. *EGFR* and *KRAS* mutations were analyzed using polymerase chain reaction-based sequencing. *EGFR* copy number was analyzed using fluorescence in situ hybridization.

Results

The study included 73 patients, 59 of whom had all three potential markers successfully analyzed. *EGFR* mutation was detected in 7/71 patients (9.8%), increased *EGFR* copy number in 32/59 (54.2%), and *KRAS* mutation in 16/70 (22.8%). *EGFR* mutation ($P<.0001$) but not increased *EGFR* copy number ($P=.48$) correlated with favorable response. No survival benefit was detected in patients with either of these features. *KRAS* mutation correlated with progressive disease ($P=.04$) and shorter median time to progression ($P=.0025$) but not with survival. Patients with both *EGFR* mutation and increased *EGFR* copy number had a greater than 99.7% chance of objective response,

whereas patients with *KRAS* mutation with or without increased *EGFR* copy number had a larger than 96.5% chance of disease progression.

Conclusion

KRAS mutation should be included as indicator of resistance in the panel of markers used to predict response to EGFR-TKIs in NSCLC.

INTRODUCTION

Lung cancer remains the leading cause of cancer death in the United States and is expected to cause 162,000 deaths in the United States in 2006 (1). Epidermal growth factor receptor (EGFR), a receptor tyrosine kinase is expressed in the majority of non-small cell lung cancers (NSCLC). Gefitinib (ZD1839, Iressa; AstraZeneca, Wilmington, DE) and erlotinib (Tarceva, OSI-774; OSI Pharmaceuticals, New York, NY), small-molecule inhibitors that target the tyrosine kinase domain of the EGFR, produce responses in approximately 10% of patients with NSCLC that has progressed with prior chemotherapy (2-6). In patients with NSCLC who benefit from gefitinib or erlotinib, the responses can be dramatic and may last for longer than a year (2-6).

Several markers have been identified that predict response to the EGFR-specific tyrosine kinase inhibitors (EGFR-TKIs) in patients with NSCLC. Activating mutations in the *EGFR* tyrosine kinase domain (exons 18 to 21), increased *EGFR* copy number, and increased EGFR protein expression have been associated with favorable response to EGFR-TKIs (7-17). In contrast, *KRAS* gene mutation, which occurs in 20% to 30% of NSCLCs, mainly in adenocarcinomas (30%) and smokers, (18) has been reported to be associated with poor response to EGFR-TKIs (19-23).

Studies have also investigated potential markers of survival in patients with NSCLC treated with EGFR-TKIs. Whether activating mutations in the *EGFR* tyrosine kinase domain are associated with a survival advantage from gefitinib or erlotinib, especially in Western populations with NSCLC, is controversial. Several retrospective studies showed prolonged survival in gefitinib-treated patients with tyrosine kinase activating mutations, mostly in Asian populations (8-14), whereas in the BR.21 study, the

hazard ratio for death was almost identical in patients with mutated and wild type *EGFR* (0.73 and 0.77, respectively) (16). *EGFR* increased copy number has been shown to predict favorable survival outcomes after EGFR-TKI therapy (7, 13, 15, 17).

Several studies have shown that *EGFR* mutation and *KRAS* mutation are mutually exclusive (19, 24, 25) and *EGFR* mutation and genomic gain are associated (7), but the relationship between increased *EGFR* copy number and *KRAS* mutation and the effect of this combination on response to EGFR-TKI therapy have not yet been investigated. The purpose of this retrospective study was to investigate the concomitant presence of increased *EGFR* copy number and *KRAS* mutation in tumor specimens from patients with NSCLC and to clarify the predictive value of combinations of *EGFR* mutation status, *EGFR* copy number status, and *KRAS* mutation status in predicting response and survival in patients with NSCLC treated with EGFR-TKIs.

MATERIALS AND METHODS

Patients and Data Collection

Tumor specimens were obtained from patients with advanced NSCLC treated with gefitinib or erlotinib at The University of Texas M. D. Anderson Cancer Center between May 1999 and December 2004. Patients either received gefitinib as part of an extended-access protocol approved by the institutional review board or received gefitinib or erlotinib after the drugs were approved by the United States Food and Drug Administration. Both drugs were administered orally once daily: gefitinib at 250 mg and erlotinib at 150 mg. Only patients with at least four formalin-fixed, paraffin-embedded

tissue sections with at least 1,000 tumor cells per section (necessary for DNA extraction and mutation analyses) were eligible.

This study was approved by the M. D. Anderson Cancer Center. All specimens were histologically classified according to the World Health Organization classification for lung cancer by an experienced thoracic pathologist (I.I.W.) (26). Imaging studies were assessed by a medical oncologist (E.M.), who graded responses according to the Response Evaluation Criteria in Solid Tumors (27). In case of stable disease, measurements had to meet the stable disease criteria at least once after the first evaluation at a minimum interval of 6 to 8 weeks. All the investigators were blinded to patient outcomes.

EGFR and KRAS Mutation Analysis

Exons 18 through 21 of *EGFR* and exon 2 of *KRAS* were polymerase chain reaction (PCR)-amplified using intron-based primers as previously described (25, 28, 29). From microdissected formalin-fixed, paraffin-embedded cells, ~200 cells were used for each PCR amplification, as previously described (29). All PCR products were directly sequenced using the Applied Biosystems PRISM dye terminator cycle sequencing method (Foster City, CA). All sequence variants were confirmed by independent PCR amplifications from at least two independent microdissections and sequenced in both directions.

EGFR Copy Number Analysis

EGFR copy number per cell was investigated using fluorescence in situ hybridization (FISH) performed with the LSI EGFR SpectrumOrange/CEP 7 SpectrumGreen probe (Vysis, Abbott Laboratories, IL) according to a published protocol (7, 30). Serial 5- μ m-thick tissue sections were incubated at 56°C overnight, deparaffinized, and dehydrated in 100% ethanol. After incubation in 2x saline sodium citrate buffer (2x SSC; pH 7.0) at 75°C for 15 to 25 minutes, sections were digested with proteinase K (0.25 mg/mL in 2x SSC; pH 7.0) at 37°C for 15 to 25 minutes, rinsed in 2x SSC (pH 7.0) at room temperature for 5 minutes, and dehydrated using ethanol in increasing concentrations (70%, 85%, and 100%). The EGFR/CEP 7 probe set was applied per the manufacturer's instructions to an area of the slide containing tumor foci, and the hybridization area was covered with a glass coverslip and sealed with rubber cement. The slides were incubated at 80 °C for 8-10 minutes to permit codenaturation of chromosomal and probe DNA and were then placed in a humidified chamber at 37°C and left for 20 to 24 hours to allow hybridization. Posthybridization washes were performed in 1.5 M urea and 0.1x SSC (pH 7.0 to 7.5) at 45°C for 30 minutes and in 2x SSC for 2 minutes at room temperature. After the samples were dehydrated in ethanol, 4',6'-diamidino-2-phenylindole (DAPI; 0.3 mg/mL in Vectashield mounting medium, Vector Laboratories, Burlingame, CA) was applied for chromatin counterstaining.

FISH assessment was performed independently by two authors (M.V.-G. and A.C.X.) who were blinded to the patients' clinical characteristics and all other molecular variables. Patients were classified into six FISH strata, as previously described (7, 30). High polysomy and gene amplification categories were considered to have increased

EGFR copy number, and the categories disomy to low polysomy were considered not to have increased gene copy number.

Statistical Analysis

Data were summarized using standard descriptive statistics and frequency tabulation. Associations between categorical variables were assessed using cross-tabulation, the chi-squared test, and Fisher's exact test. The Kruskal-Wallis test and Wilcoxon rank-sum test were performed to assess differences in continuous variables between clinical-pathologic groups. Logistic regression analysis was applied to estimate the effect of covariates on response (complete response + partial response *vs.* other). Time to disease progression (TTP) and overall survival (OS) were measured for each patient from the first day of treatment with gefitinib or erlotinib. Survival curves were estimated using the Kaplan-Meier method. Univariate and multivariate Cox proportional hazards models were applied to assess the effect of covariates on TTP and OS from the first day of TKI therapy.

One of our interests in this research was in addressing the question, what is the probability that the response rate in the group *i*th is greater than the response rates in all other groups? Bayesian methods provide a natural framework to address the above question. Bayesian methods, unlike classical methods, treat the probability of response as a quantity about which the investigator has some degree of uncertainty. This uncertainty is quantified directly via probability. We assume that the response data for each group follows a binomial distribution. The probability of response in the *i*th group is denoted by p_i . We also assume non-informative the prior distribution for p_i follows a non-informative

beta (0.5,0.5) distribution (for all i). Given these assumptions we now calculate the posterior probability

$$\Pr(p_i > \max(p_1, \dots, p_{i-1}, p_{i+1}, p_M) | Data)$$

The multi-dimensional integration underlying the calculation of this probability statement was performed via Monte Carlo simulation (50,000 interactions).

All computations were carried out in SAS (Cary, NC) or S-plus 2000 (Cambridge, MA).

RESULTS

Patient Population

Seventy-three patients with advanced NSCLC were treated at M. D. Anderson with gefitinib (n= 72) or erlotinib (n= 1) during the study period and had sufficient tissue sections available for DNA extraction and *EGFR* and *KRAS* mutation analyses. However, of those 73 patients, only 59 had enough tumor cells (at least 200) in the remaining tissue sections for FISH analysis. Specimens were obtained prior to the start of TKI therapy in 62 patients and within a median time of 5 months (range 2 to 19 months) after the start of the TKI therapy in 11 patients.

Correlation of *EGFR* and *KRAS* Abnormalities with Patients' Clinical and Pathologic Features

Seventy-one patients were successfully tested for *EGFR* mutation, 59 for *EGFR* gene copy number, and 70 for *KRAS* mutation. Clinical and pathologic characteristics and their correlation with genetic abnormalities are shown in Table 1.

EGFR mutation was identified in 7 (9.8%) of the 71 tested patients. *EGFR* mutations were significantly more frequent in Asian patients ($P = .03$) and patients with better performance status at the beginning of TKI treatment ($P = .01$) (Table 1). Six of the seven patients with *EGFR* mutations had a 15-bp deletion (E746-E750) in exon 19; the other patient had a point mutation in exon 18 (G719A).

EGFR gene copy number analysis revealed one patient (1.7%) with disomy, nine (15.2%) with low trisomy, 17 (28.8%) with low polysomy, 21 (35.6%) with high polysomy, and 11 (18.7%) with gene amplification. Thus, 32 (54.2%) of the 59 patients tested had increased *EGFR* copy number. There was a statistically significant association between increased *EGFR* gene copy number and the presence of brain metastasis at the start of TKI therapy ($P = .02$) (Table 1).

KRAS mutation was identified in 16 (22.8%) of the 70 tested patients. Fourteen patients had a single-amino-acid substitution in codon 12, and 2 patients had a codon 13 mutation.

None of the tumor samples analyzed harbored concomitant *KRAS* and *EGFR* mutation. In the cohort of cases ($n = 59$) analyzed for all three markers, increased *EGFR* copy number was detected in five (83%) of the six *EGFR*-mutant cases and eight (57%) of the 14 *KRAS*-mutant cases.

Correlation of *EGFR* and *KRAS* Abnormalities with Response to EGFR-TKIs

Seven patients (9.6%) had an objective response to TKI therapy (complete response in one and partial response in six), 11 patients (15.1%) had stable disease, and 55 patients (75.3%) had progressive disease. No significant differences in demographic and clinical

characteristics were observed between the different response groups (Table 2). The presence of *EGFR* mutation was significantly associated with objective response to TKI treatment ($P < .0001$) (Table 3). Four (80%) of the five responders with available FISH data had increased *EGFR* copy number, but this finding was not statistically significant (Table 3). The presence of *KRAS* mutation was significantly associated with lack of response to TKI treatment ($P = .04$) (Table 3).

Testing for *EGFR* mutation, *EGFR* copy number, and *KRAS* mutation was performed in 59 patients, and the correlations between genetic alterations and response rate are shown in Table 4. The group of patients with both mutated *EGFR* and increased *EGFR* copy number had the highest response rate (80%), and the probability of having the highest response rate (calculated via Bayesian analysis described in the statistical considerations) was calculated as being greater than 92.6% (if the single patient *EGFR* mutation positive/*EGFR* gene copy number negative/*KRAS* mutation negative is removed this probability increases to 99.7%). In contrast, the group of patients with mutated *KRAS*, independent of the *EGFR* copy number status, had the highest rate of progressive disease (100%), and this group's probability of having the highest progressive-disease rate was calculated as being greater than 96.5% (Table 4).

In the group of eleven cases collected after the *EGFR*-TKI start date, two (18%) patients obtained a partial response, two (18%) patients had stable disease and 7 patients progressed (64%). Of the two cases (18%) with *EGFR* mutation, one had partial response and the other progressive disease. No *KRAS* mutation was detected in the eleven patients. Increased *EGFR* copy number was detected in 6 of the seven (86%) cases tested for the combination of the three markers. Two cases showed both *EGFR* mutation and increased

copy number. When statistical analyses included only the cohort of 62 tumors collected before the EGFR-TKI therapy start date, data previously showed with the larger dataset (n= 73) were largely confirmed. In summary, *EGFR* mutation resulted to be a predictor of best response to *EGFR* TKI treatment ($P= .0001$) and increased gene copy number did not show a statistical association with response ($P= .68$). *KRAS* mutation was borderline associated with poor response ($P= .06$). In the cohort of 52 tumor cases collected before the EGFR-TKI therapy start date cases tested for the combination of the three markers, the group of tumors with mutated *EGFR* and increased *EGFR* copy number (n=3) was confirmed to have the highest response rate (100%), and the probability of having the highest response rate was calculated as being larger than 99.8%. In contrast, the group of patients with mutated *KRAS*, with (n=8) or without (n=6) increased *EGFR* copy number, had the highest rate of progressive disease (100%), and this group's probability of having the highest progressive-disease rate was calculated as being larger than 95%.

Correlation of *EGFR* and *KRAS* Abnormalities with Survival

With a median follow-up of 3.2 years, 57 patients had died, and 72 had experienced disease progression. A trend toward better OS was observed for the patients with mutant *EGFR*, but this did not reach statistical significance (log-rank test, $P = .08$) (Table 3). In the multivariate analysis for OS, age (hazard ratio [HR] = 1.02, $P = .07$), male gender (HR = 1.96, $P = .01$), and performance status ≥ 2 (HR = 1.68, $P = .07$) were important predictors of OS. Median TTP was significantly shorter in the patients with mutated *KRAS* (log-rank test, $P = .0025$, Table 3). Longer median TTP was also observed in patients with mutated *EGFR*, but this finding was not statistically significant (Table 3).

The multivariable Cox model indicated that, adjusted for age (HR = 1.02, $P = .04$), *KRAS* mutation (HR = 2.14, $P = .01$) remained a statistically significant predictor of TTP.

The group of patients with both mutated *EGFR* mutant and increased *EGFR* copy number had the longest TTP, whereas the group of patients with mutated *KRAS* had the shortest TTP (log-rank test, $P = .008$). Similar results were obtained when only patients whose tumor specimens were collected before the start of TKI treatment ($n = 62$) were included in the analysis, and at multivariable Cox model *KRAS* mutation remained a strong predictor of poor TTP (HR=2.45, $P = .004$).

DISCUSSION

In the current study, we found differences in response and outcome in patients with advanced NSCLC treated with EGFR-TKIs by *EGFR* mutation status, *EGFR* copy number, and *KRAS* mutation status. To our knowledge, this is the first study to analyze the combination of *EGFR* mutation, *EGFR* FISH copy number, and *KRAS* mutation in predicting response to EGFR-TKIs.

The frequencies of *EGFR* (9.8%) and *KRAS* (22.8%) mutation, the finding that these mutations were mutually exclusive, and the clinical-pathologic characteristics of the patients in our series are similar to previously published data (21). Our findings that *EGFR* mutations were detected only in adenocarcinomas and were common in Asian patients and never-smokers whereas *KRAS* mutations were identified mostly in adenocarcinomas and were more common in smokers support the notion that there are at least two molecular pathways involved in the pathogenesis of lung adenocarcinoma: a

non-smoking EGFR signaling-associated pathway, and a smoking KRAS signaling-associated pathway (31).

Whereas several recent studies have shown that increased *EGFR* copy number predicts favorable response to and outcome after treatment with EGFR-TKIs in patients with NSCLC (7, 13, 15, 17), *KRAS* mutation is known to predict poor outcome after treatment with EGFR-TKIs in patients with NSCLC (19-23). However, to our knowledge, our study is the first to show that activating *KRAS* mutation overcomes the potential favorable role of increased *EGFR* copy number in predicting response and survival of NSCLC patients after treatment with EGFR-TKIs. In fact, in our study, all sixteen patients with *KRAS* mutations experienced progressive disease as the best response to treatment with EGFR-TKIs, including eight patients whose tumors had increased *EGFR* copy number. The strong association between the presence of *KRAS* mutation and poor response to treatment was also observed when the eleven patients whose specimens tested for the three markers were obtained after the start of TKI therapy (median time of 5 months, range 2 to 19 months) were excluded.

Our findings that *EGFR* mutation was a significant predictor of favorable response to EGFR-TKIs ($P < .0001$) and that *EGFR* mutation was associated with a trend toward longer OS ($P = .08$) (Table 3) are in line with the existing literature (7-17, 32). However, in contrast with previous studies, we did not find significant correlation between *EGFR* copy number and response or outcome in this cohort of patients (15, 17). Interestingly, eight tumors with increased *EGFR* copy number also carried *KRAS* mutation and reported poor response rate (Table 4) and TTP ($P = .008$). Conversely, the group of patients with concomitant *EGFR* mutation and increased *EGFR* copy number

had the longest TTP interval ($P = .008$). This might be due to the association between *EGFR* mutation and increased *EGFR* gene copy number previously described by Cappuzzo et al. (7). In fact, among the five *EGFR*-mutant patients who responded to TKI therapy, four also had increased *EGFR* copy number (two had high polysomy and two had gene amplification). Of the two *EGFR*-mutant patients who did not respond to TKI therapy, one had high polysomy and the other had low polysomy. Another interesting finding is the absence of *EGFR* mutations in tumors from patients who had stable disease (Table 3), three of whom had stable disease for more than 1 year. A similar observation was previously reported by other authors (7) and underscores the importance of defining selection criteria to identify which patients are most likely to benefit from EGFR-TKIs.

In summary, our findings indicate that in patients with NSCLC, *KRAS* mutation is an important predictor of resistance to EGFR-TKIs and should be included in the panel of markers to be used to predict response to such therapy.

REFERENCES

1. Jemal A., Siegel R., Ward E., et al. Cancer statistics, 2006. CA Cancer J Clin, 2006;56: 106-130.
2. Fukuoka M., Yano S., Giaccone G. et al. Multi-institutional randomized phase II trial of gefitinib for previously treated patients with advanced non-small-cell lung cancer (the IDEAL 1 trial). J Clin Oncol, 2003;21: 2237-2246.
3. Kris M. G., Natale R. B., Herbst R. S., et al. Efficacy of gefitinib, an inhibitor of the epidermal growth factor receptor tyrosine kinase, in symptomatic patients with non-small cell lung cancer: a randomized trial. JAMA, 2003;290: 2149-2158.
4. Perez-Soler R., Chachoua A., Hammond L. A., et al. Determinants of tumor response and survival with erlotinib in patients with non--small-cell lung cancer. J Clin Oncol, 2004;22: 3238-3247.
5. Shepherd F. A., Rodrigues Pereira J., Ciuleanu T., et al. Erlotinib in previously treated non-small-cell lung cancer. N Engl J Med, 2005;353: 123-132.
6. Thatcher N., Chang A., Parikh P., Rodrigues Pereira J., et al. Gefitinib plus best supportive care in previously treated patients with refractory advanced non-small-cell lung cancer: results from a randomised, placebo-controlled, multicentre study (Iressa Survival Evaluation in Lung Cancer). Lancet, 2005;366: 1527-1537.
7. Cappuzzo F., Hirsch F. R., Rossi E., et al. Epidermal growth factor receptor gene and protein and gefitinib sensitivity in non-small-cell lung cancer. J Natl Cancer Inst, 2005;97: 643-655.

8. Lynch T. J., Bell D. W., Sordella R., et al. Activating mutations in the epidermal growth factor receptor underlying responsiveness of non-small-cell lung cancer to gefitinib. *N Engl J Med*, 2004;350: 2129-2139.
9. Paez J. G., Janne P. A., Lee J. C., et al. EGFR mutations in lung cancer: correlation with clinical response to gefitinib therapy. *Science*, 2004;304: 1497-1500.
10. Cortes-Funes H., Gomez C., Rosell R., et al. Epidermal growth factor receptor activating mutations in Spanish gefitinib-treated non-small-cell lung cancer patients. *Ann Oncol*, 2005;16: 1081-1086.
11. Han S. W., Kim T. Y., Hwang P. G., et al. Predictive and prognostic impact of epidermal growth factor receptor mutation in non-small-cell lung cancer patients treated with gefitinib. *J Clin Oncol*, 2005;23: 2493-2501.
12. Mitsudomi T., Kosaka T., Endoh H., et al. Mutations of the epidermal growth factor receptor gene predict prolonged survival after gefitinib treatment in patients with non-small-cell lung cancer with postoperative recurrence. *J Clin Oncol*, 2005;23: 2513-2520.
13. Takano T., Ohe Y., Sakamoto H., et al. Epidermal growth factor receptor gene mutations and increased copy numbers predict gefitinib sensitivity in patients with recurrent non-small-cell lung cancer. *J Clin Oncol*, 2005;23: 6829-6837.
14. Taron M., Ichinose Y., Rosell R., et al. Activating mutations in the tyrosine kinase domain of the epidermal growth factor receptor are associated with improved survival in gefitinib-treated chemorefractory lung adenocarcinomas. *Clin Cancer Res*, 2005;11: 5878-5885.

15. Hirsch F. R., Varella-Garcia M., McCoy J., et al. Increased epidermal growth factor receptor gene copy number detected by fluorescence in situ hybridization associates with increased sensitivity to gefitinib in patients with bronchioloalveolar carcinoma subtypes: a Southwest Oncology Group Study. *J Clin Oncol*, 2005;23: 6838-6845.
16. Tsao M. S., Sakurada A., Cutz J. C., et al. Erlotinib in lung cancer - molecular and clinical predictors of outcome. *N Engl J Med*, 2005;353: 133-144.
17. Hirsch F. R., Varella-Garcia M., Bunn P. A., Jr., et al. Molecular predictors of outcome with gefitinib in a phase III placebo-controlled study in advanced non-small-cell lung cancer. *J Clin Oncol*, 2006;24: 5034-5042.
18. Graziano S. L., Gamble G. P., Newman N. B., et al. Prognostic significance of K-ras codon 12 mutations in patients with resected stage I and II non-small-cell lung cancer. *J Clin Oncol*, 1999;17: 668-675.
19. Pao W., Wang T. Y., Riely G. J., et al. KRAS mutations and primary resistance of lung adenocarcinomas to gefitinib or erlotinib. *PLoS Medicine*, 2005;2: e17.
20. Tam I. Y., Chung L. P., Suen W. S., et al. Distinct epidermal growth factor receptor and KRAS mutation patterns in non-small cell lung cancer patients with different tobacco exposure and clinicopathologic features. *Clin Cancer Res*, 2006;12: 1647-1653.
21. Eberhard D. A., Johnson B. E., Amler L. C., et al. Mutations in the epidermal growth factor receptor and in KRAS are predictive and prognostic indicators in patients with non-small-cell lung cancer treated with chemotherapy alone and in combination with erlotinib. *J Clin Oncol*, 2005;23: 5900-5909.

22. Tsao MS, Zhu C., Sakurada A, et al. An analysis of the prognostic and predictive importance of K-ras mutation status in the National Cancer Institute of Canada Clinical Trials Group BR.21 study of erlotinib versus placebo in the treatment of non-small cell lung cancer. *J Clin Oncol*, 2006;24: abstr. 7005.
23. Miller V.A, Zakowski M., Riely G. J., et al. EGFR mutation and copy number, EGFR protein expression and KRAS mutation as predictors of outcome with erlotinib in bronchioloalveolar cell carcinoma (BAC): Results of a prospective phase II trial. *J Clin Oncol*, 2006;24: abstr. 7003.
24. Janne P. A., Engelman J. A., and Johnson B. E. Epidermal growth factor receptor mutations in non-small-cell lung cancer: implications for treatment and tumor biology. *J Clin Oncol*, 2005;23: 3227-3234.
25. Shigematsu H., Lin L., Takahashi T., et al. Clinical and biological features associated with epidermal growth factor receptor gene mutations in lung cancers. *J Natl Cancer Inst*, 2005;97: 339-346.
26. Travis W.D., Brambilla E., Muller-Hermelink H.K. et al. Tumours of the lung. In Travis WD (Ed), *World Health Organization Classification of Tumours: Pathology and Genetics of Tumours of the Lung, Pleura and Heart*, p. 9-124. Lyon, France: IARC Press, 2004.
27. Therasse P., Arbuck S. G., Eisenhauer E. A., et al. New guidelines to evaluate the response to treatment in solid tumors. European Organization for Research and Treatment of Cancer, National Cancer Institute of the United States, National Cancer Institute of Canada. *J Natl Cancer Inst*, 2000;92: 205-216.

28. Amann J., Kalyankrishna S., Massion P. P., et al. Aberrant epidermal growth factor receptor signaling and enhanced sensitivity to EGFR inhibitors in lung cancer. *Cancer Res*, 2005;65: 226-235.
29. Tang X., Shigematsu H., Bekele B. N., et al. EGFR tyrosine kinase domain mutations are detected in histologically normal respiratory epithelium in lung cancer patients. *Cancer Res*, 2005;65: 7568-7572.
30. Varella-Garcia, M. Stratification of non-small cell lung cancer patients for therapy with epidermal growth factor receptor inhibitors: the EGFR fluorescence in situ hybridization assay. *Diagn Pathol*, 2006;1: 19.
31. Gazdar, A. F., Shigematsu, H., Herz, J., and Minna, J. D. Mutations and addiction to EGFR: the Achilles 'heal' of lung cancers? *Trends Mol Med*, 2004;10: 481-486.
32. Sasaki H., Shimizu S., Endo K., et al. EGFR and erbB2 mutation status in Japanese lung cancer patients. *Int J Cancer*, 2006;118: 180-184.

Table 1. EGFR Mutation Status, EGFR Gene Copy Number Status, and KRAS Mutation Status by Patients' Characteristics

Characteristic	EGFR Mutation Status (Tested = 71/73)			EGFR Gene Copy Number Status (Tested = 59/73)			KRAS Mutation Status (Tested = 70/73)		
	Wild-Type (n = 64) N (%)	Mutated (n = 7) N (%)	P*	Not Increased (n = 27) N (%)	Increased (n = 32) N (%)	P*	Wild-Type (n = 54) N (%)	Mutated (n = 16) N (%)	P*
Age, median, years	60	51	.2	64	58	.19	57.5	65	.05
Gender	Female Male	36 (87.8) 28 (93.3)	5 (12.2) 2 (6.7)	.69	18 (54.5) 9 (34.6)	15 (45.5) 17 (65.4)	.19	30 (73.2) 24 (82.8)	11 (26.8) 5 (17.2)
Race	Asian Caucasian Other	4 (57.1) 52 (92.9) 8 (100)	3 (42.9) 4 (7.1) 0 (0)	.03	4 (80.0) 21 (42.9) 2 (40)	1 (20) 28 (57.1) 3 (60)	.34	41 (74.5) 6 (75)	14 (25.5) 2 (25)
Smoking history	Current smoker Former smoker Never smoker	23 (95.8) 28 (93.3) 13 (76.5)	1 (4.2) 2 (6.7) 4 (23.5)	.15	10 (50) 9 (34.6) 8 (61.5)	10 (50) 17 (65.4) 5 (38.5)	.28	18 (78.3) 20 (66.7) 16 (94.1)	5 (21.7) 10 (33.3) 1 (5.9)
Histology	Adenocarcinoma NSCLC Squamous cell Ca	40 (85.1) 13 (100) 11 (100)	7 (14.9) 0 0	.22	17 (43.6) 5 (55.6) 5 (45.5)	22 (56.4) 4 (44.4) 6 (54.5)	.93	34 (72.3) 9 (75) 11 (100)	13 (27.7) 3 (25) 0
PS (ECOG)†	0-1 2-3	32 (82.1) 32 (100)	7 (17.9) 0	.01	14 (43.8) 13 (48.1)	18 (56.3) 14 (51.9)	.8	31 (81.6) 23 (71.9)	7 (18.4) 9 (28.1)
Stage†	IIIB IV	5 (100) 59 (89.4)	0 7 (10.6)	1.0	3 (75) 24 (43.6)	1 (25) 31 (56.4)	.32	5 (100) 49 (75.4)	0 16 (24.6)
Previous chemotherapy regimens †	0 1 ≥2	10 (90.9) 23 (92) 31 (88.6)	1 (9.1) 2 (8) 4 (11.4)	1.0	6 (54.5) 11 (55) 10 (35.7)	5 (45.5) 9 (45) 18 (64.3)	.34	7 (63.6) 21 (84) 26 (76.5)	4 (36.4) 4 (16) 8 (23.5)
Pleural effusion†	No Yes	37 (88.1) 27 (93.1)	5 (11.9) 2 (6.9)	.69	15 (40.5) 12 (54.5)	22 (59.5) 10 (45.5)	.42	30 (73.2) 24 (82.8)	11 (26.8) 5 (17.2)
Brain metastasis†	No Yes	42 (91.3) 22 (88)	4 (8.7) 3 (12)	.69	21 (58.3) 6 (26.1)	15 (41.7) 17 (73.9)	.02	34 (74) 20 (83.3)	12 (26) 4 (16.7)

*Chi-squared test or Fisher's exact test.

†Data retrieved at start of gefitinib or erlotinib treatment.

Abbreviations: NSCLC, non-small cell lung cancer; Ca, carcinoma; PS, performance status; ECOG, Eastern Cooperative Oncology Group.

Table 2. Objective Responses by Patients' Characteristics

Covariate		Complete or Partial Response (7/73)	Stable Disease (11/73)	Progressive Disease (55/73)	
		N (%)	N (%)	N (%)	P*
Age, median, years		51	56	62	.06
Gender	Female	6 (14)	6 (14)	31 (72)	.37
	Male	1 (3.3)	5 (16.7)	24 (80)	
Race	Other	0	3 (37.5)	5 (62.5)	.12
	Asian	2 (28.6)	0	5 (71.4)	
	Caucasian	5 (8.6)	8 (13.8)	45 (77.6)	
Smoking history	Current smoker	1 (4.2)	5 (20.8)	18 (75)	.12
	Former smoker	2 (6.7)	2 (6.7)	26 (86.6)	
	Never smoker	4 (21.1)	4 (21.1)	11 (57.8)	
Histology	Adenocarcinoma	7 (14.6)	6 (12.5)	35 (72.9)	.44
	NSCLC	0	3 (21.4)	11 (78.6)	
	Squamous cell Ca	0	2 (18.2)	9 (81.8)	
PS (ECOG)†	0-1	5 (12.2)	8 (19.5)	28 (68.3)	.37
	2-3	2 (6.2)	3 (9.4)	27 (84.4)	
Stage†	IIIB	0	2 (33.3)	4 (66.7)	.31
	IV	7 (10.4)	9 (13.4)	51 (76.2)	
Previous chemotherapy regimens †	0	1 (9.1)	1 (9.1)	9 (81.8)	.67
	1	3 (11.5)	6 (23.1)	17 (65.4)	
	≥2	3 (8.3)	4 (11.1)	29 (80.6)	
Pleural effusion†	No	4 (9.3)	6 (14)	33 (76.7)	.92
	Yes	3 (10)	5 (16.7)	22 (73.3)	
Brain metastasis†	No	3 (6.4)	6 (12.8)	38 (80.8)	.36
	Yes	4 (16)	4 (16)	17 (68)	

*Fisher's exact test.

†Data retrieved at the start of gefitinib or erlotinib treatment.

Abbreviations: NSCLC, non-small cell lung cancer; Ca, carcinoma; PS, performance status, ECOG, Eastern Cooperative Oncology Group.

Table 3. Response Rate and Survival Data by *EGFR* Mutation Status, *EGFR* Gene Copy Number Status, and *KRAS* Mutation Status.

	<i>EGFR</i> Mutation Status (Tested = 71/73)		<i>EGFR</i> Gene Copy Number Status (Tested = 59/73)		<i>KRAS</i> Mutation Status (Tested = 70/73)	
	Wild-Type (n = 64) N (%)	Mutant (n = 7) N (%)	Not Increased (n = 27) N (%)	Increased (n = 32) N (%)	Wild-Type (n = 54) N (%)	Mutant (n = 16) N (%)
CR+PR	2 (28.6)	5 (71.4)	1 (20)	4 (80)	7 (100)	0
PD	53 (96.4)	2 (3.6)	23 (50)	23 (50)	38 (70.4)	16 (29.6)
SD	9 (100)	0	3 (37.5)	5 (62.5)	9 (100)	0
<i>P*</i>	<.0001		.48		.04	
Median OS, months	7.8	21.9	8.2	9.3	9.4	5.0
<i>P*</i>		.08		.68		.62
Median TTP, months	2.1	9.3	2.1	2.8	2.9	1.7
<i>P*</i>		.15		.44		.0025

*Log-rank test.

Abbreviations: CR, complete response; PR, partial response; SD, stable disease; PD, progressive disease; OS, overall survival; TTP, time to progression.

Table 4. Clinical Responses by Combination of *EGFR* Mutation Status, *EGFR* Gene Copy Number Status, and *KRAS* Mutation Status in the 59 NSCLC Cases Examined for All Three Markers

<i>EGFR</i> Mutation Status	<i>EGFR</i> Gene Copy No. Status	KRAS Mutation Status	No. of cases	CR+PR N (%)	SD N (%)	PD N (%)
Positive	Positive	Negative	5	4 (80)	0	1 (20)
	Positive	Negative	19	0	5 (26)	14 (74)
Negative	Negative	Negative	20	1 (5)	3 (15)	16 (80)
	Negative	Negative	1	0	0	1 (100)
Positive	Positive	Positive	8	0	0	8 (100)
	Negative	Positive	6	0	0	6 (100)

Abbreviations: CR, complete response; PR, partial response; SD, stable disease; PD, progressive disease.

Abstract ID: 725 Poster board space: 49

Molecular Imaging of Different EGFR Kinase Mutant NSCLC Carcinomas with [¹²⁴I]-Mipqa PET for Prediction of Responsiveness to EGFR Kinase Inhibitors.

Ryuchi Nishii, Asutosh Pal, Suren Soghomonyan, Julius Balatoni, Ioseb Mushkudiani, Hsin Hsien Yeh, Uday Mukophadhyay, Andrei Volgin, Aleksander Shavrin, David Maxwell, William Tong, Mian Alauddin, William Bornmann, **Juri Gelovani**, MD Anderson Cancer Center, Houston, TX, USA. Contact e-mail: jgelovani@mdanderson.org.

Purpose: To assess the efficacy of [¹²⁴I]mIPQA PET for prediction of response to therapy with EGFR kinase inhibitors in different clinically relevant NSCLC models in mice. Recently, two mutations in EGFR kinase had been identified: the L858R causes constitutive activation of EGFR kinase signaling (and sensitivity to drugs), while T790M mutation prevents drugs like Iressa and Tarceva from binding to the active site of EGFR kinase (causing resistance to drugs).

Methods: The [¹²⁴I]mIPQA was produced by no carrier added idodo destannylation method. Groups of 6 mice per tumor type were studied, including PC14 (wtEGFR, low TGF α), H441 (wtEGFR, high TGF α), H3255 (L858R EGFR), and H1975 (L858R and T790M EGFR). These orthotopic tumor xenografts were expressing GFP-Luciferase reporter gene to facilitate monitoring of growth using bioluminescence imaging (IVIS200, Xenogen). The mice were imaged on a MicroPET R4 (Siemens) first with [¹⁸F]FDG, next day [¹⁸F]FMAU, then [¹²⁴I]mIPQA at 3 and 24h, followed by euthanasia, cryosectioning for fluorescence imaging, autoradiography and histology. In a separate group of animals, therapeutic studies with Iressa (100 mg/kg for 10 days) had been performed beforehand to assess the responsiveness of these tumor models to therapy with EGFR kinase inhibitors.

Results: The level of [¹⁸F]FDG and [¹⁸F]FMAU accumulation did not predict the responsiveness to Iressa in these tumor models. In contrast, significantly higher levels of [¹²⁴I]mIPQA accumulation (especially at 24h) were observed in H441 and H3255 tumors expressing high levels of TGF α (which activates wtEGFR on tumor cells and vasculature) and dominant mutant EGFR, respectively. No accumulation or retention of [¹²⁴I]mIPQA was detectable in PC14 and H1975 tumor xenografts.

Conclusions: [¹²⁴I]mIPQA PET has a potential for predicting tumor responsiveness to EGFR kinase inhibitors from the same class of phenylamino-quinazoline analogues, such as Iressa, and could be used for stratification of patients for therapy.

Disclosure of author financial interests or relationships:

R. Nishii, None; A. Pal, None; S. Soghomonyan, None; J. Balatoni, None; I. Mushkudiani, None; H. Yeh, None; U. Mukophadhyay, None; A. Volgin, None; A. Shavrin, None; D. Maxwell, None; W. Tong, None; M. Alauddin, None; W. Bornmann, None; J. Gelovani, None.

This study was supported by the Department of Defense grant IMPACT (W81XWH-05-2-0027)

Abstract ID: 043 PET with ¹⁸F-FDG and ¹⁸F-FMAU in the Assessment of Early Response to EGFR-Targeted Therapy in Mice Bearing Human NSCLC Xenografts with Different EGFR Mutations. Ruyshi Nishii, Udhay Mukhopadhyay, Suren Soghomonyan, Andrei Volgin, Mian Alauddin, Juri Gelovani. M.D. Anderson Cancer Center, Houston, TX, USA. Contact e-mail: rnishii@di.mdacc.tmc.edu.

Goals: This study aimed to assess the efficacy of PET imaging with ¹⁸F-FDG and ¹⁸F-FMAU for monitoring early responses in human NSCLC xenografts in mice to therapy with EGFR kinase inhibitor gefitinib.

Methods: Human lung carcinoma cells PC14, H441, H3255, and H1975, expressing different EGFR mutants and various levels of TGF- α (Tab. 1), were injected s.c. (3×10^6 cells) in nu/nu mice. When tumors grew > 5 mm in diameter, PET imaging with ¹⁸F-FDG and ¹⁸F-FMAU was performed on two consecutive days and repeated after 3 and 4 days of gefitinib (100 mg/kg) therapy, respectively.

Results: Tumor-to-muscle (T/M) ratios of ¹⁸F-FDG and ¹⁸F-FMAU accumulation for different NSCLC xenografts before and after gefitinib treatment are summarized in Table 1. Pre-treatment T/M ratios of ¹⁸F-FMAU were higher than those of ¹⁸F-FDG, especially in gefitinib-resistant NSCLCs (PC14, H1975). In these tumors, the lack of decrease in ¹⁸F-FMAU and ¹⁸F-FDG T/M ratios after 3-4 days of gefitinib therapy was predictive of tumor resistance. In gefitinib-sensitive tumors (H441 and H3255), only minimal decreases in ¹⁸F-FDG and ¹⁸F-FMAU T/M ratios have been observed after 3-4 days of gefitinib therapy, especially in H3255 carcinomas.

Conclusions: PET with ¹⁸F-FMAU demonstrated higher sensitivity for the detection of NSCLCs as compared to ¹⁸F-FDG. The lack of decrease in ¹⁸F-FDG and ¹⁸F-FMAU uptake early after initiation of gefitinib therapy is predictive of tumor resistance. However, in some gefitinib sensitive NSCLCs the assessment of early treatment responses by PET may not be feasible, because of very low pre-treatment levels of uptake of both ¹⁸F-FDG and ¹⁸F-FMAU. Therefore, alternative imaging agents need to be developed for the detection of NSCLCs and for monitoring molecular-targeted therapies in patients.

	PC14	H441	H3255	H1975
EGFR status	wild-type	wild-type	L858R mut.	L858R, T790M mut.
TGF- α level	+	++++	+	++
Gefitinib IC50 (nM)	12.6	40.2	2.3	16.2
FDG before ther.	1.36 \pm 0.98	0.87 \pm 0.30	0.82 \pm 0.24	1.46 \pm 0.41
FDG after ther.	2.41 \pm 1.19	1.12 \pm 0.48	0.74 \pm 0.15	1.41 \pm 0.93
FMAU before ther.	5.21 \pm 2.11	2.51 \pm 1.13	1.22 \pm 0.35	3.51 \pm 1.79
FMAU after ther.	7.73 \pm 2.52	2.41 \pm 0.45	0.76 \pm 0.18	2.68 \pm 1.71
Tumor growth resp.	progression	more stable resp.	complete resp.	progression

Disclosure of author financial interests or relationships:

R. Nishii, None; U. Mukhopadhyay, None; S. Soghomonyan, None; A. Volgin, None; M. Alauddin, None; J. Gelovani, None.

This study was supported by the Department of Defense grant IMPACT (W81XWH-05-2-0027)

In Vivo Detection of Gold–Imidazole Self-Assembly Complexes: NIR-SERS Signal Reporters

Glauco R. Souza,^{†,‡} Carly S. Levin,[†] Amin Hajitou,[‡] Renata Pasqualini,[‡] Wadih Arap,[‡] and J. Houston Miller^{*,†}

Department of Chemistry, The George Washington University, Washington, D.C. 20052, and The University of Texas M. D. Anderson Cancer Center, 1515 Holcombe Boulevard, Houston, Texas 77030

Here we report in vitro and in vivo detection of self-assembled Au–imidazole by using near-infrared surface-enhanced Raman scattering (NIR-SERS). In vivo, the Au–imidazole structures were administered into tumor-bearing mice and detected noninvasively. The self-assembled Au–imidazole complexes were generated by the adsorption of imidazole molecules onto Au nanoparticles (NP) and were then characterized as aqueous suspensions by using NIR-SERS, angle-dependent light scattering with fractal dimension analysis, and visible extinction spectroscopy. The structure and optical activity was sensitive to imidazole concentration and Au NP size. Specifically, the Au–imidazole assemblies formed at lower imidazole concentrations had the lowest fractal dimension ($D_f = 1.2$) and the largest Raman enhancement factors for the dominant NIR-SERS feature, a ring-breathing vibrational mode at 954 cm^{-1} . Changes in elastic scattering intensity, fractal dimension, and surface plasmon absorption were observed with increasing imidazole concentration. The Raman enhancement factor was also found to range between 10^6 and 10^9 with different primary Au nanoparticle sizes. For the higher enhancement factor systems, NIR-SERS detection of Au–imidazole was performed with data acquisitions time of only 5 s. The largest enhancement was observed for the 954 cm^{-1} feature at an imidazole concentration of $1.9\text{ }\mu\text{M}$ when coupled to 54-nm-diameter Au NPs (the largest NP tested). Finally, we show the first demonstration of in vivo, noninvasive, and real-time SERS detection.

Development of signal reporters based on near-infrared surface-enhanced Raman scattering (NIR-SERS) is required for application of this technology in biomolecular imaging.^{1–3} Biological tissues show minimal NIR radiation (700–900 nm) absorption, thus

allowing efficient light penetration for imaging and phototherapy applications in vivo.^{4–6} We have coupled Au nanoparticles (NPs) with imidazole (Au–imidazole) into self-assembled NPs, which can be used for real-time, in vivo NIR-SERS detection. The strong affinity between imidazole and Au induces the aggregation of the Au NPs, which results in a shift in the surface plasmon resonance absorption into the NIR wavelengths along with changes in fractal structure and optical properties. All of these attributes are desirable for noninvasive detection in tissue.

Here we present proof of principle for the use of NIR-SERS in noninvasive, in vivo, and real-time detection of self-assembled nanoparticle complexes. We show the optical and structural characterization of these assemblies by using SERS, UV–visible extinction, and angle-dependent light scattering (ADLS) coupled with fractal dimension analysis. We also show detection in vivo by using a fiber-optic probe to deliver and collect light through the skin of tumor-bearing mice injected with Au–imidazole complexes.

Imidazole has been the target of several prior SERS studies using Ag NPs and electrodes.^{7–10} Holze¹¹ reported the only prior study of SERS for imidazole on gold, specifically on the surface of an Au electrode. The two nitrogens¹² of imidazole (Scheme 1a), the position 1 nitrogen (sp^3 as in pyrrole, $\text{p}K_a$ 6.5), and the position 3 nitrogen (sp^2 as in pyridine, $\text{p}K_a$ 14.0)¹¹ play a role in bridging metal particles⁷ (Scheme 1b). Because the in vitro work was performed at pH 8.0, one would expect electrostatic interaction between the cationic form of imidazole (Scheme 1a, right) and the negatively charged Au NP (resulting from adsorbed citrate ions from Au synthesis). Imidazole and its derivatives are associated with corrosion prevention and serve as precursors for the adsorption of other molecules onto metal surfaces.^{7–10,13,14} The

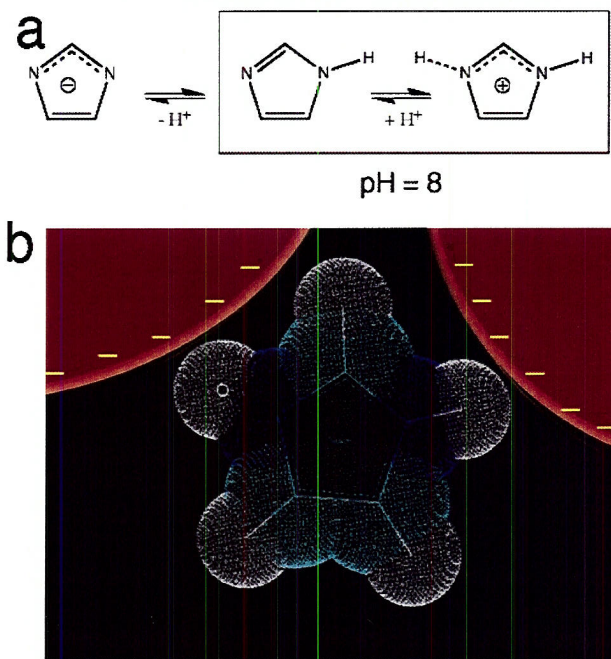
* Corresponding author. Phone: 202-994-7474. Fax: 202-994-5873. E-mail: Houston@gwu.edu.

[†] The George Washington University.

[‡] The University of Texas M. D. Anderson Cancer Center.

- (1) Souza, G. R.; Christianson, D. R.; Staquicini, F. I.; Ozawa, M. G.; Snyder, E. Y.; Sidman, R. L.; Miller, J. H.; Arap, W.; Pasqualini, R. *Proc. Natl. Acad. Sci. U.S.A.* **2006**, *103*, 1215–1220.
- (2) Kneipp, J.; Kneipp, H.; Rice, W. L.; Kneipp, K. *Anal. Chem.* **2005**, *77*, 2381–2385.
- (3) Schwartzberg, A. M.; Grant, C. D.; Wolcott, A.; Talley, C. E.; Huser, T. R.; Bogomolni, R.; Zhang, J. *Z. J. Phys. Chem. B* **2004**, *108*, 19191–19197.
- (4) Kneipp, K.; Kneipp, H.; Itzkan, I.; Dasari, R. R.; Feld, M. S. *Chem. Rev.* **1999**, *99*, 2957–2976.
- (5) Kerker, M.; Wang, D. S.; Chew, H. *Appl. Opt.* **1980**, *19*, 3373–3388.
- (6) Broderick, J. B.; Natan, M. J.; O'Halloran, T. V.; Van Duyne, R. P. *Biochemistry* **1993**, *32*, 13771–13776.
- (7) Xue, G.; Dai, Q.; Jiang, S. *J. Am. Chem. Soc.* **1988**, *110*, 2393–2395.
- (8) Cao, P.; Gu, R.; Tian, Z. *J. Phys. Chem. B* **2003**, *107*, 769–777.
- (9) Wang, G.; Shi, J.; Yang, H.; Wu, X.; Zhang, Z.; Gu, R.; Cao, P. *J. Raman Spectrosc.* **2002**, *33*, 125–130.
- (10) Carter, D. A.; Pemberton, J. E. *Langmuir* **1992**, *8*, 1218–1225.
- (11) Holze, R. *Electrochim. Acta* **1993**, *38*, 947–956.
- (12) Davis, K. L.; McGlashen, M. L.; Morris, M. D. *Langmuir* **1992**, *8*, 1654–1658.
- (13) Carter, D. A.; Pemberton, J. E.; Woelfel, K. *J. Phys. Chem. B* **1998**, *102*, 9870–9880.

Scheme 1. (a) Imidazole Neutral and Ionic Forms. (b) Au–Imidazole Assembly Interaction



interaction between imidazole and metals is also of biological relevance,^{15–19} as it is the functional moiety of several biomolecules, such as nucleic acids, histidine, and histamine. With the growing interest in combining NPs for detection of biomolecules,^{1,20–23} biological imaging, and targeted drug delivery,^{1,24,25} it is central to understand the interaction of molecules, such as imidazole, with dispersed metal NPs in aqueous environments. Essentially, this work provides the basis for application of imidazole (an inexpensive, soluble, and relatively nontoxic molecule) as a practical and sensitive NIR-SERS signal reporter.

EXPERIMENTAL SECTION

Gold Nanoparticle Self-Assembly Preparation. Samples consisted of 500 μ L of Nanopure water, 500 μ L of 100 mM borate buffer at pH 8.0, 3 μ L of imidazole solution at 99.5% (Fluka), with 500 μ L of 0.32 nM Au solution added last. To ensure that the system had reached equilibrium, all measurements were made 12 h after sample preparation. Samples were vigorously mixed to guarantee homogeneity before each measurement. Imidazole solutions consisted of 12 separate dilutions (in Nanopure water)

ranging from 0.24 to 500 μ M. The Au NPs were prepared by the standard method of citrate reduction of gold(III) chloride²⁶ (99.99+% from Aldrich) in which different sizes were obtained by varying gold(III) chloride and citrate molar ratios. Resulting particle sizes were determined through extinction and transmission electron microscope (TEM) measurements. For all measurements reported below, there was a constant molar concentration of gold atoms, which results in a variable concentration of Au NP in solutions. For 17-nm particles, molar extinction at 520 nm indicated a concentration of 1.96×10^{14} particles/L.

Spectroscopy Measurements. The NIR-SERS measurements were obtained using a Raman Systems R2001 spectrophotometer equipped with a 785-nm laser coupled to a fiber-optic probe. The incident laser power was maintained at 250 mW and was operated in a continuous wave mode. The integration time of each SERS spectrum varied from 5 to 60 s. Extinction measurements were obtained in a diode array spectrophotometer (Hewlett-Packard 8452A). The scattering measurements were obtained using a custom-made ADLS apparatus²⁷ equipped with a CCD detector and a 5-mW, 532-nm laser. Nanopure water served as the blank in all three types of measurements for the purpose of background subtraction.

TEM Measurements. Nickel mesh grids previously coated with Formvar and evaporated with carbon were floated on drops of 0.1% poly(L-lysine) (Sigma Diagnostics) on Parafilm for 5 min. Excess solution was removed from the grid by carefully touching the edge of the grid onto filter paper. The grids were not allowed to dry completely in any of the following steps. The grids were floated on drops of sample on Parafilm for 1 h. Excess fluid was removed as above, and the grids were then floated on drops of 1% ammonium molybdate in 0.02% BSA in distilled water, pH 7.0 for 60 s. Excess fluid was removed, and the grids were allowed to dry overnight. TEM images were captured by a transmission electron microscope (JEOL JEM-1010) fitted with an AMT Advantage digital CCD camera system. Au NP size was determined by averaging a population of primary particle sizes (and aspect ratios) for representative TEM images using the ImageJ software.²⁸

RESULTS AND DISCUSSION

NIR-SERS, UV–Visible, and ADLS of Au–Imidazole Assemblies. Figure 1 shows quantitatively and qualitatively the optical characteristics of Au–imidazole complexes. Figure 1a compares the NIR-SERS from a mixture of 3.9×10^{-6} M imidazole and 17-nm Au NPs (blue spectrum), with the normal Raman spectrum of 0.33 M imidazole aqueous solution (red spectrum). The prominent feature at 954 cm^{-1} in the SERS spectrum is assignable to the $\gamma(\text{NH}) + \delta_{\text{ring}}$ vibration observed weakly at 931 cm^{-1} in the unenhanced Raman spectrum of imidazole in aqueous solutions⁸ (Table 1). A comparison of the intensity of the SERS signal with the normal Raman serves to estimate an enhancement factor of 2×10^6 for this sample. We defined the Raman signal enhancement for a given feature as the ratio of Raman intensities

- (14) Carter, D. A.; Pemberton, J. E. *J. Raman Spectrosc.* **1997**, *28*, 939–946.
- (15) Kendall, P. A.; Barnard, E. A. *Biochim. Biophys. Acta* **1969**, *188*, 10–24.
- (16) Caswell, D. S.; Spiro, T. G. *J. Am. Chem. Soc.* **1986**, *108*, 6470–6477.
- (17) Salama, S.; Spiro, T. G. *J. Am. Chem. Soc.* **1978**, *100*, 1105–1111.
- (18) Yoshida, C. M.; Freedman, T. B.; Loehr, T. M. *J. Am. Chem. Soc.* **1975**, *97*, 1028–1032.
- (19) Pack, D. W.; Putnam, D.; Langer, R. *Biotechnol. Bioeng.* **2000**, *67*, 217–223.
- (20) Mirkin, C. A.; Letsinger, R. L.; Mucic, R. C.; Storhoff, J. J. *Nature* **1996**, *382*, 607–611.
- (21) Souza, G. R.; Miller, J. H. *J. Am. Chem. Soc.* **2001**, *123*, 6734–6735.
- (22) Natan, M. J. *J. Phys. Chem.* **1998**, *102*, 9404–9413.
- (23) Hirsch, L. R.; Jackson, J. B.; Lee, A.; Halas, N. J.; West, J. L. *Anal. Chem.* **2003**, *75*, 2377–2381.
- (24) Sershen, S. R.; Westcott, S. L.; Halas, N. J.; West, J. L. *J. Biomed. Mater. Res.* **2000**, *51*, 293–298.
- (25) Shen, W. C. *Biochim. Biophys. Acta* **1990**, *1034*, 122–124.

- (26) Geoghegan, W. D.; Ackerman, G. A. *J. Histochem. Cytochem.* **1977**, *25*, 1187–1200.
- (27) Souza, G. R.; Miller, J. H. In *Annual Reviews in Plasmonics*; Geddes, C., Ed.; Kluwer Academic/Plenum Publishers: New York, Vol. 2006. In press.
- (28) Rasband, W. S. *ImageJ*, U.S. National Institutes of Health, Bethesda, MD, 1997–2006.

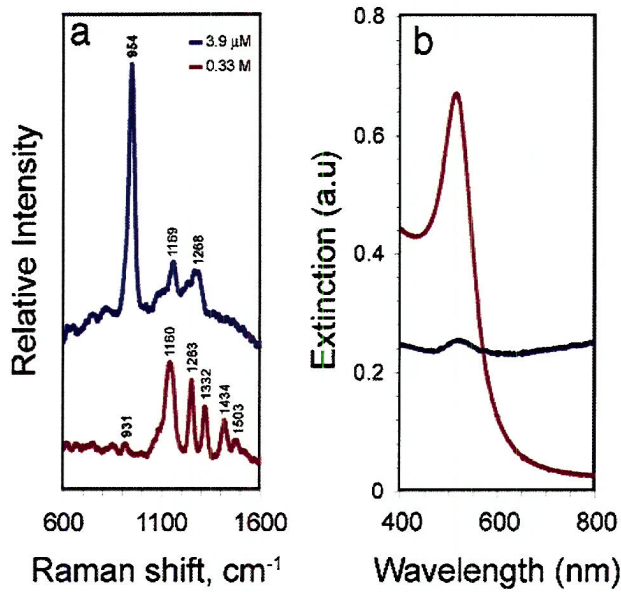


Figure 1. (a) Raman signal of 3.9 μM imidazole in 0.33 mM borate buffer pH 8.0 (borate buffer) enhanced by interaction with 17-nm Au NPs (blue spectrum, 60-s integration) and Raman spectrum of 0.3 M imidazole in borate buffer (red spectrum). Plots are offset for clarity. (b) UV-visible absorption spectra of a mixture of 3.9 μM imidazole in borate buffer with 17-nm Au NPs (blue spectrum) and 17-nm Au in borate buffer (red spectrum).

Table 1. Assignment of Raman and SERS Modes of Imidazole

work	Au-imidazole (cm ⁻¹)	imidazole (cm ⁻¹)	imidazole SERS ^{8,11} (cm ⁻¹)	vibrational assignment ^{8,11a}
	650		628	$\text{A}_2^{\text{d}}\delta_{\text{ring}}$
	764		743	$\text{A}_1\delta_{\text{ring}}$
	838		832	$\text{A}_1\delta_{\text{ring}}$
	954	931	950	$\text{A}_2\delta(\text{NH}) + \text{A}_1\delta_{\text{ring}}$
	1109		1097	$\text{A}_1\delta(\text{CH}) + \text{A}_1\nu_{\text{ring}}$
	1169	1160	1164	$\text{A}_1\delta_{\text{ring}}$
	1268	1263	1265	$\text{A}_1\delta(\text{CH})$
	1328		1329	$\text{A}_1\nu_{\text{ring}}$

^a δ , in-plane bending; γ , out-of-plane bending; ν , stretching.

normalized by imidazole concentration in samples with and without gold present, as follows:

$$E_{\text{SERS}} = \frac{I_{\text{SERS}}}{C_{\text{SERS}}} \frac{C_{\text{Neat}}}{I_{\text{Neat}}}$$

where C_{SERS} is the concentration of imidazole in solution with Au NPs and C_{Neat} is the concentration of imidazole aqueous solution without any Au NP. Of note, this estimation is only applicable for features observed in both normal and enhanced Raman spectra.

Color change from red to gray-blue occurred after mixing Au nanoparticles with imidazole solution (Figure 1b). To explore these optical changes, visible extinction spectra and angle-dependent light scattering data were collected for each sample. Figure 1b shows extinction spectra of Au solutions with and without imidazole, clearly showing a red shift in the surface plasmon absorption wavelength from 520 nm for the dispersed, isolated

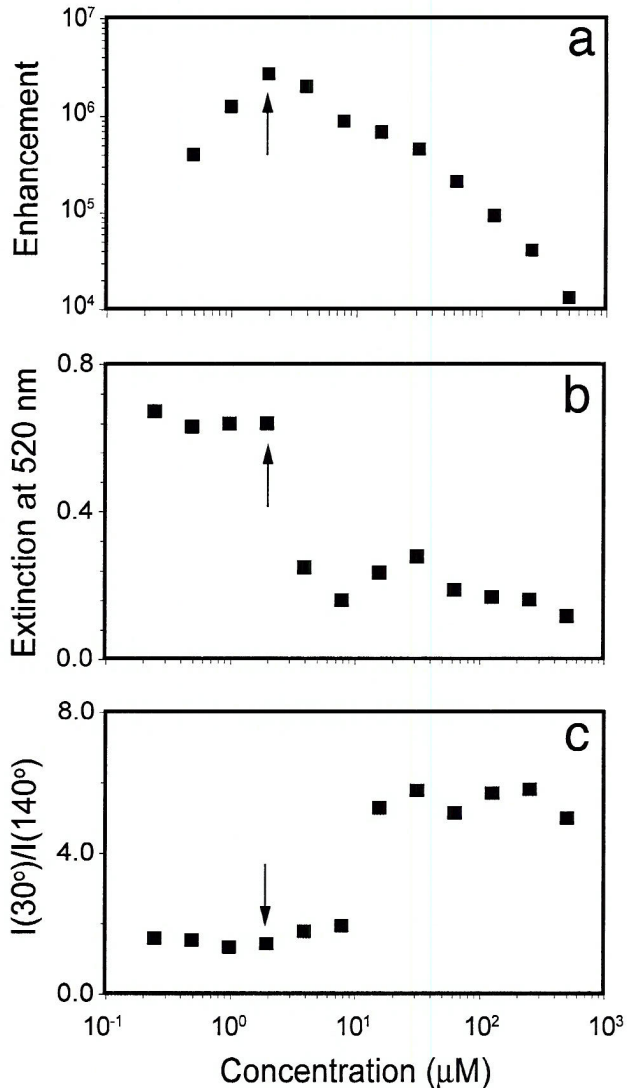


Figure 2. (a) Surface enhancement of 954-cm⁻¹ mode relative to the imidazole concentration; (b) light extinction by the sample measured by light absorption at 520 nm; and (c) dissymmetry ratio of light scattering signal of Au NPs as a function of imidazole concentration.

particles (red spectrum) to longer wavelengths for the imidazole-containing solutions (blue spectrum). As a red shift in Au surface plasmon is indicative of Au NP aggregation,^{29,30} this observation implicates participation of imidazole in the NP assembly process. Often, excitation at a surface plasmon resonance of metal NPs is associated with the SERS signal from adsorbed molecules.^{4,31}

The dependence of several experimental observables on the concentration of imidazole were performed using 17-nm Au NPs (Figure 2). The surface enhancement in the SERS signal at 954 cm⁻¹ is shown, in which largest enhancement of $\sim 3 \times 10^6$ was observed for an imidazole concentration of 1.9 μM (Figure 2a). The magnitude of the extinction feature at 520 nm, characteristic

(29) Bohren, C. F.; Huffman, D. R. *Absorption and Scattering of Light by Small Particles*; John Wiley and Sons: New York, 1983.

(30) Weisbecker, C. S.; Merritt, M. V.; Whitesides, G. M. *Langmuir* 1996, 12, 3763–3772.

(31) Wang, H.; Levin, C. S.; Halas, N. J. *J. Am. Chem. Soc.* 2005, 127, 14992–14993.

of dispersed Au NPs, also changed as a function of imidazole concentration (Figure 2b). Further, the dissymmetry ratio analysis (the ratio between intensities for forward scattering at 30° and backscattering at 140°) of the scattering data are shown in (Figure 2c). The dissymmetry ratio provides a qualitative measure of the relative size of NP aggregates,³² with larger aggregates possessing a larger dissymmetry ratio.

All three experiments indicate “threshold” behavior when imidazole concentrations are in the range of 1.9–15.6 μM (Figure 2). In order of appearance with increasing imidazole concentration, maximum Raman enhancement precedes the sharp decrease in extinction at 520 nm, which in turn precedes the sharp increase in the dissymmetry ratio. Notably, the maximum enhancement factor is observed at a concentration (1.9 μM) where change in 520-nm SP extinction is not significant (Figure 2b). Moreover, large changes in surface plasmon absorbance, resulting from increase in NP aggregation at higher imidazole concentrations ($\geq 3.9 \mu\text{M}$), did not provide additional signal enhancement. Together, these data suggest that the SERS signal originates from small aggregates consisting of the assembly of relatively few cross-linked primary Au NP.

The surface coverage of imidazole on the Au NP can be estimated by comparing the available imidazole in solution with the number of molecules required for monolayer coverage. For the latter, we first estimated the surface area of 17-nm particles (assuming spherical symmetry) and divided this number by the footprint of imidazole by assuming edge-on adsorption. Imidazole size was estimated from a semiempirical structure optimization by using Hyperchem 7.0. Essentially, the results of these calculations suggest that 1 μM imidazole represents coverage of ~ 1 –2 monolayers, assuming that all of the imidazole in solution has been adsorbed. It has been postulated^{33,34} that the greatest Raman enhancement will occur near the contact point of metallic NPs where the plasmon field is the greatest. In an evenly distributed monolayer coverage, only a fraction of adsorbed molecules would be at these contact points, suggesting that the actual enhancement may be much greater than that estimated above.

Fractal Dimension Analysis of Au–Imidazole Assemblies.

There has been recent interest in understanding the relationship between large enhancements and fractal dimension characteristics of metal surfaces and metal NP assemblies.^{4,35–37} Here we used fractal dimension analysis of the ADLS signal (Figure 3a) to structurally characterize and correlate D_f structure with the observed surface enhancement of self-assembled Au–imidazole complexes.

Fractal theory^{27,38–41} postulates that the relationship between the number of primary particles (N) in a fractal aggregate follows the relationship, $N = k(R_g/a)^{D_f}$. The angle-dependent light scattering signal is related to the fractal dimension of an aggregate

(32) Hunter, R. J. *Introduction to Modern Colloid Science*; Oxford Science Publications: New York, 1993.

(33) Jiang, J.; Bosnick, K.; Maillard, M.; Brus, L. *J. Phys. Chem. B* 2003, 107, 9964–9972.

(34) Li, K.; Stockman, M. I.; Bergman, D. J. *Phys. Rev. Lett.* 2003, 91, 227402.

(35) Micic, M.; Klymyshyn, N.; Lu, H. P. *J. Phys. Chem. B* 2004, 108, 2939–2947.

(36) Kneipp, K.; Kneipp, H.; Dresselhaus Mildred, S.; Lefrant, S. *Philos. Trans., Ser. A* 2004, 362, 2361–2373.

(37) Garcia-Ramos, J. V.; Sanchez-Gil, J. A. *Proc. SPIE* 1999, 3572, 461–464.

(38) Avnir, D.; Farin, D.; Pfeifer, P. *Nature* 1984, 308, 261–263.

(39) Farias, T. L.; Koylu, U. O.; Carvalho, M. G. *Appl. Opt.* 1996, 35, 6560.

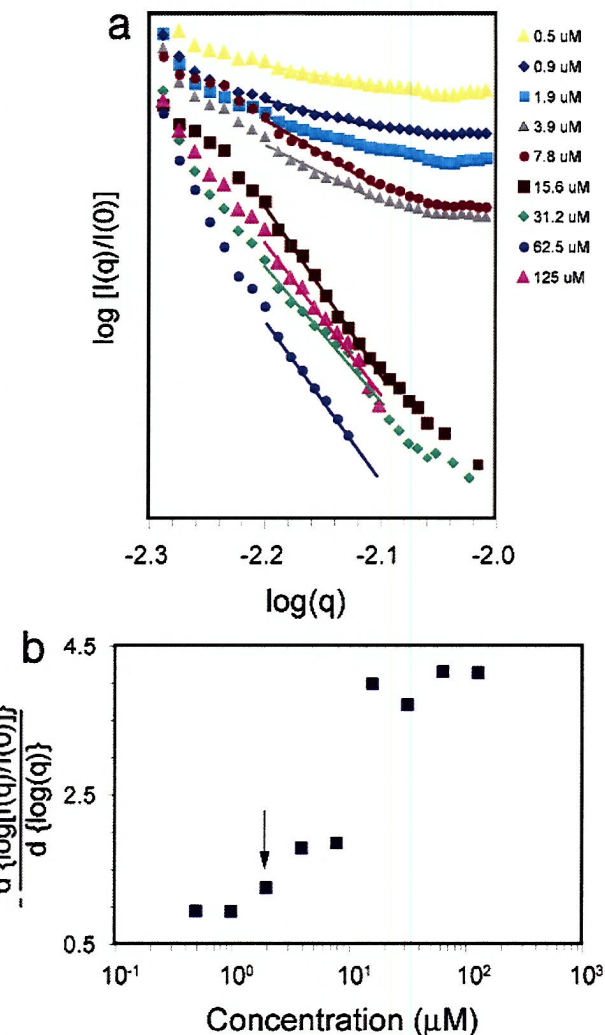


Figure 3. (a) Angle-dependent light scattering signal from Au agglomerates formed from 17-nm Au in the presence of different imidazole concentrations. (b) Fractal dimension analysis resulting from the measurement of the slope of the curves in (a) between $-2.2 < \log(q) < -2.1$.

according to $I(q) \propto q(\theta)^{-D_f}$, where $I(q)$ is the angle-dependent scattered light intensity, $q(\theta)$ is the scattering wavevector, which is a function of the scattering angle (θ) and wavelength of incident light (λ), and D_f is the fractal dimension of the scattering aggregate, which is the negative of the slope of the curves in Figure 3a. This relationship results from the interference between the scattered electromagnetic waves from individual particles forming the fractal aggregates. Numerical results for the fractal dimension analysis of the ADLS signal shown in Figure 3a are plotted in Figure 3b, where $((d\{\log [I(q)/I(0)]\})/(d\{\log (q)\}))$ is the slope of the scattering curves in Figure 3a. The data in Figure 3 indicate that the morphology of the aggregates is a strong function of imidazole concentration. These results also show that the fractal dimension of these assemblies also follow a threshold-type behavior shown in Figure 2, where the slope increases

(40) Mandelbrot, B. B. *The Fractal Geometry of Nature*; Freeman: San Francisco, 1982.

(41) Dewey, T. G. *Fractals in Molecular Biophysics*; Oxford University Press: New York, 1997.

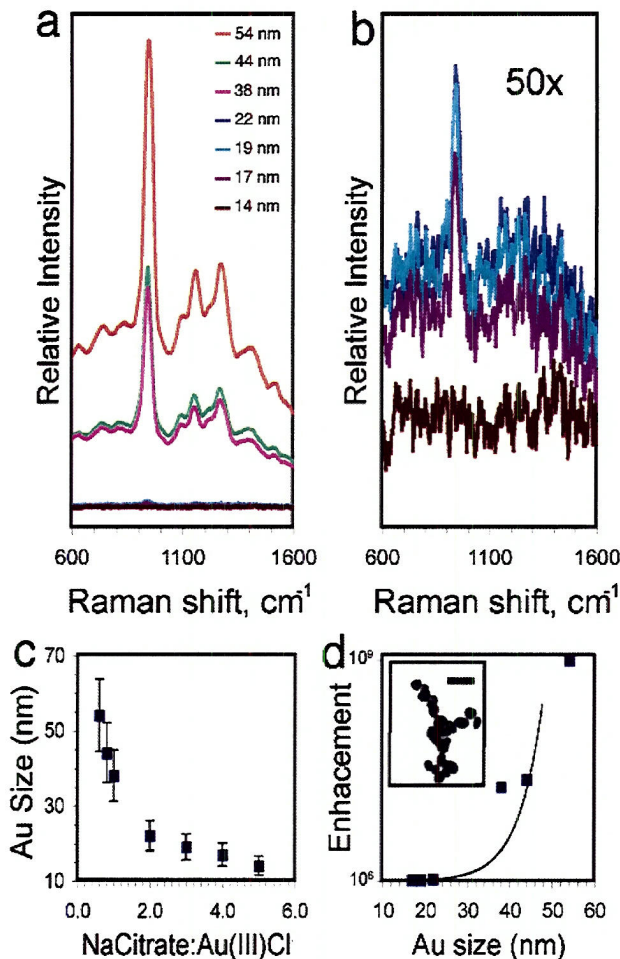


Figure 4. (a) NIR-SERS spectra from imidazole in the presence of different Au sizes (5-s integration time). (b) Magnified spectra (50x) of (a) for imidazole solutions prepared with 14-, 17-, 19-, and 22-nm Au NP sizes. (c) Au NP size as a function of sodium citrate to $\text{Au}^{III}\text{Cl}^-$ ratio during Au NP synthesis. (d) Surface enhancement of 954-cm^{-1} mode relative to Au size (inset, TEM of representative Au-imidazole clusters formed with 54-nm Au at $1.9\text{ }\mu\text{M}$ imidazole; $100\text{ }\mu\text{m}$, scale bar).

sharply between 7.8 and $15.6\text{ }\mu\text{M}$ imidazole indicating structural transition from predominantly fractal aggregates ($\leq 7.8\text{ }\mu\text{M}$ imidazole) to more homogeneous⁴¹ and compact particle assemblies ($\geq 15.6\text{ }\mu\text{M}$ of imidazole; slope ≥ 3).

Notably, the largest Raman enhancement factor was observed with systems with low fractal dimension (Figure 3b, D_f of 1.2 for $1.9\text{ }\mu\text{M}$ imidazole). Recent reports have shown that surface enhancement is greatest in NP clusters containing only a few primary particles (dimers and trimers),^{42,43} systems expected to have near-unity fractal dimensions. These results have implications for the use of NP assemblies as biomolecular labels. The characteristic high surface area of low-dimension fractal aggregates^{1,44} provides improved coupling efficiency and accessibility to binding sites, both of which are relevant for fabricating tissue-targeting image systems.

(42) Hao, E.; Schatz, G. C. *J. Chem. Phys.* 2004, 120, 357–366.

(43) Talley, C. E.; Jackson, J. B.; Oubre, C.; Grady, N. K.; Hollars, C. W.; Lane, S. M.; Huser, T. R.; Nordlander, P.; Halas, N. J. *Nano Lett.* 2005, 5, 1569–1574.

(44) West, G. B.; Brown, J. H.; Enquist, B. J. *Science* 1999, 284, 1677–1679.

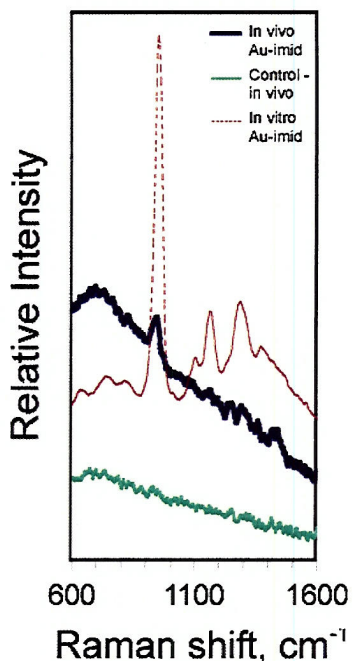


Figure 5. Noninvasive NIR-SERS detection across skin in a tumor-bearing mouse that received $300\text{ }\mu\text{L}$ of Au-imidazole clusters ($7.8\text{ }\mu\text{M}$ imidazole) administered locally in the tumor xenograft. SERS spectra description: the blue curve (in vivo) is the spectrum generated by the Au-imidazole assemblies inside the tumor with 15-s integration; red curve (in vivo) is the spectrum from tumor prior to administration of Au-imidazole assemblies injection with 15-s integration; and green (in vitro) is the spectrum from Au-imidazole complexes in solution measured in a glass cuvette with 5-s integration.

Enhancement as a Function of Au Size. Panels a and b in Figure 4 show the NIR-SERS from Au-imidazole clusters as a function of Au NP size for an imidazole concentration of $1.9\text{ }\mu\text{M}$ (indicated by the arrow in Figures 2 and 3b). As stated above, particle size is related to the ratio of sodium citrate to $\text{Au}^{III}\text{Cl}^-$ salt in the Au synthesis procedure (Figure 4c). Surface enhancement increased sharply with NP size (Figure 4d); an enhancement on the order of 10^9 was observed for Au NP of 54 nm . Large enhancements for Au NPs of $>40\text{ nm}$ have been reported previously.⁴⁵ The pronounced SERS signal from assemblies formed with 38 , 44 , and 54-nm Au NP are obtained with data acquisition time of only 5 s. Such strong enhancements indicate that these assemblies would provide desirable characteristics required for targeted biological imaging and detection,¹ such as reduced data acquisition time and laser light exposure.

In Vivo NIR-SERS Detection. To demonstrate the feasibility of using NIR-SERS for noninvasive detection of Au-imidazole assemblies *in vivo*, $300\text{ }\mu\text{L}$ of a solution of Au-imidazole clusters ($7.8\text{ }\mu\text{M}$ imidazole in H_2O) were injected into the tumors of tumor-bearing mice. Specifically, six tumor-bearing mice were tested. Of this group, three were injected with Au-imidazole solutions and the other three were injected with water as a control population. Then, a fiber-optic probe with a focal length of 7 mm was positioned 3 mm above the tumor to deliver and collect light through the exposed skin (i.e., the fur had been shaved off). Figure 5 compares the *in vitro* spectrum of Au-imidazole clusters

(45) Lee, C. R.; Kim, S. I.; Yoon, C. J.; Gong, M. S.; Choi, B. K.; Kim, K.; Joo, S. *W. J. Colloid Interface Sci.* 2004, 271, 41–46.

with the *in vivo* spectrum, clearly showing the 954-cm⁻¹ ring-breathing mode of imidazole. Only the three mice injected with Au-imidazole presented this SERS spectral feature. Although the 3-mm standoff distance resulted in the best signal, it has been our experience that this distance can be varied by $\sim \pm 2$ mm without significant degradation in the signal. Finally, the instrumentation used in this demonstration study was not designed for *in vivo* detection; thus, it is likely that further instrument optimization will markedly improve these initial results.

CONCLUSION

We report NIR-SERS signals resulting from nanoparticle self-assembly triggered by the imidazole adsorption onto Au nanoparticles. The ADLS and UV-visible extinction serve to monitor the assembly and optical properties of the Au nanoparticle aggregates as they interact with imidazole. Enhancements of up to 10⁹, measured in solution, are observed for a ring-breathing vibrational mode of imidazole for low fractal dimension aggregates of 54-nm primary particle size. The onset of the enhancement in Raman scattering at lower imidazole concentrations preceded the onset of marked changes in elastic scattering, indicating that the largest surface enhancement results from small Au nanoparticles assemblies. Finally, we have shown the *in vivo* detection of these assemblies in a preclinical tumor-bearing mouse model. We have

for the first time demonstrated that optics, spectroscopy, and Au-imidazole signal reporting can be effectively combined to observe intratissue NIR-SERS signals *in vivo*. While direct injection was used as proof of concept, the long-term goal is to use systemic delivery of targeted nanoparticles, such as was demonstrated for “nanoshuttles”, assemblies of gold nanoparticles, and bacteriophage.¹ The use of such nanostructures has the potential to overcome many of the difficulties associated with *in vivo* detection by allowing faster data acquisition time and reduced laser power in a biologically transparent wavelength region.

ACKNOWLEDGMENT

This work was supported by the George Washington University Research Enhancement Funds (to J.H.M), awards from the Gillson-Longenbaugh Foundation, and grants from Department of Defense, and National Institutes of Health (to R.P. and W.A.). We thank Corazon D. Bucana, Kenneth Dunner, Jr., and Jacqueline Ryan for assistance with TEM imaging and analysis.

Received for review March 16, 2006. Accepted June 7, 2006.

AC060483A

Differential Immunohistochemical Expression Pattern of HER Family Receptors and Ligands is Detected in Primary Lung Cancers and Corresponding Brain Metastases.

Menghong Sun¹, Erminia Massarelli², Lei Feng³, Natalie Ozburn², Guosheng Yin³, Ritsuko Komaki⁴, Waun Ki Hong², Kenneth D. Aldape¹, Ignacio I. Wistuba^{1,2}

Departments of Pathology¹, Thoracic, Head & Neck Medical Oncology², Biostatistics³, Radiation Oncology⁴, MD Anderson Cancer Center, 1515 Holcombe Blvd, Houston, Texas 77030

The brain is one of the main metastatic sites for lung cancer patients and those metastases occur in ~50% of patients with non-small cell lung carcinoma (NSCLC). Despite recent advances in lung cancer targeted therapy research, there is limited information on the molecular characteristics of lung cancer brain metastases and on markers that can predict their development. In NSCLC, the over-expression of HER family receptors and ligands has been involved in tumor pathogenesis and progression, and some of those markers have been associated to EGFR tyrosine kinase inhibitors prediction of response. We investigated the level of immunohistochemical (IHC) expression of 3 HER family receptors and 3 ligands in a series of primary NSCLCs and corresponding brain metastasis (N=57 pairs), and compared the level of expression of markers between primary tumors with (N=57 cases) and without (N=81 controls) brain metastasis. Archival formalin-fixed tissues obtained from surgically resected primary tumors and metastases were placed in tissue microarrays and examined for semi-quantitative IHC expression of EGFR, phosphorylated-EGFR (pEGFR), Her2, Her3, phosphorylated-Her3 (pHer3), EGF, amphiregulin (AR) and TGFr. All markers were examined at membranous (M), cytoplasmic (C) and nuclear (N) localization in tumor cells. Statistically significant higher levels of N-(P<0.001) and M-AR (P=0.06), M-pHer3 (P=0.001), and M- and C-pEGFR (P<0.001) were found in brain metastasis compared to corresponding primary tumor tissues. In contrast, brain metastasis showed lower levels (P=0.018) of C-TGFr expression than primary tumors. Interestingly, in multivariate analysis the IHC expression of M-pHer3 in primary tumors correlated (P=0.02, HR 1.02, 95%CI=1.003-1.043) with shorter time to brain metastasis development. Primary lung tumors with brain metastases showed statistically significant higher expression of C- and M-EGF (P<0.0001) and C-Her2 (P=0.003) compared to primary tumors without such metastasis. In contrast, M-AR, C-, M- and N-pHer3, M-EGFR, M- and C-pEGFR markers showed statistically significant higher levels of expression in primary tumors without brain metastasis. Our data indicate that there is differential expression pattern of HER family receptors and ligands in lung cancer and corresponding brain metastasis, with AR, pHer3 and pEGFR being significantly over-expressed in metastasis sites. A complex pattern of expression of HER family receptors and ligands differentiate primary NSCLC tumors with and without brain metastasis. We conclude that brain metastasis sites must be examined for molecular target expression to better predict response to targeted therapy in lung cancer patients.

(Grant IMPACT W81XWH-05-0027).

Selection, Isolation, and Identification of Targeting Peptides for Ligand-directed Gene Delivery

Martin Trepel,* Wadih Arap,† and Renata Pasqualini†

*University of Freiburg Medical Center, Department of Hematology and Oncology and Institute for Molecular Medicine and Cell Research, D-79106 Freiburg, Germany; †The University of Texas M.D. Anderson Cancer Center, Houston, Texas 77030-4095

ABSTRACT

Parenchymal, stromal, and vascular endothelial cells within organs express differential surface receptors depending on their tissue localization and functional state *in vivo*. On the basis of this receptor diversity, random phage display peptide libraries can be selected to isolate peptide ligands that home to tissue-specific cell surface receptors. Following systemic administration of the library, homing bacteriophage clones can be recovered by harvesting target tissues, amplified by infection of a bacterial host, and validated. The recovered peptide ligands then serve to identify their corresponding receptors and to target agents to specific cell types. A functional vascular map of such tissue-specific and angiogenesis-related receptors has been increasingly extended and refined by screening strategies in isolated receptors, cell lines, experimental animal models, *ex vivo* in clinical samples, and directly in patients. Recently, a new class of ligand-directed hybrid adeno-associated virus (AAV) phage vectors has been designed for targeted gene delivery to accessible cell surface receptors after systemic administration. Ultimately, these advances may lead to clinical applications in human disease.

INTRODUCTION, 360

PROTOCOL 1, 363

Selection of Random Phage Display Peptide Libraries *In Vivo*, 363

MATERIALS, 363

Reagents, 363

Equipment, 364

METHODS, 364

Injection of Phage Display Library, 364

Transcardial Perfusion and Washing, 364

Growth of K91kan Bacteria, 365

Recovery of Phage from Cell Pellets, 365

Recovery of Phage from Bacterial Culture, 365

PROTOCOL 2, 367

Phage Titering, 367

MATERIALS, 367

Reagents, 367

Equipment, 367

METHOD, 367

ACKNOWLEDGMENTS, 367

REFERENCES, 368

INTRODUCTION

Tissue-specific Vascular Receptor and Phage Display Library Selection

Tissues express specific patterns of cell surface proteins not only in their parenchymal and stromal components, but also in their vascular endothelium (for review, see Trepel et al. 2002; Hajitou et al. 2006a). Some of these cell surface proteins serve as growth factor receptors during normal development or pathological conditions. Moreover, tissue-specific endothelial cell surface proteins can serve as receptors for tissue-specific homing of circulating ligands or cells such as leukocytes. These tissue-specific endothelial receptors can be defined as functional vascular addresses by using systematic criteria (Marchiò et al. 2004). Such validated addresses can be targeted systematically through the circulation.

Ligand-directed targeting involves profiling of vascular addresses in normal organs as well as under pathological conditions. This can be readily accomplished by using random phage display peptide libraries. Such libraries represent large collections of phage particles displaying random peptides (typically $\sim 10^9$ unique sequences) (Smith and Scott 1993). Selection of phage libraries *in vivo* allows the recovery of displayed peptides that bind to tissue-specific vascular receptors and home preferentially to target organs. Briefly, libraries are injected intravenously, and the target tissue is surgically collected after a short circulation time. Phage clones displaying homing ligands present in the harvested tissue are rescued and reamplified by bacterial infection. Amplified mixtures are reinjected for further enrichment of clones displaying peptides with optimal homing capacity. After three or four rounds of selection, recovered phage clones are sequenced to identify the DNA corresponding to the inserts displayed, which should ideally share common peptide motifs (typically consisting of three to five residues). This technology has been used widely to identify tissue-specific ligand-receptor interactions *in vivo*. Different peptide motifs binding tissue-specific receptors have been recovered from several normal organs (Pasqualini and Ruoslahti 1996; Arap et al. 1998, 2002a,b; Rajotte et al. 1998; Porkka et al. 1999; Trepel et al. 2001; Essler and Ruoslahti 2002; Kolonin et al. 2002, 2004, 2006b; Laakkonen et al. 2002; Porkka et al. 2002). Likewise, targeting peptides recovered from known tissue-specific receptors or such receptors overexpressed on cells *in vitro* were used to study homing *in vivo* (Pasqualini et al. 1997; Burg et al. 1999; Arap et al. 2004; Marchiò et al. 2004; Zurita et al. 2004; Giordano et al. 2005).

An Emerging Human Vascular Ligand Receptor Map

The systematic mapping of receptors in human blood vessels (the so-called vascular ZIP codes) is required for development of clinically applicable targeted therapy. Recent studies showed that the tissue distribution of circulating peptides *in vivo* in humans is nonrandom and recovered a ligand interleukin-11 mimic peptide from the prostate (Arap et al. 2002b). Subsequently, the corresponding interleukin-11 receptor was validated as a morphologic and functional marker during human prostate cancer progression in a large panel of patient samples (Zurita et al. 2004). Recent refinements in methodology have enabled synchronous combinatorial selection of ligands from multiple organs in mice (Kolonin et al. 2006b) and have also adapted this strategy for use in patients (W. Arap et al., unpubl.). The challenges of accurate mapping are complicated further by studies in the mouse pancreas (Yao et al. 2005) which suggest that vascular heterogeneity in tissues may extend to functionally distinct regions within single organs.

Applications of Targeting Peptides

Receptor-targeting peptides can potentially serve in several applications. These include the identification of tissue-specific receptors accessible to circulating ligands (Rajotte and Ruoslahti 1999; Pasqualini et al. 2000; Giordano et al. 2001; Arap et al. 2002b; Kolonin et al. 2002, 2004; Christian

et al. 2003; Yao et al. 2005), targeting therapeutic agents (Arap et al. 1998, 2002a, 2004; Ellerby et al. 1999; Koivunen et al. 1999b; Trepel et al. 2001; Curnis et al. 2002; Kolonin et al. 2004; Zurita et al. 2004) or diagnostic compounds (Chen et al. 2004; Kolonin et al. 2006a; Souza et al. 2006) to the tissue of interest, and targeting gene-transfer vectors to specific receptors (Reynolds et al. 1999; Nicklin et al. 2000, 2001; Trepel et al. 2000b; Grifman et al. 2001; White et al. 2001, 2004; Shi and Bartlett 2003). The latter application is the most pertinent to this chapter and hence is discussed in more detail.

Ligand-directed Hybrid Vectors for Targeted Transgene Delivery

Current gene therapy vectors present problems of unintended transduction of certain tissues, adverse immune reactions, and lack of efficient transduction of the cells of interest (Somia and Verma 2000; Trepel et al. 2000a; Thomas et al. 2003). Specific targeting of vectors offers a solution to these concerns. Peptides have been exploited for viral vector targeting by using bispecific molecular conjugates consisting of antivector antibodies and peptide ligands directed toward the target receptor (Trepel et al. 2000b), as well as insertion of specific peptide ligands into the vector capsid (Girod et al. 1999; Reynolds et al. 1999; Grifman et al. 2001; Nicklin et al. 2001; White et al. 2001, 2004; Loiler et al. 2003; Müller et al. 2003; Shi and Bartlett 2003; Work et al. 2004). The latter strategy has many advantages such as ease of handling, better stability in vitro and in vivo, maintenance of the small size of the vector particle, and avoidance of additional immunogenicity elicited by conjugates.

The incorporation of peptide ligand sequences isolated by phage display libraries into eukaryotic vectors is possible (Reynolds et al. 1999; Grifman et al. 2001; Loiler et al. 2003; Shi and Bartlett 2003; White et al. 2004), but the reported success rate is quite variable. Only about 20–30% of selected ligand peptides function as well in targeted phage particles as in modified common gene-transfer vector capsids such as adenovirus or AAV. One explanation is that the phage-derived peptides are selected only for cell or receptor binding but not for subsequent post-targeting cell entry required for gene transfer. In addition, the binding potential of a ligand peptide may change when incorporated within a viral envelope. Taking such limitations into account, random peptide-display libraries based on the gene therapy vector capsid itself were developed for AAVs (Müller et al. 2003; Perabo et al. 2003) and retroviruses (Bupp and Roth 2003; Khare et al. 2003a,b; Hartl et al. 2005). This approach allows the selection of peptide ligands specifically binding to a cell type of interest within the specific viral capsid protein context. Consequently, such selections yield vectors that specifically and efficiently transduce the cell types on which they have been selected.

These approaches—the use of phage-derived peptides for targeted gene delivery and the use of peptides in the structural protein context in which they have been selected—can now be combined. This is achieved by using the targeted phage particle itself for gene delivery. However, bacteriophage species have generally been considered unsuitable vehicles for mammalian cell transduction. On the one hand, phage particles have no tropism for mammalian cells (Barrow and Soothill 1997) that must be neutralized for retargeting, and in recent years they have even been used for transduction of eukaryotic cells (Larocca et al. 1999; Poul and Marks 1999; Piersanti et al. 2004). Still, inefficient transduction and immunogenicity have remained major obstacles for phage vectors to overcome for applications in eukaryotic cells. We have thus introduced the AAV phage (AAVP) vector system (Hajitou et al. 2006b). This is a new hybrid containing genetic *cis*-elements from AAV and from a single-stranded M13 bacteriophage derivative. Incorporation of AAV-inverted terminal repeats into the phage transgene cassette is associated with improved intracellular fate of the delivered transgene (Hajitou et al. 2006b). A targeted AAVP prototype has been established by targeting α_v integrins up-regulated in tumor vessels. AAVP can mediate tissue-specific ligand-directed transduction in vivo after systemic administration of the vector. AAVP-mediated transfer of reporter genes has also been used for molecular genetic imaging and

suicide gene therapy strategies (Hajitou et al. 2006b). AAVP represents a new class of targeted prokaryotic/eukaryotic viral hybrid vectors that may serve in a wide range of applications in biomedical research. The method outlined here describes only the selection of tissue-targeted phage *in vivo*. Methods for modifying recovered phage into targeted AAVP are presented elsewhere (Hajitou et al. 2006b).

Protocol 1

Selection of Random Phage Display Peptide Libraries In Vivo

The following protocol is described for use in mice. However, it can be adapted for use in other species with modifications based on the dose of phage particles applied and phage recovery strategy. This procedure is confined to the screening of one organ at a time. However, an approach for simultaneous screening of multiple organs with phage display libraries in the mouse model has also been established (Kolonin et al. 2006b), following methodological principles similar to those outlined in this protocol.

MATERIALS

CAUTION: See Appendix for appropriate handling of materials marked with <!>.

Reagents

Anesthetic <!>

BALB/c mice (2 months old)

Despite being less cost-effective, nude mice are preferred to minimize fur-related bacterial cross-contamination. Most ligand receptors isolated thus far seem to be found across various mouse strains.

Dulbecco's modified Eagle's medium (DMEM) tissue-culture medium

K91kan bacteria

Any other F-pilus-positive *Escherichia coli* bacteria can be used for phage amplification.

Kanamycin <!>

Luria broth medium

NZY broth medium

Phage display random peptide libraries

The generation and production of phage display random peptide libraries have been described elsewhere (Smith and Scott 1993; Koivunen et al. 1999). Several libraries in different types of vectors are also commercially available. Suitable libraries comprise a diversity of $\geq 10^8$ unique phage peptide sequences. Usually, peptide lengths of ≤ 9 random residues are preferred as their selection can yield good affinity ligands. The potential diversity of larger library inserts is so high that such libraries may not be practically useful. Quality control of the phage library is crucial after each step of targeting in vivo. Amplified libraries (as opposed to primary libraries) may not always serve for this application if insertless or mutant phage clone frequencies are a concern.

Polyethylene glycol (PEG)/NaCl <!>

Dissolve 100 g of PEG (particle size 8000) and 110 g of NaCl in 450 ml of H₂O. Shake vigorously.

Sterilize by autoclaving. Shake repeatedly while cooling.

Phosphate-buffered saline (PBS)

Protease inhibitor cocktail (Roche)

TB supplement

Dissolve 11.55 g of K₂HPO₄ and 105 g of K₂HPO₄ in 500 ml of H₂O. Sterilize by autoclaving.

Dilute 1:10 in Terrific Broth prior to use.

Terrific Broth (TB) medium

Tetracycline <!>

Tris-buffered saline (TBS)

Equipment

Cannulae (butterfly IV 23-gauge blue)
 Cell culture flasks
 Glass tissue grinder
 Luria Broth agar plates
 Shaking incubator (37°C)
 Surgical tools
 Syringes

METHODS

Injection of Phage Display Library

1. Dilute the chosen phage library in DMEM or PBS to approximately 3.3×10^{10} transducing units (TU)/ml.
2. Administer 10^{10} TU of phage library intravenously into the tail vein of the subject animal. The volume should not exceed 300 μ l.
3. Maintain animal viability for 3–5 minutes while the library circulates.

Transcardial Perfusion and Washing

Transcardial perfusion of the experimental animal prior to surgical harvesting of the target organ can decrease nonspecific background phage recovery. However, for certain organs (e.g., kidney), perfusion increases phage trapping and may worsen the outcome. In addition, perfusion is not recommended for the initial round of selection as excessive stringency can eliminate potential binding peptides present in small numbers. To decrease background phage recovery from the blood if perfusion is not performed, the mouse can be exsanguinated completely.

4. Ensure that the experimental animal is under very deep surgical anesthesia.
5. Dissect away the skin at the level of the diaphragm to expose the chest and abdominal walls.
6. Open the peritoneum just below the sternum.
 It is important not to damage the liver, heart, or any large blood vessels at this point.
7. Make a section underneath and along the costal arch.
8. Dissect the lateral edges of the thorax through the diaphragm up to the axilla. Avoid damaging the lungs.
9. Fold the anterior chest wall cranially to expose the heart. Secure in position with a clamp.
10. Insert a cannula connected to a syringe containing approximately 5 ml of room-temperature DMEM in the left ventricle.
11. Make a small incision in the right atrium to provide a blood outlet.
12. Perfusion with low pressure to avoid vascular damage.
 Up to 50 ml can be perfused through the heart. The relative stringency is generally thought to be directly proportional to the volume used. During the first round of selection (if perfusion is performed), consider perfusion with lower volumes.
13. Surgically remove the target organ and at least one control organ (such as the lung or brain). Place on ice immediately to avoid bound phage internalization.
14. Weigh organs. Homogenize with a glass tissue grinder.

15. Add 1 ml of ice-cold DMEM supplemented with the protease inhibitor cocktail to the tissue homogenate. Vortex. Centrifuge at 3000 rpm for 4 minutes at 4°C. Remove the supernatant.
16. Repeat Step 15 (three washes total, or one to two washes for the first round of selection).
17. After the last centrifugation, remove the supernatant. Keep the pellet on ice until addition of bacteria.

Growth of K91kan Bacteria

18. Inoculate 5 ml of TB supplemented with 200 µg/ml kanamycin and 10% TB supplement with a streak from a K91kan agar plate.
19. Shake inoculum at regular speed for 2–4 hours at 37°C.
It is recommended that the growth of the bacteria be started after injection of the library into the animal.
20. Dilute an aliquot of inoculum 1:10 with TB. Determine OD₆₀₀.
When the OD₆₀₀ is 0.16–0.20, decrease the shaker speed to regenerate sheared pili. Use the bacteria within 30 minutes.

Recovery of Phage from Cell Pellets

21. Add 1500 µl of the K91kan culture to the phage-cell pellet (from Step 17). Resuspend pellet gently but thoroughly. Incubate for 30 minutes at 37°C. Swirl or invert the sample at 10-minute intervals.
22. Transfer bacteria to a 500-ml cell culture flask. Add 100 ml of prewarmed NZY medium containing 0.2 µg/ml tetracycline. Incubate for 30 minutes at 37°C.
23. Remove 10- and 100-µl aliquots from the suspension. Plate on LB agar plates containing 40 µg/ml tetracycline to estimate the number of transducing phage units recovered from each tissue.
24. Adjust the tetracycline concentration in the remaining culture to 20 µg/ml. Grow overnight at 37°C in the shaker.
Cultures should be grown for at least 12 hours, but no more than 16 hours.

Recovery of Phage from Bacterial Culture

25. Centrifuge the bacterial culture at 8000 rpm for 15 minutes. Decant the supernatant into a clean tube. Take care that the pellet is on the upper side of the tube when decanting.
26. Add 1.5 ml of PEG/NaCl per each 10 ml of supernatant. Shake well. Incubate for at least 1 hour on ice.
Samples can be incubated with PEG/NaCl overnight at 4°C.
27. Centrifuge at 8000 rpm for 20 minutes at 4°C. Decant and discard the supernatant.
28. Insert the tube in the rotor such that the side of the tube containing the pellet is toward the outside of the rotor. Centrifuge the pellet again at 8000 rpm for 5 minutes to remove all PEG and to further concentrate the pellet.
29. Promptly and carefully remove the supernatant with a vacuum aspirator or a 200 µl-pipette.
30. Add TBS to the phage pellet (~200–400 µl, depending on the size of the pellet). Shake for 10 minutes.
Avoid resuspending the phage pellet with the pipette as frothing can occur that might harm the phage or displayed peptides.

31. Transfer the solution to an Eppendorf tube. Centrifuge at 14,000 rpm for 10 minutes to remove any bacterial debris.
32. Carefully transfer the supernatant (phage solution) to a new labeled Eppendorf tube. Do not touch the pellet when transferring the supernatant.
33. Titer the recovered phage solution (see Protocol 2).
34. Repeat the phage selection (Steps 1–32) using 1×10^9 to 5×10^9 transducing units of the recovered phage for each successive round of selection.
For most applications, three to four rounds are sufficient to yield tissue-specific phage.
35. Sequence colonies after the third round to identify the peptides recovered from the target tissue.

The number of sequenced clones per selection round should be at least 30. For sequencing of the random phage insert, we use the primer 5'-GCAAGCTGATAAACCGATAAAATT-3'. The recognition pattern for the insert in the phage genome is 5'-GCCGACGGGGCT-insert-GGGCCGCTGGG-3'.

Protocol 2

Phage Titering

MATERIALS

CAUTION: See Appendix for appropriate handling of materials marked with <!>.

Reagents

K91kan bacteria
Kanamycin <!>
Terrific Broth (TB) medium
Tetracycline <!>

Equipment

Luria Broth agar plates
Shaking incubator (37°C)

METHOD

1. Grow *K91kan* bacteria as described in Protocol 1, Steps 18–20.
2. In separate Eppendorf tubes, prepare five serial dilutions of the phage stock (from Protocol 1, Step 32) corresponding to 10^{-5} to 10^{-9} μ l of the initial stock.
3. Add 180 μ l of the *K91kan* bacteria culture to each of the tubes.
4. Incubate phage with bacteria for 30 minutes at room temperature.
5. Plate 100 μ l of each solution on LB plates containing tetracycline. Grow overnight in the incubator at 37°C.
6. Count the colonies on the plates.
7. Multiply the number of colonies by the dilution factor to determine the number of TU/ μ l of phage solution.

Only plates with 20–600 colonies yield reliable results.

ACKNOWLEDGMENTS

This work was funded by grants from the National Institutes of Health (including the SPORE) and DOD (including the IMPACT) and by awards from the Gillson-Longenbaugh, the Keck Foundation, the Prostate Cancer Foundation (to R.P. and W.A.), and the Deutsche Forschungsgemeinschaft (to M.T.).

REFERENCES

Arap M.A., Lahdenranta J., Mintz P.J., Hajitou A., Sarkis A.S., Arap W., and Pasqualini R. 2004. Cell surface expression of the stress response chaperone GRP78 enables tumor targeting by circulating ligands. *Cancer Cell* 6: 275–284.

Arap W., Pasqualini R., and Ruoslahti E. 1998. Cancer treatment by targeted drug delivery to tumor vasculature in a mouse model. *Science* 279: 377–380.

Arap W., Haedicke W., Bernasconi M., Kain R., Rajotte D., Krajewski S., Ellerby H.M., Bredesen D.E., Pasqualini R., and Ruoslahti E. 2002a. Targeting the prostate for destruction through a vascular address. *Proc. Natl. Acad. Sci.* 99: 1527–1531.

Arap W., Kolonin M.G., Trepel M., Lahdenranta J., Cardo-Vila M., Giordano R.J., Mintz P.J., Ardelt P.U., Yao V.J., Vidal C.I., et al. 2002b. Steps toward mapping the human vasculature by phage display. *Nat. Med.* 8: 121–127.

Barrow P.A. and Soothill J.S. 1997. Bacteriophage therapy and prophylaxis: Rediscovery and renewed assessment of potential. *Trends Microbiol.* 5: 268–271.

Bupp K. and Roth M.J. 2003. Targeting a retroviral vector in the absence of a known cell-targeting ligand. *Hum. Gene Ther.* 14: 1557–1564.

Burg M.A., Pasqualini R., Arap W., Ruoslahti E., and Stallcup W.B. 1999. NG2 proteoglycan-binding peptides target tumor neovasculature. *Cancer Res.* 59: 2869–2874.

Chen L., Zurita A.J., Ardelt P.U., Giordano R.J., Arap W., and Pasqualini R. 2004. Design and validation of a bifunctional ligand display system for receptor targeting. *Chem. Biol.* 11: 1081–1091.

Christian S., Pilch J., Akerman M.E., Porkka K., Laakkonen P., and Ruoslahti E. 2003. Nucleolin expressed at the cell surface is a marker of endothelial cells in angiogenic blood vessels. *J. Cell Biol.* 163: 871–878.

Curnis F., Arrigoni G., Sacchi A., Fischetti L., Arap W., Pasqualini R., and Corti A. 2002. Differential binding of drugs containing the NGR motif to CD13 isoforms in tumor vessels, epithelia, and myeloid cells. *Cancer Res.* 62: 867–874.

Ellerby H.M., Arap W., Ellerby L.M., Kain R., Andrusiak, R., Rio G.D., Krajewski S., Lombardo C.R., Rao R., Ruoslahti E., Bredesen D.E., and Pasqualini R. 1999. Anti-cancer activity of targeted pro-apoptotic peptides. *Nat. Med.* 5: 1032–1038.

Essler M. and Ruoslahti E. 2002. Molecular specialization of breast vasculature: A breast-homing phage-displayed peptide binds to aminopeptidase P in breast vasculature. *Proc. Natl. Acad. Sci.* 99: 2252–2257.

Giordano R.J., Cardo-Vila M., Lahdenranta J., Pasqualini R., and Arap W. 2001. Biopanning and rapid analysis of selective interactive ligands. *Nat. Med.* 7: 1249–1253.

Giordano R.J., Anobom C.D., Cardo-Vila M., Kalil J., Valente A.P., Pasqualini R., Almeida F.C., and Arap W. 2005. Structural basis for the interaction of a vascular endothelial growth factor mimic peptide motif and its corresponding receptors. *Chem. Biol.* 12: 1075–1083.

Girod A., Ried M., Wobus C., Lahm H., Leike K., Kleinschmidt J., Deleage G., and Hallek M. 1999. Genetic capsid modifications allow efficient re-targeting of adeno-associated virus type 2. *Nat. Med.* 5: 1052–1056.

Grifman M., Trepel M., Specce P., Gilbert L.B., Arap W., Pasqualini R., and Weitzman M.D. 2001. Incorporation of tumor-targeting peptides into recombinant adeno-associated virus capsids. *Mol. Ther.* 3: 964–975.

Hajitou A., Pasqualini R., and Arap W. 2006a. Vascular targeting: Recent advances and therapeutic perspectives. *Trends Cardiovasc. Med.* 16: 80–88.

Hajitou A., Trepel M., Lilley C.E., Soghomonyan S., Alauddin M.M., Marini F.C., III, Restel B.H., Ozawa M.G., Moya C.A., Rangel R., et al. 2006b. A hybrid vector for ligand-directed tumor targeting and molecular imaging. *Cell* 125: 385–398.

Hartl I., Schneider R.M., Sun Y., Medvedovska J., Chadwick M.P., Russell S.J., Cichutek K., and Buchholz C.J. 2005. Library-based selection of retroviruses selectively spreading through matrix metalloprotease-positive cells. *Gene Ther.* 2: 918–926.

Khare P.D., Russell S.J., and Federspiel M.J. 2003a. Avian leukosis virus is a versatile eukaryotic platform for polypeptide display. *Virology* 315: 303–312.

Khare P.D., Rosales A.G., Bailey K.R., Russell S.J., and Federspiel M.J. 2003b. Epitope selection from an uncensored peptide library displayed on avian leukosis virus. *Virology* 315: 313–321.

Koivunen E., Restel B.H., Rajotte D., Lahdenranta J., Hagedorn M., Arap W., and Pasqualini R. 1999a. Integrin-binding peptides derived from phage display libraries. *Methods Mol. Biol.* 129: 3–17.

Koivunen E., Arap W., Valtanen H., Rainisalo A., Medina O.P., Heikkila P., Kantor C., Gahmberg C.G., Salo T., Konttinen Y.T., et al. 1999b. Tumor targeting with a selective gelatinase inhibitor. *Nat. Biotechnol.* 17: 768–774.

Kolonin M.G., Pasqualini R., and Arap W. 2002. Teratogenicity induced by targeting a placental immunoglobulin transporter. *Proc. Natl. Acad. Sci.* 99: 13055–13060.

Kolonin M.G., Saha P.K., Chan L., Pasqualini R., and Arap W. 2004. Reversal of obesity by targeted ablation of adipose tissue. *Nat. Med.* 10: 625–632.

Kolonin M.G., Sun J., Do K.A., Vidal C.I., Ji Y., Baggerly K.A., Pasqualini R., and Arap W. 2006a. Synchronous selection of homing peptides for multiple tissues by in vivo phage display. *FASEB J.* 20: 979–981.

Kolonin M.G., Bover L., Sun J., Zurita A.J., Do K.A., Lahdenranta J., Cardo-Vila M., Giordano R.J., Jaalouk D.E., Ozawa M.G., et al. 2006b. Ligand-directed surface profiling of human cancer cells with combinatorial peptide libraries. *Cancer Res.* 66: 34–40.

Laakkonen P., Porkka K., Hoffman J.A., and Ruoslahti E. 2002. A tumor-homing peptide with a targeting specificity related to lymphatic vessels. *Nat. Med.* 8: 751–755.

Larocca D., Kassner P.D., Witte A., Ladner R.C., Pierce G.F., and Baird A. 1999. Gene transfer to mammalian cells using genetically targeted filamentous bacteriophage. *FASEB J.* 13: 727–734.

Loiler S.A., Conlon T.J., Song S., Tang Q., Warrington K.H., Agarwal A., Kapturczak M., Li C., Ricordi C., Atkinson M.A., et al. 2003. Targeting recombinant adeno-associated virus vectors to enhance gene transfer to pancreatic islets and liver. *Gene Ther.* 10: 1551–1558.

Marchiò S., Lahdenranta J., Schlingemann R.O., Valdembri D., Wesseling P., Arap M.A., Hajitou A., Ozawa M.G., Trepel M., Giordano R.J., et al. 2004. Aminopeptidase A is a functional target in angiogenic blood vessels. *Cancer Cell* 5: 151–162.

Müller O.J., Kaul F., Weitzman M.D., Pasqualini R., Arap W., Kleinschmidt J.A., and Trepel M. 2003. Random peptide libraries displayed on adeno-associated virus to select for targeted gene therapy vectors. *Nat. Biotechnol.* 21: 1040–1046.

Nicklin S.A., White S.J., Watkins S.J., Hawkins R.E., and Baker A.H. 2000. Selective targeting of gene transfer to vascular endothelial cells by use of peptides isolated by phage display. *Circulation* **102**: 231–237.

Nicklin S.A., Von Seggern D.J., Work L.M., Pek D.C., Dominiczak A.F., Nemerow G.R., and Baker A.H. 2001. Ablating adenovirus type 5 fiber-CAR binding and HI loop insertion of the SIGYPLP peptide generate an endothelial cell-selective adenovirus. *Mol. Ther.* **4**: 534–542.

Pasqualini R. and Ruoslahti E. 1996. Organ targeting in vivo using phage display peptide libraries. *Nature* **380**: 364–366.

Pasqualini R., Koivunen E., and Ruoslahti E. 1997. α_v integrins as receptors for tumor targeting by circulating ligands. *Nat. Biotechnol.* **15**: 542–546.

Pasqualini R., Koivunen E., Kain R., Lahdenranta J., Sakamoto M., Stryhn A., Ashmun R.A., Shapiro L.H., Arap W., and Ruoslahti E. 2000. Aminopeptidase N is a receptor for tumor-homing peptides and a target for inhibiting angiogenesis. *Cancer Res.* **60**: 722–727.

Perabo L., Buning H., Kofler D.M., Ried M.U., Girod A., Wendtner C.M., Enssle R., and Hallek M. 2003. In vitro selection of viral vectors with modified tropism: The adeno-associated virus display. *Mol. Ther.* **8**: 151–157.

Piersanti S., Cherubini G., Martina Y., Salone B., Avitabile D., Grosso F., Cundari E., Di Zenzo G., and Saggio I. 2004. Mammalian cell transduction and internalization properties of λ phages displaying the full-length adenoviral penton base or its central domain. *J. Mol. Med.* **82**: 467–476.

Porkka K., Laakkonen P., Hoffman J.A., Bernasconi M., and Ruoslahti E. 2002. A fragment of the HMGN2 protein homes to the nuclei of tumor cells and tumor endothelial cells in vivo. *Proc. Natl. Acad. Sci.* **99**: 7444–7449.

Porkka K., Laakkonen P., Rajotte D., Hoffman J., and Ruoslahti E. 1999. Bone marrow homing peptides from phage display libraries. *Blood* **94**: 1107.

Poul M.A. and Marks J.D. 1999. Targeted gene delivery to mammalian cells by filamentous bacteriophage. *J. Mol. Biol.* **288**: 203–211.

Rajotte D. and Ruoslahti E. 1999. Membrane dipeptidase is the receptor for a lung-targeting peptide identified by in vivo phage display. *J. Biol. Chem.* **274**: 11593–11598.

Rajotte D., Arap W., Hagedorn M., Koivunen E., Pasqualini R., and Ruoslahti E. 1998. Molecular heterogeneity of the vascular endothelium revealed by in vivo phage display. *J. Clin. Invest.* **102**: 430–437.

Reynolds P., Dmitriev I., and Curiel D. 1999. Insertion of an RGD motif into the HI loop of adenovirus fiber protein alters the distribution of transgene expression of the systemically administered vector. *Gene Ther.* **6**: 1336–1339.

Shi W.F. and Bartlett J.S. 2003. RGD inclusion in VP3 provides adeno-associated virus type 2 (AAV2)-based vectors with a heparan sulfate-independent cell entry mechanism. *Mol. Ther.* **7**: 515–525.

Smith G.P. and Scott J.K. 1993. Libraries of peptides and proteins displayed on filamentous phage. *Methods Enzymol.* **217**: 228–257.

Somia N. and Verma I.M. 2000. Gene therapy: Trials and tribulations. *Nat. Rev. Genet.* **1**: 91–99.

Souza G.R., Christianson D.R., Staquicini F.I., Ozawa M.G., Snyder E.Y., Sidman R.L., Miller J.H., Arap W., and Pasqualini R. 2006. Networks of gold nanoparticles and bacteriophage as biological sensors and cell-targeting agents. *Proc. Natl. Acad. Sci.* **103**: 1215–1220.

Thomas C.E., Ehrhardt A., and Kay M.A. 2003. Progress and problems with the use of viral vectors for gene therapy. *Nat. Rev. Genet.* **4**: 346–358.

Trepel M., Arap W., and Pasqualini R. 2000a. Exploring vascular heterogeneity for gene therapy targeting. *Gene Ther.* **7**: 2059–2060.

—. 2001. Modulation of the immune response by systemic targeting of antigens to lymph nodes. *Cancer Res.* **61**: 8110–8112.

—. 2002. In vivo phage display and vascular heterogeneity: Implications for targeted medicine. *Curr. Opin. Chem. Biol.* **6**: 399–404.

Trepel M., Grifman M., Weitzman M.D., and Pasqualini R. 2000b. Molecular adaptors for vascular-targeted adenoviral gene delivery. *Hum. Gene Ther.* **11**: 1971–1981.

White S.J., Nicklin S.A., Sawamura T., and Baker A.H. 2001. Identification of peptides that target the endothelial cell-specific LOX-1 receptor. *Hypertension* **37**: 449–455.

White S.J., Nicklin S.A., Buning H., Brosnan M.J., Leike K., Papadakis E.D., Hallek M., and Baker A.H. 2004. Targeted gene delivery to vascular tissue in vivo by tropism-modified adeno-associated virus vectors. *Circulation* **109**: 513–519.

Work L.M., Nicklin S.A., Brain N.J.R., Dishart K.L., Von Seggern D.J., Hallek M., Buning H., and Baker A.H. 2004. Development of efficient viral vectors selective for vascular smooth muscle cells. *Mol. Ther.* **9**: 198–208.

Yao V.J., Ozawa M.G., Trepel M., Arap W., McDonald D.M., and Pasqualini R. 2005. Targeting pancreatic islets with phage display assisted by laser pressure catapult microdissection. *Am. J. Pathol.* **166**: 625–636.

Zurita A.J., Troncoso P., Cardo-Vila M., Logothetis C.J., Pasqualini R., and Arap W. 2004. Combinatorial screenings in patients: The interleukin-11 receptor α as a candidate target in the progression of human prostate cancer. *Cancer Res.* **64**: 435–439.